THE EUROPEAN
PHYSICAL JOURNAL C

CrossMark

A dispersive treatment of $K_{\ell 4}$ decays

Gilberto Colangelo[1], **Emilie Passemar**[2,3,4], **Peter Stoffer**[1,5,a]

[1] Albert Einstein Center for Fundamental Physics, Institute for Theoretical Physics, University of Bern, Sidlerstrasse 5, 3012 Bern, Switzerland
[2] Department of Physics, Indiana University, Bloomington, IN 47405, USA
[3] Center for Exploration of Energy and Matter, Indiana University, Bloomington, IN 47403, USA
[4] Theory Center, Thomas Jefferson National Accelerator Facility, Newport News, VA 23606, USA
[5] Helmholtz-Institut für Strahlen- und Kernphysik (Theory) and Bethe Center for Theoretical Physics, University of Bonn, 53115 Bonn, Germany

Abstract $K_{\ell 4}$ decays have several features of interest: they allow an accurate measurement of $\pi\pi$-scattering lengths; they provide the best source for the determination of some low-energy constants of χPT; one form factor is directly related to the chiral anomaly, which can be measured here. We present a dispersive treatment of $K_{\ell 4}$ decays that provides a resummation of $\pi\pi$- and $K\pi$-rescattering effects. The free parameters of the dispersion relation are fitted to the data of the high-statistics experiments E865 and NA48/2. The matching to χPT at NLO and NNLO enables us to determine the LECs L_1^r, L_2^r and L_3^r. With recently published data from NA48/2, the LEC L_9^r can be determined as well. In contrast to a pure chiral treatment, the dispersion relation describes the observed curvature of one of the form factors, which we understand as a rescattering effect beyond NNLO.

Contents

[a] e-mail: stoffer@itp.unibe.ch

Springer

1 Introduction

$K_{\ell 4}$ denotes the semileptonic decay of a kaon into two pions
and a lepton pair. Its amplitude has a similar structure to that
of $K\pi$ scattering, with the difference that in $K_{\ell 4}$ decays one
of the axial currents couples to an external field, the W boson,
which decays into the lepton pair – the q^2 of this axial current
is therefore variable rather than being stuck at M_K^2 as in $K\pi$
scattering. This difference has the important consequence
that in $K_{\ell 4}$ decays the allowed kinematical region reaches
down to lower energies, $E \leq M_K$, whereas in $K\pi$ scattering
$E \geq M_K + M_\pi$. From the point of view of chiral perturbation
theory (χPT) [1–3], the low-energy effective theory of QCD,
$K_{\ell 4}$ decays offer similar information as $K\pi$ scattering, but
in a kinematical region where the chiral expansion is more
reliable.

Due to its two-pion final state, $K_{\ell 4}$ is also one of the clean-
est sources of information on $\pi\pi$ interaction [4–6].

The latest high-statistics $K_{\ell 4}$ experiments E865 at BNL
[7,8] and NA48/2 at CERN [6,9] have achieved an impres-
sive accuracy. The statistical errors of the S-wave of one
form factor reach in both experiments the sub-percent
level. Matching this precision requires a theoretical treat-
ment beyond one-loop order in the chiral expansion. A
first treatment beyond one loop, based on dispersion rela-
tions, was already done 20 years ago [10]. The full two-
loop calculation became available in 2000 [11]. How-
ever, as we will show below, even at two loops χPT is
not able to predict the curvature of one of the form fac-
tors.

Here, we present a new dispersive treatment of $K_{\ell 4}$
decays. The form of the dispersion relation we solve
is not exact, but relies on an assumption (absence of
D- and higher wave contributions to discontinuities) that
is violated only starting at $\mathcal{O}(p^8)$ in the chiral expan-
sion. It resums two-particle rescattering effects, which we
expect to be the most important contribution beyond two

loops. Indeed, we observe that the dispersive descrip-
tion is able to reproduce the curvature of the form fac-
tor.

The dispersion relation is parameterised by subtraction
constants, which are not constrained by unitarity. These
have to be determined by theoretical input or by a fit to
data. It turns out that the available data does not con-
strain all the subtraction constants to a sufficient preci-
sion. Therefore, we use the soft-pion theorem, a low-
energy theorem for $K_{\ell 4}$ that receives only $SU(2)$ chi-
ral corrections, as well as some chiral input to constrain
the parameters that are not well determined from data
alone.

The present treatment of $K_{\ell 4}$ decays represents an exten-
sion and a major improvement of our previous dispersive
framework [12–14]. The modifications and improvements
concern the following aspects:

- Instead of a single linear combination of form factors,
  now we describe the two form factors F and G simul-
  taneously. This allows us to include more experimental
  data in the fits.
- The new framework is valid also for non-vanishing invari-
  ant energies of the lepton pair. In the previous treatment,
  we neglected the dependence on this kinematic variable.
  This approximation is no longer used and the observed
  dependence on the lepton invariant energy can be taken
  into account.
- We apply corrections for isospin-breaking effects in the
  fitted data that have not been taken into account in the
  experimental analysis.
- We perform the matching to χPT directly on the level of
  the subtraction constants, which avoids the mixing with
  the treatment of rescattering effects.
- Besides a matching to one-loop χPT, we also study the
  matching at two-loop level.

The first two points required a substantial modification
and extension of the dispersive framework from the very
start, but rendered it much more powerful. The old treat-
ment can be understood as a limiting case of the new
framework.

The outline is as follows: in Sect. 2, we derive the dis-
persion relation for the $K_{\ell 4}$ form factors, which has the
form of a set of coupled integral equations. In Sect. 3, we
describe the numerical procedure that is used to solve this
system. Section 4 is devoted to the determination of the
free parameters of the dispersion relation and the deriva-
tion of matching equations to χPT. In Sect. 5, we present
the results of the fit to data and the values of the low-energy
constants L_1^r, L_2^r and L_3^r obtained in the matching to χPT.
Section 6 concludes the main text. The appendices contain
several details on the kinematics, the derivation of the disper-

sion relation and explicit expressions for the matching equations. Further details that are omitted here can be found in [15].

2 Dispersion relation for $K_{\ell 4}$

2.1 Decay amplitude and form factors

$K_{\ell 4}$ are semileptonic decays of a kaon into two pions and a lepton-neutrino pair:

$$K^+(k) \to \pi^+(p_1)\pi^-(p_2)\ell^+(p_\ell)\nu_\ell(p_\nu), \tag{1}$$

where $\ell \in \{e, \mu\}$ is either an electron or a muon. There exist other decay modes involving neutral mesons. Their amplitudes are related to the above decay by isospin symmetry – in our dispersive treatment of $K_{\ell 4}$, we will work in the isospin limit and could therefore describe the neutral mode as well. In the present analysis, however, we only consider the charged mode because it is the one which has been measured more accurately.

In the standard model, semileptonic decays are mediated by W bosons. After integrating out the W boson from the standard model Lagrangian, we end up with a Fermi type effective current–current interaction. The matrix element of $K_{\ell 4}$ then splits up into a leptonic times a hadronic part. The leptonic matrix element can be treated in a standard way. The hadronic matrix element exhibits the usual $V - A$ structure of weak interaction:

$$_\text{out}\langle \pi^+(p_1)\pi^-(p_2)\ell^+(p_\ell)\nu_\ell(p_\nu)|K^+(k)\rangle_\text{in}$$
$$= i(2\pi)^4\delta^{(4)}(k - p_1 - p_2 - p_\ell - p_\nu)\mathcal{T}, \tag{2}$$

$$\mathcal{T} = \frac{G_F}{\sqrt{2}}V_{us}^*\bar{u}(p_\nu)\gamma^\mu(1 - \gamma_5)v(p_\ell)$$
$$\times \langle \pi^+(p_1)\pi^-(p_2)|V_\mu(0) - A_\mu(0)|K^+(k)\rangle, \tag{3}$$

where $V_\mu = \bar{s}\gamma_\mu u$ and $A_\mu = \bar{s}\gamma_\mu\gamma_5 u$. Note that although we drop the corresponding labels, the meson states are still in- and out-states with respect to the strong interaction.

The Lorentz structure of the currents allows us to write the two hadronic matrix elements as

$$\mathcal{V}_\mu^{+-} := \langle \pi^+(p_1)\pi^-(p_2)|V_\mu(0)|K^+(k)\rangle$$
$$= -\frac{H}{M_K^3}\epsilon_{\mu\nu\rho\sigma}L^\nu P^\rho Q^\sigma, \tag{4}$$

$$\mathcal{A}_\mu^{+-} := \langle \pi^+(p_1)\pi^-(p_2)|A_\mu(0)|K^+(k)\rangle$$
$$= -i\frac{1}{M_K}(P_\mu F + Q_\mu G + L_\mu R), \tag{5}$$

where $P = p_1 + p_2$, $Q = p_1 - p_2$, $L = k - p_1 - p_2$. The form factors F, G, R and H are dimensionless scalar

functions of the Mandelstam variables:

$$s = (p_1 + p_2)^2 = (k - L)^2,$$
$$t = (k - p_1)^2 = (p_2 + L)^2,$$
$$u = (k - p_2)^2 = (p_1 + L)^2. \tag{6}$$

We further define the invariant squared energy of the lepton pair $s_\ell = L^2$. For the hadronic matrix element, we regard s_ℓ as a fixed external quantity.

2.2 Analytic structure

Let us first study the general properties of matrix elements of the hadronic axial-vector current. It is instructive to draw a Mandelstam diagram for the process (see Figs. 1, 2): since $s + t + u = M_K^2 + 2M_\pi^2 + s_\ell =: \Sigma_0$ is constant (for a fixed value of s_ℓ), the Mandelstam variables can be represented in one plane, using the fact that the sum of distances of a point to the sides of an equilateral triangle is constant.

The same amplitude describes four processes:

- the decay $K^+(k) \to \pi^+(p_1)\pi^-(p_2)A_\mu^\dagger(L)$,
- the s-channel scattering $K^+(k)A_\mu(-L)\to\pi^+(p_1)\pi^-(p_2)$,
- the t-channel scattering $K^+(k)\pi^-(-p_1)\to\pi^-(p_2)A_\mu^\dagger(L)$,
- the u-channel scattering $K^+(k)\pi^+(-p_2)\to\pi^+(p_1)A_\mu^\dagger(L)$.

The physical region of the decay starts at $s = 4M_\pi^2$ and ends at $s = (M_K - \sqrt{s_\ell})^2$. The s-channel scattering starts at $s = (M_K + \sqrt{s_\ell})^2$. If $s_\ell = 0$ is assumed, the two regions touch at $s = M_K^2$ (Fig. 1).

The sub-threshold region $s < s_0 := 4M_\pi^2$, $t < t_0 := (M_K+M_\pi)^2$, $u < u_0 := (M_K+M_\pi)^2$ forms a triangle in the Mandelstam plane where the amplitude is real. Branch cuts of the amplitude start at each threshold s_0, t_0 and u_0. There, physical intermediate states are possible ($\pi\pi$ intermediate states in the s-channel, $K\pi$ states in the t- and u-channel).

2.3 Isospin decomposition

Let us study the isospin properties of the $K_{\ell 4}$ matrix element of the hadronic axial-vector current in the different channels: we decompose the physical amplitude into amplitudes with definite isospin.

2.3.1 s-channel

We consider the matrix element

$$\mathcal{A}_\mu^{+-} = \langle \pi^+(p_1)\pi^-(p_2)|A_\mu(0)|K^+(k)\rangle. \tag{7}$$
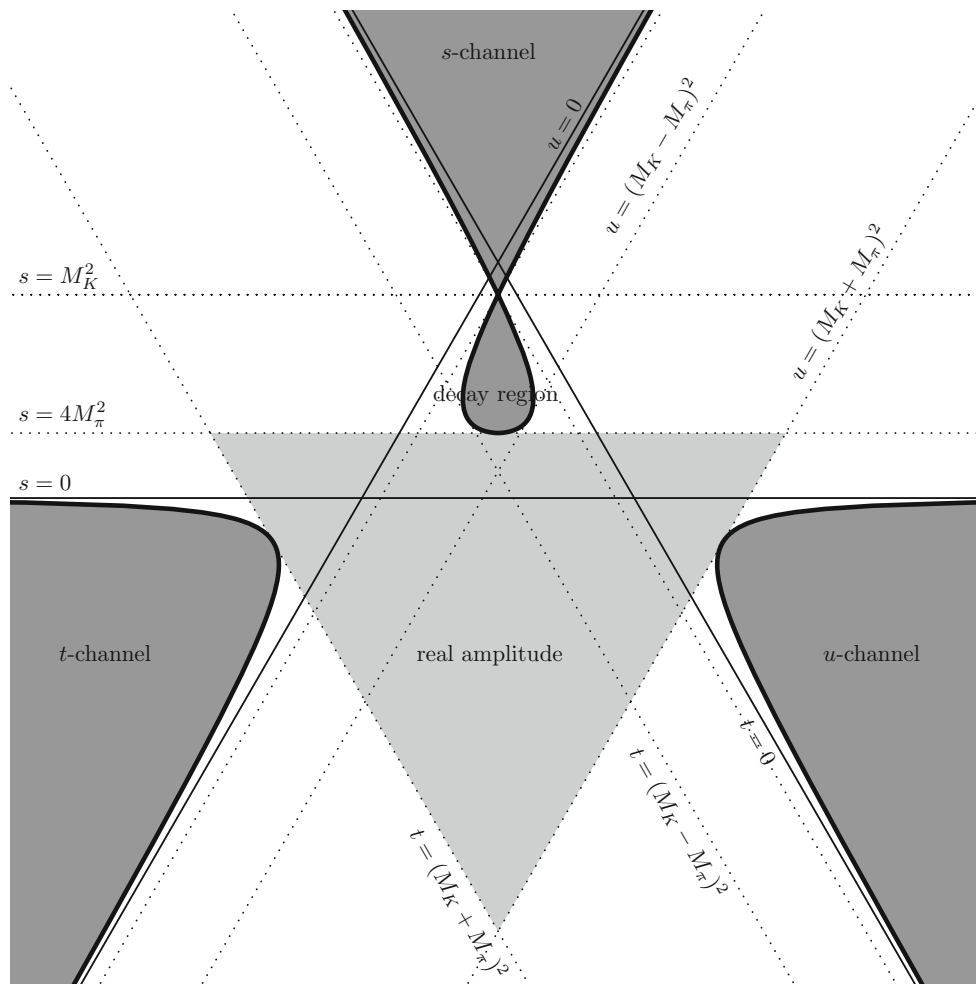
Fig. 1 Mandelstam diagram for $K_{\ell 4}$ for the case $s_\ell = 0$

As the weak current satisfies $\Delta I = \frac{1}{2}$, the initial and final states can be decomposed as

$$A_\mu(0)|K^+(k)\rangle = \frac{1}{\sqrt{2}}|1,0\rangle + \frac{1}{\sqrt{2}}|0,0\rangle,$$

$$\langle \pi^+(p_1)\pi^-(p_2)| = \frac{1}{\sqrt{6}}\langle 2,0| + \frac{1}{\sqrt{2}}\langle 1,0| + \frac{1}{\sqrt{3}}\langle 0,0|,$$

$$(8)$$

$$\langle \pi^-(p_1)\pi^+(p_2)| = \frac{1}{\sqrt{6}}\langle 2,0| - \frac{1}{\sqrt{2}}\langle 1,0| + \frac{1}{\sqrt{3}}\langle 0,0|.$$

Hence, we can write the following decomposition of the matrix element into pure isospin amplitudes:

$$\mathcal{A}_\mu^{+-} = \frac{1}{2}\mathcal{A}_\mu^{(1)} + \frac{1}{\sqrt{6}}\mathcal{A}_\mu^{(0)},$$

$$\mathcal{A}_\mu^{-+} = -\frac{1}{2}\mathcal{A}_\mu^{(1)} + \frac{1}{\sqrt{6}}\mathcal{A}_\mu^{(0)}.$$

$$(9)$$

Using $\mathcal{A}_\mu^{+-}(k, -L \to p_1, p_2) = \mathcal{A}_\mu^{-+}(k, -L \to p_2, p_1)$, we find the following relations:

$$\mathcal{A}_\mu^0(k, -L \to p_1, p_2)$$
$$= \sqrt{\frac{3}{2}}(\mathcal{A}_\mu^{+-}(k, -L \to p_1, p_2) + \mathcal{A}_\mu^{+-}(k, -L \to p_2, p_1)),$$
$$\mathcal{A}_\mu^1(k, -L \to p_1, p_2)$$
$$= (\mathcal{A}_\mu^{+-}(k, -L \to p_1, p_2) - \mathcal{A}_\mu^{+-}(k, -L \to p_2, p_1)).$$

$$(10)$$

The pure isospin form factors are related to the physical ones by

$$F^{(0)}(s,t,u) = \sqrt{\frac{3}{2}}(F(s,t,u) + F(s,u,t)),$$

$$G^{(0)}(s,t,u) = \sqrt{\frac{3}{2}}(G(s,t,u) - G(s,u,t)),$$

$$R^{(0)}(s,t,u) = \sqrt{\frac{3}{2}}(R(s,t,u) + R(s,u,t)),$$
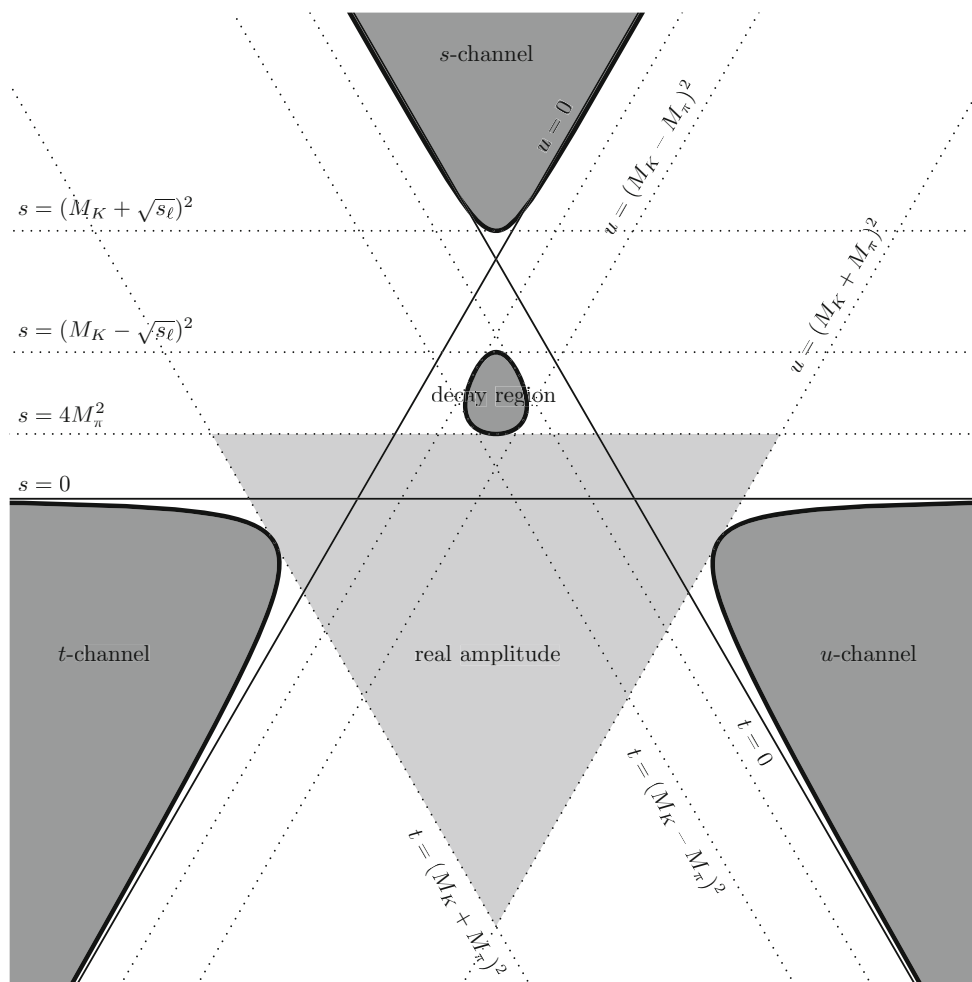
Fig. 2 Mandelstam diagram for $K_{\ell 4}$ for the case $s_\ell > 0$

$$F^{(1)}(s,t,u) = F(s,t,u) - F(s,u,t),$$
$$G^{(1)}(s,t,u) = G(s,t,u) + G(s,u,t),$$
$$R^{(1)}(s,t,u) = R(s,t,u) - R(s,u,t). \tag{11}$$

We further note that

$$\mathcal{A}_\mu^{(0)}(k, -L \rightarrow p_1, p_2) = \mathcal{A}_\mu^{(0)}(k, -L \rightarrow p_2, p_1),$$
$$\mathcal{A}_\mu^{(1)}(k, -L \rightarrow p_1, p_2) = -\mathcal{A}_\mu^{(1)}(k, -L \rightarrow p_2, p_1), \tag{12}$$

and that the form factors of the pure isospin amplitudes satisfy

$$
\begin{array}{ll}
F^{(0)}(s,t,u) = F^{(0)}(s,u,t), & F^{(1)}(s,t,u) = -F^{(1)}(s,u,t), \\
G^{(0)}(s,t,u) = -G^{(0)}(s,u,t), & G^{(1)}(s,t,u) = G^{(1)}(s,u,t), \\
R^{(0)}(s,t,u) = R^{(0)}(s,u,t), & R^{(1)}(s,t,u) = -R^{(1)}(s,u,t).
\end{array} \tag{13}
$$

2.3.2 t- and u-channel

In the crossed t-channel, we are concerned with the matrix element

$$\mathcal{A}_\mu^{+-} = \langle \pi^-(p_2)|A_\mu(0)|K^+(k)\pi^-(-p_1)\rangle. \tag{14}$$

In the u-channel, we analogously look at

$$\mathcal{A}_\mu^{+-} = \langle \pi^+(p_1)|A_\mu(0)|K^+(k)\pi^+(-p_2)\rangle. \tag{15}$$

Note that, due to crossing, these matrix elements are described by the same function – or its analytic continuation – as the corresponding s-channel matrix element.

The t-channel initial and final states have the isospin decompositions

$$|K^+(k)\pi^-(-p_1)\rangle = \sqrt{\frac{2}{3}}\left|\frac{1}{2}, -\frac{1}{2}\right\rangle + \sqrt{\frac{1}{3}}\left|\frac{3}{2}, -\frac{1}{2}\right\rangle,$$

$$\langle \pi^-(p_2)|A_\mu(0) = \sqrt{\frac{2}{3}}\left\langle\frac{1}{2}, -\frac{1}{2}\right| + \sqrt{\frac{1}{3}}\left\langle\frac{3}{2}, -\frac{1}{2}\right|, \tag{16}$$

whereas in the u-channel, we are concerned with a pure isospin 3/2 scattering:

$$|K^+(k)\pi^+(-p_2)\rangle = \left|\frac{3}{2}, \frac{3}{2}\right\rangle,$$

$$\langle\pi^+(p_1)|A_\mu(0) = \left\langle\frac{3}{2}, \frac{3}{2}\right|. \tag{17}$$

We find the following isospin relation:

$$\mathcal{A}_\mu^{(3/2)}(k, -p_2 \to L, p_1) = \mathcal{A}_\mu^{+-}(k, -L \to p_1, p_2)$$
$$= \frac{2}{3}\mathcal{A}_\mu^{(1/2)}(k, -p_1 \to L, p_2)$$
$$+ \frac{1}{3}\mathcal{A}_\mu^{(3/2)}(k, -p_1 \to L, p_2). \tag{18}$$

Note that the third component of the isospin does not alter the amplitude: just insert an isospin rotation matrix together with its inverse between in- and out-state to rotate the third component.

The amplitude that describes pure isospin 1/2 scattering in the t-channel is then

$$\mathcal{A}_\mu^{(1/2)}(k, -p_1 \to L, p_2) = \frac{3}{2}\mathcal{A}_\mu^{(3/2)}(k, -p_2 \to L, p_1)$$
$$- \frac{1}{2}\mathcal{A}_\mu^{(3/2)}(k, -p_1 \to L, p_2). \tag{19}$$

Defining analogous form factors for the isospin 1/2 amplitude, we find

$$F^{(1/2)}(s, t, u) = \frac{3}{2}F(s, t, u) - \frac{1}{2}F(s, u, t),$$

$$G^{(1/2)}(s, t, u) = \frac{3}{2}G(s, t, u) + \frac{1}{2}G(s, u, t),$$

$$R^{(1/2)}(s, t, u) = \frac{3}{2}R(s, t, u) - \frac{1}{2}R(s, u, t). \tag{20}$$

In the case $s_\ell = 0$, it may be convenient to look at a certain linear combination of the form factors F and G, as we did in [12–14]:

$$F_1 := XF + (u - t)\frac{PL}{2X}G, \tag{21}$$

where $X := \frac{1}{2}\lambda^{1/2}(M_K^2, s, s_\ell)$, $PL := \frac{1}{2}(M_K^2 - s - s_\ell)$ and $\lambda(a, b, c) := a^2 + b^2 + c^2 - 2(ab + bc + ca)$ is the Källén triangle function. We will often use the abbreviations $\lambda_{K\ell}(s) := \lambda(M_K^2, s, s_\ell)$, $\lambda_{K\pi}(t) := \lambda(M_K^2, M_\pi^2, t)$ and $\lambda_{\ell\pi}(t) := \lambda(s_\ell, M_\pi^2, t)$.

Here, too, we can define the corresponding isospin 1/2 form factor:

$$F_1^{(1/2)}(s, t, u) := XF^{(1/2)}(s, t, u) + (u - t)$$
$$\times \frac{PL}{2X}G^{(1/2)}(s, t, u)$$

$$= \frac{3}{2}\left(XF(s, t, u) + (u - t)\frac{PL}{2X}G(s, t, u)\right)$$
$$- \frac{1}{2}\left(XF(s, u, t) + (t - u)\frac{PL}{2X}G(s, u, t)\right)$$
$$= \frac{3}{2}F_1(s, t, u) - \frac{1}{2}F_1(s, u, t). \tag{22}$$

2.4 Unitarity and partial-wave expansion

In this section, we will investigate the unitarity relations in the different channels and work out expansions of the form factors into partial waves with 'nice' properties with respect to unitarity and analyticity: the partial waves shall satisfy Watson's final-state theorem. As we will need analytic continuations of the partial waves, we must also be careful not to introduce kinematic singularities.

The derivation of the partial-wave expansion has been done for the s-channel in [16,17]. We now apply the same method to all channels.

2.4.1 Helicity amplitudes

The quantities that have a simple expansion into partial waves are not the form factors but the helicity amplitudes of the $2 \to 2$ scattering process [18]. However, helicity partial waves contain kinematic singularities. In order to determine them, we use the prescriptions of [19].

We obtain the helicity amplitudes by contracting the axial-vector-current matrix element with the polarisation vectors of the off-shell W boson. In the W rest frame, the polarisation vectors are given by

$$\varepsilon_t^\mu = (1, 0, 0, 0),$$
$$\varepsilon_\pm^\mu = \frac{1}{\sqrt{2}}(0, 0, \pm 1, i),$$
$$\varepsilon_0^\mu = (0, 1, 0, 0). \tag{23}$$

They are eigenvectors of the spin matrices S^2 and S_1, defined by

$$S_1 = \begin{pmatrix} 0 & 0 & 0 & 0 \\ 0 & 0 & 0 & 0 \\ 0 & 0 & 0 & -i \\ 0 & 0 & i & 0 \end{pmatrix}, \quad S_2 = \begin{pmatrix} 0 & 0 & 0 & 0 \\ 0 & 0 & 0 & i \\ 0 & 0 & 0 & 0 \\ 0 & -i & 0 & 0 \end{pmatrix},$$

$$S_3 = \begin{pmatrix} 0 & 0 & 0 & 0 \\ 0 & 0 & -i & 0 \\ 0 & i & 0 & 0 \\ 0 & 0 & 0 & 0 \end{pmatrix}, \tag{24}$$

$$S^2 = S_1^2 + S_2^2 + S_3^2 = \begin{pmatrix} 0 & 0 & 0 & 0 \\ 0 & 2 & 0 & 0 \\ 0 & 0 & 2 & 0 \\ 0 & 0 & 0 & 2 \end{pmatrix}.$$

The eigenvalues $s(s+1)$ and s_1 of S^2 and S_1 are listed below:

	ε_t^μ	$\varepsilon_\pm^\mu$	ε_0^μ
s	0	1	1
s_1	0	± 1	0

If we boost the polarisation vectors into the frame where the W momentum is given by $L = (L^0, L^1, 0, 0)$, $L^2 = s_\ell$, we obtain

$$\varepsilon_t^\mu = \frac{1}{\sqrt{s_\ell}}(L^0, L^1, 0, 0),$$

$$\varepsilon_\pm^\mu = \frac{1}{\sqrt{2}}(0, 0, \pm 1, i),$$

$$\varepsilon_0^\mu = \frac{1}{\sqrt{s_\ell}}(L^1, L^0, 0, 0). \tag{25}$$

The contractions of these basis vectors with $\mathcal{A}_\mu$ give the different helicity amplitudes:

$$\mathcal{A}_i := \mathcal{A}_\mu \varepsilon_i^\mu. \tag{26}$$

We extract the kinematic singularities by applying the recipe of [19, chapter 7.3.5], to these helicity amplitudes.

2.4.2 Partial-wave unitarity in the s-channel

Helicity partial waves   The unitarity relation for the axial-vector current matrix element reads

$$\mathrm{Im}(i\mathcal{A}_i^{(I)}(k, -L \to p_1, p_2))$$
$$= \frac{1}{4} \int \widetilde{\mathrm{d}q_1} \widetilde{\mathrm{d}q_2} (2\pi)^4 \delta^{(4)}(p_1 + p_2 - q_1 - q_2)$$
$$\times \mathcal{T}^{(I)*}(q_1, q_2 \to p_1, p_2) i\mathcal{A}_i^{(I)}(k, -L \to q_1, q_2), \tag{27}$$

where $\widetilde{\mathrm{d}q} := \frac{\mathrm{d}^3 q}{(2\pi)^3 2q^0}$ is the Lorentz-invariant measure and where a symmetry factor $1/2$ for the pions is included. $\mathcal{T}^{(I)}$ denotes the elastic isospin I $\pi\pi$-scattering amplitude. Note that this relation is valid in the physical region and that kinematic singularities have to be removed before an analytic continuation.

We perform the integrals:

$$\mathrm{Im}(i\mathcal{A}_i^{(I)}(k, -L \to p_1, p_2))$$
$$= \frac{1}{16} \frac{1}{(2\pi)^2} \frac{1}{2} \sigma_\pi(s) \int \mathrm{d}\Omega'' \, \mathcal{T}^{(I)*}(s, \cos\theta')$$
$$\times i\mathcal{A}_i^{(I)}(s, \cos\theta'', \phi''), \tag{28}$$

where $\sigma_\pi(s) = \sqrt{1 - 4M_\pi^2/s}$ and of course $\cos\theta'$ has to be understood as a function of $\cos\theta''$ and ϕ'' through the relation

$$\cos\theta' = \sin\theta \sin\theta'' \cos\phi'' + \cos\theta \cos\theta''. \tag{29}$$

If we expand $\mathcal{T}$ and $\mathcal{A}_i$ into appropriate partial waves, we can perform the remaining angular integrals and find the unitarity relations for the $K_{\ell 4}$ partial waves.

We expand the $\pi\pi$-scattering matrix element in the usual way:

$$\mathcal{T}^{(I)}(s, \cos\theta') = \sum_{l=0}^{\infty} P_l(\cos\theta') \, t_l^I(s) \tag{30}$$

with

$$t_l^I(s) = |t_l^I(s)| e^{i\delta_l^I(s)}. \tag{31}$$

The $K_{\ell 4}$ helicity amplitudes are expanded into appropriate Wigner d-functions, which satisfy $d_{00}^{(l)}(\theta) = P_l(\cos\theta)$ and $d_{10}^{(l)}(\theta) = -[l(l+1)]^{-1/2} \sin\theta \, P_l'(\cos\theta)$. We have to take care of the kinematic singularities of the helicity amplitudes [18,19]:

$$i\mathcal{A}_t^{(I)}(s, \cos\theta) = \sum_{l=0}^{\infty} P_l(\cos\theta) \left(\frac{\lambda_{K\ell}^{1/2}(s)\sigma_\pi(s)}{M_K^2} \right)^l a_{t,l}^{(I)}(s),$$

$$i\mathcal{A}_0^{(I)}(s, \cos\theta) = i\tilde{\mathcal{A}}_0^{(I)} \frac{\lambda_{K\ell}^{1/2}(s)}{M_K^2} = \frac{\lambda_{K\ell}^{1/2}(s)}{M_K^2}$$
$$\times \sum_{l=0}^{\infty} P_l(\cos\theta) \left(\frac{\lambda_{K\ell}^{1/2}(s)\sigma_\pi(s)}{M_K^2} \right)^l a_{0,l}^{(I)}(s),$$

$$i\mathcal{A}_2^{(I)}(s, \cos\theta, \phi) = i\tilde{\mathcal{A}}_2^{(I)} \sin\theta$$
$$= \sin\theta \sum_{l=1}^{\infty} P_l'(\cos\theta) \left(\frac{\lambda_{K\ell}^{1/2}(s)\sigma_\pi(s)}{M_K^2} \right)^{l-1} \cos\phi \, a_{2,l}^{(I)}(s), \tag{32}$$

where $\mathcal{A}_2^{(I)} := \mathcal{A}_+^{(I)} - \mathcal{A}_-^{(I)}$. The square roots of the Källén function cancel exactly the square root branch cuts in the Legendre polynomials between $(M_K - \sqrt{s_\ell})^2$ and $(M_K + \sqrt{s_\ell})^2$. The factor M_K^2 in the denominators appears only for dimensional reasons. All the defined partial waves $a_{i,l}^{(I)}$ are free of kinematic singularities and can be used for an analytic continuation from the decay region through the unphysical to the scattering region.

If we insert the partial-wave expansions into the unitarity relation, the remaining angular integrals can be performed and the unitarity relation for the $K_{\ell 4}$ partial waves emerges

$(i = t, 0, 2)$:

$$\text{Im}(a_{i,l}^{(I)}(s)) = \frac{1}{2l+1} \frac{1}{32\pi} \sigma_\pi(s)\, t_l^{I*}(s)\, a_{i,l}^{(I)}(s). \tag{33}$$

In particular, we find that the phases of the $K_{\ell 4}$ s-channel partial waves are given by the elastic $\pi\pi$-scattering phases (this is Watson's theorem) for all s between $4M_\pi^2$ and some inelastic threshold:

$$a_{i,l}^{(I)}(s) = |a_{i,l}^{(I)}(s)| e^{i\delta_l^I(s)}. \tag{34}$$

Partial-wave expansion of the form factors in the s-channel
In order to find the partial-wave expansions of the form factors, we write explicitly the helicity amplitudes (generalised to a generic ϕ):

$$
\begin{aligned}
i\mathcal{A}_t^{(I)} &= i\mathcal{A}_\mu^{(I)} \varepsilon_t^\mu = i\mathcal{A}_\mu^{(I)} \frac{1}{\sqrt{s_\ell}} L^\mu \\
&= \frac{1}{M_K \sqrt{s_\ell}} \left(\frac{1}{2}(M_K^2 - s - s_\ell)\, F^{(I)} \right. \\
&\quad \left. + \frac{1}{2}\sigma_\pi(s)\lambda_{K\ell}^{1/2}(s)\cos\theta\, G^{(I)} + s_\ell\, R^{(I)} \right), \\
i\mathcal{A}_0^{(I)} &= i\mathcal{A}_\mu^{(I)} \varepsilon_0^\mu \\
&= \frac{-1}{M_K \sqrt{s_\ell}} \left(\frac{1}{2}\lambda_{K\ell}^{1/2}(s)\, F^{(I)} \right. \\
&\quad \left. + \frac{1}{2}(M_K^2 - s - s_\ell)\sigma_\pi(s)\cos\theta\, G^{(I)} \right), \\
i\mathcal{A}_2^{(I)} &= i\mathcal{A}_\mu^{(I)} \varepsilon_+^\mu - i\mathcal{A}_\mu^{(I)} \varepsilon_-^\mu \\
&= \frac{-\sqrt{2}}{M_K} \left(\sqrt{s}\sigma_\pi(s)\sin\theta\cos\phi\, G^{(I)} \right).
\end{aligned} \tag{35}
$$

Since the contribution of the form factor R to the decay rate is suppressed by m_ℓ^2, it is invisible in the electron mode and we do not have any data on it. We therefore look only for linear combinations of the form factors F and G that possess a simple partial-wave expansion. We find [16]

$$
\begin{aligned}
& F^{(I)} + \frac{\sigma_\pi(s) P L(s)}{X(s)} \cos\theta\, G^{(I)} \\
&= F^{(I)} + \frac{(M_K^2 - s - s_\ell)(u-t)}{\lambda_{K\ell}(s)} G^{(I)} \\
&= -\frac{2\sqrt{s_\ell}}{M_K} \sum_{l=0}^{\infty} P_l(\cos\theta) \left(\frac{\lambda_{K\ell}^{1/2}(s)\sigma_\pi(s)}{M_K^2} \right)^l a_{0,l}^{(I)}(s), \\
& G^{(I)} = -\frac{M_K}{\sqrt{2s}\sigma_\pi(s)} \sum_{l=1}^{\infty} P_l'(\cos\theta) \\
&\quad \times \left(\frac{\lambda_{K\ell}^{1/2}(s)\sigma_\pi(s)}{M_K^2} \right)^{l-1} a_{2,l}^{(I)}(s).
\end{aligned} \tag{36}
$$

We write the partial-wave expansions of F and G in the form

$$
\begin{aligned}
F^{(I)} &= \sum_{l=0}^{\infty} P_l(\cos\theta) \left(\frac{\lambda_{K\ell}^{1/2}(s)\sigma_\pi(s)}{M_K^2} \right)^l f_l^{(I)}(s) \\
&\quad - \frac{\sigma_\pi P L}{X} \cos\theta\, G^{(I)}, \\
G^{(I)} &= \sum_{l=1}^{\infty} P_l'(\cos\theta) \left(\frac{\lambda_{K\ell}^{1/2}(s)\sigma_\pi(s)}{M_K^2} \right)^{l-1} g_l^{(I)}(s),
\end{aligned} \tag{37}
$$

where the partial waves $f_l^{(I)}$ and $g_l^{(I)}$ satisfy Watson's theorem in the region $s > 4M_\pi^2$:

$$f_l^{(I)}(s) = |f_l^{(I)}(s)| e^{i\delta_l^I(s)}, \quad g_l^{(I)}(s) = |g_l^{(I)}(s)| e^{i\delta_l^I(s)}. \tag{38}$$

2.4.3 Partial-wave unitarity in the t-channel

Helicity partial waves The discussion in the crossed channels is a bit simpler because we are interested in partial-wave expansions only in the region $t > (M_K + M_\pi)^2$ or $u > (M_K + M_\pi)^2$, i.e. above all initial- and final-state thresholds and pseudo-thresholds. Therefore, we do not have to worry about kinematic singularities, since we will not perform analytic continuations into the critical regions.

In the crossed channels, we consider $K\pi$ intermediate states in the unitarity relation:

$$
\begin{aligned}
& \text{Im}(i\mathcal{A}_i^{(1/2)}(k, -p_1 \to L, p_2)) \\
&= \frac{1}{2} \int \widetilde{dq_K}\, \widetilde{dq_\pi}\, (2\pi)^4 \delta^{(4)}(k - p_1 - q_K - q_\pi) \\
&\quad \times \mathcal{T}^{(1/2)*}(q_K, q_\pi \to k, -p_1) i\mathcal{A}_i^{(1/2)}(q_K, q_\pi \to L, p_2),
\end{aligned} \tag{39}
$$

where $\mathcal{T}^{(1/2)}$ is the isospin $1/2$ elastic $K\pi$-scattering amplitude. By performing the integrals we obtain

$$
\begin{aligned}
& \text{Im}(i\mathcal{A}_i^{(1/2)}(k, -p_1 \to L, p_2)) \\
&= \frac{1}{8} \frac{1}{(2\pi)^2} \frac{\lambda_{K\pi}^{1/2}(t)}{2t} \int d\Omega_t'' \, \mathcal{T}^{(1/2)*}(t, \cos\theta_t') \\
&\quad \times i\mathcal{A}_i^{(1/2)}(t, \cos\theta_t'', \phi_t'').
\end{aligned} \tag{40}
$$

The $K\pi$ scattering matrix element is expanded in the usual way:

$$\mathcal{T}^{(1/2)}(t, \cos\theta_t) = \sum_{l=0}^{\infty} P_l(\cos\theta_t) t_l^{1/2}(t) \tag{41}$$

with

$$t_l^{1/2}(t) = |t_l^{1/2}(t)| e^{i\delta_l^{1/2}(t)}. \tag{42}$$

We expand the $K_{\ell 4}$ helicity amplitudes as follows:

$$
\begin{aligned}
&i\mathcal{A}_t^{(1/2)}(t, \cos\theta_t) \\
&= \sum_{l=0}^{\infty} P_l(\cos\theta_t) \left(\frac{\lambda_{K\pi}^{1/2}(t)\lambda_{\ell\pi}^{1/2}(t)}{M_K^4}\right)^l a_{t,l}^{(1/2)}(t), \\
&i\mathcal{A}_0^{(1/2)}(t, \cos\theta_t) \\
&= \sum_{l=0}^{\infty} P_l(\cos\theta_t) \left(\frac{\lambda_{K\pi}^{1/2}(t)\lambda_{\ell\pi}^{1/2}(t)}{M_K^4}\right)^l a_{0,l}^{(1/2)}(t), \\
&i\mathcal{A}_2^{(1/2)}(t, \cos\theta_t, \phi_t) \\
&= i\mathcal{A}_+^{(1/2)}(t, \cos\theta_t, \phi_t) - i\mathcal{A}_-^{(1/2)}(t, \cos\theta_t, \phi_t) \\
&= \sin\theta_t \cos\phi_t \sum_{l=1}^{\infty} P_l'(\cos\theta_t) \left(\frac{\lambda_{K\pi}^{1/2}(t)\lambda_{\ell\pi}^{1/2}(t)}{M_K^4}\right)^{l-1} a_{2,l}^{(1/2)}(t).
\end{aligned}
\tag{43}
$$

By inserting these expansions into the unitarity relation (40), we find that all the partial waves satisfy Watson's theorem ($i = t, 0, 2$):

$$
\begin{aligned}
&\mathrm{Im}(a_{i,l}^{(1/2)}(t)) = \frac{1}{2l+1}\frac{1}{16\pi}\frac{\lambda_{K\pi}^{1/2}(t)}{t} t_l^{1/2*}(t)a_{i,l}^{(1/2)}(t), \\
&a_{i,l}^{(1/2)}(t) = |a_{i,l}^{(1/2)}(t)|e^{i\delta_l^{1/2}(t)}.
\end{aligned}
\tag{44}
$$

Partial-wave expansion of the form factors in the t-channel
By contracting the axial-vector current matrix element in the t-channel with the polarisation vectors, we find the helicity amplitudes (for a generic ϕ_t). As we are not interested in R, we do not need the $\mathcal{A}_t^{(1/2)}$ component:

$$
\begin{aligned}
i\mathcal{A}_0^{(1/2)} &= i\mathcal{A}_\mu^{(1/2)}\varepsilon_0^\mu = \frac{-1}{M_K\sqrt{s_\ell}} \\
&\times \left(\frac{1}{4t}(\lambda_{K\pi}^{1/2}(t)(M_\pi^2 - s_\ell - t)\cos\theta_t \right. \\
&\quad + \lambda_{\ell\pi}^{1/2}(t)(M_K^2 - M_\pi^2 + t))F^{(1/2)} \\
&\quad + \frac{1}{4t}(\lambda_{K\pi}^{1/2}(t)(M_\pi^2 - s_\ell - t)\cos\theta_t \\
&\quad \left. + \lambda_{\ell\pi}^{1/2}(t)(M_K^2 - M_\pi^2 - 3t))G^{(1/2)}\right), \\
i\mathcal{A}_2^{(1/2)} &= i\mathcal{A}_\mu^{(1/2)}\varepsilon_+^\mu - i\mathcal{A}_\mu^{(1/2)}\varepsilon_-^\mu \\
&= \frac{1}{\sqrt{2}M_K}\left(\frac{\lambda_{K\pi}^{1/2}(t)}{\sqrt{t}}\sin\theta_t\cos\phi_t\,(F^{(1/2)}+G^{(1/2)})\right).
\end{aligned}
\tag{45}
$$

This results in the following partial-wave expansions of the form factors:

$$
\begin{aligned}
F^{(1/2)} &= \sum_{l=0}^{\infty} P_l(\cos\theta_t)\left(\frac{\lambda_{K\pi}^{1/2}(t)\lambda_{\ell\pi}^{1/2}(t)}{M_K^4}\right)^l f_l^{(1/2)}(t) \\
&\quad -\frac{1}{2t}\left(M_K^2 - M_\pi^2 - 3t + (M_\pi^2 - s_\ell - t)\frac{\lambda_{K\pi}^{1/2}(t)}{\lambda_{\ell\pi}^{1/2}(t)}\cos\theta_t\right) \\
&\quad \times \sum_{l=1}^{\infty} P_l'(\cos\theta_t)\left(\frac{\lambda_{K\pi}^{1/2}(t)\lambda_{\ell\pi}^{1/2}(t)}{M_K^4}\right)^{l-1} g_l^{(1/2)}(t), \\
G^{(1/2)} &= -\sum_{l=0}^{\infty} P_l(\cos\theta_t)\left(\frac{\lambda_{K\pi}^{1/2}(t)\lambda_{\ell\pi}^{1/2}(t)}{M_K^4}\right)^l f_l^{(1/2)}(t) \\
&\quad +\frac{1}{2t}\left(M_K^2 - M_\pi^2 + t + (M_\pi^2 - s_\ell - t)\frac{\lambda_{K\pi}^{1/2}(t)}{\lambda_{\ell\pi}^{1/2}(t)}\cos\theta_t\right) \\
&\quad \times \sum_{l=1}^{\infty} P_l'(\cos\theta_t)\left(\frac{\lambda_{K\pi}^{1/2}(t)\lambda_{\ell\pi}^{1/2}(t)}{M_K^4}\right)^{l-1} g_l^{(1/2)}(t),
\end{aligned}
\tag{46}
$$

where also the new partial waves $f_l^{(1/2)}$ and $g_l^{(1/2)}$ satisfy Watson's theorem in the region $t > (M_K + M_\pi)^2$:

$$
\begin{aligned}
f_l^{(1/2)}(t) &= |f_l^{(1/2)}(t)|e^{i\delta_l^{1/2}(t)}, \\
g_l^{(1/2)}(t) &= |g_l^{(1/2)}(t)|e^{i\delta_l^{1/2}(t)}.
\end{aligned}
\tag{47}
$$

2.4.4 Partial-wave unitarity in the u-channel

Helicity partial waves   The u-channel (i.e. the isospin 3/2 case) can be treated in complete analogy to the t-channel. We start with the unitarity relation:

$$
\begin{aligned}
&\mathrm{Im}(i\mathcal{A}_i^{(3/2)}(k, -p_2 \to L, p_1)) \\
&= \frac{1}{2}\int \widetilde{dq_K}\,\widetilde{dq_\pi}(2\pi)^4\delta^{(4)}(k - p_2 - q_K - q_\pi) \\
&\quad \times \mathcal{T}^{(3/2)*}(q_K, q_\pi \to k, -p_2)\,i\mathcal{A}_i^{(3/2)}(q_K, q_\pi \to L, p_1) \\
&= \frac{1}{8}\frac{1}{(2\pi)^2}\frac{\lambda_{K\pi}^{1/2}(u)}{2u} \\
&\quad \times \int d\Omega_u''\,\mathcal{T}^{(3/2)*}(u, \cos\theta_u')\,i\mathcal{A}_i^{(3/2)}(u, \cos\theta_u'', \phi_u'').
\end{aligned}
\tag{48}
$$

The $K\pi$-scattering matrix element is expanded as

$$
\begin{aligned}
\mathcal{T}^{(3/2)}(u, \cos\theta_u) &= \sum_{l=0}^{\infty} P_l(\cos\theta_u)t_l^{3/2}(u), \\
t_l^{3/2}(u) &= |t_l^{3/2}(u)|e^{i\delta_l^{3/2}(u)}
\end{aligned}
\tag{49}
$$

and the $K_{\ell 4}$ helicity amplitudes according to

$$
i\mathcal{A}_t^{(3/2)}(u,\cos\theta_u)
$$
$$
= \sum_{l=0}^{\infty} P_l(\cos\theta_u)\left(\frac{\lambda_{K\pi}^{1/2}(u)\lambda_{\ell\pi}^{1/2}(u)}{M_K^4}\right)^l a_{t,l}^{(3/2)}(u),
$$
$$
i\mathcal{A}_0^{(3/2)}(u,\cos\theta_u)
$$
$$
= \sum_{l=0}^{\infty} P_l(\cos\theta_u)\left(\frac{\lambda_{K\pi}^{1/2}(u)\lambda_{\ell\pi}^{1/2}(u)}{M_K^4}\right)^l a_{0,l}^{(3/2)}(u),
$$
$$
i\mathcal{A}_2^{(3/2)}(u,\cos\theta_u,\phi_u)
$$
$$
= i\mathcal{A}_+^{(3/2)}(u,\cos\theta_u,\phi_u) - i\mathcal{A}_-^{(3/2)}(u,\cos\theta_u,\phi_u)
$$
$$
= \sin\theta_u\cos\phi_u\sum_{l=1}^{\infty} P_l'(\cos\theta_u)
$$
$$
\times \left(\frac{\lambda_{K\pi}^{1/2}(u)\lambda_{\ell\pi}^{1/2}(u)}{M_K^4}\right)^{l-1} a_{2,l}^{(3/2)}(u). \tag{50}
$$

Performing the angular integrals in the unitarity relation, we find that the partial waves satisfy Watson's theorem ($i = t, 0, 2$):

$$
\mathrm{Im}(a_{i,l}^{(3/2)}(u)) = \frac{1}{2l+1}\frac{1}{16\pi}\frac{\lambda_{K\pi}^{1/2}(u)}{u}\, t_l^{3/2*}(u)a_{i,l}^{(3/2)}(u),
$$
$$
a_{i,l}^{(3/2)}(u) = |a_{i,l}^{(3/2)}(u)|e^{i\delta_l^{3/2}(u)}. \tag{51}
$$

Partial-wave expansion of the form factors in the u-channel

The contraction of the axial-vector current matrix element with the polarisation vectors yields

$$
i\mathcal{A}_0^{(3/2)} = i\mathcal{A}_\mu^{(3/2)}\varepsilon_0^\mu = \frac{-1}{M_K\sqrt{s_\ell}}
$$
$$
\times\left(\frac{1}{4u}(\lambda_{K\pi}^{1/2}(u)(M_\pi^2 - s_\ell - u)\cos\theta_u \right.
$$
$$
+ \lambda_{\ell\pi}^{1/2}(u)(M_K^2 - M_\pi^2 + u))F
$$
$$
- \frac{1}{4u}(\lambda_{K\pi}^{1/2}(u)(M_\pi^2 - s_\ell - u)\cos\theta_u
$$
$$
\left. + \lambda_{\ell\pi}^{1/2}(u)(M_K^2 - M_\pi^2 - 3u))G\right),
$$
$$
i\mathcal{A}_2^{(3/2)} = i\mathcal{A}_\mu^{(3/2)}\varepsilon_+^\mu - i\mathcal{A}_\mu^{(3/2)}\varepsilon_-^\mu
$$
$$
= \frac{1}{\sqrt{2}M_K}\left(\frac{\lambda_{K\pi}^{1/2}(u)}{\sqrt{u}}\sin\theta_u\cos\phi_u(F-G)\right). \tag{52}
$$

Hence, the partial-wave expansion of the form factors is given by

$$
F = \sum_{l=0}^{\infty} P_l(\cos\theta_u)\left(\frac{\lambda_{K\pi}^{1/2}(u)\lambda_{\ell\pi}^{1/2}(u)}{M_K^4}\right)^l f_l^{(3/2)}(u)
$$
$$
- \frac{1}{2u}\left(M_K^2 - M_\pi^2 - 3u + (M_\pi^2 - s_\ell - u)\frac{\lambda_{K\pi}^{1/2}(u)}{\lambda_{\ell\pi}^{1/2}(u)}\cos\theta_u\right)
$$

$$
\times \sum_{l=1}^{\infty} P_l'(\cos\theta_u)\left(\frac{\lambda_{K\pi}^{1/2}(u)\lambda_{\ell\pi}^{1/2}(u)}{M_K^4}\right)^{l-1} g_l^{(3/2)}(u),
$$
$$
G = \sum_{l=0}^{\infty} P_l(\cos\theta_u)\left(\frac{\lambda_{K\pi}^{1/2}(u)\lambda_{\ell\pi}^{1/2}(u)}{M_K^4}\right)^l f_l^{(3/2)}(u)
$$
$$
- \frac{1}{2u}\left(M_K^2 - M_\pi^2 + u + (M_\pi^2 - s_\ell - u)\frac{\lambda_{K\pi}^{1/2}(u)}{\lambda_{\ell\pi}^{1/2}(u)}\cos\theta_u\right)
$$
$$
\times \sum_{l=1}^{\infty} P_l'(\cos\theta_u)\left(\frac{\lambda_{K\pi}^{1/2}(u)\lambda_{\ell\pi}^{1/2}(u)}{M_K^4}\right)^{l-1} g_l^{(3/2)}(u), \tag{53}
$$

where the partial waves $f_l^{(3/2)}$ and $g_l^{(3/2)}$ satisfy Watson's theorem in the region $u > (M_K + M_\pi)^2$:

$$
f_l^{(3/2)}(u) = |f_l^{(3/2)}(u)|e^{i\delta_l^{3/2}(u)},
$$
$$
g_l^{(3/2)}(u) = |g_l^{(3/2)}(u)|e^{i\delta_l^{3/2}(u)}. \tag{54}
$$

2.4.5 Projection and analytic structure of the partial waves

The several partial waves $f_l^{(I)}$ and $g_l^{(I)}$ can be calculated by angular projections:

$$
f_l^{(I)}(s) = \left(\frac{M_K^2}{\lambda_{K\ell}^{1/2}(s)\sigma_\pi(s)}\right)^l \frac{2l+1}{2}
$$
$$
\times \int_{-1}^{1} dz\, P_l(z)\left(F^{(I)}(s,z) + \frac{\sigma_\pi(s)PL(s)}{X(s)}zG^{(I)}(s,z)\right),
$$
$$
g_l^{(I)}(s) = \left(\frac{M_K^2}{\lambda_{K\ell}^{1/2}(s)\sigma_\pi(s)}\right)^{l-1}
$$
$$
\times \int_{-1}^{1} dz\,\frac{P_{l-1}(z) - P_{l+1}(z)}{2}G^{(I)}(s,z), \tag{55}
$$

where $X^{(I)}(s,z) := X^{(I)}(s,t(s,z),u(s,z))$, $X \in \{F,G\}$, $I \in \{0,1\}$ and

$$
t(s,z) = \frac{1}{2}(\Sigma_0 - s - 2X\sigma_\pi z),
$$
$$
u(s,z) = \frac{1}{2}(\Sigma_0 - s + 2X\sigma_\pi z). \tag{56}
$$

Since $t(s,-z) = u(s,z)$, the definition of the pure isospin form factors (11) implies

$$
f_l^{(0)}(s) = g_l^{(0)}(s) = 0 \quad \forall\ l\ \text{odd},
$$
$$
f_l^{(1)}(s) = g_l^{(1)}(s) = 0 \quad \forall\ l\ \text{even}. \tag{57}
$$

Hence, we can as well directly use the partial waves of the physical form factors:

$$
f_l(s) = \left(\frac{M_K^2}{\lambda_{K\ell}^{1/2}(s)\sigma_\pi(s)}\right)^l \frac{2l+1}{2}
$$
$$
\times \int_{-1}^{1} dz\, P_l(z)\left(F(s,z) + \frac{\sigma_\pi(s)PL(s)}{X(s)} z G(s,z)\right),
$$
$$
g_l(s) = \left(\frac{M_K^2}{\lambda_{K\ell}^{1/2}(s)\sigma_\pi(s)}\right)^{l-1} \int_{-1}^{1} dz\, \frac{P_{l-1}(z)-P_{l+1}(z)}{2} G(s,z),
$$
(58)

which still fulfil Watson's theorem,

$$
f_l(s) = |f_l(s)|e^{i\delta_l^I(s)}, \quad g_l(s) = |g_l(s)|e^{i\delta_l^I(s)},
$$
(59)

where $I = (l \mod 2)$.

In the crossed channels, the partial wave projections are given by

$$
f_l^{(1/2)}(t) = \left(\frac{M_K^4}{\lambda_{K\pi}^{1/2}(t)\lambda_{\ell\pi}^{1/2}(t)}\right)^l \frac{2l+1}{2}
$$
$$
\times \int_{-1}^{1} dz_t\, P_l(z_t)\left(\frac{F^{(1/2)}(t,z_t) - G^{(1/2)}(t,z_t)}{2}\right.
$$
$$
+ \frac{1}{2t}\left(M_K^2 - M_\pi^2 - t + (M_\pi^2 - s_\ell - t)\frac{\lambda_{K\pi}^{1/2}(t)}{\lambda_{\ell\pi}^{1/2}(t)}z_t\right)
$$
$$
\left. \times \frac{F^{(1/2)}(t,z_t) + G^{(1/2)}(t,z_t)}{2}\right),
$$
$$
g_l^{(1/2)}(t) = \left(\frac{M_K^4}{\lambda_{K\pi}^{1/2}(t)\lambda_{\ell\pi}^{1/2}(t)}\right)^{l-1}
$$
$$
\times \int_{-1}^{1} dz_t\, \frac{P_{l-1}(z_t)-P_{l+1}(z_t)}{2}\frac{F^{(1/2)}(t,z_t)+G^{(1/2)}(t,z_t)}{2},
$$
$$
f_l^{(3/2)}(u) = \left(\frac{M_K^4}{\lambda_{K\pi}^{1/2}(u)\lambda_{\ell\pi}^{1/2}(u)}\right)^l \frac{2l+1}{2}
$$
$$
\times \int_{-1}^{1} dz_u\, P_l(z_u)\left(\frac{F(u,z_u) + G(u,z_u)}{2}\right.
$$
$$
+ \frac{1}{2u}\left(M_K^2 - M_\pi^2 - u + (M_\pi^2 - s_\ell - u)\frac{\lambda_{K\pi}^{1/2}(u)}{\lambda_{\ell\pi}^{1/2}(u)}z_u\right)
$$
$$
\left. \times \frac{F(u,z_u) - G(u,z_u)}{2}\right),
$$
$$
g_l^{(3/2)}(u) = \left(\frac{M_K^4}{\lambda_{K\pi}^{1/2}(u)\lambda_{\ell\pi}^{1/2}(u)}\right)^{l-1}
$$
$$
\times \int_{-1}^{1} dz_u\, \frac{P_{l-1}(z_u)-P_{l+1}(z_u)}{2}\frac{F(u,z_u) - G(u,z_u)}{2},
$$
(60)

where $X^{(I)}(t,z_t) := X^{(I)}(s(t,z_t),t,u(t,z_t))$, $X^{(I)}(u,z_u) := X^{(I)}(s(u,z_u),t(u,z_u),u)$, $X \in \{F,G\}$ and

$$
s(t,z_t) = \frac{1}{2}\left(\Sigma_0 - t + \frac{1}{t}(z_t\,\lambda_{K\pi}^{1/2}(t)\lambda_{\ell\pi}^{1/2}(t) - \Delta_{K\pi}\Delta_{\ell\pi})\right),
$$
$$
u(t,z_t) = \frac{1}{2}\left(\Sigma_0 - t - \frac{1}{t}(z_t\,\lambda_{K\pi}^{1/2}(t)\lambda_{\ell\pi}^{1/2}(t) - \Delta_{K\pi}\Delta_{\ell\pi})\right),
$$
$$
s(u,z_u) = \frac{1}{2}\left(\Sigma_0 - u + \frac{1}{u}(z_u\,\lambda_{K\pi}^{1/2}(u)\lambda_{\ell\pi}^{1/2}(u) - \Delta_{K\pi}\Delta_{\ell\pi})\right),
$$
$$
t(u,z_u) = \frac{1}{2}\left(\Sigma_0 - u - \frac{1}{u}(z_u\,\lambda_{K\pi}^{1/2}(u)\lambda_{\ell\pi}^{1/2}(u) - \Delta_{K\pi}\Delta_{\ell\pi})\right).
$$
(61)

The construction of the partial waves has been done in a way that excludes kinematic singularities for $s > 4M_\pi^2$ and $t, u > (M_K + M_\pi)^2$. There may still be kinematic singularities present below these regions, but they do not bother us. But also the analytic structure of the partial waves with respect to dynamic singularities is not trivial.

For the s-channel partial waves, there is of course the right-hand cut at $s > 4M_\pi^2$. Further cuts can appear through the angular integration, i.e. at points where the integration contour in the t- or u-plane touches the crossed channel cuts. If s lies in the physical decay region, the integration path is just a horizontal line from one end of the decay region to the other (see the Mandelstam diagram in Fig. 2). When we continue analytically into the region $(M_K - \sqrt{s_\ell})^2 < s < (M_K + \sqrt{s_\ell})^2$, the integration path moves into the complex t- and u-plane and crosses the real Mandelstam plane at $t = u$: the square root of the Källén function $X = \frac{1}{2}\lambda_{K\ell}^{1/2}(s)$ is purely imaginary in this region. One has to know which branch of the square root should be taken. The correct sign is found by taking s real and shifting $M_K \to M_K + i\epsilon$ (see [20]). With this prescription, the Källén function turns counterclockwise around $\lambda_{K\ell} = 0$ when s runs from $s < (M_K - \sqrt{s_\ell})^2$ to $s > (M_K + \sqrt{s_\ell})^2$. The square root of the Källén function therefore takes the following values:

$$
\lambda_{K\ell}^{1/2}(s)
$$
$$
= \begin{cases} +|\lambda_{K\ell}^{1/2}(s)|, & s < (M_K - \sqrt{s_\ell})^2, \\ +i|\lambda_{K\ell}^{1/2}(s)|, & (M_K - \sqrt{s_\ell})^2 < s < (M_K + \sqrt{s_\ell})^2, \\ -|\lambda_{K\ell}^{1/2}(s)|, & (M_K + \sqrt{s_\ell})^2 < s. \end{cases}
$$
(62)

In the region $s > (M_K + \sqrt{s_\ell})^2$, the integration path again lies in the real Mandelstam plane from one to the other end of the scattering region.

As we are away from the t- and u-channel unitarity cuts at $t, u > (M_K + M_\pi)^2$, this extension of the integration path

into the complex t- and u-plane is the only subtlety that has to be taken into account.

In the region $s < 4M_\pi^2$, there is a left-hand cut at $s \in (-\infty, 0)$: the integration path extends again into the complex t- and u-plane in the region $0 < s < 4M_\pi^2$ (due to the second square root). It diverges at $s = 0$ and returns to the real axis at $s < 0$, but this time it touches the t- and u-channel unitarity cuts at $t, u > (M_K + M_\pi)^2$, which produces the left-hand cut of the s-channel partial waves.

This left-hand cut can be most easily found by looking at the end-points of the integration paths: solving the equation

$$t_\pm = u_\mp = \frac{1}{2}(\Sigma_0 - s \mp 2X(s)\sigma_\pi(s)) \tag{63}$$

for $t_\pm > (M_K + M_\pi)^2$ gives the left-hand cut $s \in (-\infty, 0)$.

Let us consider the crossed t-channel (the situation in the u-channel is analogous). We have defined the partial-wave expansion in the scattering region $t > (M_K + M_\pi)^2$. Therefore, we also define the square root branches of the Källén functions $\lambda_{K\pi}^{1/2}$ and $\lambda_{\ell\pi}^{1/2}$ in this region. The sign of the square root branch can be absorbed into the definition of the partial waves.

The right-hand t-channel unitarity cut at $t > (M_K + M_\pi)^2$ also shows up in the partial waves. A second possibility for singularities in the t-channel partial waves arises when the integration path touches the s- or u-channel unitarity cuts. For $t > (M_K + M_\pi)^2$, the integration path lies on the negative real axis of the s- and u-planes (this can be seen in the Mandelstam diagram in Fig. 2). In the region $(M_K - M_\pi)^2 < t < (M_K + M_\pi)^2$, the integration path extends into the complex s- and u-plane. For the value of t fulfilling $\frac{1}{2}\left(\Sigma_0 - t - \frac{1}{t}\Delta_{K\pi}\Delta_{\ell\pi}\right) = 4M_\pi^2$, the integration path in the s-plane touches the s-channel branch cut. From this point on towards smaller values of t, the integration path has to be deformed in the s-plane. Since the u-channel cut appears only at $u > (M_K + M_\pi)^2$, such a deformation is not needed in the u-plane. At $t = (M_K - M_\pi)^2$, the integration path in the s-plane has then the shape of a horseshoe wrapped around the s-channel cut. For even smaller values of t, the path unwraps itself in a continuous way, such that for $t < \frac{1}{2}(M_K^2 - 2M_\pi^2 + s_\ell)$, the integration path lies completely on the upper side of the s-channel cut.

The cut structure in the t-channel partial wave is rather complicated, at least for $s_\ell > 0$: The left-hand cuts can be found by solving the equations

$$s_\pm = \frac{1}{2}\left(\Sigma_0 - t + \frac{1}{t}(\pm \lambda_{K\pi}^{1/2}(t)\lambda_{\ell\pi}^{1/2}(t) - \Delta_{K\pi}\Delta_{\ell\pi})\right),$$
$$u_\pm = \frac{1}{2}\left(\Sigma_0 - t - \frac{1}{t}(\pm \lambda_{K\pi}^{1/2}(t)\lambda_{\ell\pi}^{1/2}(t) - \Delta_{K\pi}\Delta_{\ell\pi})\right), \tag{64}$$
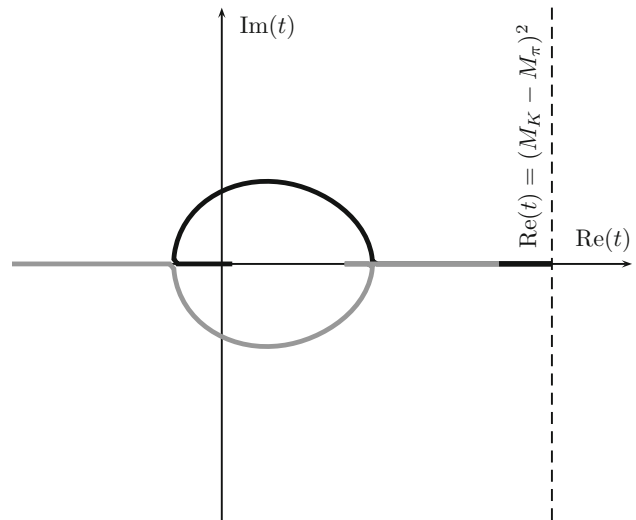
Fig. 3 The left-hand cut of the t-channel partial waves ($s_\ell = 0.3M_\pi^2$)

for $s_\pm > 4M_\pi^2$ and $u_\pm > (M_K + M_\pi)^2$. While the second equation results in a cut along the real axis, the first equation produces an egg-shaped cut structure in the complex t-plane with $\mathrm{Re}(t) < (M_K - M_\pi)^2$, shown in Fig. 3. The exact shape depends on the value of s_ℓ.

2.4.6 Simplifications for $s_\ell \to 0$

In the experiment, a dependence on s_ℓ has been observed only in the first partial wave of the form factor F [6,9]. If we neglect this dependence on s_ℓ and assume that $s_\ell = 0$, the treatment can be significantly simplified.

- The square root of the Källén function simplifies to

$$\lim_{s_\ell \to 0} \lambda_{K\ell}^{1/2}(s) = M_K^2 - s,$$

 the square root branch cut disappears. Hence, the integration path for the angular integrals in the s-channel always lies on the real axis.
- The left-hand cut structure of t- and u-channel partial waves simplifies to a straight line along the real axis. The egg-shaped branch cuts disappear in the limit $s_\ell \to 0$.
- From (37), we see that the quantity

$$\lim_{s_\ell \to 0} F_1^{(I)} = \lim_{s_\ell \to 0} \left(\frac{1}{2}\lambda_{K\ell}^{1/2}(s)F^{(I)}\right.$$
$$\left. + \frac{1}{2}\frac{(M_K^2 - s - s_\ell)(u - t)}{\lambda_{K\ell}^{1/2}(s)}G^{(I)}\right)$$
$$= \frac{M_K^2 - s}{2}F^{(I)} + \frac{u - t}{2}G^{(I)} \tag{65}$$

has a simple s-channel partial-wave expansion into Legendre polynomials. If we consider (46) in the limit $s_\ell \to 0$, we find that exactly the same linear combination of the form factors $F^{(1/2)}$ and $G^{(1/2)}$ has a simple t-channel partial-wave expansion into Legendre polynomials. The same follows from (53) for the u-channel. In this limit, the form factor F_1 can therefore be treated independently from the other form factors. This is the procedure that has been followed in [12–14].

There are several reasons why we abstain here from taking the limit $s_\ell \to 0$, which would result in a substantial simplification of the whole treatment. The experiments provide data on both form factors F and G. In order to include all the available information, we deal with both form factors at the same time. There is also some data available on the dependence on s_ℓ, which we include in this treatment. Finally, the matching to χPT becomes much cleaner if it is performed with F and G directly, since these are the form factors with the simplest chiral representation.

2.5 Reconstruction theorem

Since the form factors F and G describe a hadronic four-'particle' process, they depend on the three Mandelstam variables s, t and u and therefore possess a rather complicated analytic structure. However, it is possible to decompose the form factors into a sum of functions that depend only on a single Mandelstam variable. Such a decomposition provides a major simplification of the problem and leads to a powerful dispersive description. This procedure is known under the name of 'reconstruction theorem' and was first applied to $\pi\pi$-scattering [21]. For $K\pi$ scattering, it was generalised to the case of unequal masses in [22]. In [23], it was formulated for a general $2 \to 2$ scattering process of the pseudoscalar octet mesons. We presented its first application to a $K_{\ell 4}$ form factor in [12–14]. In [24], it was again used for the $K_{\ell 4}$ form factors in order to study isospin-breaking effects in the phases at two loops in a dispersive framework.

2.5.1 Decomposition of the form factors

The explicit derivation of the decomposition of the form factors F and G into functions of a single Mandelstam variable can be found in [15]. It is based on fixed-s, fixed-t and fixed-u dispersion relations. We have to assume a certain asymptotic behaviour of the form factors, e.g. for fixed u, we assume

$$\lim_{|s| \to \infty} \frac{X_s^u(s)}{s^n} = \lim_{|t| \to \infty} \frac{X_t^u(t)}{t^n} = 0, \qquad (66)$$

where the Froissart bound [25] suggests $n = 2$. However, we are also interested in the case $n = 3$ in order to meet the asymptotic behaviour of the NNLO χPT form factors. We therefore write down either a twice- or thrice-subtracted dispersion relation for the form factors. Then we use the partial-wave expansions derived in the previous section. We neglect the imaginary parts of D- and higher waves, an approximation that is violated only at $\mathcal{O}(p^8)$ in the chiral power counting. It implements the case $s_\ell \neq 0$.

The result of the decomposition is the following:

$$F(s, t, u) = M_0(s) + \frac{u - t}{M_K^2} M_1(s)$$
$$+ \frac{2}{3} N_0(t) + \frac{2}{3} \frac{t(s - u) + \Delta_{K\pi}\Delta_{\ell\pi}}{M_K^4} N_1(t) - \frac{2}{3} \frac{\Delta_{K\pi} - 3t}{2M_K^2} \tilde{N}_1(t)$$
$$+ \frac{1}{3} R_0(t) + \frac{1}{3} \frac{t(s - u) + \Delta_{K\pi}\Delta_{\ell\pi}}{M_K^4} R_1(t) - \frac{1}{3} \frac{\Delta_{K\pi} - 3t}{2M_K^2} \tilde{R}_1(t)$$
$$+ R_0(u) + \frac{u(s - t) + \Delta_{K\pi}\Delta_{\ell\pi}}{M_K^4} R_1(u) - \frac{\Delta_{K\pi} - 3u}{2M_K^2} \tilde{R}_1(u)$$
$$+ \mathcal{O}(p^8),$$

$$G(s, t, u) = \tilde{M}_1(s)$$
$$- \frac{2}{3} N_0(t) - \frac{2}{3} \frac{t(s - u) + \Delta_{K\pi}\Delta_{\ell\pi}}{M_K^4} N_1(t) + \frac{2}{3} \frac{\Delta_{K\pi} + t}{2M_K^2} \tilde{N}_1(t)$$
$$- \frac{1}{3} R_0(t) - \frac{1}{3} \frac{t(s - u) + \Delta_{K\pi}\Delta_{\ell\pi}}{M_K^4} R_1(t) + \frac{1}{3} \frac{\Delta_{K\pi} + t}{2M_K^2} \tilde{R}_1(t)$$
$$+ R_0(u) + \frac{u(s - t) + \Delta_{K\pi}\Delta_{\ell\pi}}{M_K^4} R_1(u) - \frac{\Delta_{K\pi} + u}{2M_K^2} \tilde{R}_1(u)$$
$$+ \mathcal{O}(p^8). \qquad (67)$$

In the case $n = 2$, the various functions of one variable are given by

$$M_0(s) = m_0^0 + m_0^1 \frac{s}{M_K^2} + \frac{s^2}{\pi} \int_{s_0}^\infty \frac{\mathrm{Im} f_0(s')}{(s' - s - i\epsilon)s'^2} \mathrm{d}s',$$

$$M_1(s) = m_1^0 + \frac{s}{\pi} \int_{s_0}^\infty \frac{1}{(s' - s - i\epsilon)s'}$$
$$\times \mathrm{Im}\left(f_1(s') - \frac{2PL(s')M_K^2}{\lambda_{K\ell}(s')} g_1(s')\right) \mathrm{d}s',$$

$$\tilde{M}_1(s) = \tilde{m}_1^0 + \tilde{m}_1^1 \frac{s}{M_K^2} + \frac{s^2}{\pi} \int_{s_0}^\infty \frac{\mathrm{Im} g_1(s')}{(s' - s - i\epsilon)s'^2} \mathrm{d}s',$$

$$N_0(t) = n_0^1 \frac{t}{M_K^2} + \frac{t^2}{\pi} \int_{t_0}^\infty \frac{\mathrm{Im} f_0^{(1/2)}(t')}{(t' - t - i\epsilon)t'^2} \mathrm{d}t',$$

$$N_1(t) = \frac{1}{\pi} \int_{t_0}^\infty \frac{1}{t' - t - i\epsilon}$$
$$\times \mathrm{Im}\left(f_1^{(1/2)}(t') + \frac{(\Delta_{\ell\pi} + t')M_K^4}{2t'\lambda_{\ell\pi}(t')} g_1^{(1/2)}(t')\right) \mathrm{d}t',$$

$$\tilde{N}_1(t) = \frac{t}{\pi} \int_{t_0}^{\infty} \frac{M_K^2}{t'} \frac{\mathrm{Im}\, g_1^{(1/2)}(t')}{(t'-t-i\epsilon)t'} dt',$$

$$R_0(t) = \frac{t^2}{\pi} \int_{t_0}^{\infty} \frac{\mathrm{Im}\, f_0^{(3/2)}(t')}{(t'-t-i\epsilon)t'^2} dt',$$

$$R_1(t) = \frac{1}{\pi} \int_{t_0}^{\infty} \frac{1}{t'-t-i\epsilon}$$
$$\times \mathrm{Im}\left(f_1^{(3/2)}(t') + \frac{(\Delta_{\ell\pi} + t')M_K^4}{2t'\lambda_{\ell\pi}(t')} g_1^{(3/2)}(t') \right) dt',$$

$$\tilde{R}_1(t) = \frac{t}{\pi} \int_{t_0}^{\infty} \frac{M_K^2}{t'} \frac{\mathrm{Im}\, g_1^{(3/2)}(t')}{(t'-t-i\epsilon)t'} dt', \tag{68}$$

while for $n = 3$, the functions of one variable are

$$M_0(s) = m_0^0 + m_0^1 \frac{s}{M_K^2} + m_0^2 \frac{s^2}{M_K^4}$$
$$+ \frac{s^3}{\pi} \int_{s_0}^{\infty} \frac{\mathrm{Im}\, f_0(s')}{(s'-s-i\epsilon)s'^3} ds',$$

$$M_1(s) = m_1^0 + m_1^1 \frac{s}{M_K^2} + \frac{s^2}{\pi} \int_{s_0}^{\infty} \frac{1}{(s'-s-i\epsilon)s'^2}$$
$$\times \mathrm{Im}\left(f_1(s') - \frac{2PL(s')M_K^2}{\lambda_{K\ell}(s')} g_1(s') \right) ds',$$

$$\tilde{M}_1(s) = \tilde{m}_1^0 + \tilde{m}_1^1 \frac{s}{M_K^2} + \tilde{m}_1^2 \frac{s^2}{M_K^4}$$
$$+ \frac{s^3}{\pi} \int_{s_0}^{\infty} \frac{\mathrm{Im}\, g_1(s')}{(s'-s-i\epsilon)s'^3} ds',$$

$$N_0(t) = n_0^1 \frac{t}{M_K^2} + n_0^2 \frac{t^2}{M_K^4} + \frac{t^3}{\pi} \int_{t_0}^{\infty} \frac{\mathrm{Im}\, f_0^{(1/2)}(t')}{(t'-t-i\epsilon)t'^3} dt',$$

$$N_1(t) = n_1^0 + \frac{t}{\pi} \int_{t_0}^{\infty} \frac{1}{(t'-t-i\epsilon)t'}$$
$$\times \mathrm{Im}\left(f_1^{(1/2)}(t') + \frac{(\Delta_{\ell\pi} + t')M_K^4}{2t'\lambda_{\ell\pi}(t')} g_1^{(1/2)}(t') \right) dt',$$

$$\tilde{N}_1(t) = \tilde{n}_1^1 \frac{t}{M_K^2} + \frac{t^2}{\pi} \int_{t_0}^{\infty} \frac{M_K^2}{t'} \frac{\mathrm{Im}\, g_1^{(1/2)}(t')}{(t'-t-i\epsilon)t'^2} dt',$$

$$R_0(t) = \frac{t^3}{\pi} \int_{t_0}^{\infty} \frac{\mathrm{Im}\, f_0^{(3/2)}(t')}{(t'-t-i\epsilon)t'^3} dt',$$

$$R_1(t) = \frac{t}{\pi} \int_{t_0}^{\infty} \frac{1}{(t'-t-i\epsilon)t'}$$
$$\times \mathrm{Im}\left(f_1^{(3/2)}(t') + \frac{(\Delta_{\ell\pi} + t')M_K^4}{2t'\lambda_{\ell\pi}(t')} g_1^{(3/2)}(t') \right) dt',$$

$$\tilde{R}_1(t) = \frac{t^2}{\pi} \int_{t_0}^{\infty} \frac{M_K^2}{t'} \frac{\mathrm{Im}\, g_1^{(3/2)}(t')}{(t'-t-i\epsilon)t'^2} dt'. \tag{69}$$

Actually, since the P-wave of isospin $I = 3/2$ $K\pi$ scattering is real at $\mathcal{O}(p^6)$, so are the partial waves $f_1^{(3/2)}$ and $g_1^{(3/2)}$. Hence, the functions $R_1(t)$ and $\tilde{R}_1(t)$ could be dropped alto-

gether in the decomposition. The phase $\delta_1^{3/2}$ is also known to be tiny in phenomenology.

2.5.2 Ambiguity of the decomposition

We have decomposed the form factors F and G into functions of one variable $M_0(s), \ldots$. However, while the form factors are observable quantities, these functions are not. It is possible to redefine the functions $M_0(s), \ldots$ without changing the form factors and hence without changing the physics.

Therefore, let us study this ambiguity of the decomposition of the form factors. We require the form factors to be invariant under a change of the functions of one variable:

$$M_0(s) \mapsto M_0(s) + \delta M_0(s),$$
$$M_1(s) \mapsto M_1(s) + \delta M_1(s),$$
$$\ldots, \tag{70}$$

which we call 'gauge transformation'. The shifts have to satisfy

$$0 = \delta M_0(s) + \frac{u-t}{M_K^2} \delta M_1(s) + \frac{2}{3} \delta N_0(t)$$
$$+ \frac{2}{3} \frac{t(s-u) + \Delta_{K\pi}\Delta_{\ell\pi}}{M_K^4} \delta N_1(t) - \frac{2}{3} \frac{\Delta_{K\pi} - 3t}{2M_K^2} \delta\tilde{N}_1(t)$$
$$+ \frac{1}{3} \delta R_0(t) + \frac{1}{3} \frac{t(s-u) + \Delta_{K\pi}\Delta_{\ell\pi}}{M_K^4} \delta R_1(t)$$
$$- \frac{1}{3} \frac{\Delta_{K\pi} - 3t}{2M_K^2} \delta\tilde{R}_1(t) + \delta R_0(u)$$
$$+ \frac{u(s-t) + \Delta_{K\pi}\Delta_{\ell\pi}}{M_K^4} \delta R_1(u) - \frac{\Delta_{K\pi} - 3u}{2M_K^2} \delta\tilde{R}_1(u), \tag{71}$$

$$0 = \delta\tilde{M}_1(s) - \frac{2}{3} \delta N_0(t)$$
$$- \frac{2}{3} \frac{t(s-u) + \Delta_{K\pi}\Delta_{\ell\pi}}{M_K^4} \delta N_1(t) + \frac{2}{3} \frac{\Delta_{K\pi} + t}{2M_K^2} \delta\tilde{N}_1(t)$$
$$- \frac{1}{3} \delta R_0(t) - \frac{1}{3} \frac{t(s-u) + \Delta_{K\pi}\Delta_{\ell\pi}}{M_K^4} \delta R_1(t)$$
$$+ \frac{1}{3} \frac{\Delta_{K\pi} + t}{2M_K^2} \delta\tilde{R}_1(t) + \delta R_0(u)$$
$$+ \frac{u(s-t) + \Delta_{K\pi}\Delta_{\ell\pi}}{M_K^4} \delta R_1(u) - \frac{\Delta_{K\pi} + u}{2M_K^2} \delta\tilde{R}_1(u). \tag{72}$$

The solution to these equations is found in the following way: we substitute one of the three kinematic variables by means of $s + t + u = \Sigma_0$. Then we take the derivative with respect to one of the two remaining variables and substitute back

$\Sigma_0 = s + t + u$. After four or five such differentiations, one gets differential equations for single functions $\delta M_0, \ldots$ with the following solution:

$$\delta M_0(s) = c_0^{M_0} + c_1^{M_0} s + c_2^{M_0} s^2,$$

$$\delta M_1(s) = c_0^{M_1} + c_1^{M_1} s + c_2^{M_1} s^2,$$

$$\delta \tilde{M}_1(s) = c_0^{\tilde{M}_1} + c_1^{\tilde{M}_1} s + c_2^{\tilde{M}_1} s^2 + c_3^{\tilde{M}_1} s^3,$$

$$\delta N_0(t) = c_{-1}^{N_0} t^{-1} + c_0^{N_0} + c_1^{N_0} t + c_2^{N_0} t^2,$$

$$\delta N_1(t) = c_{-1}^{N_1} t^{-1} + c_0^{N_1} + c_1^{N_1} t, \qquad (73)$$

$$\delta \tilde{N}_1(t) = c_{-1}^{\tilde{N}_1} t^{-1} + c_0^{\tilde{N}_1} + c_1^{\tilde{N}_1} t + c_2^{\tilde{N}_1} t^2,$$

$$\delta R_0(t) = c_{-1}^{R_0} t^{-1} + c_0^{R_0} + c_1^{R_0} t + c_2^{R_0} t^2,$$

$$\delta R_1(t) = c_{-1}^{R_1} t^{-1} + c_0^{R_1} + c_1^{R_1} t,$$

$$\delta \tilde{R}_1(t) = c_{-1}^{\tilde{R}_1} t^{-1} + c_0^{\tilde{R}_1} + c_1^{\tilde{R}_1} t + c_2^{\tilde{R}_1} t^2.$$

Inserting these solutions into the various differential equations results in algebraic equations for the diverse coefficients. In the end, there remain 13 independent parameters. In complete generality, we therefore have a gauge freedom of 13 parameters in the decomposition (67). The gauge can be fixed by imposing constraints on the Taylor expansion or the asymptotic behaviour of the functions $M_0(s), \ldots$.

First, let us restrict the gauge freedom by imposing the same vanishing Taylor coefficients as in (68), i.e. we exclude all the pole terms, the constants in N_0, $\tilde{N}_1$, R_0, $\tilde{R}_1$ and even a linear term in R_0. Then we further demand that asymptotically the functions behave at most as in (69), i.e. like $M_1(s) = \mathcal{O}(s)$, $\tilde{M}_1(s) = \mathcal{O}(s^2)$, $N_1(t) = \mathcal{O}(1)$, $\tilde{N}_1(t) = \mathcal{O}(t)$, $R_1(t) = \mathcal{O}(1)$ and $\tilde{R}_1(t) = \mathcal{O}(t)$. After imposing these constraints, we are left with a restricted gauge freedom of 3 parameters, which we call C^{R_0}, A^{R_1} and $B^{\tilde{R}_1}$:

$$\delta M_0(s) = (2A^{R_1} - B^{\tilde{R}_1} + 2C^{R_0}) \frac{(\Sigma_0 - s)^2 - \Delta_{K\pi} \Delta_{\ell\pi}}{2M_K^4},$$

$$\delta M_1(s) = -(A^{R_1} + B^{\tilde{R}_1} + 2C^{R_0}) \frac{\Sigma_0}{M_K^2} + B^{\tilde{R}_1} \frac{\Delta_{K\pi}}{2M_K^2}$$
$$\qquad + (B^{\tilde{R}_1} + 2C^{R_0}) \frac{s}{M_K^2},$$

$$\delta \tilde{M}_1(s) = ((B^{\tilde{R}_1} - 2C^{R_0})\Sigma_0^2 - (2A^{R_1} + B^{\tilde{R}_1} - 2C^{R_0})$$
$$\qquad \times \Delta_{K\pi} \Delta_{\ell\pi} + B^{\tilde{R}_1} \Sigma_0 \Delta_{K\pi}) \frac{1}{2M_K^4}$$
$$\qquad - (B^{\tilde{R}_1} \Delta_{K\pi} + (A^{R_1} + B^{\tilde{R}_1} - 2C^{R_0})2\Sigma_0) \frac{s}{2M_K^4}$$
$$\qquad + (2A^{R_1} + B^{\tilde{R}_1} - 2C^{R_0}) \frac{s^2}{2M_K^4},$$

$$\delta N_0(t) = -(2A^{R_1} - B^{\tilde{R}_1} + 2C^{R_0}) \frac{3t(\Delta_{K\pi} + 2\Sigma_0)}{8M_K^4}$$

$$\qquad + (6A^{R_1} - 3B^{\tilde{R}_1} - 10C^{R_0}) \frac{t^2}{8M_K^4},$$

$$\delta N_1(t) = -\frac{1}{4}(2A^{R_1} + 3B^{\tilde{R}_1} - 6C^{R_0}),$$

$$\delta \tilde{N}_1(t) = -(6A^{R_1} + 5B^{\tilde{R}_1} + 6C^{R_0}) \frac{t}{4M_K^2},$$

$$\delta R_0(t) = C^{R_0} \frac{t^2}{M_K^4},$$

$$\delta R_1(t) = A^{R_1},$$

$$\delta \tilde{R}_1(t) = B^{\tilde{R}_1} \frac{t}{M_K^2}. \qquad (74)$$

In order to fix the gauge completely, we have to impose further conditions. We will use two different gauges. The first one corresponds to the case of an asymptotic behaviour that needs $n = 2$ subtractions. It is most suitable for our numerical dispersive representation of the form factors and for the NLO chiral result. In this case, the asymptotic behaviour excludes quadratic terms in $\delta M_0(s)$ and $\delta \tilde{M}_1(s)$ or a linear term in $\delta M_1(s)$. Hence, in the representation (68), the gauge is completely fixed.

The chiral representation, being an expansion in the masses and momenta, does not necessarily reproduce the correct asymptotic behaviour. The $\mathcal{O}(p^6)$ chiral expressions show an asymptotic behaviour that needs $n = 3$ subtractions. In this case, one has to fix the gauge rather with the Taylor coefficients, e.g. by excluding a quadratic term in R_0, a constant term in R_1 and a linear term in $\tilde{R}_1$. Therefore, also in the representation (69), the gauge is completely fixed.

Note that the second representation (69) makes less restrictive assumptions as regards the asymptotic behaviour. Therefore, the first representation (68) is a special case of the second (69). One can easily switch from the first to the second representation with the help of the gauge transformation (74). In this case, the additional subtraction constants will be given by sum rules.

2.5.3 Simplifications for $s_\ell \to 0$

As a test of the decomposition, let us study the linear combination

$$F_1(s, t, u) = \frac{1}{2}(M_K^2 - s)F(s, t, u) + \frac{1}{2}(u - t)G(s, t, u) \qquad (75)$$

in the limit $s_\ell \to 0$. We neglect the contribution of the isospin 3/2 P-wave:

$$\lim_{s_\ell \to 0} F_1(s, t, u)$$
$$= \lim_{s_\ell \to 0} \left(\frac{M_K^2 - s}{2} F(s, t, u) + \frac{u - t}{2} G(s, t, u) \right)$$

$$= \frac{M_K^2 - s}{2} M_0(s)$$

$$+ \frac{u - t}{2} \left[\frac{M_K^2 - s}{M_K^2} M_1(s) + \tilde{M}_1(s) \right]$$

$$+ \frac{2}{3} [(t - M_\pi^2) N_0(t)]$$

$$+ \frac{1}{3} [(t - M_\pi^2) R_0(t)] + (u - M_\pi^2) R_0(u)$$

$$- \frac{2}{3} (t(u - s) + (M_K^2 - M_\pi^2) M_\pi^2)$$

$$\times \left[\frac{t - M_\pi^2}{M_K^4} N_1(t) - \frac{1}{2M_K^2} \tilde{N}_1(t) \right]. \tag{76}$$

By identifying

$$M_0^{F_1}(s) = \frac{M_K^2 - s}{2} M_0(s),$$

$$M_1^{F_1}(s) = \frac{1}{2} \left(\frac{M_K^2 - s}{M_K^2} M_1(s) + \tilde{M}_1(s) \right),$$

$$N_0^{F_1}(t) = (t - M_\pi^2) N_0(t),$$

$$R_0^{F_1}(t) = (t - M_\pi^2) R_0(t),$$

$$N_1^{F_1}(t) = \frac{t - M_\pi^2}{M_K^4} N_1(t) - \frac{1}{2M_K^2} \tilde{N}_1(t), \tag{77}$$

we recover the decomposition of the form factor F_1 used in [12–14]. We further note that the imaginary parts of the functions of one variable in this decomposition are given by

$$\text{Im} M_0^{F_1}(s) = \frac{M_K^2 - s}{2} \text{Im} f_0(s),$$

$$\text{Im} M_1^{F_1}(s) = \frac{M_K^2 - s}{2M_K^2} \text{Im} f_1(s),$$

$$\text{Im} N_0^{F_1}(t) = (t - M_\pi^2) \text{Im} f_0^{(1/2)}(t), \tag{78}$$

$$\text{Im} R_0^{F_1}(t) = (t - M_\pi^2) \text{Im} f_0^{(3/2)}(t),$$

$$\text{Im} N_1^{F_1}(t) = \frac{t - M_\pi^2}{M_K^4} \text{Im} f_1^{(1/2)}(t),$$

and repeat the observation of Sect. 2.4.6 that in the limit $s_\ell \to 0$, these partial waves are given by projections of F_1 in all three channels. Hence, the form factor F_1 decouples in this limit and can be treated independently in the above decomposition.

2.6 Integral equations

The decomposition of the form factors (67) signifies a major simplification, since we only have to deal with functions of a single Mandelstam variable. We will now derive integral equations of the inhomogeneous Omnès type [26,27] for the

single-variable functions, which can be solved numerically and will lead to a resummation of $\pi\pi$ and $K\pi$ rescattering effects. This is the same strategy that we used in [12–14] for the limiting case $s_\ell \to 0$.

The reconstruction theorem for the $K_{\ell 4}$ form factors was used in [24] in a different context. There a dispersive description was constructed that includes isospin-breaking effects due to mass differences. While in our case, we will use the physical phases as input to perform a resummation of rescattering effects, the dispersion relation of [24] is not based on an Omnès representation and was used to analytically calculate the phases (but not the real parts) of the form factors at two-loop level.

2.6.1 Omnès representation

The single-variable functions (68, 69) are constructed in such a way that they only contain the right-hand cut of the corresponding partial wave. Their imaginary part on the upper rim of their cut is given by

$$\text{Im} M_0(s) = \text{Im} f_0(s),$$

$$\text{Im} M_1(s) = \text{Im} \left(f_1(s) - \frac{2PL(s)M_K^2}{\lambda_{K\ell}(s)} g_1(s) \right),$$

$$\text{Im} \tilde{M}_1(s) = \text{Im} g_1(s),$$

$$\text{Im} N_0(t) = \text{Im} f_0^{(1/2)}(t),$$

$$\text{Im} N_1(t) = \text{Im} \left(f_1^{(1/2)}(t) + \frac{(\Delta_{\ell\pi} + t)M_K^4}{2t\lambda_{\ell\pi}(t)} g_1^{(1/2)}(t) \right),$$

$$\text{Im} \tilde{N}_1(t) = \text{Im} \left(\frac{M_K^2}{t} g_1^{(1/2)}(t) \right), \tag{79}$$

$$\text{Im} R_0(t) = \text{Im} f_0^{(3/2)}(t),$$

$$\text{Im} R_1(t) = \text{Im} \left(f_1^{(3/2)}(t) + \frac{(\Delta_{\ell\pi} + t)M_K^4}{2t\lambda_{\ell\pi}(t)} g_1^{(3/2)}(t) \right),$$

$$\text{Im} \tilde{R}_1(t) = \text{Im} \left(\frac{M_K^2}{t} g_1^{(3/2)}(t) \right).$$

Therefore, we can write

$$M_0(s) + \hat{M}_0(s) = f_0(s),$$

$$M_1(s) + \hat{M}_1(s) = f_1(s) - \frac{2PL(s)M_K^2}{\lambda_{K\ell}(s)} g_1(s),$$

$$\tilde{M}_1(s) + \hat{\tilde{M}}_1(s) = g_1(s),$$

$$N_0(t) + \hat{N}_0(t) = f_0^{(1/2)}(t),$$

$$N_1(t) + \hat{N}_1(t) = f_1^{(1/2)}(t) + \frac{(\Delta_{\ell\pi} + t)M_K^4}{2t\lambda_{\ell\pi}(t)} g_1^{(1/2)}(t),$$

$$\tilde{N}_1(t) + \hat{\tilde{N}}_1(t) = \frac{M_K^2}{t} g_1^{(1/2)}(t),$$

$$R_0(t) + \hat{R}_0(t) = f_0^{(3/2)}(t),$$

$$R_1(t) + \hat{R}_1(t) = f_1^{(3/2)}(t) + \frac{(\Delta_{\ell\pi} + t)M_K^4}{2t\lambda_{\ell\pi}(t)} g_1^{(3/2)}(t),$$

$$\tilde{R}_1(t) + \hat{\tilde{R}}_1(t) = \frac{M_K^2}{t} g_1^{(3/2)}(t), \tag{80}$$

where the 'hat functions' $\hat{M}_0(s)$, ... are real on the cut: indeed, they do not possess a right-hand cut, but contain the (possibly complicated) left-hand cut structure of the partial waves (see Sect. 2.4.5). Writing $\mathrm{Im}\, f_0(s) = f_0(s)\mathrm{e}^{-i\delta_0^0(s)}\sin\delta_0^0(s)$, ... leads directly to the following equations:

$$\mathrm{Im} M_0(s) = (M_0(s) + \hat{M}_0(s))\mathrm{e}^{-i\delta_0^0(s)}\sin\delta_0^0(s),$$

$$\mathrm{Im} M_1(s) = (M_1(s) + \hat{M}_1(s))\mathrm{e}^{-i\delta_1^1(s)}\sin\delta_1^1(s),$$

$$\mathrm{Im}\tilde{M}_1(s) = (\tilde{M}_1(s) + \hat{\tilde{M}}_1(s))\mathrm{e}^{-i\delta_1^1(s)}\sin\delta_1^1(s),$$

$$\mathrm{Im} N_0(t) = (N_0(t) + \hat{N}_0(t))\mathrm{e}^{-i\delta_0^{1/2}(t)}\sin\delta_0^{1/2}(t),$$

$$\mathrm{Im} N_1(t) = (N_1(t) + \hat{N}_1(t))\mathrm{e}^{-i\delta_1^{1/2}(t)}\sin\delta_1^{1/2}(t),$$

$$\mathrm{Im}\tilde{N}_1(t) = (\tilde{N}_1(t) + \hat{\tilde{N}}_1(t))\mathrm{e}^{-i\delta_1^{1/2}(t)}\sin\delta_1^{1/2}(t),$$

$$\mathrm{Im} R_0(t) = (R_0(t) + \hat{R}_0(t))\mathrm{e}^{-i\delta_0^{3/2}(t)}\sin\delta_0^{3/2}(t),$$

$$\mathrm{Im} R_1(t) = (R_1(t) + \hat{R}_1(t))\mathrm{e}^{-i\delta_1^{3/2}(t)}\sin\delta_1^{3/2}(t),$$

$$\mathrm{Im}\tilde{R}_1(t) = (\tilde{R}_1(t) + \hat{\tilde{R}}_1(t))\mathrm{e}^{-i\delta_1^{3/2}(t)}\sin\delta_1^{3/2}(t), \tag{81}$$

where, below some inelastic threshold, the phases δ_l^I agree with the elastic $\pi\pi$- or $K\pi$-scattering phase shifts. Therefore, the functions M_0, ... are given by the solution to the inhomogeneous Omnès problem. The minimal number of subtractions appearing in the Omnès representation is determined by the asymptotic behaviour of the functions M_0, ... and the phases δ_l^I.

Let us extend these equations even to the region above inelastic thresholds by replacing $\delta \mapsto \omega$,

$$\mathrm{Im} M_0(s) = (M_0(s) + \hat{M}_0(s))\mathrm{e}^{-i\omega_0^0(s)}\sin\omega_0^0(s),$$

$$\dots, \tag{82}$$

where $\omega_l^I(s) = \delta_l^I(s) + \eta_l^I(s)$ and $\eta_l^I(s) = 0$ below the inelastic threshold $s = \Lambda^2$.

We define the usual once-subtracted Omnès function

$$\Omega(s) := \exp\left(\frac{s}{\pi}\int_{s_0}^\infty \frac{\delta(s')}{(s'-s-i\epsilon)s'}\mathrm{d}s'\right). \tag{83}$$

If the asymptotic behaviour of the phase is $\lim_{s\to\infty}\delta(s) = m\pi$, the Omnès function behaves asymptotically as $\mathcal{O}(s^{-m})$. Provided that the function $M(s)$ behaves asymptotically as

$\mathcal{O}(s^k)$, we can write a dispersion relation for M/Ω that leads to a modified Omnès solution

$$M(s)$$
$$= \Omega(s)\Bigg\{P_{n-1}(s) + \frac{s^n}{\pi}\int_{s_0}^{\Lambda^2} \frac{\hat{M}(s')\sin\delta(s')}{|\Omega(s')|(s'-s-i\epsilon)s'^n}\mathrm{d}s'$$
$$+ \frac{s^n}{\pi}\int_{\Lambda^2}^\infty \frac{\hat{M}(s')\sin\delta(s')}{|\Omega(s')|(s'-s-i\epsilon)s'^n}\mathrm{d}s'$$
$$+ \frac{s^n}{\pi}\int_{\Lambda^2}^\infty \frac{(\hat{M}(s')+\mathrm{Re}M(s'))\sin\eta(s')}{|\Omega(s')|\cos(\delta(s')+\eta(s'))(s'-s-i\epsilon)s'^n}\mathrm{d}s'\Bigg\}, \tag{84}$$

where the order of the subtraction polynomial is $n - 1 = k + m$.

Actually, we do not know the phase δ at high energies. Inelasticities due to multi-Goldstone boson intermediate states, i.e. more than two Goldstone bosons, appear only at $\mathcal{O}(p^8)$ [21], hence the most important inelastic contribution would certainly be a $K\bar{K}$ intermediate state in the s-channel. This could be included by using experimental input on η up to $s \approx (1.4\,\mathrm{GeV})^2$.

We could make a Taylor expansion of the inelasticity integral and neglect terms that only contribute at $\mathcal{O}(p^8)$ to the form factors by applying the power counting $\frac{s}{\Lambda^2} \sim p^2$. This would introduce quite a lot of unknown Taylor coefficients. Here, we follow another strategy: we set $\eta = 0$ and assign a large error to the phases δ at high energies. We assume further that δ reaches a multiple of π above a certain $s = \Lambda^2$. The two high-energy integrals in (84) drop in this case.

Assuming that the phases behave asymptotically like $\delta_0^0 \to \pi$, $\delta_1^1 \to \pi$ and all other $\delta_l^I \to 0$, we find the following solution for the case of $n = 2$ subtractions:

$$M_0(s) = \Omega_0^0(s)\Bigg\{a^{M_0} + b^{M_0}\frac{s}{M_K^2} + c^{M_0}\frac{s^2}{M_K^4}$$
$$+ \frac{s^3}{\pi}\int_{s_0}^{\Lambda^2} \frac{\hat{M}_0(s')\sin\delta_0^0(s')}{|\Omega_0^0(s')|(s'-s-i\epsilon)s'^3}\mathrm{d}s'\Bigg\},$$

$$M_1(s) = \Omega_1^1(s)\Bigg\{a^{M_1} + b^{M_1}\frac{s}{M_K^2}$$
$$+ \frac{s^2}{\pi}\int_{s_0}^{\Lambda^2} \frac{\hat{M}_1(s')\sin\delta_1^1(s')}{|\Omega_1^1(s')|(s'-s-i\epsilon)s'^2}\mathrm{d}s'\Bigg\},$$

$$\tilde{M}_1(s) = \Omega_1^1(s)\Bigg\{a^{\tilde{M}_1} + b^{\tilde{M}_1}\frac{s}{M_K^2} + c^{\tilde{M}_1}\frac{s^2}{M_K^4}$$
$$+ \frac{s^3}{\pi}\int_{s_0}^{\Lambda^2} \frac{\hat{\tilde{M}}_1(s')\sin\delta_1^1(s')}{|\Omega_1^1(s')|(s'-s-i\epsilon)s'^3}\mathrm{d}s'\Bigg\},$$

$$N_0(t) = \Omega_0^{1/2}(t)\Bigg\{b^{N_0}\frac{t}{M_K^2}$$
$$+ \frac{t^2}{\pi}\int_{t_0}^{\Lambda^2} \frac{\hat{N}_0(t')\sin\delta_0^{1/2}(t')}{|\Omega_0^{1/2}(t')|(t'-t-i\epsilon)t'^2}\mathrm{d}t'\Bigg\},$$

$$N_1(t) = \Omega_1^{1/2}(t) \left\{ \frac{1}{\pi} \int_{t_0}^{\Lambda^2} \frac{\hat{N}_1(t') \sin \delta_1^{1/2}(t')}{|\Omega_1^{1/2}(t')|(t'-t-i\epsilon)} dt' \right\},$$

$$\tilde{N}_1(t) = \Omega_1^{1/2}(t) \left\{ \frac{t}{\pi} \int_{t_0}^{\Lambda^2} \frac{\hat{\tilde{N}}_1(t') \sin \delta_1^{1/2}(t')}{|\Omega_1^{1/2}(t')|(t'-t-i\epsilon)t'} dt' \right\},$$

$$R_0(t) = \Omega_0^{3/2}(t) \left\{ \frac{t^2}{\pi} \int_{t_0}^{\Lambda^2} \frac{\hat{R}_0(t') \sin \delta_0^{3/2}(t')}{|\Omega_0^{3/2}(t')|(t'-t-i\epsilon)t'^2} dt' \right\},$$

$$R_1(t) = \Omega_1^{3/2}(t) \left\{ \frac{1}{\pi} \int_{t_0}^{\Lambda^2} \frac{\hat{R}_1(t') \sin \delta_1^{3/2}(t')}{|\Omega_1^{3/2}(t')|(t'-t-i\epsilon)} dt' \right\},$$

$$\tilde{R}_1(t) = \Omega_1^{3/2}(t) \left\{ \frac{t}{\pi} \int_{t_0}^{\Lambda^2} \frac{\hat{\tilde{R}}_1(t') \sin \delta_1^{3/2}(t')}{|\Omega_1^{3/2}(t')|(t'-t-i\epsilon)t'} dt' \right\},$$

$$(85)$$

where we have fixed some of the subtraction constants in N_0, $\tilde{N}_1$, R_0 and $\tilde{R}_1$ to zero by imposing the same Taylor expansion as in the defining equation (68).

Note that driving the $K\pi$ phases to 0 is somewhat artificial. They are rather supposed to reach π at high energies. However, this would introduce three more subtraction constants in our framework. Since the high-energy behaviour of the phases does not have an important influence on our results, we abstain from introducing more subtractions and take these effects into account in the systematic uncertainty.

In the case of $n = 3$ subtractions, six additional subtraction constants appear in the Omnès representation. The conversion of a solution for $n = 2$ into a solution for $n = 3$ requires a gauge transformation in the Omnès representation, as explained in Appendix C.1.

2.6.2 Hat functions

The hat functions appearing in the Omnès solution to the functions of one variable (85) can be computed through partial-wave projections of the form factors: (80) should be understood as the defining equation of the hat functions. One has to compute the partial-wave projections of the decomposed form factors F and G (67) and subtract the function of one variable (M_0, ...). Finally, one obtains an expression for the hat functions in terms of angular averages of the single-variable functions. The explicit expressions for the hat functions are given in Appendix C.2.

3 Numerical solution of the dispersion relation

3.1 Iterative solution of the dispersion relation

The reconstruction theorem has allowed us to decompose the form factors into functions of one variable, (67). The nine functions of one variable are given unambiguously by the Omnès solutions (85). The hat functions appearing in the dispersive integrals are given by angular integrals of the nine functions of one variable and link these functions together. Therefore, we face a set of coupled integral equations, parameterised by the nine subtraction constants a^{M_0}, b^{M_0}, ... as defined in (85). In this section we discuss a method for solving these equations numerically. We will assume an asymptotic behaviour of the form factors that requires only $n = 2$ subtractions.

A crucial property of this set of equations is that they are linear in the subtraction constants. Any solution can be written as a linear combination of nine basis solutions. Our main task is therefore to determine numerically these nine basis solutions.

So far, the invariant squared energy of the dilepton system, s_ℓ, has been treated as an external parameter. On the one hand, it appears in the definition of the hat functions. On the other hand, the subtraction constants have an implicit dependence on s_ℓ. To make this dependence explicit we write the form factors as:

$$X(s, t, u) = \sum_{i=1}^{9} a_i(s_\ell) X_i(s, t, u),$$ (86)

where $X \in \{F, G\}$, $\{a_i\}_i = \{a^{M_0}, b^{M_0}, \ldots, b^{N_0}\}$ and where X_i denotes the basis solution with $a_k = \delta_{ik}$, $k \in \{1, \ldots, 9\}$. If s_ℓ is allowed to vary, the 'functions of one variable' become actually functions of two variables, $M_0(s, s_\ell)$, ...

Our strategy is as follows. We determine the basis solutions by a numerical iteration of the coupled integral equations. Each basis solution is a function of s, t and u, where $s + t + u = \Sigma_0 = M_K^2 + 2M_\pi^2 + s_\ell$, or equivalently a function of s, s_ℓ and $\cos\theta$. Since s_ℓ is a fixed external parameter in the integral equations, the iterative solution has to be performed for each value of s_ℓ separately. Once the basis solutions are computed, the subtraction constants (or rather functions) have to be determined by suitable means, such as a fit to data, the soft-pion theorem and χPT input. As the dependence on s_ℓ has been found to be rather weak in experiments, the subtraction functions can be well approximated by a low-order polynomial in s_ℓ.

In summary, we need the nine basis solutions for a set of values of s_ℓ, so as to allow us to calculate them for any value of s_ℓ by interpolation. Again, since the dependence on s_ℓ appears to be rather weak, we will need only a low number of values of s_ℓ.

To calculate each of the basis solutions we use the following iterative procedure:

1. set the initial value of the functions M_0, ... to Omnès function × subtraction polynomial (the polynomial is in
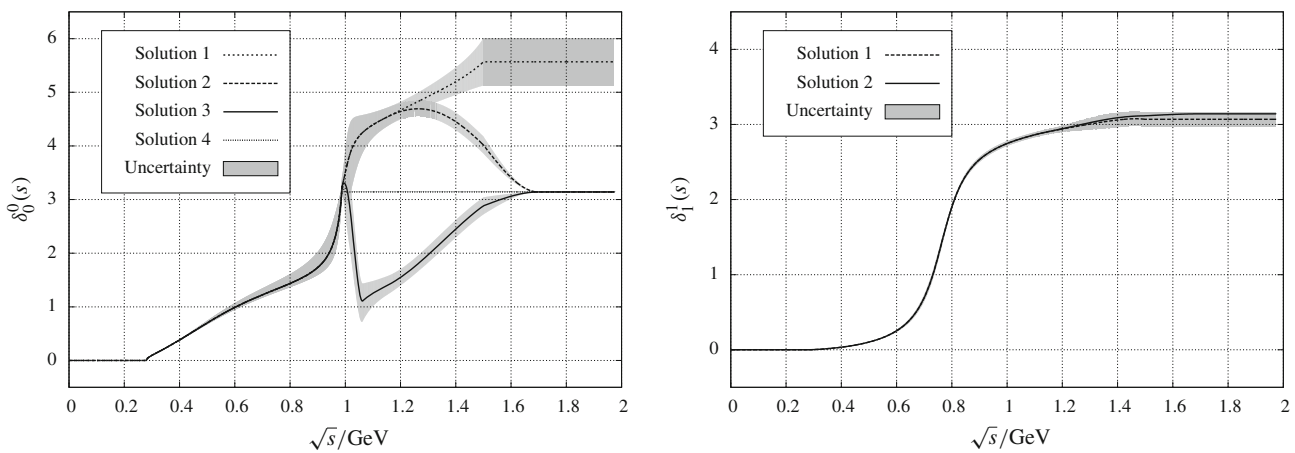
Fig. 4 $\pi\pi$ phase shift inputs

fact either 0 or a simple monomial with coefficient 1 for a particular basis solution);

2. calculate the hat functions $\hat{M}_0, \ldots$ by means of angular integrals of the functions $M_0, \ldots$;
3. calculate the new values of the functions $M_0, \ldots$ as Omnès function $\times$ (polynomial + dispersive part), where in the dispersion integral the hat function calculated in step 2 appears;
4. go to step 2 and iterate this procedure until convergence.

It turns out that this iteration converges quickly. After five or six iterations, the relative changes are of order 10^{-6}.

3.2 Phase input

3.2.1 $\pi\pi$ phase shifts

For the pion scattering phase shifts, we use the parameterisation of [28,29]. The solution depends on 28 parameters that can vary within a certain range. The curve labelled as Solution 1 in Fig. 4 shows the central solution for the phase shifts as well as the error band due to uncertainty in the parameters (summed in quadrature).

Two aspects deserve special attention. First, the phase for Solution 1 is just taken constant above $\sqrt{s} \approx 1.5$ GeV. Our derivation of the dispersion relation, however, relies on the assumption that $\delta_0^0(s) \to \pi$, $\delta_1^1(s) \to \pi$ for $s \to \infty$. We should therefore change the high-energy behaviour of the phases such that they reach π at $s = \Lambda^2$. The exact way how this is achieved should not have influence on the result at low energies, especially in the physical region of the decay. We choose to interpolate smoothly between the value of Solution 1 and π:

$$\delta_0^0(s)_{\text{sol.2}} := (1 - f_{\text{int}}(s_1, s_2, s))\delta_0^0(s)_{\text{sol.1}} + f_{\text{int}}(s_1, s_2, s)\pi,$$
$$\delta_1^1(s)_{\text{sol.2}} := (1 - f_{\text{int}}(s_1, s_2, s))\delta_1^1(s)_{\text{sol.1}} + f_{\text{int}}(s_1, s_2, s)\pi,$$

$$f_{\text{int}}(s_1, s_2, s) := \begin{cases} 0 & \text{if } s < s_1, \\ \frac{(s-s_1)^2(3s_2-2s-s_1)}{(s_2-s_1)^3} & \text{if } s_1 \leq s < s_2, \\ 1 & \text{if } s_2 \leq s. \end{cases} \tag{87}$$

Figure 4 shows Solution 2 with $s_1 = 68M_\pi^2$ and $s_2 = 148M_\pi^2$. These values can be varied and should not have an important influence.

The second subtlety is the problem of the behaviour around the $K\bar{K}$ threshold [30]: are the $K_{\ell4}$ partial waves expected to have a peak or a dip in the vicinity of the $K\bar{K}$ threshold, i.e. do they rather behave like the strange or the non-strange scalar form factor of the pion? The answer to this question could be obtained from a coupled-channel analysis of the $K_{\ell4}$ amplitude, which, however, goes beyond the scope of this paper. In case of a dip we have to modify the phase such that it follows $\delta_0^0(s) - \pi$ above the $K\bar{K}$ threshold. The third solution shown in Fig. 4 is given by

$$\delta_0^0(s)_{\text{sol.3}} := (1 - f_{\text{int}}(s_1, s_2, s))(\delta_0^0(s)_{\text{sol.1}} - f_{\text{int}}(\tilde{s}_1, \tilde{s}_2, s)\pi)$$
$$+ f_{\text{int}}(s_1, s_2, s)\pi, \tag{88}$$

with $\tilde{s}_1 = 4M_K^2$ and $\tilde{s}_2 = \tilde{s}_1 + 8M_\pi^2$.

The solution 4 in Fig. 4 corresponds to Solution 2 but with $s_1 = 4M_K^2$ and $s_2 = s_1 + M_\pi^2$.

As the question of the correct behaviour around the $K\bar{K}$ threshold is not easy to answer, we declare Solution 3 as the 'central' one and use all the other solutions to determine the systematic uncertainty.

3.2.2 $K\pi$ phase shifts

For the crossed channels, we also need the $K\pi$ phase shifts as an input. We use the phase shifts and uncertainties of [31,32], but add by hand a more conservative uncertainty that reaches $20°$ at $t = 150M_\pi^2$. For the very small phase $\delta_1^{3/2}$, we just
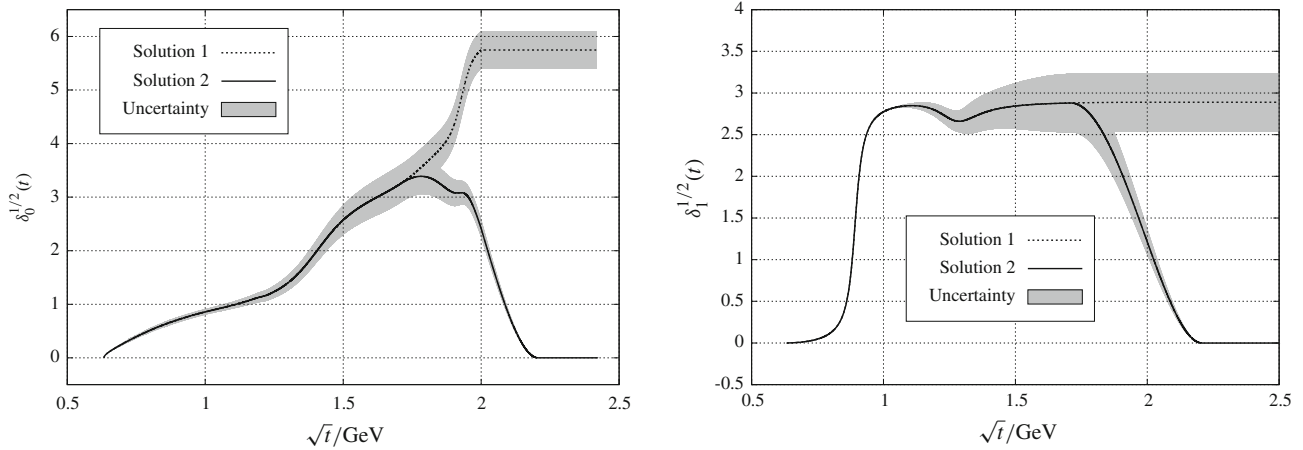
Fig. 5 $K\pi$ phase shift inputs, isospin $I = 1/2$
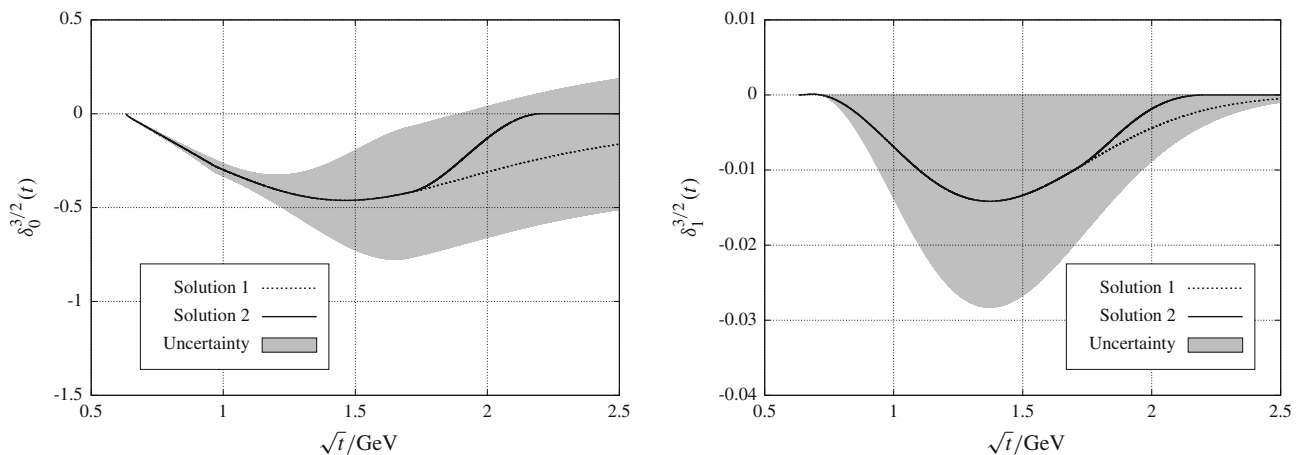
Fig. 6 $K\pi$ phase shift inputs, isospin $I = 3/2$

assume a 100 % uncertainty. These phase solutions are shown in Figs. 5 and 6 as 'Solution 1'.

In the derivation of the dispersion relation, we assume that the $K\pi$ phases go to zero at high energies. We implement this by interpolating smoothly between Solution 1 and zero with $f_{\text{int}}(t_1, t_2, t)$. These modified phase shifts with $t_1 = 150 M_\pi^2$ and $t_2 = 250 M_\pi^2$ are displayed as 'Solution 2' in Figs. 5 and 6. The difference between 'Solution 1' and 'Solution 2' is taken as a measure of the systematic uncertainty due to the high-energy behaviour of the $K\pi$ phases.

3.3 Omnès functions

In a first step, the six Omnès functions are computed, defined by

$$\Omega_l^I(s) := \exp\left(\frac{s}{\pi} \int_{s_0}^\infty \frac{\delta_l^I(s')}{(s' - s - i\epsilon)s'} \mathrm{d}s'\right), \qquad (89)$$

where s_0 denotes the respective threshold. We show only the results for the $\pi\pi$ Omnès functions; see Figs. 7 and 8. In the case of Ω_0^0, the Omnès function is computed for the phase Solution 3 – the corresponding uncertainty is obtained by summing in quadrature the variations generated by the uncertainties of all 28 parameters. The differences, appropriately weighted, are summed up in quadrature to give the error band. For the phase Solutions 1, 2 and 4, only the central curve is shown. Note that the differences between the various high-energy phase solutions are much larger than the error band due to the phase parameters. However, at low energy these differences are well described by polynomials and can be absorbed at low energies by the subtraction constants of the dispersion relation. This implies that the uncertainty generated by the unknown high-energy behaviour of the phase shifts will be moderate.

3.4 Hat functions and angular projection

During the iterative solution of the dispersion relation, the hat functions have to be computed by means of angular aver-
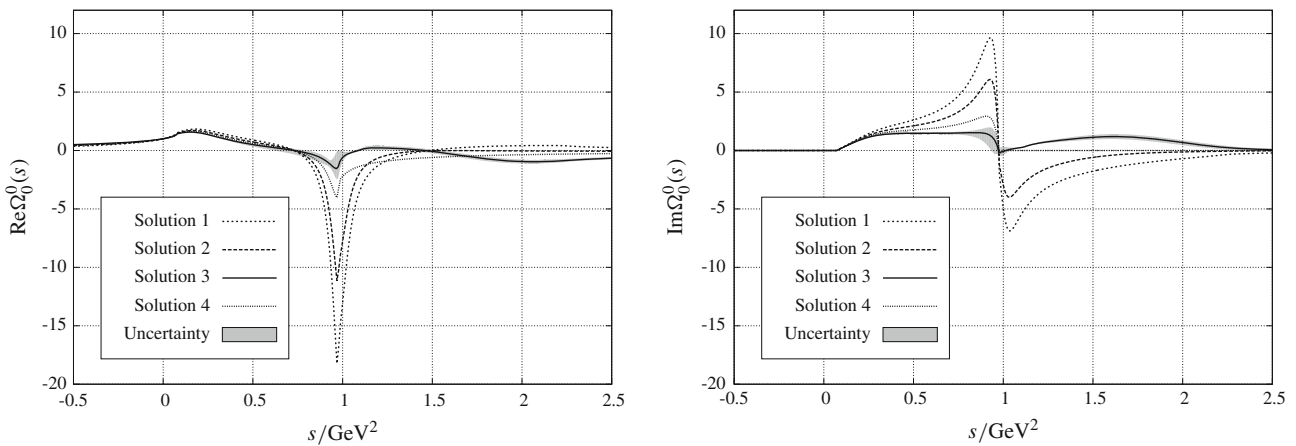
Fig. 7 $\pi\pi$ S-wave Omnès function, isospin $I = 0$
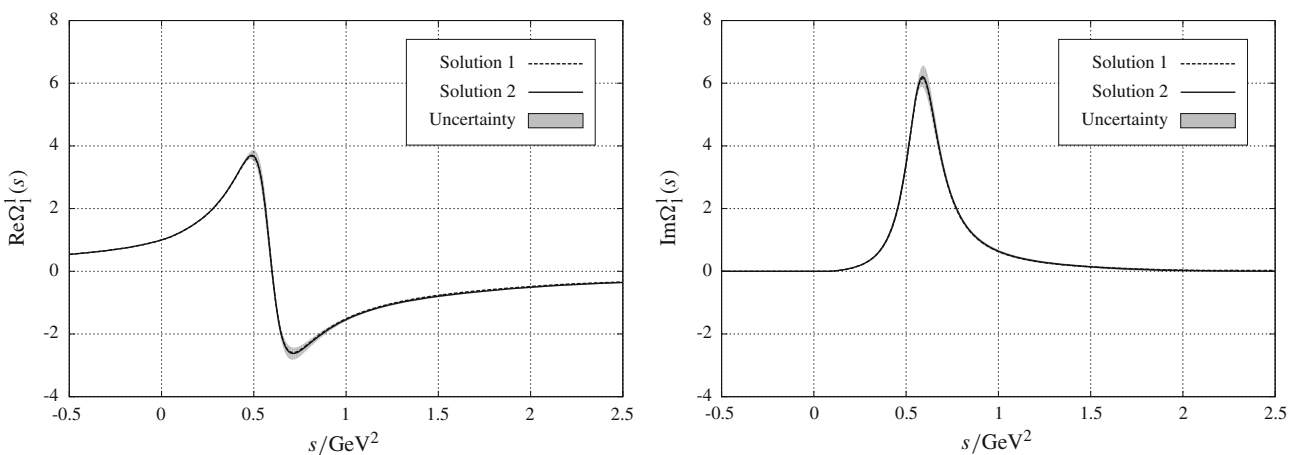
Fig. 8 $\pi\pi$ P-wave Omnès function, isospin $I = 1$

ages. Since the hat functions appear in the integrand of the dispersive integrals, they have to be known just on the real axis above the threshold of the respective channel.

In the $s_\ell = 0$ case, the calculation of the angular integrals is straightforward. The functions $M_0, \ldots$ need to be computed on the real axis, also for negative values of their argument. As described in Sect. 2.4.5, a subtlety arises in the case $s_\ell \neq 0$: in the calculation of the s-channel hat functions, we have to know the angular integrals of the t- and u-channel functions $N_0, \ldots$. In the region $(M_K - \sqrt{s_\ell})^2 < s < (M_K + \sqrt{s_\ell})^2$, the angular integration path extends into the complex t- or u-plane. Therefore, the t- and u-channel functions $N_0, \ldots$ have to be computed not only on the real axis but also in the complex plane. Since the region where this happens is much below the t- or u-channel cut, we have two options how to perform this:

- Integrate on a straight line in the complex t- or u-plane. The functions $N_0(t), \ldots$ have to be known in an egg-shaped region of s_ℓ-dependent size. The egg lies within $M_\pi^2 - M_K \sqrt{s_\ell} < \mathrm{Re}(t) < M_\pi^2 + M_K \sqrt{s_\ell}$. The functions

$N_0(t), \ldots$ can be computed on a two-dimensional grid covering this egg and then e.g. interpolated with a 2D spline.

- Since the functions $N_0(t), \ldots$ are analytic in the region of the egg, the angular integration path can be deformed to lie always on the border of the egg. Therefore, the functions $N_0(t), \ldots$ only have to be computed on points lying on this border (in addition to the real axis) and 1D interpolation methods can be applied.

The first method is more straightforward, the second needs less computing time. The second one requires a change of variable that we briefly describe.

We want to compute the angular integral

$$\langle z^n X \rangle_{t_s}(s) = \frac{1}{2} \int_{-1}^{1} \mathrm{d}z \, z^n X(t(s, z)), \tag{90}$$

where e.g. $X = N_0$ and

$$t(s, z) = \frac{1}{2}(\Sigma_0 - s - \lambda_{K\ell}^{1/2}(s)\sigma_\pi(s)z). \tag{91}$$
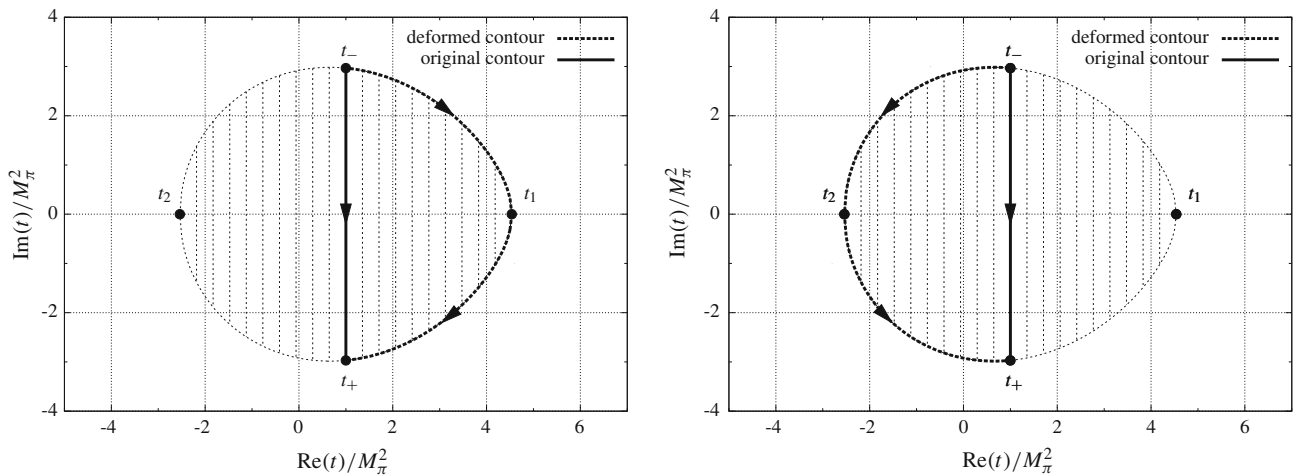
Fig. 9 Angular integration contours for $s_\ell = M_\pi^2$

The square root of the Källén function is defined by (62) and the critical region is $s_- < s < s_+$, where we define

$$s_\pm := \left(M_K \pm \sqrt{s_\ell}\right)^2. \tag{92}$$

In this region, the angular integration path in the complex t-plane runs from $t_- := t(s, -1)$ to $t_+ := t(s, 1)$. Due to the analyticity of the function $X(t)$, the straight contour can be deformed along the border of the egg, either to pass $t_1 := t(s_-, z)$ or $t_2 := t(s_+, z)$; see the two plots in Fig. 9.

Defining

$$z_s(t) = \frac{1}{\lambda_{K\ell}^{1/2}(s)\sigma_\pi(s)}(\Sigma_0 - s - 2t), \tag{93}$$

we rewrite the angular integral as a complex integral:

$$
\begin{aligned}
\langle z^n X \rangle_{t_s} &= \frac{1}{2} \int_{t_-}^{t_+} \frac{\mathrm{d}z_s}{\mathrm{d}t} \mathrm{d}t \, z_s^n(t) X(t) \\
&= -\frac{1}{\lambda_{K\ell}^{1/2}(s)\sigma_\pi(s)} \int_{t_-}^{t_+} \mathrm{d}t \, z_s^n(t) X(t) \\
&= -\frac{1}{\lambda_{K\ell}^{1/2}(s)\sigma_\pi(s)} \\
&\quad \times \left(\int_{t_-}^{t_1} \mathrm{d}t \, z_s^n(t) X(t) - \int_{t_+}^{t_1} \mathrm{d}t \, z_s^n(t) X(t) \right),
\end{aligned}
\tag{94}
$$

or equivalently

$$
\begin{aligned}
\langle z^n X \rangle_{t_s} &= -\frac{1}{\lambda_{K\ell}^{1/2}(s)\sigma_\pi(s)} \\
&\quad \times \left(\int_{t_-}^{t_2} \mathrm{d}t \, z_s^n(t) X(t) - \int_{t_+}^{t_2} \mathrm{d}t \, z_s^n(t) X(t) \right).
\end{aligned}
\tag{95}
$$

We parametrise the border of the egg by the following curves:

$$
\begin{aligned}
t_s^\pm(\xi) &:= t(\xi, \pm 1) = \frac{1}{2}(\Sigma_0 - \xi \mp \lambda_{K\ell}^{1/2}(\xi)\sigma_\pi(\xi)), \\
&\quad \xi \in [s_-, s_+],
\end{aligned}
\tag{96}
$$

hence

$$
\begin{aligned}
\langle z^n X \rangle_{t_s} &= -\frac{1}{\lambda_{K\ell}^{1/2}(s)\sigma_\pi(s)} \\
&\quad \times \left(\int_s^{s_-} \mathrm{d}\xi \, \frac{\mathrm{d}t_s^-(\xi)}{\mathrm{d}\xi} z_s^n(t_s^-(\xi)) X(t_s^-(\xi)) \right. \\
&\quad \left. - \int_s^{s_-} \mathrm{d}\xi \, \frac{\mathrm{d}t_s^+(\xi)}{\mathrm{d}\xi} z_s^n(t_s^+(\xi)) X(t_s^+(\xi)) \right),
\end{aligned}
\tag{97}
$$

or

$$
\begin{aligned}
\langle z^n X \rangle_{t_s} &= -\frac{1}{\lambda_{K\ell}^{1/2}(s)\sigma_\pi(s)} \\
&\quad \times \left(\int_s^{s_+} \mathrm{d}\xi \, \frac{\mathrm{d}t_s^-(\xi)}{\mathrm{d}\xi} z_s^n(t_s^-(\xi)) X(t_s^-(\xi)) \right. \\
&\quad \left. - \int_s^{s_+} \mathrm{d}\xi \, \frac{\mathrm{d}t_s^+(\xi)}{\mathrm{d}\xi} z_s^n(t_s^+(\xi)) X(t_s^+(\xi)) \right),
\end{aligned}
\tag{98}
$$

where

$$\frac{dt_s^\pm(\xi)}{d\xi} = \frac{1}{2}\left(-1 \mp \frac{d(\lambda_{K\ell}^{1/2}(\xi)\sigma_\pi(\xi))}{d\xi}\right)$$

$$= \frac{1}{2}\left(-1 \mp \frac{2M_K^4 M_\pi^2 - M_K^2\left(4M_\pi^2 s_\ell + \xi^2\right) + (s_\ell - \xi)\left(2M_\pi^2(\xi + s_\ell) - \xi^2\right)}{\xi^2 \lambda_{K\ell}^{1/2}(\xi)\sigma_\pi(\xi)}\right), \tag{99}$$

$$z_s(t_s^\pm(\xi)) = \frac{1}{\lambda_{K\ell}^{1/2}(s)\sigma_\pi(s)}(\xi - s \pm \lambda_{K\ell}^{1/2}(\xi)\sigma_\pi(\xi)).$$

Note that

$$z_s(t_s^+(\xi)) = -z_s(t_s^-(\xi))^*,$$
$$t_s^+(\xi) = t_s^-(\xi)^*, \tag{100}$$
$$\frac{dt_s^+(\xi)}{d\xi} = \left(\frac{dt_s^-(\xi)}{d\xi}\right)^*$$

and hence, due to the Schwarz reflection principle,

$$X(t_s^+(\xi)) = X(t_s^-(\xi))^*. \tag{101}$$

Therefore, the function X has to be computed only on the 'upper half-egg':

$$\langle z^n X\rangle_{t_s} = \frac{1}{\lambda_{K\ell}^{1/2}(s)\sigma_\pi(s)}$$
$$\times \int_{s_-}^{s} d\xi\left(\frac{dt_s^-(\xi)}{d\xi}z_s^n(t_s^-(\xi))X(t_s^-(\xi))\right.$$
$$\left. -(-1)^n\left(\frac{dt_s^-(\xi)}{d\xi}z_s^n(t_s^-(\xi))X(t_s^-(\xi))\right)^*\right) \tag{102}$$

or

$$\langle z^n X\rangle_{t_s} = -\frac{1}{\lambda_{K\ell}^{1/2}(s)\sigma_\pi(s)}$$
$$\times \int_{s}^{s_+} d\xi\left(\frac{dt_s^-(\xi)}{d\xi}z_s^n(t_s^-(\xi))X(t_s^-(\xi))\right.$$
$$\left. -(-1)^n\left(\frac{dt_s^-(\xi)}{d\xi}z_s^n(t_s^-(\xi))X(t_s^-(\xi))\right)^*\right). \tag{103}$$

Although both descriptions are valid in the range $s_- < s < s_+$, one may choose to use the first in the region $s_- < s < s_m$ and the second in the region $s_m < s < s_+$, where s_m lies somewhere in the middle of s_- and s_+, e.g. $s_m = (s_- + s_+)/2$. The motivation to do so is to avoid numerical instabilities: the integral from s_- to s with $s \to s_+$ must tend to zero to give a finite value for the hat function. The integral over the whole half-egg, however, accumulates a numerical uncertainty.

3.5 Results for the basis solutions

We have now all the ingredients to compute the nine basis solutions of the dispersion relation. The final result will be a linear combination thereof. In Sect. 4, we will describe how to determine this linear combination. We will fit experimental data on the partial waves defined by

$$F_s(s, s_\ell) = (M_0(s, s_\ell) + \hat{M}_0(s, s_\ell))e^{-i\delta_0^0(s)},$$
$$\tilde{F}_p(s, s_\ell) = (M_1(s, s_\ell) + \hat{M}_1(s, s_\ell))e^{-i\delta_1^1(s)},$$
$$G_p(s, s_\ell) = (\tilde{M}_1(s, s_\ell) + \hat{\tilde{M}}_1(s, s_\ell))e^{-i\delta_1^1(s)}. \tag{104}$$

The Figs. 10 and 11 show the partial waves of the basis solutions in the case $s_\ell = 0$. They are computed with the phase solutions that reach the asymptotic values of π in the case of the $\pi\pi$ phases and 0 in the case of the $K\pi$ phases. For δ_0^0, the solution with the drop around the $K\bar{K}$ threshold is used. The figures illustrate what can be learnt also from the definitions (85) and (104): the data on the partial wave F_s will constrain mainly the subtraction constants appearing in M_0, the data on F_p mainly the constants in M_1 and the data on G_p mainly the constants in $\tilde{M}_1$. An exception is the constant
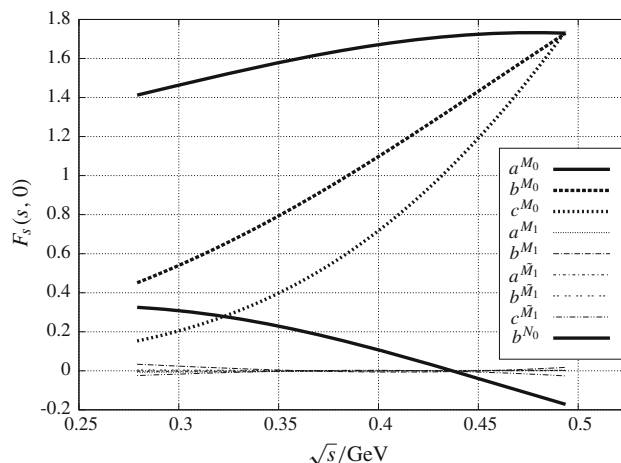
Fig. 10 S-wave of the form factor F for the different basis solutions for $s_\ell = 0$
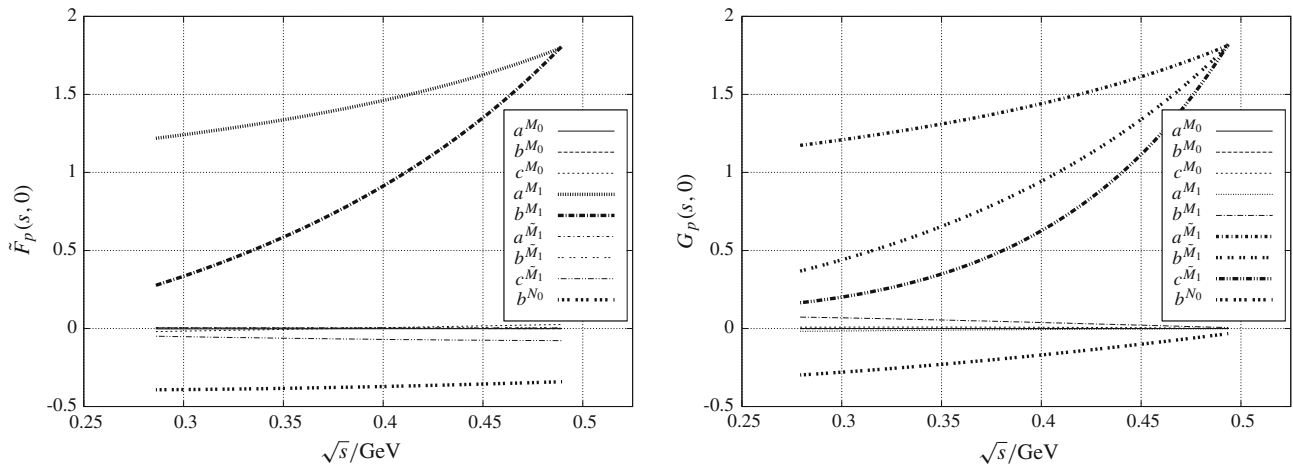
Fig. 11 P-waves of the form factors F and G for the different basis solutions for $s_\ell = 0$

Table 1 Values of the two relevant combinations of the form factors F and G at the soft-pion points, computed for the basis solutions

Basis solution	$(F - G)_{\text{SPP1}}$	$(F + G)_{\text{SPP2}}$
a^{M_0}	1.06	1.05
b^{M_0}	0.08	0.09
c^{M_0}	0.03	-0.01
a^{M_1}	-1.03	0.93
b^{M_1}	0.05	0.11
$a^{\tilde{M}_1}$	-1.07	1.02
$b^{\tilde{M}_1}$	-0.05	0.09
$c^{\tilde{M}_1}$	-0.10	-0.01
b^{N_0}	1.62	-0.01

b^{N_0}: through the hat functions, it is constrained by the data on all partial waves.

Besides experimental data on the partial waves, we will also use two soft-pion theorems as an additional source of information. Table 1 shows the values of $(F - G)(M_\pi^2, M_K^2, M_\pi^2)$ and $(F + G)(M_\pi^2, M_\pi^2, M_K^2)$ for the basis solutions. The first soft-pion theorem, which implies $(F - G)(M_\pi^2, M_K^2, M_\pi^2) \approx 0$, constrains mainly a linear combination of a^{M_0}, a^{M_1}, $a^{\tilde{M}_1}$ and b^{N_0}.

4 Determination of the subtraction constants

In the previous chapter, we have described how to solve numerically the Omnès dispersion relation for the form factors F and G. The solution is parameterised in terms of the subtraction constants $a^{M_0}, \ldots$. The next task is now to determine these subtraction constants in order to fix the parametric freedom. We use three different sources of information for the determination of the subtraction constants:

- experimental data on the $K_{\ell 4}$ form factors,
- the soft-pion theorem, providing relations between F, G and the $K_{\ell 3}$ vector form factor,
- input from χPT.

The soft-pion theorem (SPT) is valid up to corrections of $\mathcal{O}(M_\pi^2)$ and hence can be considered as a strong constraint. From the two high-statistics experiments NA48/2 and E865 we have data on the S- and P-waves of the form factors. Although these experiments have achieved impressive results, the data alone does not determine all the subtraction constants with satisfactory precision. Therefore, we use chiral input to fix some of the subtraction constants that are not well determined by the fit to data.

In the following, we describe in more detail what data we use for the fits and how these fits are performed. We were provided with additional unpublished data from the E865 experiment and include the data sets of NA48/2 that became available only recently as an addendum to the original publication [9]. Therefore, our fits include the maximal amount of experimental information on the $K_{\ell 4}$ form factors F and G that is currently available.

4.1 Experimental data

The NA48/2 experiment defines the partial wave expansion of the form factors as

$$
\begin{aligned}
F &= F_s \mathrm{e}^{i\delta_s} + F_p \mathrm{e}^{i\delta_p} \cos\theta + \cdots, \\
G &= G_p \mathrm{e}^{i\delta_p} + \cdots
\end{aligned}
\tag{105}
$$

and further defines the linear combination

$$
\tilde{G}_p := G_p + \frac{X}{\sigma_\pi P L} F_p.
\tag{106}
$$

For us, it is convenient to define the partial wave

$$\tilde{F}_p := \frac{M_K^2}{2X\sigma_\pi} F_p. \tag{107}$$

In our former treatment of the form factor F_1 [12–14], it was most convenient to use the data on F_s and $\tilde{G}_p$ (which corresponds to the P-wave of F_1). Now that we describe both form factors F and G, we prefer to fit the three partial waves F_s, $\tilde{F}_p$ and G_p.

The comparison with our definition of the s-channel partial-wave expansions

$$F = \sum_{l=0}^{\infty} P_l(\cos\theta) \left(\frac{2X\sigma_\pi}{M_K^2}\right)^l f_l - \frac{\sigma_\pi P L}{X} \cos\theta \, G,$$

$$G = \sum_{l=1}^{\infty} P_l'(\cos\theta) \left(\frac{2X\sigma_\pi}{M_K^2}\right)^{l-1} g_l, \tag{108}$$

allows us to identify

$$F_s \mathrm{e}^{i\delta_s} = f_0,$$
$$F_p \mathrm{e}^{i\delta_p} = \frac{2X\sigma_\pi}{M_K^2} f_1 - \frac{\sigma_\pi P L}{X} g_1,$$
$$G_p \mathrm{e}^{i\delta_p} = g_1. \tag{109}$$

The phase shifts are just given by the $\pi\pi$ phases that we use as input. With (80), we find the fitting equations:

$$F_s(s, s_\ell) = (M_0(s, s_\ell) + \hat{M}_0(s, s_\ell))\mathrm{e}^{-i\delta_0^0(s)},$$
$$\tilde{F}_p(s, s_\ell) = (M_1(s, s_\ell) + \hat{M}_1(s, s_\ell))\mathrm{e}^{-i\delta_1^1(s)},$$
$$G_p(s, s_\ell) = (\tilde{M}_1(s, s_\ell) + \hat{\tilde{M}}_1(s, s_\ell))\mathrm{e}^{-i\delta_1^1(s)}. \tag{110}$$

The NA48/2 collaboration has performed phenomenological fits of the form [6,9]

$$\frac{F_s(s, s_\ell)}{f_s} = 1 + \frac{f_s'}{f_s} q^2 + \frac{f_s''}{f_s} q^4 + \frac{f_e'}{f_s} \frac{s_\ell}{4 M_\pi^2},$$
$$\frac{F_p(s, s_\ell)}{f_s} = \frac{f_p}{f_s},$$
$$\frac{G_p(s, s_\ell)}{f_s} = \frac{g_p}{f_s} + \frac{g_p'}{f_s} q^2, \tag{111}$$

where $q^2 = \frac{s}{4 M_\pi^2} - 1$. In a first step, only the normalised coefficients were measured [6]. In a second step, the normalisation f_s was determined from the branching ratio measurement and a phase-space integration, using the parameterisation (111) and the fitted normalised coefficients [9].

However, one should note that from (109) it follows that F_p has to vanish at the $\pi\pi$ threshold like $\sim \sqrt{q^2}$. The phenomenological fit (111) of [6,9], which assumes F_p to be constant in q^2, gives a wrong threshold behaviour. We have not tried to estimate its influence on the determination of the

normalisation f_s. For our purpose, we find it convenient to work with $\tilde{F}_p$, which does not contain kinematic prefactors.

Because all the basis solutions use the same $\pi\pi$ phase as input, the real quantities F_s, $\tilde{F}_p$ and G_p are still linear combinations of the corresponding quantities computed with the basis solutions. Note that the partial waves can be negative, i.e. one really has to rotate the $\pi\pi$ phase away and not just take the absolute value.

For our fits, we use the experimental values of NA48/2 [6,9] and E865 [7,8] on the partial waves. Some remarks on these numbers are appropriate.

- Originally, the published NA48/2 data consisted of 10 bins in s-direction. Very recently, a two-dimensional data set on $F_s(s, s_\ell)$ has become available (addendum to [9]): in this set, not only a single bin but up to 10 bins are used in s_ℓ-direction.
- The barycentre values of s_ℓ for the original 10 bins of NA48/2 also became available in the addendum to [9]. A value of s_ℓ could also be extracted from the relation (106) between F_p, G_p and $\tilde{G}_p$ [33]. However, this value does not agree with the barycentre.
- We compute the value of $\tilde{F}_p$ with (107) using the values of F_p and the barycentre values of s and s_ℓ.
- There is a discrepancy between [6] and [9]. The statistical and systematic uncertainties for F_s in the NA48/2 data have to be calculated from the normalised coefficients in [6]. The correct uncertainties are also listed in the addendum to [9].
- The published values of F_s in the 10 bins of NA48/2 have been normalised in such a way that a fit of the form (111) with $f_e' = 0$ results in $F_s(0,0)/f_s = 1$, although a non-zero value of f_e' has been obtained from a fit to the two-dimensional data set. In order to take the s_ℓ-dependence consistently into account, we have to increase the values of F_s by 0.77 %.
- The E865 experiment has assumed in the analysis that the form factors do not depend on s_ℓ. The values of s_ℓ for each bin were not published.[1]
- The E865 experiment only provides data on the first partial waves F_s and G_p.
- The E865 papers [7,8] include the fully correlated error of the normalisation of 1.2 % in their systematic errors (added in quadrature).[2] It needs a special treatment for unbiased fitting.

In the data analysis of both experiments, radiative corrections have been applied to some extent. More reliable radia-

---

[1] We thank Peter Truöl and Andries van der Schaaf, who performed a new analysis of the Brookhaven data in order to extract the barycentre values of s_ℓ.

[2] We thank Stefan Pislak and Peter Truöl for this additional unpublished information.

tive corrections based on a fixed-order calculation [33] can be applied a posteriori at least to the NA48/2 data. Furthermore, neither the E865 nor the NA48/2 experiment has corrected the isospin-breaking effects due to the quark and meson mass differences. The calculation of [33] also allows for their correction. The resulting numbers are given in Appendix D. We add the uncertainties of the isospin corrections (without the higher-order estimate) in quadrature to the systematic errors. The one-dimensional NA48/2 values also include the mentioned correction of the normalisation of F_s by 0.77 % due to the s_ℓ-dependence.

In addition to the statistical and systematic errors, we take into account the correlations between F_p and G_p of the NA48/2 data, which also became available with the addendum to [9]. There are, however, several correlations that we neglect, either because they are not available or because we assume them to play a minor role. These include the bin-to-bin correlations of the P-waves and the correlations with the S-wave. We also neglect the correlation due to the isospin-breaking corrections and correlations between the two experiments due to external input. We do not expect any of these neglected correlations to significantly affect our fits, but of course it would be better to check this. If the complete set of experimental correlations will become available, it will be possible to do that.

4.2 Soft-pion theorem

In addition to the experimental input on the partial waves, we use the well-known soft-pion theorem (SPT) [34–37] as a second source of information to determine the subtraction constants. The SPT was already employed for the determination of subtraction constants in a different context in [38].

There are two different soft-pion theorems for $K_{\ell 4}$, depending on which pion is taken to be soft. If the momentum p_1 of the positively charged pion is sent to zero, the Mandelstam variables become $s = M_\pi^2, t = M_K^2, u = s_\ell$. Since the SPT is valid only at $\mathcal{O}(M_\pi^2)$, we set $u = s_\ell + M_\pi^2$, such that the relation $s + t + u = M_K^2 + 2M_\pi^2 + s_\ell$ remains valid and one does not need to worry about defining an off-shell form factor.

The first SPT states [12]

$$F(M_\pi^2, M_K^2, M_\pi^2 + s_\ell) - G(M_\pi^2, M_K^2, M_\pi^2 + s_\ell) = \mathcal{O}(M_\pi^2).$$
(112)

If the momentum p_2 of the negatively charged pion is sent to zero, the Mandelstam variables become $s = M_\pi^2, t = s_\ell, u = M_K^2$. We set $t = s_\ell + M_\pi^2$.

The second SPT gives a relation to the $K_{\ell 3}$ vector form factor:

$$F(M_\pi^2, M_\pi^2 + s_\ell, M_K^2) + G(M_\pi^2, M_\pi^2 + s_\ell, M_K^2)$$

$$- \frac{\sqrt{2}M_K}{F_\pi} f_+(M_\pi^2 + s_\ell) = \mathcal{O}(M_\pi^2).$$
(113)

At leading order in χPT, the SPTs are fulfilled exactly, i.e. the right-hand sides of Eqs. (112) and (113) vanish, at NLO and NNLO, there appear $\mathcal{O}(M_\pi^2)$ corrections.

Numerically, it turns out that the first SPT is fulfilled to a higher precision than the second SPT. At NLO, the correction to the first SPT is about 0.4 % for $s_\ell = 0$, the second SPT gets a correction of 2.0 % if $f_+(M_\pi^2)$ is used. If we make the arbitrary replacement $f_+(M_\pi^2) \mapsto f_+(0)$, again an $\mathcal{O}(M_\pi^2)$ effect, the deviation in the second SPT increases to 4.9 %. This confirms that the size of the observed deviations from the SPT is natural.

At NNLO, the corrections become slightly larger.[3] If the $\mathcal{O}(p^6)$ LECs C_i^r are all put to zero and $s_\ell = 0$ as well, the first SPT is fulfilled at 1.0 %, the second at 4.4 % with $f_+(M_\pi^2)$ or 7.6 % with $f_+(0)$. If the C_i^r parts are replaced by the estimates of [11,39] (resonances estimates in the case of $K_{\ell 4}$), the accuracy of the first SPT is 1.5 %, the one of the second SPT 5.4 % using $f_+(M_\pi^2)$ or again 7.6 % using $f_+(0)$.

We use the size of the NNLO corrections to the SPT as an estimate of the tolerance that we allow in the fits when using the SPTs as constraints.

4.3 Fitting method

In the following, we describe how we perform the fit. Basically, we have to deal with a simple linear fit. The only subtlety is the fact that the data contains a fully correlated uncertainty of the normalisation, which is a multiplicative quantity. The fact that we use two experiments with different normalisation errors asks for a special fitting method to avoid a bias [40,41]. We apply the 't_0-method' of [41].

First, we construct a covariance matrix for the observations as follows.

- For all the partial-wave data that we want to fit we construct the covariance matrix with the squared statistical errors on the diagonal and the statistical covariance between the P-waves as off-diagonal elements.
- We add the uncorrelated systematic errors, which do not contain the error of the normalisation, in quadrature to the diagonal entries.
- We may or may not include the two soft-pion theorems as additional observations. If we do so, we take e.g. $F - G$ at the first soft-pion point (SPP) and $F + G$ at the second SPP as observations. As uncertainties, we take a value typical for the deviation in χPT at NNLO, e.g. 1 or 2 %

---

[3] We thank Johan Bijnens and Ilaria Jemos for providing the C++ implementation of the NNLO expressions.

of the LO value of F for the first SPT and a few percent of $\sqrt{2}M_K/F_\pi f_+(0)$ for the second SPT.

- We add the errors of the normalisation to the covariance matrix, which are in block-diagonal form for the data of the two experiments:

$$(\text{cov})_{ij} = (\text{rel.cov.})_{ij} + (\text{norm.cov.})_{ij},$$

$$(\text{norm.cov.})_{ij} = \Delta_I^2 \, f(s^i, s_\ell^i) f(s^j, s_\ell^j)\delta_{I_i,I_j}, \qquad (114)$$

where Δ_I denotes the error of the normalisation for experiment I. I_i is the index of the experiment (1 or 2) corresponding to the data point i and $f(s^i, s_\ell^i)$ is the value of the *fitted* partial wave. In a first step, this value has to be computed under the assumption of some starting values for the fit parameters.

The fit requires then an iteration. One has to minimise the error function defined by

$$\chi^2 = v^T P v, \qquad (115)$$

where v is the vector of the residues, i.e. the differences between the observations and computed values. P is the inverse of the covariance matrix constructed above: $P = (\text{cov})^{-1}$. The minimum of the χ^2 function can be either found with some minimisation routine or, since the fit is linear, directly with the explicit solution

$$\text{par} = (A^T P A)^{-1} A^T P O, \qquad (116)$$

where O is the vector of observations and

$$A_{ij} = \frac{\partial f(s^i, s_\ell^i)}{\partial \text{param}_j} \qquad (117)$$

is the design matrix to be determined with the values of the basis solutions.

With these new values for the fit parameters, one again computes the new covariance matrix (the contribution for the normalisation changes) and iterates this procedure. It turns out that only very few iterations are needed to reach convergence.

If we do not want to determine a parameter through the fit but fix it beforehand to a non-zero value, we have to subtract the fixed contribution from the observations O, such that O is purely linear in the parameters and contains no constant contributions.

In the above discussion, we have not specified what we use as fit parameters. One option is to fit the subtraction constants. Since we want to include an s_ℓ-dependence in the subtraction constants, we write e.g.

$$a^{M_0}(s_\ell) = a_0^{M_0} + a_1^{M_0} \frac{s_\ell}{M_K^2} + \cdots, \qquad (118)$$

where $a_0^{M_0}, a_1^{M_0}, \ldots$ are now the parameters collected in the above vector 'par'. Another option is to use the matching equations to χPT, which provide a linear relation between the subtraction constants and the LECs we are interested in, and perform the fit directly with the LECs.

4.4 Matching to χPT

The final goal of this treatment is the determination of low-energy constants of χPT. Instead of fitting directly the $K_{\ell 4}$ data with the chiral expressions, we use the dispersive representation as an intermediate step. The dispersion relation provides a model-independent resummation of final-state rescattering effects. Therefore, we expect that even the most important effects beyond $\mathcal{O}(p^6)$ are included in the dispersion relation. Of course, in order to extract values for the LECs, one has to perform a matching of the dispersive and the chiral representations. This can be done e.g. on the level of the form factors [12–14]. Since the dispersion relation describes the energy dependence, the matching point can be outside the physical region, i.e. even at lower energies, where χPT is expected to converge better.

Here, we follow an improved strategy for the matching: we match the dispersive and the chiral representations not on the level of form factors but directly on the level of subtraction constants. Since the decomposition (67) is valid up to terms of $\mathcal{O}(p^8)$, the one-loop and even the two-loop result can be written in this form, which allows us to extract a chiral representation of the subtraction constants. This procedure has the advantage that the matching is performed for each function of one variable $M_0(s), \ldots$ at its subtraction point, i.e. at $s = 0$, $t = 0$ and $u = 0$, where indeed the chiral representation is expected to be reliable.

4.4.1 Matching equations at $\mathcal{O}(p^4)$

Reconstruction of the χPT form factors   Let us start by reconstructing the NLO form factors in the standard dispersive form (68).

The LO χPT form factors are given by

$$F_{\text{LO}} = G_{\text{LO}} = \frac{M_K}{\sqrt{2}F_\pi}. \qquad (119)$$

With the partial wave projections (58), we find

$$f_0^{\text{LO}}(s) = \frac{M_K}{\sqrt{2}F_\pi},$$

$$f_1^{\text{LO}}(s) = \frac{M_K}{\sqrt{2}F_\pi}\frac{M_K^2 PL}{2X^2},$$

$$g_1^{\text{LO}}(s) = \frac{M_K}{\sqrt{2}F_\pi}. \qquad (120)$$

The isospin 1/2 form factors (20) are given by

$$F_{\text{LO}}^{(1/2)} = \frac{M_K}{\sqrt{2}F_\pi}, \quad G_{\text{LO}}^{(1/2)} = \frac{\sqrt{2}M_K}{F_\pi}. \tag{121}$$

Hence, the partial waves in the crossed channels (60) are

$$f_{0,\text{LO}}^{(1/2)}(t) = \frac{M_K}{\sqrt{2}F_\pi}\frac{3\Delta_{K\pi} - 5t}{4t},$$

$$f_{1,\text{LO}}^{(1/2)}(t) = \frac{M_K}{\sqrt{2}F_\pi}\frac{3M_K^4(M_\pi^2 - s_\ell - t)}{4t\lambda_{\ell\pi}(t)},$$

$$g_{1,\text{LO}}^{(1/2)}(t) = \frac{3M_K}{2\sqrt{2}F_\pi}, \tag{122}$$

$$f_{0,\text{LO}}^{(3/2)}(u) = \frac{M_K}{\sqrt{2}F_\pi},$$

$$f_{1,\text{LO}}^{(3/2)}(u) = 0,$$

$$g_{1,\text{LO}}^{(3/2)}(u) = 0.$$

The $\pi\pi$-scattering amplitude can be written as [2]

$$T^{(0)}(s,t,u) = 3A(s,t,u) + A(t,u,s) + A(u,s,t),$$
$$T^{(1)}(s,t,u) = A(t,u,s) - A(u,s,t), \tag{123}$$

where at LO

$$A^{\text{LO}}(s,t,u) = \frac{s - M_\pi^2}{F_\pi^2}. \tag{124}$$

The Mandelstam variables for $\pi\pi$ scattering satisfy

$$s + t + u = 4M_\pi^2,$$
$$t = -2q^2(1 - z), \tag{125}$$

where $q^2 = \frac{s}{4} - M_\pi^2$, $z = \cos\theta$. Hence, the $\pi\pi$ partial waves are

$$t_{0,\text{LO}}^0(s) = \frac{1}{2}\int_{-1}^1 \mathrm{d}z\, T_{\text{LO}}^{(0)}(s,z) = \frac{2s - M_\pi^2}{F_\pi^2},$$

$$t_{1,\text{LO}}^1(s) = \frac{3}{2}\int_{-1}^1 \mathrm{d}z\, z T_{\text{LO}}^{(1)}(s,z) = \frac{s - 4M_\pi^2}{F_\pi^2}. \tag{126}$$

The $K\pi$-scattering amplitude is given by [42]

$$T^{(1/2)}(s,t,u) = \frac{3}{2}T^{(3/2)}(u,t,s) - \frac{1}{2}T^{(3/2)}(s,t,u), \tag{127}$$

and at LO

$$T^{(3/2)}(s,t,u) = \frac{1}{2F_\pi^2}(M_K^2 + M_\pi^2 - s). \tag{128}$$

Of course, the Mandelstam variables satisfy here $s + t + u = 2M_K^2 + 2M_\pi^2$. The partial waves are given by

$$t_{0,\text{LO}}^{1/2}(s) = \frac{1}{8sF_\pi^2}(5s^2 - 2s(M_K^2 + M_\pi^2) - 3\Delta_{K\pi}^2),$$

$$t_{1,\text{LO}}^{1/2}(s) = \frac{1}{8sF_\pi^2}(3s^2 - 6s(M_K^2 + M_\pi^2) + 3\Delta_{K\pi}^2), \tag{129}$$

$$t_{0,\text{LO}}^{3/2}(s) = \frac{1}{2F_\pi^2}(M_K^2 + M_\pi^2 - s),$$

$$t_{1,\text{LO}}^{3/2}(s) = 0.$$

Using the unitarity relation for the $K_{\ell4}$ partial waves, we can now easily construct their imaginary parts at NLO:

$$\text{Im} f_l^{\text{NLO}}(s) = \frac{1}{2l+1}\frac{1}{32\pi}\sigma_\pi(s)t_{l,\text{LO}}^{I*}(s)f_l^{\text{LO}}(s),$$

$$\text{Im} g_l^{\text{NLO}}(s) = \frac{1}{2l+1}\frac{1}{32\pi}\sigma_\pi(s)t_{l,\text{LO}}^{I*}(s)g_l^{\text{LO}}(s),$$

$$\text{Im} f_{l,\text{NLO}}^{(I)}(t) = \frac{1}{2l+1}\frac{1}{16\pi}\frac{\lambda_{K\pi}^{1/2}(t)}{t}t_{l,\text{LO}}^{I*}(t)f_{l,\text{LO}}^{(I)}(t), \tag{130}$$

$$\text{Im} g_{l,\text{NLO}}^{(I)}(t) = \frac{1}{2l+1}\frac{1}{16\pi}\frac{\lambda_{K\pi}^{1/2}(t)}{t}t_{l,\text{LO}}^{I*}(t)g_{l,\text{LO}}^{(I)}(t),$$

hence

$$\text{Im} f_0^{\text{NLO}}(s) = \frac{1}{32\pi}\sigma_\pi(s)\frac{M_K(2s - M_\pi^2)}{\sqrt{2}F_\pi^3},$$

$$\text{Im} f_1^{\text{NLO}}(s) = \frac{1}{3}\frac{1}{32\pi}\sigma_\pi(s)\frac{M_K(s - 4M_\pi^2)}{\sqrt{2}F_\pi^3}\frac{M_K^2 PL}{2X^2},$$

$$\text{Im} g_1^{\text{NLO}}(s) = \frac{1}{3}\frac{1}{32\pi}\sigma_\pi(s)\frac{M_K(s - 4M_\pi^2)}{\sqrt{2}F_\pi^3},$$

$$\text{Im} f_{0,\text{NLO}}^{(1/2)}(t) = \frac{1}{16\pi}\frac{\lambda_{K\pi}^{1/2}(t)}{t}\frac{M_K}{32\sqrt{2}t^2 F_\pi^3}$$
$$\times (5t^2 - 2t(M_K^2 + M_\pi^2) - 3\Delta_{K\pi}^2)$$
$$\times (3\Delta_{K\pi} - 5t),$$

$$\text{Im} f_{1,\text{NLO}}^{(1/2)}(t) = \frac{1}{16\pi}\frac{\lambda_{K\pi}^{1/2}(t)}{t}\frac{M_K}{8\sqrt{2}t F_\pi^3}$$
$$\times (3t^2 - 6t(M_K^2 + M_\pi^2) + 3\Delta_{K\pi}^2)$$
$$\times \frac{M_K^4(M_\pi^2 - s_\ell - t)}{4t\lambda_{\ell\pi}(t)},$$

$$\text{Im} g_{1,\text{NLO}}^{(1/2)}(t) = \frac{1}{16\pi}\frac{\lambda_{K\pi}^{1/2}(t)}{t}\frac{M_K}{16\sqrt{2}t F_\pi^3}$$
$$\times (3t^2 - 6t(M_K^2 + M_\pi^2) + 3\Delta_{K\pi}^2),$$

$$\mathrm{Im} f_{0,\mathrm{NLO}}^{(3/2)}(u) = \frac{1}{16\pi} \frac{\lambda_{K\pi}^{1/2}(u)}{u} \frac{M_K}{2\sqrt{2}F_\pi^3} (M_K^2 + M_\pi^2 - u),$$

$$\mathrm{Im} f_{1,\mathrm{NLO}}^{(3/2)}(u) = 0,$$

$$\mathrm{Im} g_{1,\mathrm{NLO}}^{(3/2)}(u) = 0. \tag{131}$$

By inserting these imaginary parts into the dispersion integrals in (68), we can reconstruct the NLO form factors. For the comparison with the explicit loop calculation, we rewrite the dispersive integrals in terms of loop functions (see Appendix A):

$$M_0^{\mathrm{NLO}}(s) = m_{0,\mathrm{NLO}}^0 + m_{0,\mathrm{NLO}}^1 \frac{s}{M_K^2} + \frac{M_K}{2\sqrt{2}F_\pi^3}$$

$$\times ((2s - M_\pi^2)(\bar{B}_{\pi\pi}(s) - \bar{B}_{\pi\pi}(0))$$

$$+ M_\pi^2 s \bar{B}_{\pi\pi}'(0)),$$

$$M_1^{\mathrm{NLO}}(s) = m_{1,\mathrm{NLO}}^0,$$

$$\tilde{M}_1^{\mathrm{NLO}}(s) = \tilde{m}_{1,\mathrm{NLO}}^0 + \tilde{m}_{1,\mathrm{NLO}}^1 \frac{s}{M_K^2} + \frac{M_K}{6\sqrt{2}F_\pi^3}$$

$$\times ((s - 4M_\pi^2)(\bar{B}_{\pi\pi}(s) - \bar{B}_{\pi\pi}(0))$$

$$+ 4M_\pi^2 s \bar{B}_{\pi\pi}'(0)),$$

$$N_0^{\mathrm{NLO}}(t) = n_{0,\mathrm{NLO}}^1 \frac{t}{M_K^2} + \frac{M_K}{32\sqrt{2}F_\pi^3}$$

$$\times \Bigg((-25t + 5(5M_K^2 - M_\pi^2))$$

$$\times (\bar{B}_{K\pi}(t) - \bar{B}_{K\pi}(0))$$

$$+ \frac{3\Delta_{K\pi}}{t^2} (t(3M_K^2 - 7M_\pi^2) - 3\Delta_{K\pi}^2)$$

$$\times \Bigg(\bar{B}_{K\pi}(t) - \bar{B}_{K\pi}(0) - t \bar{B}_{K\pi}'(0)$$

$$- \frac{t^2}{2} \bar{B}_{K\pi}''(0) \Bigg) - 5t(5M_K^2 - M_\pi^2)\bar{B}_{K\pi}'(0)$$

$$+ \frac{3}{2} t \Delta_{K\pi}^3 \bar{B}_{K\pi}'''(0) \Bigg),$$

$$N_1^{\mathrm{NLO}}(t) = 0,$$

$$\tilde{N}_1^{\mathrm{NLO}}(t) = \frac{3M_K^3}{16\sqrt{2}F_\pi^3} \Bigg(\frac{1}{t^2}(t^2 - 2t(M_K^2 + M_\pi^2) + \Delta_{K\pi}^2)$$

$$\times (\bar{B}_{K\pi}(t) - \bar{B}_{K\pi}(0)) + \frac{1}{t}(2t(M_K^2 + M_\pi^2)$$

$$- \Delta_{K\pi}^2)\bar{B}_{K\pi}'(0) - \frac{\Delta_{K\pi}^2}{2} \bar{B}_{K\pi}''(0) \Bigg),$$

$$R_0^{\mathrm{NLO}}(u) = \frac{M_K}{2\sqrt{2}F_\pi^3} ((M_K^2 + M_\pi^2 - u)(\bar{B}_{K\pi}(u) - \bar{B}_{K\pi}(0))$$

$$- (M_K^2 + M_\pi^2)u \bar{B}_{K\pi}'(0)),$$

$$R_1^{\mathrm{NLO}}(u) = 0,$$

$$\tilde{R}_1^{\mathrm{NLO}}(u) = 0. \tag{132}$$

We can now compare this expression with the one-loop calculation [10,43,44]. As in our dispersive treatment, we only consider $\pi\pi$ intermediate states in the s-channel and $K\pi$ intermediate states in the crossed channels, the $K\bar{K}$ and $\eta\eta$ loops in the s-channel and the $K\eta$ loops in the t-channel have to be expanded in a Taylor series and absorbed by the subtraction polynomial. The comparison of the dispersive representation with the loop calculation then allows for the extraction of the $\mathcal{O}(p^4)$ values for the subtraction constants.

Note that the only contributions that we neglect when writing the $\mathcal{O}(p^4)$ loop calculation in the dispersive form are the second- and higher-order Taylor coefficients of the expanded loop functions of higher intermediate states ($K\bar{K}$, $\eta\eta$ and $K\eta$). The result for the $\mathcal{O}(p^4)$ subtraction constants can be found in Appendix E.1.

χPT *form factors in the Omnès representation*   The reason why we do not use the standard dispersive form (68) for the numerical solution of the dispersion relation but rather the Omnès representation (85) is mainly the separation of final-state rescattering effects: the Omnès function resums the most important rescattering effects. The remaining dispersive integrals take the interplay of the different channels into account.

It is therefore desirable to perform the matching to χPT not on the level of the standard dispersive form but directly with the Omnès representation. This should avoid mixing the final-state resummation with the determination of the LECs.

However, it is not possible to write directly the χPT representation in the Omnès form, because the chiral expansion of the phase shifts does not have the correct asymptotic behaviour. At LO, the phases grow linearly, hence the Omnès dispersion integral (83) is logarithmically divergent. Therefore, we subtract the dispersion integral once more:

$$\Omega(s) = \exp\left(\frac{s}{\pi} \int_{s_0}^{\infty} \frac{\delta(s')}{(s'-s-i\epsilon)s'} ds' \right)$$

$$= \exp\left(\frac{s}{\pi} \int_{s_0}^{\infty} \frac{\delta(s')}{s'^2} ds' + \frac{s^2}{\pi} \int_{s_0}^{\infty} \frac{\delta(s')}{(s'-s-i\epsilon)s'^2} ds' \right)$$

$$=: \exp\left(\omega \frac{s}{M_K^2} + \frac{s^2}{\pi} \int_{s_0}^{\infty} \frac{\delta(s')}{(s'-s-i\epsilon)s'^2} ds' \right). \tag{133}$$

ω is divergent if evaluated in χPT. Let us postpone the determination of this constant for a moment.

Let us now use the Omnès representation to reconstruct the NLO result for the form factors. At LO, the functions of one variable are simply given by

$$M_0^{\text{LO}}(s) = \tilde{M}_1^{\text{LO}}(s) = \frac{M_K}{\sqrt{2}F_\pi},$$
$$M_1^{\text{LO}}(s) = N_0^{\text{LO}}(t) = N_1^{\text{LO}}(t) = \tilde{N}_1^{\text{LO}}(t)$$
$$= R_0^{\text{LO}}(u) = R_1^{\text{LO}}(u) = \tilde{R}_1^{\text{LO}}(u) = 0. \qquad (134)$$

We start by calculating the hat functions at LO:

$$\hat{M}_0^{\text{LO}}(s) = \hat{M}_1^{\text{LO}}(s) = \hat{\tilde{M}}_1^{\text{LO}}(s) = \hat{N}_1^{\text{LO}}(t) = \hat{R}_1^{\text{LO}}(u)$$
$$= \hat{\tilde{R}}_1^{\text{LO}}(u) = 0,$$
$$\hat{N}_0^{\text{LO}}(t) = \frac{M_K}{\sqrt{2}F_\pi}\frac{3\Delta_{K\pi} - 5t}{4t},$$
$$\hat{\tilde{N}}_1^{\text{LO}}(t) = \frac{M_K}{\sqrt{2}F_\pi}\frac{3M_K^2}{2t},$$
$$\hat{R}_0^{\text{LO}}(u) = \frac{M_K}{\sqrt{2}F_\pi}. \qquad (135)$$

Further, we need the phase shifts at LO:

$$\delta_{0,\text{LO}}^0(s) = \frac{1}{32\pi F_\pi^2}(2s - M_\pi^2)\sigma_\pi(s),$$

$$\delta_{1,\text{LO}}^1(s) = \frac{1}{96\pi F_\pi^2}(s - 4M_\pi^2)\sigma_\pi(s),$$

$$\delta_{0,\text{LO}}^{1/2}(t) = \frac{1}{128\pi F_\pi^2}(5t^2 - 2t(M_K^2 + M_\pi^2) - 3\Delta_{K\pi}^2)\frac{\lambda_{K\pi}^{1/2}(t)}{t^2},$$

$$\delta_{1,\text{LO}}^{1/2}(t) = \frac{1}{384\pi F_\pi^2}(3t^2 - 6t(M_K^2 + M_\pi^2) + 3\Delta_{K\pi}^2)\frac{\lambda_{K\pi}^{1/2}(t)}{t^2},$$

$$\delta_{0,\text{LO}}^{3/2}(u) = \frac{1}{32\pi F_\pi^2}(M_K^2 + M_\pi^2 - u)\frac{\lambda_{K\pi}^{1/2}(u)}{u},$$

$$\delta_{1,\text{LO}}^{3/2}(u) = 0. \qquad (136)$$

We expand the Omnès representation (85) at NLO:

$$M_0^{\text{NLO}}(s) = \left(1 + \omega_0^0\frac{s}{M_K^2} + \frac{s^2}{\pi}\int_{s_0}^\infty\frac{\delta_{0,\text{LO}}^0(s')}{(s'-s-i\epsilon)s'^2}ds'\right)$$
$$\times\left(a^{M_0} + b^{M_0}\frac{s}{M_K^2} + c^{M_0}\frac{s^2}{M_K^4}\right),$$

$$M_1^{\text{NLO}}(s) = \left(1 + \omega_1^1\frac{s}{M_K^2} + \frac{s^2}{\pi}\int_{s_0}^\infty\frac{\delta_{1,\text{LO}}^1(s')}{(s'-s-i\epsilon)s'^2}ds'\right)$$

$$\times\left(a^{M_1} + b^{M_1}\frac{s}{M_K^2}\right),$$

$$\tilde{M}_1^{\text{NLO}}(s) = \left(1 + \omega_1^1\frac{s}{M_K^2} + \frac{s^2}{\pi}\int_{s_0}^\infty\frac{\delta_{1,\text{LO}}^1(s')}{(s'-s-i\epsilon)s'^2}ds'\right)$$
$$\times\left(a^{\tilde{M}_1} + b^{\tilde{M}_1}\frac{s}{M_K^2} + c^{\tilde{M}_1}\frac{s^2}{M_K^4}\right),$$

$$N_0^{\text{NLO}}(t) = \left(1 + \omega_0^{1/2}\frac{t}{M_K^2} + \frac{t^2}{\pi}\int_{t_0}^\infty\frac{\delta_{0,\text{LO}}^{1/2}(t')}{(t'-t-i\epsilon)t'^2}dt'\right)$$
$$\times\left(b^{N_0}\frac{t}{M_K^2} + \frac{t^2}{\pi}\int_{t_0}^\infty\frac{\hat{N}_0^{\text{LO}}(t')\delta_{0,\text{LO}}^{1/2}(t')}{(t'-t-i\epsilon)t'^2}dt'\right),$$

$$N_1^{\text{NLO}}(t) = 0,$$

$$\tilde{N}_1^{\text{NLO}}(t) = \left(1 + \omega_1^{1/2}\frac{t}{M_K^2} + \frac{t^2}{\pi}\int_{t_0}^\infty\frac{\delta_{1,\text{LO}}^{1/2}(t')}{(t'-t-i\epsilon)t'^2}dt'\right)$$
$$\times\left(\frac{t}{\pi}\int_{t_0}^\infty\frac{\hat{\tilde{N}}_1^{\text{LO}}(t')\delta_{1,\text{LO}}^{1/2}(t')}{(t'-t-i\epsilon)t'}dt'\right),$$

$$R_0^{\text{NLO}}(u) = \left(1 + \omega_0^{3/2}\frac{u}{M_K^2} + \frac{u^2}{\pi}\int_{u_0}^\infty\frac{\delta_{0,\text{LO}}^{3/2}(u')}{(u'-u-i\epsilon)u'^2}du'\right)$$
$$\times\left(\frac{u^2}{\pi}\int_{u_0}^\infty\frac{\hat{R}_0^{\text{LO}}(u')\delta_{0,\text{LO}}^{3/2}(u')}{(u'-u-i\epsilon)u'^2}du'\right),$$

$$R_1^{\text{NLO}}(u) = 0,$$
$$\tilde{R}_1^{\text{NLO}}(u) = 0. \qquad (137)$$

If we further expand these expressions chirally and neglect higher orders, we obtain (note that only a^{M_0} and $a^{\tilde{M}_1}$ do not vanish at LO)

$$M_0^{\text{NLO}}(s) = a_{\text{LO}}^{M_0}\left(1 + \omega_0^0\frac{s}{M_K^2} + \frac{s^2}{\pi}\int_{s_0}^\infty\frac{\delta_{0,\text{LO}}^0(s')}{(s'-s-i\epsilon)s'^2}ds'\right)$$
$$+ \Delta a_{\text{NLO}}^{M_0} + b_{\text{NLO}}^{M_0}\frac{s}{M_K^2} + c_{\text{NLO}}^{M_0}\frac{s^2}{M_K^4},$$

$$M_1^{\text{NLO}}(s) = a_{\text{NLO}}^{M_1} + b_{\text{NLO}}^{M_1}\frac{s}{M_K^2},$$

$$\tilde{M}_1^{\text{NLO}}(s) = a_{\text{LO}}^{\tilde{M}_1}\left(1 + \omega_1^1\frac{s}{M_K^2} + \frac{s^2}{\pi}\int_{s_0}^\infty\frac{\delta_{1,\text{LO}}^1(s')}{(s'-s-i\epsilon)s'^2}ds'\right)$$
$$+ \Delta a_{\text{NLO}}^{\tilde{M}_1} + b_{\text{NLO}}^{\tilde{M}_1}\frac{s}{M_K^2} + c_{\text{NLO}}^{\tilde{M}_1}\frac{s^2}{M_K^4},$$

$$N_0^{\text{NLO}}(t) = b_{\text{NLO}}^{N_0}\frac{t}{M_K^2} + \frac{t^2}{\pi}\int_{t_0}^\infty\frac{\hat{N}_0^{\text{LO}}(t')\delta_{0,\text{LO}}^{1/2}(t')}{(t'-t-i\epsilon)t'^2}dt',$$

$$N_1^{\text{NLO}}(t) = 0,$$

$$\tilde{N}_1^{\text{NLO}}(t) = \frac{t}{\pi}\int_{t_0}^\infty\frac{\hat{\tilde{N}}_1^{\text{LO}}(t')\delta_{1,\text{LO}}^{1/2}(t')}{(t'-t-i\epsilon)t'}dt',$$

$$R_0^{\mathrm{NLO}}(u) = \frac{u^2}{\pi} \int_{u_0}^{\infty} \frac{\hat{R}_0^{\mathrm{LO}}(u')\delta_{0,\mathrm{LO}}^{3/2}(u')}{(u'-u-i\epsilon)u'^2}\,\mathrm{d}u',$$

$$R_1^{\mathrm{NLO}}(u) = 0,$$

$$\tilde{R}_1^{\mathrm{NLO}}(u) = 0, \tag{138}$$

where

$$a_{\mathrm{NLO}}^{M_0} = a_{\mathrm{LO}}^{M_0} + \Delta a_{\mathrm{NLO}}^{M_0}, \quad a_{\mathrm{LO}}^{M_0} = \frac{M_K}{\sqrt{2}F_\pi},$$
$$a_{\mathrm{NLO}}^{\tilde{M}_1} = a_{\mathrm{LO}}^{\tilde{M}_1} + \Delta a_{\mathrm{NLO}}^{\tilde{M}_1}, \quad a_{\mathrm{LO}}^{\tilde{M}_1} = \frac{M_K}{\sqrt{2}F_\pi}. \tag{139}$$

Next, we insert the LO phases and hat functions:

$$M_0^{\mathrm{NLO}}(s) = a_{\mathrm{NLO}}^{M_0} + \left(b_{\mathrm{NLO}}^{M_0} + \frac{M_K}{\sqrt{2}F_\pi}\omega_0^0\right)\frac{s}{M_K^2} + c_{\mathrm{NLO}}^{M_0}\frac{s^2}{M_K^4},$$
$$+\frac{s^2}{\pi}\int_{s_0}^{\infty}\frac{1}{(s'-s-i\epsilon)s'^2}\frac{\sigma_\pi(s')}{32\pi}$$
$$\times\frac{M_K(2s'-M_\pi^2)}{\sqrt{2}F_\pi^3}\,\mathrm{d}s',$$

$$M_1^{\mathrm{NLO}}(s) = a_{\mathrm{NLO}}^{M_1} + b_{\mathrm{NLO}}^{M_1}\frac{s}{M_K^2},$$

$$\tilde{M}_1^{\mathrm{NLO}}(s) = a_{\mathrm{NLO}}^{\tilde{M}_1} + \left(b_{\mathrm{NLO}}^{\tilde{M}_1} + \frac{M_K}{\sqrt{2}F_\pi}\omega_1^1\right)\frac{s}{M_K^2} + c_{\mathrm{NLO}}^{\tilde{M}_1}\frac{s^2}{M_K^4}$$
$$+\frac{s^2}{\pi}\int_{s_0}^{\infty}\frac{1}{(s'-s-i\epsilon)s'^2}\frac{\sigma_\pi(s')}{32\pi}$$
$$\times\frac{M_K(s'-4M_\pi^2)}{3\sqrt{2}F_\pi^3}\,\mathrm{d}s',$$

$$N_0^{\mathrm{NLO}}(t) = b_{\mathrm{NLO}}^{N_0}\frac{t}{M_K^2} + \frac{t^2}{\pi}\int_{t_0}^{\infty}\frac{1}{(t'-t-i\epsilon)t'^2}$$
$$\times\frac{\lambda_{K\pi}^{1/2}(t')}{16\pi t'}\frac{M_K(3\Delta_{K\pi}-5t')}{32\sqrt{2}t'^2F_\pi^3}$$
$$\times(5t'^2-2t'(M_K^2+M_\pi^2)-3\Delta_{K\pi}^2)\mathrm{d}t',$$

$$N_1^{\mathrm{NLO}}(t) = 0,$$

$$\tilde{N}_1^{\mathrm{NLO}}(t) = \frac{t}{\pi}\int_{t_0}^{\infty}\frac{1}{(t'-t-i\epsilon)t'}\frac{\lambda_{K\pi}^{1/2}(t')}{16\pi t'}\frac{M_K^3}{16\sqrt{2}t'^2F_\pi^3}$$
$$\times(3t'^2-6t'(M_K^2+M_\pi^2)+3\Delta_{K\pi}^2)\mathrm{d}t',$$

$$R_0^{\mathrm{NLO}}(u) = \frac{u^2}{\pi}\int_{u_0}^{\infty}\frac{1}{(u'-u-i\epsilon)u'^2}\frac{\lambda_{K\pi}^{1/2}(u')}{16\pi u'}\frac{M_K}{2\sqrt{2}F_\pi^3}$$
$$\times(M_K^2+M_\pi^2-u')\mathrm{d}u',$$

$$R_1^{\mathrm{NLO}}(u) = 0,$$

$$\tilde{R}_1^{\mathrm{NLO}}(u) = 0. \tag{140}$$

We see that the form of the Omnès representation is completely equivalent to the standard representation, apart from the presence of the additional subtraction constants c^{M_0}, b^{M_1} and $c^{\tilde{M}_1}$, which also need to be determined. We expand the

t-channel $K\eta$ integrals up to linear terms in t and find

$$a_{\mathrm{NLO}}^{M_0} = m_{0,\mathrm{NLO}}^0,$$

$$b_{\mathrm{NLO}}^{M_0} = m_{0,\mathrm{NLO}}^1 - \frac{M_K}{\sqrt{2}F_\pi}\omega_0^0,$$

$$c_{\mathrm{NLO}}^{M_0} = \frac{M_K^3}{\sqrt{2}F_\pi^3}\frac{15M_\eta^4+M_K^2M_\pi^2}{1920\pi^2M_\eta^4},$$

$$a_{\mathrm{NLO}}^{M_1} = m_{1,\mathrm{NLO}}^0,$$

$$b_{\mathrm{NLO}}^{M_1} = 0, \tag{141}$$

$$a_{\mathrm{NLO}}^{\tilde{M}_1} = \tilde{m}_{1,\mathrm{NLO}}^0,$$

$$b_{\mathrm{NLO}}^{\tilde{M}_1} = \tilde{m}_{1,\mathrm{NLO}}^1 - \frac{M_K}{\sqrt{2}F_\pi}\omega_1^1,$$

$$c_{\mathrm{NLO}}^{\tilde{M}_1} = \frac{M_K^3}{\sqrt{2}F_\pi^3}\frac{1}{1920\pi^2},$$

$$b_{\mathrm{NLO}}^{N_0} = n_{0,\mathrm{NLO}}^1.$$

The constants ω_0^0 and ω_1^1 cannot be evaluated with the chiral phases. If we evaluate them with the physical phases, this leads to exactly the same matching equations for the determination of the L_i^r as if we would match the Taylor expansion of the Omnès representation with the Taylor expansion of the chiral result. Note, however, that the expressions obtained for c^{M_0}, b^{M_1} and $c^{\tilde{M}_1}$ are different. E.g. for b^{M_1}, the chiral expansion leads to $b_{\mathrm{NLO}}^{M_1} = 0$ while a Taylor expansion of the dispersion relation would require $b^{M_1} = -m_{1,\mathrm{NLO}}^0\Omega_1^{1'}(0)M_K^2$, where $\Omega_1^{1'}$ is the derivative of the Omnès function calculated with the physical phases. Of course, the difference is a higher-order effect in the chiral counting. As higher-order effects can be important if due to final-state rescattering, we would not like to intermingle them with the matching of the subtraction constants. The matching on the basis of Taylor coefficients would require the linear term of $M_1(s)$ to vanish exactly, while the matching based on the chiral expansion of the dispersion relation gives a non-zero linear term in $M_1(s)$ due to the Omnès function – this is important information which we wish to make use of in our fits.

4.4.2 Matching equations at $\mathcal{O}(p^6)$

Decomposition of the NNLO form factors   In the following, we describe the decomposition of the two-loop result such that the matching can be performed at NNLO. Since the NNLO chiral result has a different asymptotic behaviour than the NLO result and our numerical dispersive representation, we have to use the representation (69), which uses a different gauge and more subtractions than (68).

The imaginary parts of the $K_{\ell 4}$ partial waves at NNLO could again be reconstructed using the unitarity relations, e.g.

$$\text{Im} f_l^{\text{NNLO}}(s) = \frac{1}{2l+1} \frac{1}{32\pi} \sigma_\pi(s) (t_{l,\text{LO}}^{I*}(s) f_l^{\text{LO}}(s)$$

$$+ \Delta t_{l,\text{NLO}}^{I*}(s) f_l^{\text{LO}}(s) + t_{l,\text{LO}}^{I*}(s) \Delta f_l^{\text{NLO}}(s)). \tag{142}$$

However, instead of proceeding as for NLO, it is more straightforward to decompose the two-loop result directly into functions of one variable, then to impose the gauge condition and extract the Taylor coefficients of the functions of one variable.

The two-loop result for the form factors F and G was computed in [11]. We have the full expressions in form of a C++ program at hand.[4] It has the following structure:

$$X^{\text{NNLO}}(s,t,u) = X^{\text{LO}} + X_L^{\text{NLO}}(s,t,u) + X_R^{\text{NLO}}(s,t,u)$$

$$+ X_C^{\text{NNLO}}(s,t,u) + X_L^{\text{NNLO}}(s,t,u) + X_P^{\text{NNLO}}(s,t,u)$$

$$+ X_{VS}^{\text{NNLO}}(s,t,u) + X_{VT}^{\text{NNLO}}(s,t,u) + X_{VU}^{\text{NNLO}}(s,t,u), \tag{143}$$

where $X \in \{F, G\}$ and the different parts denote the following:

- X_L^{NLO}: NLO polynomial containing the LECs L_i^r,
- X_R^{NLO}: NLO loops,
- X_C^{NNLO}: NNLO polynomial containing the LECs C_i^r,
- X_L^{NNLO}: NNLO part containing $L_i^r \times L_i^r$ and $L_i^r \times$ loop,
- X_P^{NNLO}: NNLO two-loop part without vertex integrals,
- X_{VS}^{NNLO}: NNLO vertex integrals in the s-channel,
- X_{VT}^{NNLO}: NNLO vertex integrals in the t-channel,
- X_{VU}^{NNLO}: NNLO vertex integrals in the u-channel.

In Appendix E.2.1, we perform the explicit decomposition of the two-loop result into functions of one Mandelstam variable according to (67) and (69) and evaluate numerically the subtraction constants.

NNLO form factors in the Omnès representation   As we already pointed out for the NLO matching, it is desirable to use the Omnès representation rather than the standard dispersion relation for the matching and the determination of the LECs. Let us therefore derive the matching equations at NNLO in the Omnès scheme.

---

[4] We thank Johan Bijnens and Ilaria Jemos for providing the C++ implementation of the NNLO expressions.

We have to use the second gauge for the decomposition of the NNLO representation (69). As a starting point, let us find the NLO Omnès subtraction constants in the second gauge. In the first gauge, we found $R_1^{\text{NLO}} = \tilde{R}_1^{\text{NLO}} = 0$, hence

$$c_{\text{NLO}}^{R_0} = \frac{M_K}{\sqrt{2}F_\pi^3} \frac{M_K^4}{4} ((M_K^2 + M_\pi^2) \bar{B}_{K\pi}''(0) - 2\bar{B}_{K\pi}'(0)),$$

$$a_{\text{NLO}}^{R_1} = b_{\text{NLO}}^{\tilde{R}_1} = 0. \tag{144}$$

The gauge transformation (74) is then defined by

$$C_{\text{NLO}}^{R_0} = \frac{M_K}{\sqrt{2}F_\pi^3} \frac{1}{32\pi^2} \frac{M_K^4}{\Delta_{K\pi}^4}$$

$$\times \left(\frac{(M_K^2 + M_\pi^2)(M_K^4 - 8M_K^2 M_\pi^2 + M_\pi^4)}{3} + \frac{4M_K^4 M_\pi^4 \ln\left(\frac{M_K^2}{M_\pi^2}\right)}{\Delta_{K\pi}} \right),$$

$$A_{\text{NLO}}^{R_1} = B_{\text{NLO}}^{\tilde{R}_1} = 0. \tag{145}$$

At NLO, the shifts in the subtraction constants (C.5) are therefore given by

$$\delta a_{\text{NLO}}^{M_0} = \frac{\Sigma_0^2 - \Delta_{K\pi}\Delta_{\ell\pi}}{M_K^4} C_{\text{NLO}}^{R_0}, \quad \delta b_{\text{NLO}}^{M_0} = -\frac{2\Sigma_0}{M_K^2} C_{\text{NLO}}^{R_0},$$

$$\delta c_{\text{NLO}}^{M_0} = C_{\text{NLO}}^{R_0}, \quad \delta d_{\text{NLO}}^{M_0} = 0,$$

$$\delta a_{\text{NLO}}^{M_1} = -\frac{2\Sigma_0}{M_K^2} C_{\text{NLO}}^{R_0},$$

$$\delta b_{\text{NLO}}^{M_1} = 2C_{\text{NLO}}^{R_0}, \quad \delta c_{\text{NLO}}^{M_1} = 0,$$

$$\delta a_{\text{NLO}}^{\tilde{M}_1} = -\frac{\Sigma_0^2 - \Delta_{K\pi}\Delta_{\ell\pi}}{M_K^4} C_{\text{NLO}}^{R_0}, \quad \delta b_{\text{NLO}}^{\tilde{M}_1} = \frac{2\Sigma_0}{M_K^2} C_{\text{NLO}}^{R_0},$$

$$\delta c_{\text{NLO}}^{\tilde{M}_1} = -C_{\text{NLO}}^{R_0}, \quad \delta d_{\text{NLO}}^{\tilde{M}_1} = 0,$$

$$\delta b_{\text{NLO}}^{N_0} = -\frac{3(\Delta_{K\pi} + 2\Sigma_0)}{4M_K^2} C_{\text{NLO}}^{R_0}, \quad \delta c_{\text{NLO}}^{N_0} = -\frac{5}{4} C_{\text{NLO}}^{R_0},$$

$$\delta a_{\text{NLO}}^{N_1} = \frac{3}{2} C_{\text{NLO}}^{R_0}, \quad \delta b_{\text{NLO}}^{\tilde{N}_1} = -\frac{3}{2} C_{\text{NLO}}^{R_0},$$

$$\delta c_{\text{NLO}}^{R_0} = C_{\text{NLO}}^{R_0}, \quad \delta a_{\text{NLO}}^{R_1} = 0, \quad \delta b_{\text{NLO}}^{\tilde{R}_1} = 0. \tag{146}$$

When studying now the Omnès representation at NNLO, we notice that the asymptotic behaviour of the phases at NNLO is even worse than at NLO, hence we have to subtract the Omnès function three times:

$$\Omega(s) = \exp\left(\frac{s}{\pi} \int_{s_0}^{\infty} \frac{\delta(s')}{(s'-s-i\epsilon)s'} ds' \right)$$

$$= \exp\left(\frac{s}{\pi} \int_{s_0}^{\infty} \frac{\delta(s')}{s'^2} ds' \right)$$

$$+ \frac{s^2}{\pi} \int_{s_0}^{\infty} \frac{\delta(s')}{s'^3} ds' + \frac{s^3}{\pi} \int_{s_0}^{\infty} \frac{\delta(s')}{(s'-s-i\epsilon)s'^3} ds' \Big)$$

$$=: \exp\left(\omega \frac{s}{M_K^2} + \bar{\omega} \frac{s^2}{M_K^4} + \frac{s^3}{\pi} \int_{s_0}^{\infty} \frac{\delta(s')}{(s'-s-i\epsilon)s'^3} ds'\right).$$

$$(147)$$

ω and $\bar{\omega}$ are both divergent if evaluated in χPT at NNLO, hence we will use the physical phases to determine them.

In the case of the NLO matching, we have derived the relation between the standard and the Omnès subtraction constants (141) by comparing the Taylor coefficients of the chirally expanded Omnès representation with the Taylor coefficients of the standard dispersive representation. Although it is instructive to understand the chiral expansion of the Omnès representation, a shortcut can be taken. Note that the chiral expansion and the Taylor expansion are interchangeable. Therefore, we easily obtain the relations between the standard subtraction constants $m_0^0, \ldots$ and the Omnès subtraction constants $a^{M_0}, \ldots$ by chirally expanding the Taylor coefficients of the Omnès representation (C.1) and comparing it with the Taylor coefficients of (69).

This leads to the following relations between the relevant subtraction constants:

$$m_0^{0,\text{NNLO}} = a_{\text{NNLO}}^{M_0},$$

$$m_0^{1,\text{NNLO}} = b_{\text{NNLO}}^{M_0} + \omega_0^0 a_{\text{NLO}}^{M_0},$$

$$m_0^{2,\text{NNLO}} = c_{\text{NNLO}}^{M_0} + \omega_0^0 b_{\text{NLO}}^{M_0} + \frac{1}{2}\omega_0^{0^2} a_{\text{LO}}^{M_0} + a_{\text{NLO}}^{M_0}\bar{\omega}_0^0 + \text{h.o.},$$

$$m_1^{0,\text{NNLO}} = a_{\text{NNLO}}^{M_1},$$

$$m_1^{1,\text{NNLO}} = b_{\text{NNLO}}^{M_1} + \omega_1^1 a_{\text{NLO}}^{M_1},$$

$$\tilde{m}_1^{0,\text{NNLO}} = a_{\text{NNLO}}^{\tilde{M}_1},$$

$$\tilde{m}_1^{1,\text{NNLO}} = b_{\text{NNLO}}^{\tilde{M}_1} + \omega_1^1 a_{\text{NLO}}^{\tilde{M}_1},$$

$$\tilde{m}_1^{2,\text{NNLO}} = c_{\text{NNLO}}^{\tilde{M}_1} + \omega_1^1 b_{\text{NLO}}^{\tilde{M}_1} + \frac{1}{2}\omega_1^{1^2} a_{\text{LO}}^{\tilde{M}_1} + a_{\text{NLO}}^{\tilde{M}_1}\bar{\omega}_1^1 + \text{h.o.},$$

$$n_0^{1,\text{NNLO}} = b_{\text{NNLO}}^{N_0},$$

$$n_0^{2,\text{NNLO}} = c_{\text{NNLO}}^{N_0} + \omega_0^{1/2} b_{\text{NLO}}^{N_0},$$

$$n_1^{0,\text{NNLO}} = a_{\text{NNLO}}^{N_1},$$

$$\tilde{n}_1^{1,\text{NNLO}} = b_{\text{NNLO}}^{\tilde{N}_1}.$$

$$(148)$$

The NNLO chiral expansion of the full Omnès representation can be found in Appendix E.2.2 and leads to the same result. It can be used to identify all the imaginary parts and to connect the different dispersive integrals with the discontinuities of the loop diagrams.

5 Results

In this chapter, we discuss the results for the low-energy constants that we determine by fitting the dispersive representation to data and matching it to χPT. In order to understand the differences between the results at NLO and NNLO and the source of complications that appear at NNLO, it is useful to study in a first step the results of direct χPT fits. We perform direct fits at NLO and NNLO and compare our results with the literature before using the whole machinery of the dispersive framework matched to χPT at NLO and finally at NNLO.

5.1 Comparison of direct χPT fits

The most recent fits to $K_{\ell 4}$ data performed in the literature are [45]. There a global fit is performed, taking into account the threshold expansion parameters of the $K_{\ell 4}$ form factor measurement of NA48/2 [9]:

$$F = f_s + f_s' q^2 + \cdots,$$
$$f_s = 5.705 \pm 0.035, \quad f_s' = 0.867 \pm 0.050$$
$$G = g_p + g_p' q^2 + \cdots,$$
$$g_p = 4.952 \pm 0.086, \quad g_p' = 0.508 \pm 0.122, \quad (149)$$

where $q^2 = \frac{s}{4M_\pi^2} - 1$. In [45], the above quantities are fitted with the form factors at $\cos\theta = 0$ instead of the first partial wave. In addition to the $K_{\ell 4}$ form factor data, the global fit of [45] uses many other inputs, like data on the different decay constants and masses, $\pi\pi$- and $K\pi$-scattering parameters, quark mass ratios etc.

We compare now different strategies for direct fits with the results of [45]. We use only $K_{\ell 4}$ data for our fits and therefore are only sensitive to the LECs L_1^r, L_2^r and L_3^r [12]. The other LECs are taken as a fixed input.

5.1.1 Direct fits at $\mathcal{O}(p^4)$

Fits of threshold parameters In order to make the connection to [45], we first perform a direct NLO fit to the NA48/2 threshold parameters in (149). Using $\cos\theta = 0$, i.e. the first Taylor coefficient of an expansion in $z = \cos\theta$, and the LEC inputs $L_4^r = 0$ and the fitted value for L_5^r of [45], we reproduce almost exactly the result of [45] for L_1^r, L_2^r and L_3^r; see the second and third column in Table 2. If we use instead the partial-wave projection (55), the fit results for L_1^r and L_2^r change a bit, as shown in the fourth column of Table 2. The last column uses lattice results [46,47] for the input LECs.

Table 2 Comparison of direct NLO fits to the NA48/2 threshold parameters [9]. The renormalisation scale is $\mu = 770$ MeV. The last column uses the lattice determination of [46,47] for the input LECs. The uncertainties are purely statistical

	Ref. [45]	Taylor	PWE	PWE
$10^3 \cdot L_1^r$	0.98 (09)	0.99 (09)	1.15 (09)	1.17 (09)
$10^3 \cdot L_2^r$	1.56 (09)	1.57 (09)	1.48 (08)	1.50 (08)
$10^3 \cdot L_3^r$	−3.82 (30)	−3.83 (30)	−3.82 (30)	−3.87 (30)
$10^3 \cdot L_4^r$	≡0	≡0	≡0	≡0.04
$10^3 \cdot L_5^r$	1.23 (06)	≡1.23	≡1.23	≡0.84
χ^2	16	0.3	0.3	0.3
dof	5	1	1	1
χ^2/dof	3.2	0.3	0.3	0.3

Table 3 Comparison of direct NLO fits to the NA48/2 and E865 form factor measurements. The renormalisation scale is $\mu = 770$ MeV. For L_4^r and L_5^r, we use lattice input [46,47], for L_9^r the determination of [48]. The uncertainties are purely statistical

	NA48/2	NA48/2, iso	NA48/2 and E865	NA48/2 and E865, iso
$10^3 \cdot L_1^r$	0.69 (03)	0.71 (04)	0.62 (03)	0.64 (04)
$10^3 \cdot L_2^r$	1.88 (07)	1.80 (08)	1.79 (06)	1.70 (06)
$10^3 \cdot L_3^r$	−3.89 (13)	−3.93 (14)	−3.62 (11)	−3.60 (12)
$10^3 \cdot L_4^r$	≡0.04	≡0.04	≡0.04	≡0.04
$10^3 \cdot L_5^r$	≡0.84	≡0.84	≡0.84	≡0.84
$10^3 \cdot L_9^r$	≡5.93	≡5.93	≡5.93	≡5.93
χ^2	159.4	67.5	199.9	117.1
dof	27	27	39	39
χ^2/dof	5.9	2.5	5.1	3.0

Fits of the complete form factor data In a next step, we no longer fit the threshold expansion parameters (149) of the form factors, but the form factor data of NA48/2 [6,9] and E865 [7,8], discussed in Sect. 4.1. The second column of Table 3 shows the result of the NLO fit to the one-dimensional NA48/2 data without isospin corrections (but with the corrected normalisation of F_s to account for the s_ℓ-dependence). In the third column, isospin corrections are applied to the fitted data (Table 10). The fourth and fifth column show the results of a combined fit to NA48/2 and E865 data (Table 11). The smaller χ^2 value in the fits to the data with isospin-breaking corrections is due to the fact that the isospin corrections introduce an additional uncertainty in the data.

Figure 12 shows a comparison of the NA48/2 threshold parameter fit of [45] with the result of the fit to the whole form factor data set (fourth column of Table 3). It helps one to understand the difference between the fitted LECs in the two procedures: in the fit to the threshold parameters, the curvature of the form factor is neglected. Since the NLO chiral representation cannot reproduce the curvature, the data
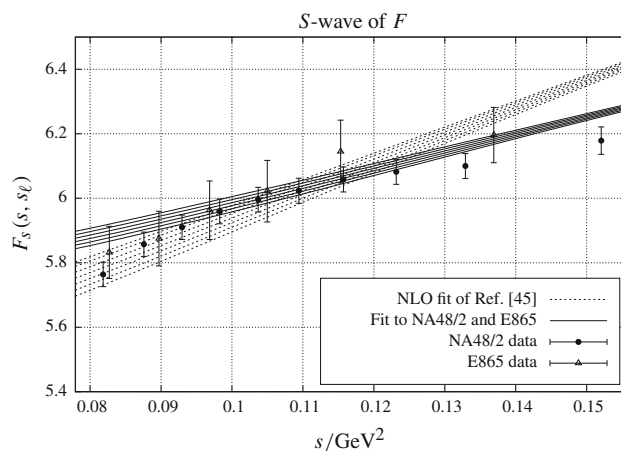
Fig. 12 Comparison of different fits for the S-wave of the form factor F: NA48/2 threshold parameter fit of [45] and a fit to the full data set. The (s, s_ℓ)-phase space is projected on the s-axis. No isospin corrections are applied

points at higher energies reduce the slope in a fit to the whole data set.

5.1.2 Direct fits at $\mathcal{O}(p^6)$

χPT at NNLO suffers from the problem that many new low-energy constants C_i^r appear in the $\mathcal{O}(p^6)$ Lagrangian. In $K_{\ell 4}$, in total 24 linearly independent combinations of the C_i^r enter in the NNLO chiral representation of the form factors F and G. A fit of so many parameters seems out of question. We would rather like to use some input values for the C_i^r. Unfortunately, only very few of the NNLO LECs are known reliably. We could either use determinations of the C_i^r with models like the chiral quark model [49], a resonance estimate [11,50] or the educated guess of [45]. These different estimates, however, do not lead to compatible results [45].

In Table 4, we display the results of our direct χPT fits at NNLO in comparison with the results of [45]. In contrast to [45], we do not use the threshold parameters but the whole form factor data sets of NA48/2 and E865 corrected by isospin-breaking effects [33]. It turns out that even at NNLO, χPT has trouble to reproduce the curvature of the F_s data. We also note that the results for the fitted LECs at NNLO differ quite significantly from the results at NLO.

5.2 Matching the dispersion relation to χPT

With the direct χPT fits, we have seen a number of problems: First, at NLO and even at NNLO, the energy dependence of the F_s form factor is not very well described. Second, at $\mathcal{O}(p^6)$, the appearance of quite a large number of additional LECs reduces the predictive power of χPT. Some input values for the C_i^r have to be assumed, as a fit of $K_{\ell 4}$ data alone cannot determine all these LECs.

Table 4 Direct NNLO fits for different choices of the C_i^r. The results of the fits of [45] are shown for comparison. The renormalisation scale is $\mu = 770$ MeV. Our results are fits to the entire form factor data including isospin corrections. The uncertainties are purely statistical. The NLO input LECs L_4^r, L_5^r, L_6^r and L_8^r are lattice determinations [46,47], L_7^r is the BE14 value [45] and L_9^r is taken from [48]

	Ref. [45]	Ref. [45]	NA48/2	NA48/2 & E865	NA48/2	NA48/2 & E865
C_i^r	$\equiv 0$	BE14	$\equiv 0$	$\equiv 0$	BE14	BE14
$10^3 \cdot L_1^r$	0.67 (06)	0.53 (06)	0.34 (03)	0.28 (02)	0.33 (03)	0.27 (02)
$10^3 \cdot L_2^r$	0.17 (04)	0.81 (04)	0.42 (06)	0.35 (05)	0.95 (06)	0.89 (05)
$10^3 \cdot L_3^r$	−1.76 (21)	−3.07 (20)	−1.54 (14)	−1.25 (11)	−3.06 (14)	−2.80 (11)
$10^3 \cdot L_4^r$	0.73 (10)	$\equiv 0.3$	$\equiv 0.04$	$\equiv 0.04$	$\equiv 0.04$	$\equiv 0.04$
$10^3 \cdot L_5^r$	0.65 (05)	1.01 (06)	$\equiv 0.84$	$\equiv 0.84$	$\equiv 0.84$	$\equiv 0.84$
$10^3 \cdot L_6^r$	0.25 (09)	0.14 (05)	$\equiv 0.07$	$\equiv 0.07$	$\equiv 0.07$	$\equiv 0.07$
$10^3 \cdot L_7^r$	−0.17 (06)	−0.34 (09)	$\equiv -0.34$	$\equiv -0.34$	$\equiv -0.34$	$\equiv -0.34$
$10^3 \cdot L_8^r$	0.22 (08)	0.47 (10)	$\equiv 0.36$	$\equiv 0.36$	$\equiv 0.36$	$\equiv 0.36$
$10^3 \cdot L_9^r$			$\equiv 5.93$	$\equiv 5.93$	$\equiv 5.93$	$\equiv 5.93$
χ^2	26	1.0	81.3	128.7	52.5	91.2
dof	9		27	39	27	39
χ^2/dof	2.9		3.0	3.3	1.9	2.3

We now turn to the results using the dispersive representation as an intermediate step in the determination of the LECs: we fit the $K_{\ell 4}$ form factor data with the dispersion relation. The matching to χPT relates the subtraction constants of the dispersion relation to the LECs. As the dispersion relation provides a resummation of final-state rescattering effects, we trust that we will obtain a better description of the energy dependence of the form factors. However, it is clear that the matching of the dispersion relation to NNLO χPT will not be free of the problem related to the large number of LECs. We will alleviate the situation by including additional constraints on the chiral convergence in the fit. This will enable us to fit partially the contribution of the NNLO LECs to the subtraction constants.

5.2.1 Matching at $\mathcal{O}(p^4)$

Our numerical solution of the dispersion relation (85) is parameterised by nine subtraction constants, which in fact are functions of s_ℓ. If we use the matching at NLO to provide a chiral representation of the subtraction constants, we see that $a_{\text{NLO}}^{M_0}$ and $a_{\text{NLO}}^{\tilde{M}_1}$ are linear in s_ℓ, while the other subtraction constants do not depend on s_ℓ. We therefore introduce this s_ℓ-dependence according to (118) and have to determine in total 11 parameters.

We fit our dispersive representation to the data of both experiments, shown in Appendix D. In the case of NA48/2, the use of the two-dimensional instead of the one-dimensional data set has basically no effect on the determination of the LECs L_1^r, L_2^r and L_3^r but gives us the option to fit the s_ℓ-dependence and therefore to determine also L_9^r. In order to test the influence of the isospin-breaking corrections, we also perform fits to the data without isospin corrections.

An unconstrained fit with the 11 subtraction parameters leads to a low relative χ^2 of 0.77 (with 94 degrees of freedom, dof) for the NA48/2 data alone or 0.74 (106 dof) for the combined data set of NA48/2 and E865. However, the soft-pion theorems in such a fit are not well reproduced. Therefore, we chose to use the soft-pion theorems as constraints in the fit: the first soft-pion theorem (112) with a tolerance of 2 % and the second soft-pion theorem (113) of 5 %. These numbers are inspired by the typical NNLO deviation. In these fits the relative χ^2 slightly increases to 0.79 (96 dof) for the NA48/2 fit and 0.77 (108 dof) for the combined fit. This shows that in a fit with all 11 parameters, the soft-pion theorems are not fulfilled automatically but are not a strong additional constraint.

In an unconstrained fit, the result for the subtraction constants turns out to be rather unstable: the statistical uncertainties are large and some of the subtraction constants change drastically if the E865 data is included. We consider these fits of little interest and fix to an a priori value those subtraction constants that have the largest statistical uncertainty: these are the subtraction constants of highest order in each function and the one parametrising the s_ℓ-dependence in G_p, i.e. c^{M_0}, b^{M_1}, $c^{\tilde{M}_1}$ and $a_1^{\tilde{M}_1}$. We fix these subtraction constants to the NLO chiral prediction in the matching (141): while c^{M_0}, b^{M_1} and $c^{\tilde{M}_1}$ are purely numerical, $a_1^{\tilde{M}_1}$ depends on L_2^r and L_9^r. We take those two LECs as input and iterate the fit after the matching to reach self-consistency for L_2^r (and L_9^r if this LEC is determined in the matching as well).

Seven subtraction constants $a_0^{M_0}$, $a_1^{M_0}$, b^{M_0}, a^{M_1}, $a_0^{\tilde{M}_1}$, $b^{\tilde{M}_1}$ and b^{N_0} remain to be fitted to the data. In the matching equations (i.e. 141 together with Appendix E.1), the LECs L_1^r, L_2^r, L_3^r and L_9^r are overdetermined. Hence, we have to use a second χ^2 minimisation to fix these LECs. As an alternative

Table 5 Fit results for the dispersion relation matched to χPT at NLO. The renormalisation scale is $\mu = 770$ MeV

	NA48/2	NA48/2 and E865	NA48/2	NA48/2 and E865	NA48/2	NA48/2 and E865
Isospin corr.	✗	✗	✓	✓	✓	✓
σ_{SPT1}	–	–	–	–	2 %	2 %
σ_{SPT2}	–	–	–	–	5 %	5 %
$10^3 \cdot L_1^r$	0.52 (02) (05)	0.48 (02) (05)	0.54 (02) (05)	0.50 (02) (05)	0.54 (02) (05)	0.50 (02) (05)
$10^3 \cdot L_2^r$	1.00 (05) (07)	0.94 (04) (07)	0.94 (05) (07)	0.88 (05) (07)	0.94 (05) (07)	0.88 (05) (07)
$10^3 \cdot L_3^r$	−3.03 (11) (07)	−2.83 (09) (07)	−2.99 (11) (07)	−2.79 (10) (07)	−2.99 (11) (07)	−2.80 (10) (07)
$10^3 \cdot L_9^r$	4.70 (40) (63)	4.64 (39) (61)	4.51 (43) (63)	4.44 (43) (61)	4.52 (43) (63)	4.45 (43) (61)
χ^2	100.9	133.3	86.1	116.8	98.0	128.8
dof	101	113	101	113	103	115
χ^2/dof	1.0	1.2	0.9	1.0	1.0	1.1

to this two-step procedure (first fit to the data, then matching to χPT), we can directly use the NLO chiral representation of the subtraction constants and perform the fit of the dispersive representation to the data with the LECs as fitting parameters. As expected, these two strategies lead to almost identical numerical results for the LECs.

In Table 5, we show the results of the fits of the dispersion relation matched to NLO χPT. For the input LECs, we use lattice results [46,47]:

$$10^3 \cdot L_4^r = 0.04(14),$$
$$10^3 \cdot L_5^r = 0.84(38). \tag{150}$$

The χ^2 and degrees of freedom correspond to the strategy of using the LECs as fitting parameters. If we use the two-step fitting/matching strategy instead, the χ^2/dof of the fit of the subtraction constants to the data is good: around 0.8 for the fit to NA48/2 and around 1.0 for the fit to both experiments. At the same time, the relative χ^2/dof of the matching is bad (between 2.9 and 6.1). This is not surprising because the sum of the total χ^2 of the two steps is approximately equal to the total χ^2 in the one-step procedure, while the dof in the second step are drastically reduced.

The first bracket indicates the statistical uncertainty due to the fitted data. The second bracket gives the systematic uncertainty. In Sect. 5.3, we will discuss in more detail the different sources of uncertainty.

The fit results for L_9^r are not in agreement with the determination of [48],

$$10^3 \cdot L_9^r = 5.93(43). \tag{151}$$

Note that the influence of L_9^r on L_1^r, L_2^r and L_3^r is minimal: if L_9^r is fixed to (151), we find $10^3 \cdot L_1^r = 0.51(02)(06)$, $10^3 \cdot L_2^r = 0.89(05)(07)$ and $10^3 \cdot L_3^r = -2.82(10)(07)$.

While the final results for the LECs do not differ significantly in the one-step and two-step strategies, a difference can be observed concerning the soft-pion theorems. If we use the two-step matching strategy, the soft-pion theorems

are not automatically satisfied, but if they are imposed as a fitting constraint, they can be perfectly satisfied with only a slight increase of the χ^2. In contrast, in the one-step strategy, where the subtraction constants have to fulfil the chiral constraints, the accuracy of the soft-pion theorems lies at $\sim$4 and $\sim$10 %, respectively. This does not change with the soft-pion constraints added to the fit, which only increases the χ^2 a bit.

The influence of the isospin-breaking corrections of [33] is about the size of the statistical uncertainty in the case of L_1^r and L_2^r, while L_3^r is less sensitive to the isospin effects.

A plot of the data points indicates that the two experiments NA48/2 and E865 are in agreement, which is confirmed by the fit results. We find it worthwhile to stress that this is only the case if the normalisation of the F_s data points of NA48/2 is determined including the s_ℓ-dependence (for the values in the 10 published bins, this requires the normalisation to be increased by 0.77 %). If the published values are used, which are normalised neglecting the s_ℓ-dependence, a quite strong tension between the two experiments is observed, resulting in higher χ^2 values for combined fits.

We note that the χ^2 in the dispersive treatment is clearly improved compared to the direct fit with χPT at NLO: in a fit to the one-dimensional data in Appendix D, the χ^2 of a dispersive fit is 1.2 instead of 2.5 for the direct chiral fit (both with 27 dof). This is illustrated in Fig. 13: in contrast to a pure chiral treatment, the dispersion relation allows to describe the curvature of the S-wave of the form factor F. We interpret this as the result of the resummation of final-state rescattering effects. Figure 14 shows the fitted P-waves of F and G.

5.2.2 Matching at $\mathcal{O}(p^6)$

We have seen that when using one-loop χPT, the dispersive treatment clearly exhibits its powers, and the advantage over a pure chiral treatment is evident: the dispersive representation is able to describe the energy dependence of the form
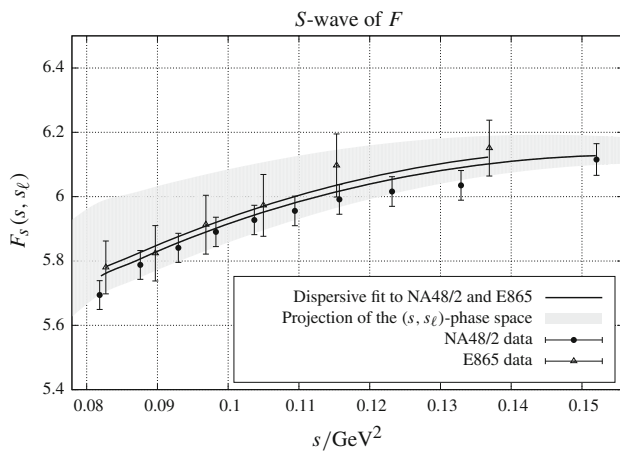
Fig. 13 Fit result for the S-wave of the form factor F. The dispersive description reproduces beautifully the curvature of the form factor. The (s, s_ℓ)-phase space is projected on the s-axis, the *plotted lines* correspond to splines through the (s, s_ℓ)-values of the two data sets

factors, hence the χ^2 of the fit to the whole form factor data is much better. Due to the resummation of final-state rescattering effects, we expect the dispersive representation to capture the most important higher-order contributions and to render the determination of the LECs more robust.

In combination with two-loop χPT, the treatment becomes more difficult. The matching equations at NNLO relate the subtraction constants to chiral expressions that contain the $\mathcal{O}(p^6)$ LECs C_i^r. The largest obstacle in a chiral treatment at NNLO is the large number of poorly known C_i^r. In the dispersive treatment with NNLO matching, the same problem occurs. It turns out that the determination of the NLO LECs is still strongly affected by the choice of the C_i^r, a situation known from direct χPT fits [45,50].

In order to alleviate this problem, we note that not all choices of the input C_i^r lead to a good convergence of the chiral expansion. In our dispersion relation, there appear nine subtraction constants, which are gauge-dependent quantities.

Since the gauge transformation (74) is described by three parameters, we can find six gauge-invariant linear combinations of subtraction constants. For these linear combinations, we require a good chiral convergence. We obtain this by modifying the fitting procedure as follows.

- We introduce nine additional fitting parameters, corresponding to the contribution of the C_i^r to the subtraction constants.
- We add to the χ^2 nine observations of these parameters corresponding to the input values of the C_i^r with a 50 % tolerance for the linear combinations of the C_i^r.
- We add to the χ^2 six observations of the total $\mathcal{O}(p^6)$ correction to the gauge-invariant linear combinations of subtraction constants. The observation is zero ± 5.6 % of the $\mathcal{O}(p^4)$ contribution (5.6 % corresponds to $M_\eta^2/(4\pi F_\pi)^2$).

With this setup, we are able to perform the NNLO matching with a reduced dependence on the input values of the C_i^r. In Table 6, we present the matching results at NNLO, using the 'preferred values' of [45] as input for the C_i^r.

The fit results with L_9^r taken as input are shown in the second and third column of Table 6. Here, the corrections from NLO to NNLO matching for all three LECs are smaller than the corrections between NLO and NNLO observed in direct χPT fits. The larger uncertainties with respect to the NLO matching are explained by the additional fitting parameters for the C_i^r contribution to the subtraction constants. If we take as input for the C_i^r the resonance estimate of [50], we obtain $\{L_1^r, L_2^r, L_3^r\} = \{0.65, 0.26, -1.79\} \cdot 10^{-3}$. With the C_i^r input taken from the chiral quark model [49], we find $\{L_1^r, L_2^r, L_3^r\} = \{0.49, 0.65, -2.44\} \cdot 10^{-3}$. We prefer the BE14 input values for the C_i^r, because they lead to the best chiral convergence and the best χ^2 of the fit.

The fit results change quite drastically if we include L_9^r in the fit. These fit results are shown in the fourth and fifth
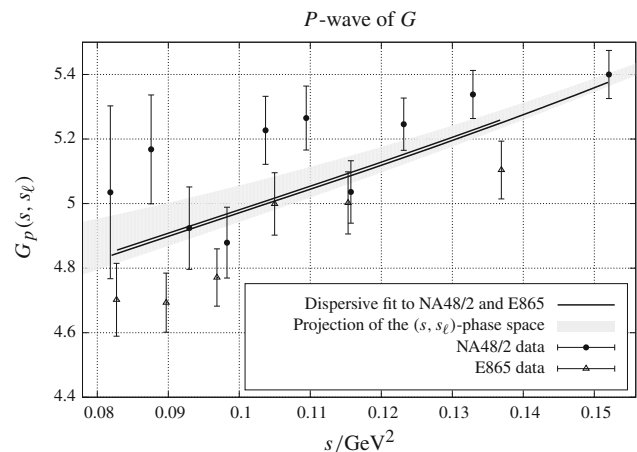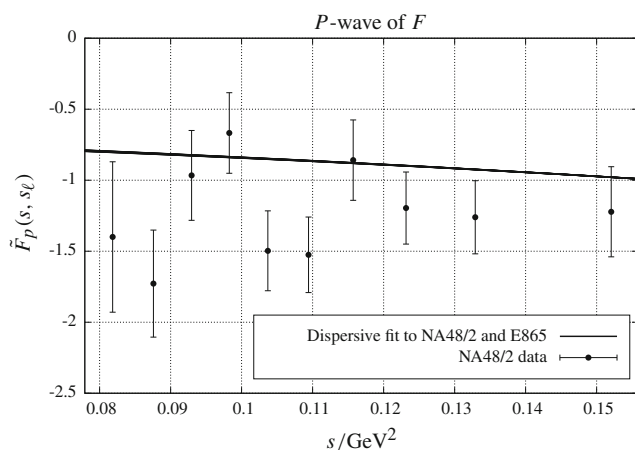

Fig. 14 Fit results for the P-waves of the form factors F and G. The (s, s_ℓ)-phase space is again projected on the s-axis

Table 6 Fit results for the dispersion relation matched to χPT at NNLO. The renormalisation scale is $\mu = 770$ MeV. As in Table 4, we use lattice input for L_4^r, L_5^r, L_6^r and L_8^r [46,47], L_7^r is the BE14 value [45] and the input value for L_9^r is taken from [48]

	NA48/2	NA48/2 and E865	NA48/2	NA48/2 and E865
$10^3 \cdot L_1^r$	0.82 (16) (09)	0.69 (16) (08)	0.93 (17) (04)	0.78 (17) (03)
$10^3 \cdot L_2^r$	0.71 (10) (10)	0.63 (09) (10)	1.11 (17) (08)	0.97 (17) (08)
$10^3 \cdot L_3^r$	−3.10 (40) (27)	−2.63 (39) (24)	−3.96 (49) (14)	−3.38 (48) (10)
$10^3 \cdot L_9^r$	≡5.93	≡5.93	8.36 (87) (48)	8.05 (86) (39)
χ^2	91.8	123.9	83.1	115.3
dof	110	122	109	121
χ^2/dof	0.8	1.0	0.8	1.0

Table 7 Matching results for the LECs at NLO and NNLO. The scale is $\mu = 770$ MeV

	NLO	NNLO
$10^3 \cdot L_1^r(\mu)$	0.51 (02) (06)	0.69 (16) (08)
$10^3 \cdot L_2^r(\mu)$	0.89 (05) (07)	0.63 (09) (10)
$10^3 \cdot L_3^r(\mu)$	−2.82 (10) (07)	−2.63 (39) (24)

Table 8 Statistical and systematic correlations of the fitted LECs at NLO

Statistical correlation	L_2^r	L_3^r	Systematic correlation	L_2^r	L_3^r
L_1^r	0.49	−0.72	L_1^r	−0.69	−0.31
L_2^r		−0.95	L_2^r		−0.29

Table 9 Statistical and systematic correlations of the fitted LECs at NNLO

Statistical correlation	L_2^r	L_3^r	Systematic correlation	L_2^r	L_3^r
L_1^r	0.31	−0.32	L_1^r	0.23	−0.83
L_2^r		−0.84	L_2^r		−0.70

column of Table 6. In the matching equations at NNLO, a stronger correlation between L_9^r and the other LECs is introduced due to their appearance in the s_ℓ-dependence. At present, alternative determinations of L_9^r are clearly more reliable than this one, and we therefore prefer here the fits with L_9^r taken as input. However, if the s_ℓ-dependence of the form factors will be measured in forthcoming experiments with even higher statistics, this could provide a new reliable way to determine L_9^r.

5.3 Error analysis

In the following, we analyse the different sources of uncertainties in the determination of the LECs using the NLO and NNLO matching. In table 7 we give once more the NLO and NNLO values for the LECs, obtained from the combined fits to the NA48/2 and E865 data, where L_9^r is taken as a fixed input [48].

The first error indicates the statistical one, i.e. the error calculated in the linear fit of the parameters. This error is due to the uncertainty of the fitted data including isospin corrections. In the case of NNLO matching, it includes also the uncertainty introduced with the 50 % tolerance of the C_i^r contribution to the subtraction constants. The second error is due to the systematics of our approach. The corresponding statistical and systematic correlations are shown in Tables 8 and 9.

Figures 15, 16 and 17 show bar charts of the uncertainties of the LECs. The fractional uncertainties are summed in squares and determined as follows:

- The uncertainty due to the $K_{\ell 4}$ form factor data is the statistical uncertainty of a fit where no isospin corrections are included and the C_i^r contributions are fixed to the fitted values.
- The uncertainty due to isospin corrections is the difference in squares of the statistical uncertainties of fits to data with and without isospin corrections, again with the C_i^r contributions fixed to the fitted values.
- The uncertainty due to the C_i^r is the difference in squares of the statistical uncertainties of fits to isospin corrected data with the C_i^r contributions either fitted or fixed to the fitted values.
- For the $\pi\pi$ phases [28,29], we vary all the 28 parameters and sum the variations of the LECs in squares. In the bar charts, this is the uncertainty labelled by '$\pi\pi$ phases, low energy'.
- The next fractional uncertainty is due to the high-energy behaviour of the $\pi\pi$ phases. We sum in squares the differences between the high-energy solutions explained in Sect. 3.2.1.
- The $K\pi$ phases are simply varied between the centre and upper/lower limit of the error bands. This influence is labelled as '$K\pi$ phases, low energy'.
- The uncertainty due to the high-energy behaviour of the $K\pi$ phases is estimated with the two solutions for each of the $K\pi$ phases as explained in Sect. 3.2.2.
- The input LECs are varied by their uncertainties given in (150) and (151).
- We have checked that the numerical uncertainties due to the discretisation, interpolation and numerical integration

Fig. 15 Contributions to the uncertainty of L_1^r in the $\mathcal{O}(p^4)$ and $\mathcal{O}(p^6)$ matching in units of 10^{-5}

Fig. 16 Contributions to the uncertainty of L_2^r in the $\mathcal{O}(p^4)$ and $\mathcal{O}(p^6)$ matching in units of 10^{-5}
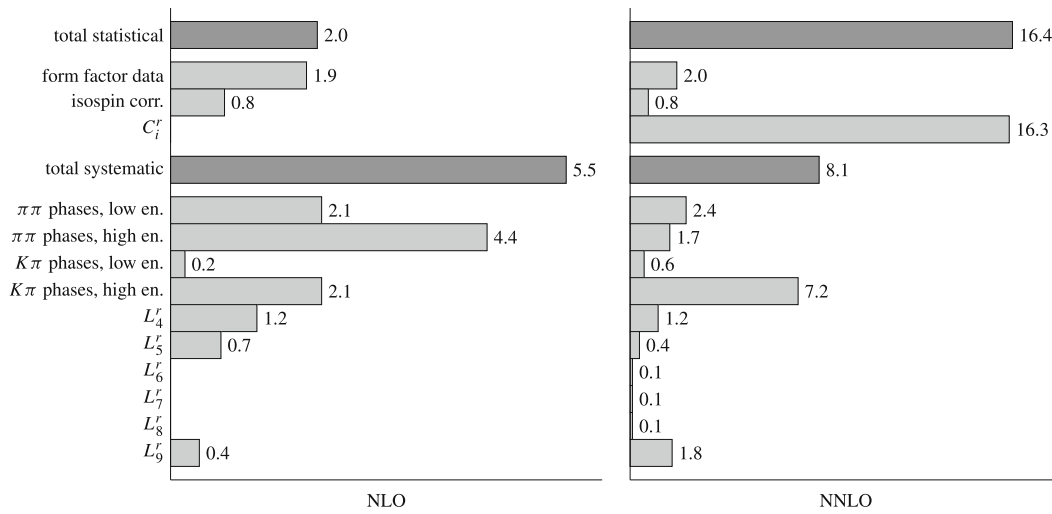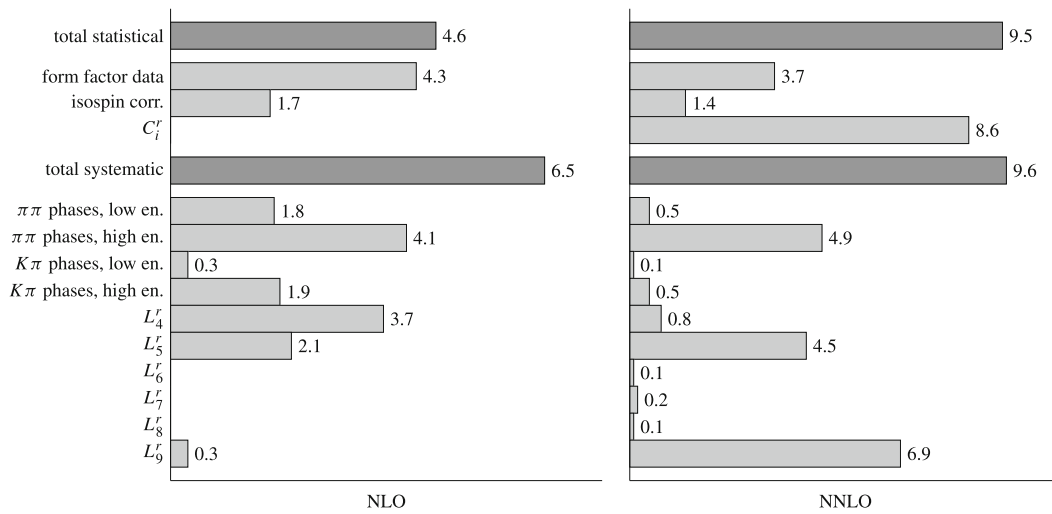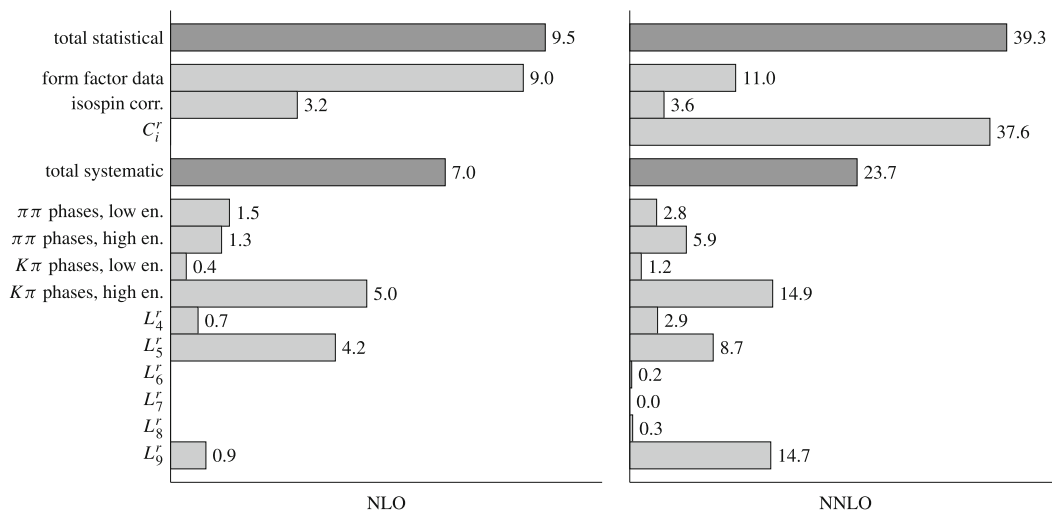

Fig. 17 Contributions to the uncertainty of L_3^r in the $\mathcal{O}(p^4)$ and $\mathcal{O}(p^6)$ matching in units of 10^{-5}

of the functions as well as the iteration procedure are completely negligible.

We note that at NLO, the largest contribution to the systematic errors comes from the high-energy behaviour of the phase shifts, either from the $\pi\pi$ phases in the case of L_1^r and L_2^r or the $K\pi$ phases in the case of L_3^r. The uncertainties due to the low-energy parameterisation of the phases are small. The uncertainty due to the input LEC L_9^r is very small as well.

At NNLO, the high-energy behaviour of the phases is again a large contribution to the uncertainty. L_9^r has now a large impact on the uncertainty of L_2^r. The additional LECs L_6^r, L_7^r and L_8^r have almost no influence on the uncertainty. The largest uncertainty is due to the fitted contribution of the C_i^r, which is part of the statistical uncertainty.

6 Conclusion and outlook

We have presented a new dispersive treatment of $K_{\ell 4}$ decays, which provides a very accurate description of the hadronic form factors F and G. The dispersion relation is valid up to and including $\mathcal{O}(p^6)$ in the chiral counting. Furthermore, it provides a resummation of final-state $\pi\pi$- and $K\pi$-rescattering effects, which we believe to be the most important contribution beyond $\mathcal{O}(p^6)$.

Our dispersion relation for $K_{\ell 4}$ is written in the form of an Omnès representation. It consists of a set of coupled integral equations. We have solved this system numerically with an iterative procedure. The solutions are parameterised by subtraction constants, which we have determined in a fit to the data and by using the soft-pion theorem as well as chiral input. In contrast to a pure chiral description, the dispersion relation describes perfectly the experimentally observed curvature of the S-wave of the form factor F, which we interpret as a result of significant $\pi\pi$-rescattering effects. This is yet another case in which high-precision data clearly call for effects which go even beyond NNLO in χPT. These effects only concern the momentum dependence of the form factors: we see no sign that quark mass dependence beyond NNLO is required by data.

By using the matching equations to χPT we have extracted the values of the low-energy constants L_1^r, L_2^r and L_3^r. The correction from NLO to NNLO, when matching the chiral and dispersive representations and fitting the latter to the data are smaller than the corrections from NLO to NNLO observed in direct χPT fits. Constraints on the chiral convergence of the subtraction constants allow us to reduce the dependence on the input values for the C_i^r. Still, the poorly known values of the C_i^r are responsible for the larger uncertainties in the matching at NNLO.

Our results for the LECs obtained by matching χPT at NLO are:

$$L_1^r = 0.51(06) \cdot 10^{-3}, \quad L_2^r = 0.89(09) \cdot 10^{-3},$$
$$L_3^r = -2.82(12) \cdot 10^{-3}, \tag{152}$$

whereas the matching at NNLO gives

$$L_1^r = 0.69(18) \cdot 10^{-3}, \quad L_2^r = 0.63(13) \cdot 10^{-3},$$
$$L_3^r = -2.63(46) \cdot 10^{-3}. \tag{153}$$

The two-dimensional NA48/2 data set for the S-wave of F, which shows both the s- and the s_ℓ-dependence, has allowed us to extract a value for L_9^r, which is roughly compatible with previous determinations. In accuracy, however, it cannot yet compete, as it reflects the low precision in the measurement of the s_ℓ-dependence of F. The determination of L_9^r is also quite strongly dependent on whether the matching is done at NLO or NNLO.

A Scalar loop functions

We use the following conventions for the scalar one-loop functions in n dimensions:

$$A_0(m^2) := \frac{1}{i} \int \frac{d^n q}{(2\pi)^n} \frac{1}{[q^2 - m^2]},$$
$$B_0(p^2, m_1^2, m_2^2) := \frac{1}{i} \int \frac{d^n q}{(2\pi)^n} \frac{1}{[q^2 - m_1^2][(q+p)^2 - m_2^2]}.$$
$$\tag{A.1}$$

These loop functions are UV-divergent. We define the renormalised loop functions in the $\overline{MS}$ scheme:

$$A_0(m^2) = -2m^2\lambda + \bar{A}_0(m^2) + \mathcal{O}(4-n),$$
$$B_0(p^2, m_1^2, m_2^2) = -2\lambda + \bar{B}_0(p^2, m_1^2, m_2^2) + \mathcal{O}(4-n),$$
$$\tag{A.2}$$

where

$$\lambda = \frac{\mu^{n-4}}{16\pi^2}\left(\frac{1}{n-4} - \frac{1}{2}(\ln(4\pi) + 1 - \gamma_E)\right). \qquad (A.3)$$

μ denotes the renormalisation scale.

The renormalised loop functions are given by [11]

$$\bar{A}_0(m^2) = -\frac{m^2}{16\pi^2}\ln\left(\frac{m^2}{\mu^2}\right),$$

$$\bar{B}_0(p^2, m_1^2, m_2^2) = -\frac{1}{16\pi^2}\frac{m_1^2\ln\left(\frac{m_1^2}{\mu^2}\right) - m_2^2\ln\left(\frac{m_2^2}{\mu^2}\right)}{m_1^2 - m_2^2}$$

$$\qquad (A.4)$$

$$+ \frac{1}{32\pi^2}\left(2 + \left(-\frac{\Delta}{p^2} + \frac{\Sigma}{\Delta}\right)\ln\left(\frac{m_1^2}{m_2^2}\right)\right.$$

$$\left. - \frac{\nu}{p^2}\ln\left(\frac{(p^2+\nu)^2 - \Delta^2}{(p^2-\nu)^2 - \Delta^2}\right)\right),$$

where

$$\Delta := m_1^2 - m_2^2,$$
$$\Sigma := m_1^2 + m_2^2, \qquad (A.5)$$
$$\nu := \lambda^{1/2}(s, m_1^2, m_2^2).$$

The renormalised two-point function fulfils a once-subtracted dispersion relation:

$$\bar{B}_0(s, m_1^2, m_2^2) = \bar{B}_0(0, m_1^2, m_2^2)$$
$$+ \frac{s}{\pi}\int_{(m_1+m_2)^2}^{\infty}\frac{\mathrm{Im}\,\bar{B}_0(s', m_1^2, m_2^2)}{(s' - s - i\epsilon)s'}\mathrm{d}s',$$
$$\qquad (A.6)$$

where the imaginary part is given by

$$\mathrm{Im}\,\bar{B}_0(s, m_1^2, m_2^2) = \frac{1}{16\pi}\frac{\lambda^{1/2}(s, m_1^2, m_2^2)}{s} \qquad (A.7)$$

and the value at $s = 0$ is

$$B_0(0, m_1^2, m_2^2) = -\frac{1}{16\pi^2}\frac{m_1^2\ln\left(\frac{m_1^2}{\mu^2}\right) - m_2^2\ln\left(\frac{m_2^2}{\mu^2}\right)}{m_1^2 - m_2^2}. \qquad (A.8)$$

The first and second derivative at $s = 0$ are

$$B_0'(0, m_1^2, m_2^2) = \frac{1}{32\pi^2}\frac{\Delta\Sigma - 2m_1^2 m_2^2 \ln\left(\frac{m_1^2}{m_2^2}\right)}{\Delta^3},$$

$$B_0''(0, m_1^2, m_2^2) = \frac{1}{48\pi^2}\frac{\Delta(m_1^4 + 10m_1^2 m_2^2 + m_2^4) - 6m_1^2 m_2^2 \Sigma \ln\left(\frac{m_1^2}{m_2^2}\right)}{\Delta^5}.$$
$$\qquad (A.9)$$

B Kinematics

For each channel, the partial-wave expansion is performed in the corresponding rest frame, i.e. in the $\pi\pi$ centre-of-mass frame for the s-channel and in one of the $K\pi$ centre-of-mass frames for the t- and u-channel. Therefore, we work out explicitly the kinematics in the three different frames.

B.1 Legendre polynomials and spherical harmonics

For the partial-wave expansions, we make use of several relations between spherical harmonics and Legendre polynomials.

We use the addition theorem for the spherical harmonics and the relations between Legendre polynomials or derivatives of Legendre polynomials to spherical harmonics:

$$P_l(\cos\theta') = \frac{4\pi}{2l+1}\sum_{m=-l}^{l}Y_l^m(\theta, 0)Y_l^{m*}(\theta'', \phi''), \qquad (B.1)$$

$$P_{l'}(\cos\theta'') = \sqrt{\frac{4\pi}{2l'+1}}Y_{l'}^0(\theta'', \phi'') \quad \text{(for any } \phi''\text{)}, \quad (B.2)$$

$$P_{l'}'(\cos\theta'')\sin\theta'' = (-1)\sqrt{\frac{4\pi}{2l'+1}}\sqrt{\frac{(l'+1)!}{(l'-1)!}}$$
$$\times Y_{l'}^{1*}(\theta'', \phi'')e^{i\phi''}, \qquad (B.3)$$

where $P_l'(z) := \frac{\mathrm{d}}{\mathrm{d}z}P_l(z)$. The different angles are defined in Fig. 18.

We can now easily derive the addition theorem for the Legendre polynomials:

$$\int \mathrm{d}\Omega'' P_l(\cos\theta')P_{l'}(\cos\theta'')$$

$$= \int \mathrm{d}\Omega''\frac{4\pi}{2l+1}\sum_{m=-l}^{l}Y_l^m(\theta, 0)Y_l^{m*}(\theta'', \phi'')$$

$$\times\sqrt{\frac{4\pi}{2l'+1}}Y_{l'}^0(\theta'', \phi'')$$
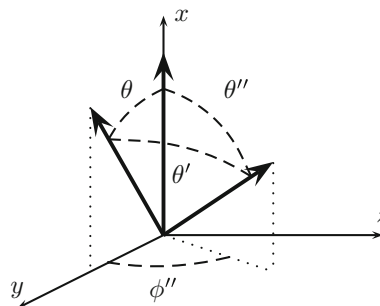
Fig. 18 Vectors and angles appearing in the addition theorem for spherical harmonics

$$= \sum_{m=-l}^{l} Y_l^m(\theta,0) \frac{4\pi}{2l+1} \sqrt{\frac{4\pi}{2l'+1}}$$

$$\times \underbrace{\int d\Omega'' Y_l^{m*}(\theta'',\phi'') Y_{l'}^0(\theta'',\phi'')}_{\delta_{ll'}\delta_{m0}}$$

$$= \delta_{ll'} \frac{4\pi}{2l+1} \sqrt{\frac{4\pi}{2l'+1}} Y_l^0(\theta,0) = \delta_{ll'} \frac{4\pi}{2l+1} P_l(\cos\theta),$$
(B.4)

as well as the following relation:

$$\int d\Omega'' P_l(\cos\theta') P_{l'}'(\cos\theta'') \sin\theta'' e^{-i\phi''}$$

$$= \int d\Omega'' \frac{4\pi}{2l+1} \sum_{m=-l}^{l} Y_l^{m*}(\theta,0) Y_l^m(\theta'',\phi'')(-1)$$

$$\times \sqrt{\frac{4\pi}{2l'+1}} \sqrt{\frac{(l'+1)!}{(l'-1)!}} Y_{l'}^{1*}(\theta'',\phi'')$$

$$= \sum_{m=-l}^{l} Y_l^{m*}(\theta,0) \frac{4\pi}{2l+1} (-1) \sqrt{\frac{4\pi}{2l'+1}} \sqrt{\frac{(l'+1)!}{(l'-1)!}}$$

$$\times \underbrace{\int d\Omega'' Y_l^m(\theta'',\phi'') Y_{l'}^{1*}(\theta'',\phi'')}_{\delta_{ll'}\delta_{m1}}$$

$$= \delta_{ll'} \frac{4\pi}{2l+1} (-1) \sqrt{\frac{4\pi}{2l'+1}} \sqrt{\frac{(l+1)!}{(l-1)!}} Y_l^{1*}(\theta,0)$$

$$= \delta_{ll'} \frac{4\pi}{2l+1} P_l'(\cos\theta) \sin\theta.$$
(B.5)

Since the right-hand side is real, we conclude that

$$\int d\Omega'' P_l(\cos\theta') P_{l'}'(\cos\theta'') \sin\theta'' \cos\phi''$$

$$= \delta_{ll'} \frac{4\pi}{2l+1} P_l'(\cos\theta) \sin\theta,$$

$$\int d\Omega'' P_l(\cos\theta') P_{l'}'(\cos\theta'') \sin\theta'' \sin\phi'' = 0.$$
(B.6)

B.2 Kinematics in the s-channel

In the $\pi\pi$ centre-of-mass frame, the four-momenta of the different particles take the following values:

$$k = \left(\sqrt{M_K^2 + \vec{k}^2}, \vec{k}\right), \quad -L = \left(-\sqrt{s_\ell + \vec{k}^2}, -\vec{k}\right),$$

$$q_1 = \left(\sqrt{M_\pi^2 + \vec{q}^2}, \vec{q}\right), \quad q_2 = \left(\sqrt{M_\pi^2 + \vec{q}^2}, -\vec{q}\right),$$

$$p_1 = \left(\sqrt{M_\pi^2 + \vec{p}^2}, \vec{p}\right), \quad p_2 = \left(\sqrt{M_\pi^2 + \vec{p}^2}, -\vec{p}\right), \quad \text{(B.7)}$$
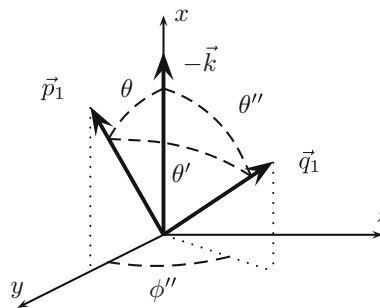
Fig. 19 Vectors and angles in the s-channel centre-of-mass frame

where q_1 and q_2 will be the momenta of intermediate pions. Note that we choose here the decay region (L^0 is positive), but we could have equally well chosen the scattering region.

Inserting these expressions into $s = (k - L)^2 = (q_1 + q_2)^2 = (p_1 + p_2)^2$ gives the values of $\vec{k}^2$, $\vec{q}^2$ and $\vec{p}^2$. We choose the directions of the three-vectors according to Fig. 19, i.e. the angles are defined as $\theta := \angle(-\vec{k}, \vec{p}_1)$, $\theta' := \angle(\vec{p}_1, \vec{q}_1)$, $\theta'' := \angle(-\vec{k}, \vec{q}_1)$.

We end up with the following explicit expressions for the four-vectors:

$$k = \left(\frac{M_K^2 + s - s_\ell}{2\sqrt{s}}, -\frac{\lambda_{K\ell}^{1/2}(s)}{2\sqrt{s}}, 0, 0\right),$$

$$L = \left(\frac{M_K^2 - s - s_\ell}{2\sqrt{s}}, -\frac{\lambda_{K\ell}^{1/2}(s)}{2\sqrt{s}}, 0, 0\right),$$

$$q_1 = \left(\frac{\sqrt{s}}{2}, \sqrt{\frac{s}{4} - M_\pi^2}\cos\theta'', \sqrt{\frac{s}{4} - M_\pi^2}\sin\theta''\cos\phi'', \right.$$
$$\left. \sqrt{\frac{s}{4} - M_\pi^2}\sin\theta''\sin\phi''\right),$$

$$q_2 = \left(\frac{\sqrt{s}}{2}, -\sqrt{\frac{s}{4} - M_\pi^2}\cos\theta'', -\sqrt{\frac{s}{4} - M_\pi^2}\sin\theta''\cos\phi'', \right.$$
$$\left. -\sqrt{\frac{s}{4} - M_\pi^2}\sin\theta''\sin\phi''\right),$$

$$p_1 = \left(\frac{\sqrt{s}}{2}, \sqrt{\frac{s}{4} - M_\pi^2}\cos\theta, \sqrt{\frac{s}{4} - M_\pi^2}\sin\theta, 0\right),$$

$$p_2 = \left(\frac{\sqrt{s}}{2}, -\sqrt{\frac{s}{4} - M_\pi^2}\cos\theta, -\sqrt{\frac{s}{4} - M_\pi^2}\sin\theta, 0\right),$$
(B.8)

where $\lambda_{K\ell}(s) := \lambda(M_K^2, s_\ell, s)$. Note that $\lambda_{K\ell}^{1/2}(s)$ has a square root branch cut in the s-plane between $\left(M_K - \sqrt{s_\ell}\right)^2$ and $\left(M_K + \sqrt{s_\ell}\right)^2$ and changes sign when we continue it analytically to the scattering region. We will have to pay attention that we do not introduce this kinematic singularity into the partial-wave expansion.

In order to express the s-channel scattering angle θ with the Mandelstam variables, we calculate:

$$t - u = (k - p_1)^2 - (k - p_2)^2$$

$$= k^2 + p_1^2 - 2kp_1 - k^2 - p_2^2 + 2kp_2$$

$$= 2k(p_2 - p_1)$$

$$= 2(k^0(p_2^0 - p_1^0) - \vec{k} \cdot (\vec{p}_2 - \vec{p}_1))$$

$$= \frac{\lambda_{K\ell}^{1/2}(s)}{\sqrt{s}} \left(-2\sqrt{\frac{s}{4} - M_\pi^2} \cos\theta \right)$$

$$= -\lambda_{K\ell}^{1/2}(s) \sqrt{1 - \frac{4M_\pi^2}{s}} \cos\theta$$

$$= -2X(s)\sigma_\pi(s)\cos\theta, \tag{B.9}$$

hence

$$\cos\theta = \frac{u - t}{2X\sigma_\pi}, \tag{B.10}$$

where $\sigma_\pi(s) := \sqrt{1 - 4M_\pi^2/s}$ and $X(s) = \frac{1}{2}\lambda_{K\ell}^{1/2}(s)$ as before.

B.3 Kinematics in the t-channel

In the t-channel, we are in the $K\pi$ centre-of-mass frame and look at the t-channel scattering region:

$$k = \left(\sqrt{M_K^2 + \vec{k}^2}, \vec{k} \right), \quad -p_1 = \left(\sqrt{M_\pi^2 + \vec{k}^2}, -\vec{k} \right),$$

$$q_K = \left(\sqrt{M_K^2 + \vec{q}_K^2}, \vec{q}_K \right), \quad q_\pi = \left(\sqrt{M_\pi^2 + \vec{q}_K^2}, -\vec{q}_K \right),$$

$$p_2 = \left(\sqrt{M_\pi^2 + \vec{p}_2^2}, \vec{p}_2 \right), \quad L = \left(\sqrt{s_\ell + \vec{p}_2^2}, -\vec{p}_2 \right) \tag{B.11}$$

Inserting these expressions into $t = (k - p_1)^2 = (q_K + q_\pi)^2 = (p_2 + L)^2$ gives the values of $\vec{k}^2$, $\vec{q}_K^2$ and $\vec{p}_2^2$. We choose the directions of the three-vectors according to Fig. 20, i.e. the angles are defined as $\theta_t := \angle(-\vec{k}, \vec{p}_2)$, $\theta_t' := \angle(\vec{k}, \vec{q}_K)$, $\theta_t'' := \angle(-\vec{q}_K, \vec{p}_2)$.

We find the following results:

$$k = \left(\frac{t + M_K^2 - M_\pi^2}{2\sqrt{t}}, -\frac{\lambda_{K\pi}^{1/2}(t)}{2\sqrt{t}} \cos\theta_t, -\frac{\lambda_{K\pi}^{1/2}(t)}{2\sqrt{t}} \sin\theta_t, 0 \right),$$

$$p_1 = \left(\frac{M_K^2 - M_\pi^2 - t}{2\sqrt{t}}, -\frac{\lambda_{K\pi}^{1/2}(t)}{2\sqrt{t}} \cos\theta_t, -\frac{\lambda_{K\pi}^{1/2}(t)}{2\sqrt{t}} \sin\theta_t, 0 \right),$$
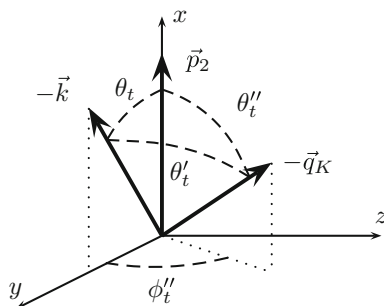
Fig. 20 Vectors and angles in the t-channel centre-of-mass frame

$$q_K = \left(\frac{t + M_K^2 - M_\pi^2}{2\sqrt{t}}, -\frac{\lambda_{K\pi}^{1/2}(t)}{2\sqrt{t}} \cos\theta_t'', -\frac{\lambda_{K\pi}^{1/2}(t)}{2\sqrt{t}} \sin\theta_t'' \cos\phi_t'', \right.$$

$$\left. -\frac{\lambda_{K\pi}^{1/2}(t)}{2\sqrt{t}} \sin\theta_t'' \sin\phi_t'' \right),$$

$$q_\pi = \left(\frac{t - M_K^2 + M_\pi^2}{2\sqrt{t}}, \frac{\lambda_{K\pi}^{1/2}(t)}{2\sqrt{t}} \cos\theta_t'', \frac{\lambda_{K\pi}^{1/2}(t)}{2\sqrt{t}} \sin\theta_t'' \cos\phi_t'', \right.$$

$$\left. \frac{\lambda_{K\pi}^{1/2}(t)}{2\sqrt{t}} \sin\theta_t'' \sin\phi_t'' \right),$$

$$p_2 = \left(\frac{t - s_\ell + M_\pi^2}{2\sqrt{t}}, \frac{\lambda_{\ell\pi}^{1/2}(t)}{2\sqrt{t}}, 0, 0 \right),$$

$$L = \left(\frac{t + s_\ell - M_\pi^2}{2\sqrt{t}}, -\frac{\lambda_{\ell\pi}^{1/2}(t)}{2\sqrt{t}}, 0, 0 \right), \tag{B.12}$$

where $\lambda_{K\pi}(t) := \lambda(M_K^2, M_\pi^2, t)$ and $\lambda_{\ell\pi}(t) := \lambda(s_\ell, M_\pi^2, t)$. Again, the square root of the first of these Källén functions has in the t-plane a branch cut between $(M_K - M_\pi)^2$ and $(M_K + M_\pi)^2$, the second between $(M_\pi - \sqrt{s_\ell})^2$ and $(M_\pi + \sqrt{s_\ell})^2$. Since we need the partial-wave expansion only in the scattering region $t > (M_K + M_\pi)^2$, these branch cuts are not relevant.

We calculate the t-channel scattering angle θ_t as a function of the Mandelstam variables:

$$s - u = (p_1 + p_2)^2 - (k - p_2)^2 = p_1^2 + p_2^2 + 2p_1p_2$$

$$- k^2 - p_2^2 + 2kp_2 = M_\pi^2 - M_K^2 + 2p_2(k + p_1)$$

$$= M_\pi^2 - M_K^2 + 2\left(\frac{t - s_\ell + M_\pi^2}{2\sqrt{t}} \frac{M_K^2 - M_\pi^2}{\sqrt{t}} + \frac{\lambda_{\ell\pi}^{1/2}(t)}{2\sqrt{t}} \frac{\lambda_{K\pi}^{1/2}(t)}{\sqrt{t}} \cos\theta_t \right), \tag{B.13}$$

hence

$$\cos\theta_t = \frac{t(s - u) + \Delta_{K\pi}\Delta_{\ell\pi}}{\lambda_{K\pi}^{1/2}(t)\lambda_{\ell\pi}^{1/2}(t)}. \tag{B.14}$$

B.4 Kinematics in the u-channel

The u-channel is completely analogous to the t-channel:

$$k = \left(\sqrt{M_K^2 + \vec{k}^2}, \vec{k} \right), \quad -p_2 = \left(\sqrt{M_\pi^2 + \vec{k}^2}, -\vec{k} \right),$$

$$q_K = \left(\sqrt{M_K^2 + \vec{q}_K^2}, \vec{q}_K \right), \quad q_\pi = \left(\sqrt{M_\pi^2 + \vec{q}_K^2}, -\vec{q}_K \right),$$

$$p_1 = \left(\sqrt{M_\pi^2 + \vec{p}_1^2}, \vec{p}_1 \right), \quad L = \left(\sqrt{s_\ell + \vec{p}_1^2}, -\vec{p}_1 \right). \tag{B.15}$$

Inserting these expressions into $u = (k - p_2)^2 = (q_K + q_\pi)^2 = (p_1 + L)^2$ gives the values of $\vec{k}^2$, $\vec{q}_K^2$ and $\vec{p}_1^2$. We choose the directions of the three-vectors according to

Fig. 21 Vectors and angles in the u-channel centre-of-mass frame

Fig. 21, i.e. the angles are defined as $\theta_u := \angle(-\vec{k}, \vec{p}_1)$, $\theta_u' := \angle(\vec{k}, \vec{q}_K)$, $\theta_u'' := \angle(-\vec{q}_K, \vec{p}_1)$.

The results for the u-channel are then

$$k = \left(\frac{u + M_K^2 - M_\pi^2}{2\sqrt{u}}, -\frac{\lambda_{K\pi}^{1/2}(u)}{2\sqrt{u}} \cos\theta_u, -\frac{\lambda_{K\pi}^{1/2}(u)}{2\sqrt{u}} \sin\theta_u, 0 \right),$$

$$p_2 = \left(\frac{M_K^2 - M_\pi^2 - u}{2\sqrt{u}}, -\frac{\lambda_{K\pi}^{1/2}(u)}{2\sqrt{u}} \cos\theta_u, -\frac{\lambda_{K\pi}^{1/2}(u)}{2\sqrt{u}} \sin\theta_u, 0 \right),$$
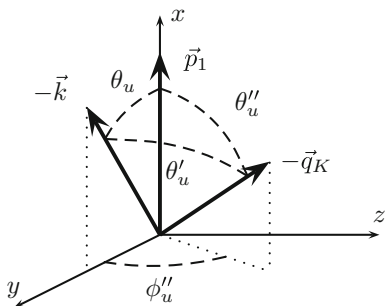
$$q_K = \left(\frac{u + M_K^2 - M_\pi^2}{2\sqrt{u}}, -\frac{\lambda_{K\pi}^{1/2}(u)}{2\sqrt{u}} \cos\theta_u'', -\frac{\lambda_{K\pi}^{1/2}(u)}{2\sqrt{u}} \sin\theta_u'' \cos\phi_u'', \right.$$
$$\left. -\frac{\lambda_{K\pi}^{1/2}(u)}{2\sqrt{u}} \sin\theta_u'' \sin\phi_u'' \right),$$

$$q_\pi = \left(\frac{u - M_K^2 + M_\pi^2}{2\sqrt{u}}, \frac{\lambda_{K\pi}^{1/2}(u)}{2\sqrt{u}} \cos\theta_u'', \frac{\lambda_{K\pi}^{1/2}(u)}{2\sqrt{u}} \sin\theta_u'' \cos\phi_u'', \right.$$
$$\left. \frac{\lambda_{K\pi}^{1/2}(u)}{2\sqrt{u}} \sin\theta_u'' \sin\phi_u'' \right),$$

$$p_1 = \left(\frac{u - s_\ell + M_\pi^2}{2\sqrt{u}}, \frac{\lambda_{\ell\pi}^{1/2}(u)}{2\sqrt{u}}, 0, 0 \right),$$

$$L = \left(\frac{u + s_\ell - M_\pi^2}{2\sqrt{u}}, -\frac{\lambda_{\ell\pi}^{1/2}(u)}{2\sqrt{u}}, 0, 0 \right). \tag{B.16}$$

Let us calculate the u-channel scattering angle θ_u as a function of the Mandelstam variables:

$$\begin{aligned}
s - t &= (p_1 + p_2)^2 - (k - p_1)^2 \\
&= p_1^2 + p_2^2 + 2p_1 p_2 - k^2 - p_1^2 + 2kp_1 \\
&= M_\pi^2 - M_K^2 + 2p_1(k + p_2) = M_\pi^2 - M_K^2 \\
&\quad + 2\left(\frac{u - s_\ell + M_\pi^2}{2\sqrt{u}} \frac{M_K^2 - M_\pi^2}{\sqrt{u}} + \frac{\lambda_{\ell\pi}^{1/2}(u)}{2\sqrt{u}} \frac{\lambda_{K\pi}^{1/2}(u)}{\sqrt{u}} \cos\theta_u \right),
\end{aligned} \tag{B.17}$$

hence

$$\cos\theta_u = \frac{u(s - t) + \Delta_{K\pi}\Delta_{\ell\pi}}{\lambda_{K\pi}^{1/2}(u)\lambda_{\ell\pi}^{1/2}(u)}. \tag{B.18}$$

C Omnès solution to the dispersion relation

C.1 Solution for $n = 3$ subtractions

For $n = 3$ subtractions, the Omnès representation reads

$$\begin{aligned}
M_0(s) &= \Omega_0^0(s)\left\{ a^{M_0} + b^{M_0}\frac{s}{M_K^2} + c^{M_0}\frac{s^2}{M_K^4} + d^{M_0}\frac{s^3}{M_K^6} \right. \\
&\quad \left. + \frac{s^4}{\pi}\int_{s_0}^{\Lambda^2} \frac{\hat{M}_0(s')\sin\delta_0^0(s')}{|\Omega_0^0(s')|(s' - s - i\epsilon)s'^4} ds' \right\},
\end{aligned}$$

$$\begin{aligned}
M_1(s) &= \Omega_1^1(s)\left\{ a^{M_1} + b^{M_1}\frac{s}{M_K^2} + c^{M_1}\frac{s^2}{M_K^4} \right. \\
&\quad \left. + \frac{s^3}{\pi}\int_{s_0}^{\Lambda^2} \frac{\hat{M}_1(s')\sin\delta_1^1(s')}{|\Omega_1^1(s')|(s' - s - i\epsilon)s'^3} ds' \right\},
\end{aligned}$$

$$\begin{aligned}
\tilde{M}_1(s) &= \Omega_1^1(s)\left\{ a^{\tilde{M}_1} + b^{\tilde{M}_1}\frac{s}{M_K^2} + c^{\tilde{M}_1}\frac{s^2}{M_K^4} + d^{\tilde{M}_1}\frac{s^3}{M_K^6} \right. \\
&\quad \left. + \frac{s^4}{\pi}\int_{s_0}^{\Lambda^2} \frac{\hat{\tilde{M}}_1(s')\sin\delta_1^1(s')}{|\Omega_1^1(s')|(s' - s - i\epsilon)s'^4} ds' \right\},
\end{aligned}$$

$$\begin{aligned}
N_0(t) &= \Omega_0^{1/2}(t)\left\{ b^{N_0}\frac{t}{M_K^2} + c^{N_0}\frac{t^2}{M_K^4} \right. \\
&\quad \left. + \frac{t^3}{\pi}\int_{t_0}^{\Lambda^2} \frac{\hat{N}_0(t')\sin\delta_0^{1/2}(t')}{|\Omega_0^{1/2}(t')|(t' - t - i\epsilon)t'^3} dt' \right\},
\end{aligned}$$

$$\begin{aligned}
N_1(t) &= \Omega_1^{1/2}(t) \\
&\quad \times \left\{ a^{N_1} + \frac{t}{\pi}\int_{t_0}^{\Lambda^2} \frac{\hat{N}_1(t')\sin\delta_1^{1/2}(t')}{|\Omega_1^{1/2}(t')|(t' - t - i\epsilon)t'} dt' \right\},
\end{aligned}$$

$$\begin{aligned}
\tilde{N}_1(t) &= \Omega_1^{1/2}(t) \\
&\quad \times \left\{ b^{\tilde{N}_1}\frac{t}{M_K^2} + \frac{t^2}{\pi}\int_{t_0}^{\Lambda^2} \frac{\hat{\tilde{N}}_1(t')\sin\delta_1^{1/2}(t')}{|\Omega_1^{1/2}(t')|(t' - t - i\epsilon)t'^2} dt' \right\},
\end{aligned}$$

$$\begin{aligned}
R_0(t) &= \Omega_0^{3/2}(t) \\
&\quad \times \left\{ \frac{t^3}{\pi}\int_{t_0}^{\Lambda^2} \frac{\hat{R}_0(t')\sin\delta_0^{3/2}(t')}{|\Omega_0^{3/2}(t')|(t' - t - i\epsilon)t'^3} dt' \right\},
\end{aligned}$$

$$\begin{aligned}
R_1(t) &= \Omega_1^{3/2}(t) \\
&\quad \times \left\{ \frac{t}{\pi}\int_{t_0}^{\Lambda^2} \frac{\hat{R}_1(t')\sin\delta_1^{3/2}(t')}{|\Omega_1^{3/2}(t')|(t' - t - i\epsilon)t'} dt' \right\},
\end{aligned}$$

$$\begin{aligned}
\tilde{R}_1(t) &= \Omega_1^{3/2}(t) \\
&\quad \times \left\{ \frac{t^2}{\pi}\int_{t_0}^{\Lambda^2} \frac{\hat{\tilde{R}}_1(t')\sin\delta_1^{3/2}(t')}{|\Omega_1^{3/2}(t')|(t' - t - i\epsilon)t'^2} dt' \right\}. \tag{C.1}
\end{aligned}$$

Let us work out how to transform the Omnès representation (85) into the one with more subtractions (C.1). We start by subtracting all the dispersive integrals once more, using the relation

$$\frac{1}{s' - s} = \frac{1}{s'} + \frac{s}{(s' - s)s'}. \tag{C.2}$$

This generates nine additional subtraction constants:

$$M_0(s) = \Omega_0^0(s)\left\{ a^{M_0} + b^{M_0}\frac{s}{M_K^2} + c^{M_0}\frac{s^2}{M_K^4} + d^{M_0}\frac{s^3}{M_K^6} \right.$$

$$+\frac{s^4}{\pi}\int_{s_0}^{\Lambda^2}\frac{\hat{M}_0(s')\sin\delta_0^0(s')}{|\Omega_0^0(s')|(s'-s-i\epsilon)s'^4}ds'\Big\},$$

$$M_1(s)=\Omega_1^1(s)\Big\{a^{M_1}+b^{M_1}\frac{s}{M_K^2}+c^{M_1}\frac{s^2}{M_K^4}$$
$$+\frac{s^3}{\pi}\int_{s_0}^{\Lambda^2}\frac{\hat{M}_1(s')\sin\delta_1^1(s')}{|\Omega_1^1(s')|(s'-s-i\epsilon)s'^3}ds'\Big\},$$

$$\tilde{M}_1(s)=\Omega_1^1(s)\Big\{a^{\tilde{M}_1}+b^{\tilde{M}_1}\frac{s}{M_K^2}+c^{\tilde{M}_1}\frac{s^2}{M_K^4}+d^{\tilde{M}_1}\frac{s^3}{M_K^6}$$
$$+\frac{s^4}{\pi}\int_{s_0}^{\Lambda^2}\frac{\hat{\tilde{M}}_1(s')\sin\delta_1^1(s')}{|\Omega_1^1(s')|(s'-s-i\epsilon)s'^4}ds'\Big\},$$

$$N_0(t)=\Omega_0^{1/2}(t)\Big\{b^{N_0}\frac{t}{M_K^2}+c^{N_0}\frac{t^2}{M_K^4}$$
$$+\frac{t^3}{\pi}\int_{t_0}^{\Lambda^2}\frac{\hat{N}_0(t')\sin\delta_0^{1/2}(t')}{|\Omega_0^{1/2}(t')|(t'-t-i\epsilon)t'^3}dt'\Big\},$$

$$N_1(t)=\Omega_1^{1/2}(t)$$
$$\times\Big\{a^{N_1}+\frac{t}{\pi}\int_{t_0}^{\Lambda^2}\frac{\hat{N}_1(t')\sin\delta_1^{1/2}(t')}{|\Omega_1^{1/2}(t')|(t'-t-i\epsilon)t'}dt'\Big\},$$

$$\tilde{N}_1(t)=\Omega_1^{1/2}(t)$$
$$\times\Big\{b^{\tilde{N}_1}\frac{t}{M_K^2}+\frac{t^2}{\pi}\int_{t_0}^{\Lambda^2}\frac{\hat{\tilde{N}}_1(t')\sin\delta_1^{1/2}(t')}{|\Omega_1^{1/2}(t')|(t'-t-i\epsilon)t'^2}dt'\Big\},$$

$$R_0(t)=\Omega_0^{3/2}(t)$$
$$\times\Big\{c^{R_0}\frac{t^2}{M_K^4}+\frac{t^3}{\pi}\int_{t_0}^{\Lambda^2}\frac{\hat{R}_0(t')\sin\delta_0^{3/2}(t')}{|\Omega_0^{3/2}(t')|(t'-t-i\epsilon)t'^3}dt'\Big\},$$

$$R_1(t)=\Omega_1^{3/2}(t)$$
$$\times\Big\{a^{R_1}+\frac{t}{\pi}\int_{t_0}^{\Lambda^2}\frac{\hat{R}_1(t')\sin\delta_1^{3/2}(t')}{|\Omega_1^{3/2}(t')|(t'-t-i\epsilon)t'}dt'\Big\},$$

$$\tilde{R}_1(t)=\Omega_1^{3/2}(t)$$
$$\times\Big\{b^{\tilde{R}_1}\frac{t}{M_K^2}+\frac{t^2}{\pi}\int_{t_0}^{\Lambda^2}\frac{\hat{\tilde{R}}_1(t')\sin\delta_1^{3/2}(t')}{|\Omega_1^{3/2}(t')|(t'-t-i\epsilon)t'^2}dt'\Big\}.\quad(\text{C.3})$$

To get rid of the subtraction constants in the R-functions, we apply a gauge transformation (74). To this end, let us write the gauge transformation in the Omnès representation:

$$\delta M_0(s)=\Omega_0^0(s)\Big\{\delta a^{M_0}+\delta b^{M_0}\frac{s}{M_K^2}+\delta c^{M_0}\frac{s^2}{M_K^4}$$
$$+\delta d^{M_0}\frac{s^3}{M_K^6}+\frac{s^4}{\pi}\int_{s_0}^{\Lambda^2}\frac{\delta\hat{M}_0(s')\sin\delta_0^0(s')}{|\Omega_0^0(s')|(s'-s-i\epsilon)s'^4}ds'\Big\},$$

$$\delta M_1(s)=\Omega_1^1(s)\Big\{\delta a^{M_1}+\delta b^{M_1}\frac{s}{M_K^2}+\delta c^{M_1}\frac{s^2}{M_K^4}$$
$$+\frac{s^3}{\pi}\int_{s_0}^{\Lambda^2}\frac{\delta\hat{M}_1(s')\sin\delta_1^1(s')}{|\Omega_1^1(s')|(s'-s-i\epsilon)s'^3}ds'\Big\},$$

$$\delta\tilde{M}_1(s)=\Omega_1^1(s)\Big\{\delta a^{\tilde{M}_1}+\delta b^{\tilde{M}_1}\frac{s}{M_K^2}+\delta c^{\tilde{M}_1}\frac{s^2}{M_K^4}$$
$$+\delta d^{\tilde{M}_1}\frac{s^3}{M_K^6}+\frac{s^4}{\pi}\int_{s_0}^{\Lambda^2}\frac{\delta\hat{\tilde{M}}_1(s')\sin\delta_1^1(s')}{|\Omega_1^1(s')|(s'-s-i\epsilon)s'^4}ds'\Big\},$$

$$\delta N_0(t)=\Omega_0^{1/2}(t)\Big\{\delta b^{N_0}\frac{t}{M_K^2}+\delta c^{N_0}\frac{t^2}{M_K^4}$$
$$+\frac{t^3}{\pi}\int_{t_0}^{\Lambda^2}\frac{\delta\hat{N}_0(t')\sin\delta_0^{1/2}(t')}{|\Omega_0^{1/2}(t')|(t'-t-i\epsilon)t'^3}dt'\Big\},$$

$$\delta N_1(t)=\Omega_1^{1/2}(t)$$
$$\times\Big\{\delta a^{N_1}+\frac{t}{\pi}\int_{t_0}^{\Lambda^2}\frac{\delta\hat{N}_1(t')\sin\delta_1^{1/2}(t')}{|\Omega_1^{1/2}(t')|(t'-t-i\epsilon)t'}dt'\Big\},$$

$$\delta\tilde{N}_1(t)=\Omega_1^{1/2}(t)$$
$$\times\Big\{\delta b^{\tilde{N}_1}\frac{t}{M_K^2}+\frac{t^2}{\pi}\int_{t_0}^{\Lambda^2}\frac{\delta\hat{\tilde{N}}_1(t')\sin\delta_1^{1/2}(t')}{|\Omega_1^{1/2}(t')|(t'-t-i\epsilon)t'^2}dt'\Big\},$$

$$\delta R_0(t)=\Omega_0^{3/2}(t)$$
$$\times\Big\{\delta c^{R_0}\frac{t^2}{M_K^4}+\frac{t^3}{\pi}\int_{t_0}^{\Lambda^2}\frac{\delta\hat{R}_0(t')\sin\delta_0^{3/2}(t')}{|\Omega_0^{3/2}(t')|(t'-t-i\epsilon)t'^3}dt'\Big\},$$

$$\delta R_1(t)=\Omega_1^{3/2}(t)$$
$$\times\Big\{\delta a^{R_1}+\frac{t}{\pi}\int_{t_0}^{\Lambda^2}\frac{\delta\hat{R}_1(t')\sin\delta_1^{3/2}(t')}{|\Omega_1^{3/2}(t')|(t'-t-i\epsilon)t'}dt'\Big\},$$

$$\delta\tilde{R}_1(t)=\Omega_1^{3/2}(t)$$
$$\times\Big\{\delta b^{\tilde{R}_1}\frac{t}{M_K^2}+\frac{t^2}{\pi}\int_{t_0}^{\Lambda^2}\frac{\delta\hat{\tilde{R}}_1(t')\sin\delta_1^{3/2}(t')}{|\Omega_1^{3/2}(t')|(t'-t-i\epsilon)t'^2}dt'\Big\}.$$
$$(\text{C.4})$$

Since the gauge transformation is a polynomial and has no discontinuity, the changes in the hat functions are given by $\delta\hat{M}_0=-\delta M_0$ etc., which ensures that the partial waves are unchanged. The shifts in the subtraction constants are most easily found by comparing the Taylor expansion of (C.4) with (74):

$$\delta a^{M_0}=(2A^{R_1}-B^{\tilde{R}_1}+2C^{R_0})\frac{\Sigma_0^2-\Delta_{K\pi}\Delta_{\ell\pi}}{2M_K^4},$$

$$\delta b^{M_0}=-(2A^{R_1}-B^{\tilde{R}_1}+2C^{R_0})\left(\frac{\Sigma_0}{M_K^2}+\omega_0^0\frac{\Sigma_0^2-\Delta_{K\pi}\Delta_{\ell\pi}}{2M_K^4}\right),$$

$$\delta c^{M_0}=(2A^{R_1}-B^{\tilde{R}_1}+2C^{R_0})$$
$$\times\left(\frac{1}{2}+\omega_0^0\frac{\Sigma_0}{M_K^2}+\left(\frac{\omega_0^{0^2}}{2}-\bar{\omega}_0^0\right)\frac{\Sigma_0^2-\Delta_{K\pi}\Delta_{\ell\pi}}{2M_K^4}\right),$$

$$\delta d^{M_0}=-(2A^{R_1}-B^{\tilde{R}_1}+2C^{R_0})\left(\frac{\omega_0^0}{2}-\left(\bar{\omega}_0^0-\frac{\omega_0^{0^2}}{2}\right)\right.$$
$$\left.\times\frac{\Sigma_0}{M_K^2}+(\omega_0^{0^3}-6\omega_0^0\bar{\omega}_0^0+6\bar{\bar{\omega}}_0^0)\frac{\Sigma_0^2-\Delta_{K\pi}\Delta_{\ell\pi}}{12M_K^4}\right),$$

$$\delta a^{M_1}=-(A^{R_1}+B^{\tilde{R}_1}+2C^{R_0})\frac{\Sigma_0}{M_K^2}+B^{\tilde{R}_1}\frac{\Delta_{K\pi}}{2M_K^2},$$

$$\delta b^{M_1}=(B^{\tilde{R}_1}+2C^{R_0})$$
$$+\omega_1^1\left((A^{R_1}+B^{\tilde{R}_1}+2C^{R_0})\frac{\Sigma_0}{M_K^2}-B^{\tilde{R}_1}\frac{\Delta_{K\pi}}{2M_K^2}\right),$$

$$\delta c^{M_1} = -\left((A^{R_1} + B^{\tilde{R}_1} + 2C^{R_0})\frac{\Sigma_0}{M_K^2} - B^{\tilde{R}_1}\frac{\Delta_{K\pi}}{2M_K^2} \right)$$

$$\times \left(\frac{\omega_1^{1\,2}}{2} - \bar{\omega}_1^1 \right) - \omega_1^1 (B^{\tilde{R}_1} + 2C^{R_0}),$$

$$\delta a^{\tilde{M}_1} = (B^{\tilde{R}_1} - 2C^{R_0})\frac{\Sigma_0^2}{2M_K^4} - (2A^{R_1} + B^{\tilde{R}_1} - 2C^{R_0})$$

$$\times \frac{\Delta_{K\pi}\Delta_{\ell\pi}}{2M_K^4} + B^{\tilde{R}_1}\frac{\Sigma_0\Delta_{K\pi}}{2M_K^4},$$

$$\delta b^{\tilde{M}_1} = -\left(B^{\tilde{R}_1}\frac{\Delta_{K\pi}}{2M_K^2} + (A^{R_1} + B^{\tilde{R}_1} - 2C^{R_0})\frac{\Sigma_0}{M_K^2} \right)$$

$$- \omega_1^1 \left((B^{\tilde{R}_1} - 2C^{R_0})\frac{\Sigma_0^2}{2M_K^4} - (2A^{R_1} + B^{\tilde{R}_1} \right.$$

$$\left. - 2C^{R_0})\frac{\Delta_{K\pi}\Delta_{\ell\pi}}{2M_K^4} + B^{\tilde{R}_1}\frac{\Sigma_0\Delta_{K\pi}}{2M_K^4} \right),$$

$$\delta c^{\tilde{M}_1} = \frac{1}{2}(2A^{R_1} + B^{\tilde{R}_1} - 2C^{R_0})$$

$$+ \omega_1^1 \left(B^{\tilde{R}_1}\frac{\Delta_{K\pi}}{2M_K^2} + (A^{R_1} + B^{\tilde{R}_1} - 2C^{R_0})\frac{\Sigma_0}{M_K^2} \right)$$

$$+ \left(\frac{\omega_1^{1\,2}}{2} - \bar{\omega}_1^1 \right)$$

$$\times \left((B^{\tilde{R}_1} - 2C^{R_0})\frac{\Sigma_0^2}{2M_K^4} - (2A^{R_1} + B^{\tilde{R}_1} - 2C^{R_0}) \right.$$

$$\left. \times \frac{\Delta_{K\pi}\Delta_{\ell\pi}}{2M_K^4} + B^{\tilde{R}_1}\frac{\Sigma_0\Delta_{K\pi}}{2M_K^4} \right),$$

$$\delta d^{\tilde{M}_1} = -\frac{1}{2}\omega_1^1(2A^{R_1} + B^{\tilde{R}_1} - 2C^{R_0}) - \left(\frac{\omega_1^{1\,2}}{2} - \bar{\omega}_1^1 \right)$$

$$\times \left(B^{\tilde{R}_1}\frac{\Delta_{K\pi}}{2M_K^2} + (A^{R_1} + B^{\tilde{R}_1} - 2C^{R_0})\frac{\Sigma_0}{M_K^2} \right)$$

$$- \frac{1}{6}(\omega_1^{1\,3} - 6\omega_1^1\bar{\omega}_1^1 + 6\bar{\bar{\omega}}_1^1)$$

$$\times \left((B^{\tilde{R}_1} - 2C^{R_0})\frac{\Sigma_0^2}{2M_K^4} - (2A^{R_1} + B^{\tilde{R}_1} - 2C^{R_0}) \right.$$

$$\left. \times \frac{\Delta_{K\pi}\Delta_{\ell\pi}}{2M_K^4} + B^{\tilde{R}_1}\frac{\Sigma_0\Delta_{K\pi}}{2M_K^4} \right),$$

$$\delta b^{N_0} = -(2A^{R_1} - B^{\tilde{R}_1} + 2C^{R_0})\frac{3(\Delta_{K\pi} + 2\Sigma_0)}{8M_K^2},$$

$$\delta c^{N_0} = \frac{1}{8}(6A^{R_1} - 3B^{\tilde{R}_1} - 10C^{R_0})$$

$$+ \omega_0^{1/2}(2A^{R_1} - B^{\tilde{R}_1} + 2C^{R_0})\frac{3(\Delta_{K\pi} + 2\Sigma_0)}{8M_K^2},$$

$$\delta a^{N_1} = -\frac{1}{4}(2A^{R_1} + 3B^{\tilde{R}_1} - 6C^{R_0}),$$

$$\delta b^{\tilde{N}_1} = -\frac{1}{4}(6A^{R_1} + 5B^{\tilde{R}_1} + 6C^{R_0}),$$

$$\delta c^{R_0} = C^{R_0}, \quad \delta a^{R_1} = A^{R_1}, \quad \delta b^{\tilde{R}_1} = B^{\tilde{R}_1}, \tag{C.5}$$

where ω, $\bar{\omega}$ and $\bar{\bar{\omega}}$ are defined by applying subtractions to the Omnès functions:

$$\Omega(s) = \exp\left(\frac{s}{\pi}\int_{s_0}^\infty \frac{\delta(s')}{(s'-s-i\epsilon)s'}\,ds' \right)$$

$$= \exp\left(\frac{s}{\pi}\int_{s_0}^\infty \frac{\delta(s')}{s'^2}\,ds' + \frac{s^2}{\pi}\int_{s_0}^\infty \frac{\delta(s')}{s'^3}\,ds' \right.$$

$$\left. + \frac{s^3}{\pi}\int_{s_0}^\infty \frac{\delta(s')}{s'^4}\,ds' + \frac{s^4}{\pi}\int_{s_0}^\infty \frac{\delta(s')}{(s'-s-i\epsilon)s'^4}\,ds' \right)$$

$$=: \exp\left(\omega\frac{s}{M_K^2} + \bar{\omega}\frac{s^2}{M_K^4} + \bar{\bar{\omega}}\frac{s^3}{M_K^6} \right.$$

$$\left. + \frac{s^4}{\pi}\int_{s_0}^\infty \frac{\delta(s')}{(s'-s-i\epsilon)s'^4}\,ds' \right). \tag{C.6}$$

In order to obtain the form (C.1), the subtraction constants in the R-functions can now be removed with the gauge transformation

$$C^{R_0} = -c^{R_0},$$
$$A^{R_1} = -a^{R_1},$$
$$B^{\tilde{R}_1} = -b^{\tilde{R}_1}. \tag{C.7}$$

C.2 Hat functions

In the following, we provide the explicit expressions for the hat functions that appear in the Omnès solution to the dispersion relation.

$$
\begin{aligned}
\hat{M}_0(s) = {} & \frac{2}{3}(\langle N_0\rangle_{t_s} + 2\langle R_0\rangle_{t_s}) - (\langle z N_0\rangle_{t_s} + 2\langle z R_0\rangle_{t_s})\frac{2\sigma_\pi PL}{3X} \\
& - (\langle N_1\rangle_{t_s} + 2\langle R_1\rangle_{t_s})\frac{3s^2 - 4s\Sigma_0 + \Sigma_0^2 - 4\Delta_{K\pi}\Delta_{\ell\pi}}{6M_K^4} \\
& + (\langle z N_1\rangle_{t_s} + 2\langle z R_1\rangle_{t_s})\frac{\sigma_\pi(-4PL\Delta_{K\pi}\Delta_{\ell\pi} + PL(3s^2 - 4s\Sigma_0 + \Sigma_0^2) - 4sX^2)}{6M_K^4 X} \\
& + (\langle z^2 N_1\rangle_{t_s} + 2\langle z^2 R_1\rangle_{t_s})\frac{2\sigma_\pi^2(PLs + X^2)}{3M_K^4} - (\langle z^3 N_1\rangle_{t_s} + 2\langle z^3 R_1\rangle_{t_s})\frac{2\sigma_\pi^3 PL X}{3M_K^4} \\
& - (\langle \tilde{N}_1\rangle_{t_s} + 2\langle \tilde{R}_1\rangle_{t_s})\frac{2\Delta_{K\pi} + 3s - 3\Sigma_0}{6M_K^2} \\
& + (\langle z\tilde{N}_1\rangle_{t_s} + 2\langle z\tilde{R}_1\rangle_{t_s})\frac{\sigma_\pi(PL(2\Delta_{K\pi} - s + \Sigma_0) - 6X^2)}{6M_K^2 X} - (\langle z^2\tilde{N}_1\rangle_{t_s} + 2\langle z^2\tilde{R}_1\rangle_{t_s})\frac{\sigma_\pi^2 PL}{3M_K^2},
\end{aligned} \tag{C.8}
$$

$$
\begin{aligned}
\hat{M}_1(s) = {} & (\langle N_0\rangle_{t_s} - \langle R_0\rangle_{t_s})\frac{M_K^2 PL}{2X^2} + (\langle z N_0\rangle_{t_s} - \langle z R_0\rangle_{t_s})\frac{M_K^2}{\sigma_\pi X} - (\langle z^2 N_0\rangle_{t_s} - \langle z^2 R_0\rangle_{t_s})\frac{3M_K^2 PL}{2X^2} \\
& + (\langle N_1\rangle_{t_s} - \langle R_1\rangle_{t_s})\frac{(4\Delta_{K\pi}\Delta_{\ell\pi} - 3s^2 + 4s\Sigma_0 - \Sigma_0^2)PL}{8M_K^2 X^2} \\
& - (\langle z N_1\rangle_{t_s} - \langle z R_1\rangle_{t_s})\frac{3s^2 + 2\sigma_\pi^2 PLs - 4s\Sigma_0 + \Sigma_0^2 - 4\Delta_{K\pi}\Delta_{\ell\pi}}{4M_K^2 \sigma_\pi X} \\
& + (\langle z^2 N_1\rangle_{t_s} - \langle z^2 R_1\rangle_{t_s})\left(\frac{3PL(3s^2 - 4s\Sigma_0 + \Sigma_0^2) - 12PL\Delta_{K\pi}\Delta_{\ell\pi}}{8M_K^2 X^2} + \frac{\sigma_\pi^2 PL - 2s}{2M_K^2}\right) \\
& + (\langle z^3 N_1\rangle_{t_s} - \langle z^3 R_1\rangle_{t_s})\frac{\sigma_\pi(3sPL + 2X^2)}{2XM_K^2} - (\langle z^4 N_1\rangle_{t_s} - \langle z^4 R_1\rangle_{t_s})\frac{3\sigma_\pi^2 PL}{2M_K^2} \\
& - (\langle \tilde{N}_1\rangle_{t_s} - \langle \tilde{R}_1\rangle_{t_s})\frac{PL(2\Delta_{K\pi} - s + \Sigma_0)}{8X^2} + (\langle z\tilde{N}_1\rangle_{t_s} - \langle z\tilde{R}_1\rangle_{t_s})\frac{3\Sigma_0 - 2\Delta_{K\pi} + \sigma_\pi^2 PL - 3s}{4\sigma_\pi X} \\
& + (\langle z^2\tilde{N}_1\rangle_{t_s} - \langle z^2\tilde{R}_1\rangle_{t_s})\left(\frac{3PL(2\Delta_{K\pi} - s + \Sigma_0)}{8X^2} - \frac{3}{2}\right) - (\langle z^3\tilde{N}_1\rangle_{t_s} - \langle z^3\tilde{R}_1\rangle_{t_s})\frac{3PL\sigma_\pi}{4X},
\end{aligned} \tag{C.9}
$$

$$
\begin{aligned}
\hat{\tilde{M}}_1(s) = {} & -(\langle N_0\rangle_{t_s} - \langle R_0\rangle_{t_s}) + (\langle z^2 N_0\rangle_{t_s} - \langle z^2 R_0\rangle_{t_s}) \\
& + (\langle N_1\rangle_{t_s} - \langle R_1\rangle_{t_s})\frac{3s^2 - 4s\Sigma_0 + \Sigma_0^2 - 4\Delta_{K\pi}\Delta_{\ell\pi}}{4M_K^4} + (\langle z N_1\rangle_{t_s} - \langle z R_1\rangle_{t_s})\frac{s\sigma_\pi X}{M_K^4} \\
& - (\langle z^2 N_1\rangle_{t_s} - \langle z^2 R_1\rangle_{t_s})\frac{3s^2 - 4s\Sigma_0 + \Sigma_0^2 + 4\sigma_\pi^2 X^2 - 4\Delta_{K\pi}\Delta_{\ell\pi}}{4M_K^4} \\
& - (\langle z^3 N_1\rangle_{t_s} - \langle z^3 R_1\rangle_{t_s})\frac{s\sigma_\pi X}{M_K^4} + (\langle z^4 N_1\rangle_{t_s} - \langle z^4 R_1\rangle_{t_s})\frac{\sigma_\pi^2 X^2}{M_K^4} \\
& + (\langle \tilde{N}_1\rangle_{t_s} - \langle \tilde{R}_1\rangle_{t_s})\frac{2\Delta_{K\pi} - s + \Sigma_0}{4M_K^2} - (\langle z\tilde{N}_1\rangle_{t_s} - \langle z\tilde{R}_1\rangle_{t_s})\frac{\sigma_\pi X}{2M_K^2} \\
& - (\langle z^2\tilde{N}_1\rangle_{t_s} - \langle z^2\tilde{R}_1\rangle_{t_s})\frac{2\Delta_{K\pi} - s + \Sigma_0}{4M_K^2} + (\langle z^3\tilde{N}_1\rangle_{t_s} - \langle z^3\tilde{R}_1\rangle_{t_s})\frac{\sigma_\pi X}{2M_K^2},
\end{aligned} \tag{C.10}
$$

$$\hat{N}_0(t) = \langle M_0\rangle_{s_t} \frac{\Delta_{K\pi} + t}{4t} - \langle zM_0\rangle_{s_t} \frac{\lambda_{K\pi}^{1/2}(t)(\Delta_{\ell\pi} + t)}{4t\lambda_{\ell\pi}^{1/2}(t)} + \langle M_1\rangle_{s_t} \frac{(\Delta_{K\pi} + t)(\Delta_{K\pi}\Delta_{\ell\pi} + t(\Sigma_0 - 3t))}{4t^2 M_K^2}$$

$$- \langle zM_1\rangle_{s_t} \frac{\lambda_{K\pi}^{1/2}(t)(\Delta_{K\pi}(\lambda_{\ell\pi}(t) + \Delta_{\ell\pi}(\Delta_{\ell\pi} + t)) + t(\lambda_{\ell\pi}(t) + (\Sigma_0 - 3t)(\Delta_{\ell\pi} + t)))}{4t^2 M_K^2 \lambda_{\ell\pi}^{1/2}(t)}$$

$$+ \langle z^2 M_1\rangle_{s_t} \frac{\lambda_{K\pi}(t)(\Delta_{\ell\pi} + t)}{4t^2 M_K^2} + \langle \tilde{M}_1\rangle_{s_t} \frac{\Delta_{K\pi} - 3t}{2t} - \langle z\tilde{M}_1\rangle_{s_t} \frac{\lambda_{K\pi}^{1/2}(t)(\Delta_{\ell\pi} + t)}{2t\lambda_{\ell\pi}^{1/2}(t)}$$

$$+ (\langle N_0\rangle_{u_t} - 4\langle R_0\rangle_{u_t})\frac{t - \Delta_{K\pi}}{6t} + (\langle zN_0\rangle_{u_t} - 4\langle zR_0\rangle_{u_t})\frac{\lambda_{K\pi}^{1/2}(t)\,(\Delta_{\ell\pi} + t)}{6t\lambda_{\ell\pi}^{1/2}(t)}$$

$$+ (\langle N_1\rangle_{u_t} - 4\langle R_1\rangle_{u_t})\frac{(\Delta_{K\pi} - t)(\Delta_{K\pi}\Delta_{\ell\pi} + t(t - \Sigma_0))(\Delta_{K\pi}\Delta_{\ell\pi} + t(\Sigma_0 - 3t))}{24t^3 M_K^4}$$

$$- (\langle zN_1\rangle_{u_t} - 4\langle zR_1\rangle_{u_t})\Bigg(\frac{\lambda_{K\pi}^{1/2}(t)(\Delta_{\ell\pi} + t)(\Delta_{K\pi}\Delta_{\ell\pi} + t(t - \Sigma_0))(\Delta_{K\pi}\Delta_{\ell\pi} + t(\Sigma_0 - 3t))}{24t^3 M_K^4 \lambda_{\ell\pi}^{1/2}(t)}$$

$$+ \frac{(\Delta_{K\pi} - t)\lambda_{K\pi}^{1/2}(t)\lambda_{\ell\pi}^{1/2}(t)(\Delta_{K\pi}\Delta_{\ell\pi} + t^2)}{12t^3 M_K^4} \Bigg)$$

$$+ (\langle z^2 N_1\rangle_{u_t} - 4\langle z^2 R_1\rangle_{u_t})\Bigg(\frac{(\Delta_{K\pi} - t)\,\lambda_{K\pi}(t)\lambda_{\ell\pi}(t)}{24t^3 M_K^4} + \frac{\lambda_{K\pi}(t)\,(\Delta_{\ell\pi} + t)\left(\Delta_{K\pi}\Delta_{\ell\pi} + t^2\right)}{12t^3 M_K^4} \Bigg)$$

$$- (\langle z^3 N_1\rangle_{u_t} - 4\langle z^3 R_1\rangle_{u_t})\frac{\lambda_{K\pi}^{3/2}(t)\lambda_{\ell\pi}^{1/2}(t)\,(\Delta_{\ell\pi} + t)}{24t^3 M_K^4}$$

$$- (\langle \tilde{N}_1\rangle_{u_t} - 4\langle \tilde{R}_1\rangle_{u_t})\frac{t\Delta_{K\pi}\,(3\Delta_{\ell\pi} + \Sigma_0 + t) + \Delta_{K\pi}^2\,(\Delta_{\ell\pi} - 2t) + 3t^2\,(\Sigma_0 - t)}{24t^2 M_K^2}$$

$$+ (\langle z\tilde{N}_1\rangle_{u_t} - 4\langle z\tilde{R}_1\rangle_{u_t})\Bigg(\frac{\lambda_{K\pi}^{1/2}(t)\,(\Delta_{\ell\pi} + t)\,(\Delta_{K\pi}\,(\Delta_{\ell\pi} - 2t) + t\,(\Sigma_0 - t))}{24t^2 M_K^2 \lambda_{\ell\pi}^{1/2}(t)} + \frac{(\Delta_{K\pi} + 3t)\,\lambda_{K\pi}^{1/2}(t)\lambda_{\ell\pi}^{1/2}(t)}{24t^2 M_K^2} \Bigg)$$

$$- (\langle z^2 \tilde{N}_1\rangle_{u_t} - 4\langle z^2 \tilde{R}_1\rangle_{u_t})\frac{\lambda_{K\pi}(t)\,(\Delta_{\ell\pi} + t)}{24t^2 M_K^2}, \tag{C.11}$$

$$\hat{N}_1(t) = \langle M_0\rangle_{s_t} \frac{3M_K^4\,(\Delta_{\ell\pi} + t)}{8t\lambda_{\ell\pi}(t)} + \langle zM_0\rangle_{s_t} \frac{3M_K^4\,(\Delta_{K\pi} + t)}{4t\lambda_{K\pi}^{1/2}(t)\lambda_{\ell\pi}^{1/2}(t)} - \langle z^2 M_0\rangle_{s_t} \frac{9M_K^4\,(\Delta_{\ell\pi} + t)}{8t\lambda_{\ell\pi}(t)}$$

$$+ \langle M_1\rangle_{s_t} \frac{3M_K^2\,(\Delta_{\ell\pi} + t)\,(\Delta_{K\pi}\Delta_{\ell\pi} + t\,(\Sigma_0 - 3t))}{8t^2 \lambda_{\ell\pi}(t)}$$

$$+ \langle zM_1\rangle_{s_t} \Bigg(\frac{3M_K^2\,(\Delta_{K\pi} + t)\,(\Delta_{K\pi}\Delta_{\ell\pi} + t\,(\Sigma_0 - 3t))}{4t^2 \lambda_{K\pi}^{1/2}(t)\lambda_{\ell\pi}^{1/2}(t)} - \frac{3M_K^2 \lambda_{K\pi}^{1/2}(t)\,(\Delta_{\ell\pi} + t)}{8t^2 \lambda_{\ell\pi}^{1/2}(t)} \Bigg)$$

$$- \langle z^2 M_1\rangle_{s_t} \Bigg(\frac{9M_K^2\,(\Delta_{\ell\pi} + t)\,(\Delta_{K\pi}\Delta_{\ell\pi} + t\,(\Sigma_0 - 3t))}{8t^2 \lambda_{\ell\pi}(t)} + \frac{3M_K^2\,(\Delta_{K\pi} + t)}{4t^2} \Bigg)$$

$$+ \langle z^3 M_1\rangle_{s_t} \frac{9M_K^2 \lambda_{K\pi}^{1/2}(t)\,(\Delta_{\ell\pi} + t)}{8t^2 \lambda_{\ell\pi}^{1/2}(t)} + \langle \tilde{M}_1\rangle_{s_t} \frac{3M_K^4\,(\Delta_{\ell\pi} + t)}{4t\lambda_{\ell\pi}(t)} + \langle z\tilde{M}_1\rangle_{s_t} \frac{3M_K^4\,(\Delta_{K\pi} - 3t)}{2t\lambda_{K\pi}^{1/2}(t)\lambda_{\ell\pi}^{1/2}(t)}$$

$$- \langle z^2 \tilde{M}_1\rangle_{s_t} \frac{9M_K^4\,(\Delta_{\ell\pi} + t)}{4t\lambda_{\ell\pi}(t)} - (\langle N_0\rangle_{u_t} - 4\langle R_0\rangle_{u_t})\frac{M_K^4\,(\Delta_{\ell\pi} + t)}{4t\lambda_{\ell\pi}(t)}$$

$$+ \left(\langle zN_0\rangle_{u_t} - 4\langle zR_0\rangle_{u_t}\right)\frac{M_K^4\,(t - \Delta_{K\pi})}{2t\lambda_{K\pi}^{1/2}(t)\lambda_{\ell\pi}^{1/2}(t)}$$

$$+ \left(\langle z^2N_0\rangle_{u_t} - 4\langle z^2R_0\rangle_{u_t}\right)\frac{3M_K^4\,(\Delta_{\ell\pi} + t)}{4t\lambda_{\ell\pi}(t)}$$

$$+ \left(\langle N_1\rangle_{u_t} - 4\langle R_1\rangle_{u_t}\right)\frac{(\Delta_{\ell\pi} + t)\,(\Delta_{K\pi}\Delta_{\ell\pi} + t\,(t - \Sigma_0))\,(\Delta_{K\pi}\Delta_{\ell\pi} + t\,(\Sigma_0 - 3t))}{16t^3\lambda_{\ell\pi}(t)}$$

$$+ \left(\langle zN_1\rangle_{u_t} - 4\langle zR_1\rangle_{u_t}\right)\left(\frac{(\Delta_{K\pi} - t)\,(\Delta_{K\pi}\Delta_{\ell\pi} + t\,(t - \Sigma_0))\,(\Delta_{K\pi}\Delta_{\ell\pi} + t\,(\Sigma_0 - 3t))}{8t^3\lambda_{K\pi}^{1/2}(t)\lambda_{\ell\pi}^{1/2}(t)}\right.$$

$$\left. - \frac{\lambda_{K\pi}^{1/2}(t)\,(\Delta_{\ell\pi} + t)\left(\Delta_{K\pi}\Delta_{\ell\pi} + t^2\right)}{8t^3\lambda_{\ell\pi}^{1/2}(t)}\right)$$

$$- \left(\langle z^2N_1\rangle_{u_t} - 4\langle z^2R_1\rangle_{u_t}\right)\left(\frac{3\,(\Delta_{\ell\pi} + t)\,(\Delta_{K\pi}\Delta_{\ell\pi} + t\,(t - \Sigma_0))\,(\Delta_{K\pi}\Delta_{\ell\pi} + t\,(\Sigma_0 - 3t))}{16t^3\lambda_{\ell\pi}(t)}\right.$$

$$\left. - \frac{\lambda_{K\pi}(t)\,(\Delta_{\ell\pi} + t)}{16t^3} + \frac{(\Delta_{K\pi} - t)\left(\Delta_{K\pi}\Delta_{\ell\pi} + t^2\right)}{4t^3}\right)$$

$$+ \left(\langle z^3N_1\rangle_{u_t} - 4\langle z^3R_1\rangle_{u_t}\right)\left(\frac{(\Delta_{K\pi} - t)\lambda_{K\pi}^{1/2}(t)\lambda_{\ell\pi}^{1/2}(t)}{8t^3} + \frac{3\lambda_{K\pi}^{1/2}(t)\,(\Delta_{\ell\pi} + t)\left(\Delta_{K\pi}\Delta_{\ell\pi} + t^2\right)}{8t^3\lambda_{\ell\pi}^{1/2}(t)}\right)$$

$$- \left(\langle z^4N_1\rangle_{u_t} - 4\langle z^4R_1\rangle_{u_t}\right)\frac{3\lambda_{K\pi}(t)\,(\Delta_{\ell\pi} + t)}{16t^3}$$

$$+ \left(\langle \tilde{N}_1\rangle_{u_t} - 4\langle \tilde{R}_1\rangle_{u_t}\right)\frac{M_K^2\,(\Delta_{\ell\pi} + t)\left(t^2 + 2t\Delta_{K\pi} - \Sigma_0 t - \Delta_{K\pi}\Delta_{\ell\pi}\right)}{16t^2\lambda_{\ell\pi}(t)}$$

$$+ \left(\langle z\tilde{N}_1\rangle_{u_t} - 4\langle z\tilde{R}_1\rangle_{u_t}\right)\left(\frac{M_K^2\lambda_{K\pi}^{1/2}(t)\,(\Delta_{\ell\pi} + t)}{16t^2\lambda_{\ell\pi}^{1/2}(t)}\right.$$

$$\left. - \frac{M_K^2\left(t\Delta_{K\pi}\,(3\Delta_{\ell\pi} + \Sigma_0 + t) + \Delta_{K\pi}^2\,(\Delta_{\ell\pi} - 2t) + 3t^2\,(\Sigma_0 - t)\right)}{8t^2\lambda_{K\pi}^{1/2}(t)\lambda_{\ell\pi}^{1/2}(t)}\right)$$

$$+ \left(\langle z^2\tilde{N}_1\rangle_{u_t} - 4\langle z^2\tilde{R}_1\rangle_{u_t}\right)\left(\frac{3M_K^2\,(\Delta_{\ell\pi} + t)\,(\Delta_{K\pi}\,(\Delta_{\ell\pi} - 2t) + t\,(\Sigma_0 - t))}{16t^2\lambda_{\ell\pi}(t)} + \frac{M_K^2\,(\Delta_{K\pi} + 3t)}{8t^2}\right)$$

$$- \left(\langle z^3\tilde{N}_1\rangle_{u_t} - 4\langle z^3\tilde{R}_1\rangle_{u_t}\right)\frac{3M_K^2\lambda_{K\pi}^{1/2}(t)\,(\Delta_{\ell\pi} + t)}{16t^2\lambda_{\ell\pi}^{1/2}(t)},\tag{C.12}$$

$$\hat{\tilde{N}}_1(t) = \langle(1 - z^2)M_0\rangle_{s_t}\frac{3M_K^2}{4t} + \langle(1 - z^2)M_1\rangle_{s_t}\frac{3\,(\Delta_{K\pi}\Delta_{\ell\pi} + t\,(\Sigma_0 - 3t))}{4t^2}$$

$$- \langle(1 - z^2)zM_1\rangle_{s_t}\frac{3\lambda_{K\pi}^{1/2}(t)\lambda_{\ell\pi}^{1/2}(t)}{4t^2} + \langle(1 - z^2)\tilde{M}_1\rangle_{s_t}\frac{3M_K^2}{2t}$$

$$- \left(\langle(1 - z^2)N_0\rangle_{u_t} - 4\langle(1 - z^2)R_0\rangle_{u_t}\right)\frac{M_K^2}{2t}$$

$$+ \left(\langle(1 - z^2)N_1\rangle_{u_t} - 4\langle(1 - z^2)R_1\rangle_{u_t}\right)\frac{(\Delta_{K\pi}\Delta_{\ell\pi} + t\,(t - \Sigma_0))\,(\Delta_{K\pi}\Delta_{\ell\pi} + t\,(\Sigma_0 - 3t))}{8t^3M_K^2}$$

$$- \left(\langle(1 - z^2)zN_1\rangle_{u_t} - 4\langle(1 - z^2)zR_1\rangle_{u_t}\right)\frac{\lambda_{K\pi}^{1/2}(t)\lambda_{\ell\pi}^{1/2}(t)\left(\Delta_{K\pi}\Delta_{\ell\pi} + t^2\right)}{4t^3M_K^2}$$

$$+ \left(\langle(1 - z^2)z^2N_1\rangle_{u_t} - 4\langle(1 - z^2)z^2R_1\rangle_{u_t}\right)\frac{\lambda_{K\pi}(t)\lambda_{\ell\pi}(t)}{8t^3M_K^2}$$

$$+ \left(\langle(1 - z^2)\tilde{N}_1\rangle_{u_t} - 4\langle(1 - z^2)\tilde{R}_1\rangle_{u_t}\right)\frac{t^2 + 2t\Delta_{K\pi} - \Sigma_0 t - \Delta_{K\pi}\Delta_{\ell\pi}}{8t^2}$$

$$+ \left(\langle(1 - z^2)z\tilde{N}_1\rangle_{u_t} - 4\langle(1 - z^2)z\tilde{R}_1\rangle_{u_t}\right)\frac{\lambda_{K\pi}^{1/2}(t)\lambda_{\ell\pi}^{1/2}(t)}{8t^2},\tag{C.13}$$

$$\hat{R}_0(u) = \langle M_0\rangle_{s_u}\frac{u+\Delta_{K\pi}}{4u} - \langle zM_0\rangle_{s_u}\frac{(u+\Delta_{\ell\pi})\lambda_{K\pi}^{1/2}(u)}{4u\lambda_{\ell\pi}^{1/2}(u)} - \langle M_1\rangle_{s_u}\frac{(u+\Delta_{K\pi})\,(u\,(\Sigma_0-3u)+\Delta_{K\pi}\Delta_{\ell\pi})}{8u^2M_K^2}$$

$$+ \langle zM_1\rangle_{s_u}\left(\frac{\lambda_{K\pi}^{1/2}(u)\lambda_{\ell\pi}^{1/2}(u)\,(u+\Delta_{K\pi})}{8u^2M_K^2} + \frac{(u+\Delta_{\ell\pi})\,(u\,(\Sigma_0-3u)+\Delta_{K\pi}\Delta_{\ell\pi}\lambda_{K\pi}^{1/2}(u))}{8u^2M_K^2\lambda_{\ell\pi}^{1/2}(u)}\right)$$

$$- \langle z^2M_1\rangle_{s_u}\frac{(u+\Delta_{\ell\pi})\lambda_{K\pi}(u)}{8u^2M_K^2} + \langle \tilde{M}_1\rangle_{s_u}\frac{3u-\Delta_{K\pi}}{4u} + \langle z\tilde{M}_1\rangle_{s_u}\frac{(u+\Delta_{\ell\pi})\lambda_{K\pi}^{1/2}(u)}{4u\lambda_{\ell\pi}^{1/2}(u)}$$

$$+ (2\langle N_0\rangle_{t_u}+\langle R_0\rangle_{t_u})\frac{\Delta_{K\pi}-u}{6u} - (2\langle zN_0\rangle_{t_u}+\langle zR_0\rangle_{t_u})\frac{(u+\Delta_{\ell\pi})\lambda_{K\pi}^{1/2}(u)}{6u\lambda_{\ell\pi}^{1/2}(u)}$$

$$- (2\langle N_1\rangle_{t_u}+\langle R_1\rangle_{t_u})\frac{(\Delta_{K\pi}-u)\,(u\,(u-\Sigma_0)+\Delta_{K\pi}\Delta_{\ell\pi})\,(u\,(\Sigma_0-3u)+\Delta_{K\pi}\Delta_{\ell\pi})}{24u^3M_K^4}$$

$$+ (2\langle zN_1\rangle_{t_u}+\langle zR_1\rangle_{t_u})\left(\frac{(\Delta_{K\pi}-u)\lambda_{K\pi}^{1/2}(u)\lambda_{\ell\pi}^{1/2}(u)\,(u^2+\Delta_{K\pi}\Delta_{\ell\pi})}{12u^3M_K^4}\right.$$

$$\left. + \frac{(u+\Delta_{\ell\pi})\,(u\,(u-\Sigma_0)+\Delta_{K\pi}\Delta_{\ell\pi})\,(u\,(\Sigma_0-3u)+\Delta_{K\pi}\Delta_{\ell\pi})\lambda_{K\pi}^{1/2}(u)}{24u^3M_K^4\lambda_{\ell\pi}^{1/2}(u)}\right)$$

$$+ (2\langle z^2N_1\rangle_{t_u}+\langle z^2R_1\rangle_{t_u})\left(\frac{(u-\Delta_{K\pi})\lambda_{K\pi}(u)\lambda_{\ell\pi}(u)}{24u^3M_K^4} - \frac{(u+\Delta_{\ell\pi})\,(u^2+\Delta_{K\pi}\Delta_{\ell\pi})\lambda_{K\pi}(u)}{12u^3M_K^4}\right)$$

$$+ (2\langle z^3N_1\rangle_{t_u}+\langle z^3R_1\rangle_{t_u})\frac{(u+\Delta_{\ell\pi})\lambda_{K\pi}^{3/2}(u)\lambda_{\ell\pi}^{1/2}(u)}{24u^3M_K^4}$$

$$+ (2\langle \tilde{N}_1\rangle_{t_u}+\langle \tilde{R}_1\rangle_{t_u})\frac{3\,(\Sigma_0-u)\,u^2+\Delta_{K\pi}\,(u+\Sigma_0+3\Delta_{\ell\pi})\,u+\Delta_{K\pi}^2\,(\Delta_{\ell\pi}-2u)}{24u^2M_K^2}$$

$$+ (2\langle z\tilde{N}_1\rangle_{t_u}+\langle z\tilde{R}_1\rangle_{t_u})\left(\frac{(u+\Delta_{\ell\pi})\,(u^2-\Sigma_0u+2\Delta_{K\pi}u-\Delta_{K\pi}\Delta_{\ell\pi})\lambda_{K\pi}^{1/2}(u)}{24u^2M_K^2\lambda_{\ell\pi}^{1/2}(u)} - \frac{(3u+\Delta_{K\pi})\lambda_{K\pi}^{1/2}(u)\lambda_{\ell\pi}^{1/2}(u)}{24u^2M_K^2}\right)$$

$$+ (2\langle z^2\tilde{N}_1\rangle_{t_u}+\langle z^2\tilde{R}_1\rangle_{t_u})\frac{(u+\Delta_{\ell\pi})\lambda_{K\pi}(u)}{24u^2M_K^2}, \tag{C.14}$$

$$\hat{R}_1(u) = \langle M_0\rangle_{s_u}\frac{3M_K^4\,(u+\Delta_{\ell\pi})}{8u\lambda_{\ell\pi}(u)} + \langle zM_0\rangle_{s_u}\frac{3M_K^4\,(u+\Delta_{K\pi})}{4u\lambda_{K\pi}^{1/2}(u)\lambda_{\ell\pi}^{1/2}(u)} - \langle z^2M_0\rangle_{s_u}\frac{9M_K^4\,(u+\Delta_{\ell\pi})}{8u\lambda_{\ell\pi}(u)}$$

$$- \langle M_1\rangle_{s_u}\frac{3M_K^2\,(u+\Delta_{\ell\pi})\,(u\,(\Sigma_0-3u)+\Delta_{K\pi}\Delta_{\ell\pi})}{16u^2\lambda_{\ell\pi}(u)}$$

$$+ \langle zM_1\rangle_{s_u}\left(\frac{3M_K^2\lambda_{K\pi}^{1/2}(u)\,(\Delta_{\ell\pi}+u)}{16u^2\lambda_{\ell\pi}^{1/2}(u)} - \frac{3M_K^2\,(\Delta_{K\pi}+u)\,(\Delta_{K\pi}\Delta_{\ell\pi}+u\,(\Sigma_0-3u))}{8u^2\lambda_{K\pi}^{1/2}(u)\lambda_{\ell\pi}^{1/2}(u)}\right)$$

$$+ \langle z^2M_1\rangle_{s_u}\left(\frac{9M_K^2\,(\Delta_{\ell\pi}+u)\,(\Delta_{K\pi}\Delta_{\ell\pi}+u\,(\Sigma_0-3u))}{16u^2\lambda_{\ell\pi}(u)} + \frac{3M_K^2\,(\Delta_{K\pi}+u)}{8u^2}\right)$$

$$- \langle z^3M_1\rangle_{s_u}\frac{9M_K^2\,(u+\Delta_{\ell\pi})\lambda_{K\pi}^{1/2}(u)}{16u^2\lambda_{\ell\pi}^{1/2}(u)} - \langle \tilde{M}_1\rangle_{s_u}\frac{3M_K^4\,(u+\Delta_{\ell\pi})}{8u\lambda_{\ell\pi}(u)} - \langle z\tilde{M}_1\rangle_{s_u}\frac{3M_K^4\,(\Delta_{K\pi}-3u)}{4u\lambda_{K\pi}^{1/2}(u)\lambda_{\ell\pi}^{1/2}(u)}$$

$$+ \langle z^2\tilde{M}_1\rangle_{s_u}\frac{9M_K^4\,(u+\Delta_{\ell\pi})}{8u\lambda_{\ell\pi}(u)} + (2\langle N_0\rangle_{t_u}+\langle R_0\rangle_{t_u})\frac{M_K^4\,(u+\Delta_{\ell\pi})}{4u\lambda_{\ell\pi}(u)}$$

$$+ (2\langle zN_0\rangle_{t_u}+\langle zR_0\rangle_{t_u})\frac{M_K^4\,(\Delta_{K\pi}-u)}{2u\lambda_{K\pi}^{1/2}(u)\lambda_{\ell\pi}^{1/2}(u)} - (2\langle z^2N_0\rangle_{t_u}+\langle z^2R_0\rangle_{t_u})\frac{3M_K^4\,(u+\Delta_{\ell\pi})}{4u\lambda_{\ell\pi}(u)}$$

$$- (2\langle N_1\rangle_{t_u} + \langle R_1\rangle_{t_u}) \frac{(u + \Delta_{\ell\pi})\left(u\left(u - \Sigma_0\right) + \Delta_{K\pi}\Delta_{\ell\pi}\right)\left(u\left(\Sigma_0 - 3u\right) + \Delta_{K\pi}\Delta_{\ell\pi}\right)}{16u^3\lambda_{\ell\pi}(u)}$$

$$+ (2\langle zN_1\rangle_{t_u} + \langle zR_1\rangle_{t_u})\left(\frac{\lambda_{K\pi}^{1/2}(u)\left(\Delta_{\ell\pi} + u\right)\left(\Delta_{K\pi}\Delta_{\ell\pi} + u^2\right)}{8u^3\lambda_{\ell\pi}^{1/2}(u)}\right.$$
$$\left. - \frac{(\Delta_{K\pi} - u)\left(\Delta_{K\pi}\Delta_{\ell\pi} + u\left(u - \Sigma_0\right)\right)\left(\Delta_{K\pi}\Delta_{\ell\pi} + u\left(\Sigma_0 - 3u\right)\right)}{8u^3\lambda_{K\pi}^{1/2}(u)\lambda_{\ell\pi}^{1/2}(u)}\right)$$

$$+ (2\langle z^2N_1\rangle_{t_u} + \langle z^2R_1\rangle_{t_u})\left(\frac{3\left(\Delta_{\ell\pi} + u\right)\left(\Delta_{K\pi}\Delta_{\ell\pi} + u\left(u - \Sigma_0\right)\right)\left(\Delta_{K\pi}\Delta_{\ell\pi} + u\left(\Sigma_0 - 3u\right)\right)}{16u^3\lambda_{\ell\pi}(u)}\right.$$
$$\left. - \frac{\lambda_{K\pi}(u)\left(\Delta_{\ell\pi} + u\right)}{16u^3} + \frac{(\Delta_{K\pi} - u)\left(\Delta_{K\pi}\Delta_{\ell\pi} + u^2\right)}{4u^3}\right)$$

$$+ (2\langle z^3N_1\rangle_{t_u} + \langle z^3R_1\rangle_{t_u})\left(\frac{(u - \Delta_{K\pi})\lambda_{K\pi}^{1/2}(u)\lambda_{\ell\pi}^{1/2}(u)}{8u^3} - \frac{3\lambda_{K\pi}^{1/2}(u)\left(\Delta_{\ell\pi} + u\right)\left(\Delta_{K\pi}\Delta_{\ell\pi} + u^2\right)}{8u^3\lambda_{\ell\pi}^{1/2}(u)}\right)$$

$$+ (2\langle z^4N_1\rangle_{t_u} + \langle z^4R_1\rangle_{t_u})\frac{3\left(u + \Delta_{\ell\pi}\right)\lambda_{K\pi}(u)}{16u^3}$$

$$+ (2\langle \tilde{N}_1\rangle_{t_u} + \langle \tilde{R}_1\rangle_{t_u})\frac{M_K^2\left(u + \Delta_{\ell\pi}\right)\left(u\left(\Sigma_0 - u\right) + \Delta_{K\pi}\left(\Delta_{\ell\pi} - 2u\right)\right)}{16u^2\lambda_{\ell\pi}(u)}$$

$$+ (2\langle z\tilde{N}_1\rangle_{t_u} + \langle z\tilde{R}_1\rangle_{t_u})\left(\frac{M_K^2\left(u\Delta_{K\pi}\left(3\Delta_{\ell\pi} + \Sigma_0 + u\right) + \Delta_{K\pi}^2\left(\Delta_{\ell\pi} - 2u\right) + 3u^2\left(\Sigma_0 - u\right)\right)}{8u^2\lambda_{K\pi}^{1/2}(u)\lambda_{\ell\pi}^{1/2}(u)}\right.$$
$$\left. - \frac{M_K^2\lambda_{K\pi}^{1/2}(u)\left(\Delta_{\ell\pi} + u\right)}{16u^2\lambda_{\ell\pi}^{1/2}(u)}\right)$$

$$+ (2\langle z^2\tilde{N}_1\rangle_{t_u} + \langle z^2\tilde{R}_1\rangle_{t_u})\left(\frac{3M_K^2\left(\Delta_{\ell\pi} + u\right)\left(-\Delta_{K\pi}\Delta_{\ell\pi} + 2u\Delta_{K\pi} + u^2 - \Sigma_0 u\right)}{16u^2\lambda_{\ell\pi}(u)} - \frac{M_K^2\left(\Delta_{K\pi} + 3u\right)}{8u^2}\right)$$

$$+ (2\langle z^3\tilde{N}_1\rangle_{t_u} + \langle z^3\tilde{R}_1\rangle_{t_u})\frac{3M_K^2\lambda_{K\pi}^{1/2}(u)\left(\Delta_{\ell\pi} + u\right)}{16u^2\lambda_{\ell\pi}^{1/2}(u)}, \tag{C.15}$$

$$\hat{\tilde{R}}_1(u) = \langle(1 - z^2)M_0\rangle_{s_u}\frac{3M_K^2}{4u} - \langle(1 - z^2)M_1\rangle_{s_u}\frac{3\left(\Delta_{K\pi}\Delta_{\ell\pi} + u\left(\Sigma_0 - 3u\right)\right)}{8u^2}$$

$$+ \langle(1 - z^2)zM_1\rangle_{s_u}\frac{3\lambda_{K\pi}^{1/2}(u)\lambda_{\ell\pi}^{1/2}(u)}{8u^2} - \langle(1 - z^2)\tilde{M}_1\rangle_{s_u}\frac{3M_K^2}{4u}$$

$$+ (2\langle(1 - z^2)N_0\rangle_{t_u} + \langle(1 - z^2)R_0\rangle_{t_u})\frac{M_K^2}{2u}$$

$$- (2\langle(1 - z^2)N_1\rangle_{t_u} + \langle(1 - z^2)R_1\rangle_{t_u})\frac{\left(\Delta_{K\pi}\Delta_{\ell\pi} + u\left(u - \Sigma_0\right)\right)\left(\Delta_{K\pi}\Delta_{\ell\pi} + u\left(\Sigma_0 - 3u\right)\right)}{8u^3M_K^2}$$

$$+ (2\langle(1 - z^2)zN_1\rangle_{t_u} + \langle(1 - z^2)zR_1\rangle_{t_u})\frac{\lambda_{K\pi}^{1/2}(u)\lambda_{\ell\pi}^{1/2}(u)\left(\Delta_{K\pi}\Delta_{\ell\pi} + u^2\right)}{4u^3M_K^2}$$

$$- (2\langle(1 - z^2)z^2N_1\rangle_{t_u} + \langle(1 - z^2)z^2R_1\rangle_{t_u})\frac{\lambda_{K\pi}(u)\lambda_{\ell\pi}(u)}{8u^3M_K^2}$$

$$+ (2\langle(1 - z^2)\tilde{N}_1\rangle_{t_u} + \langle(1 - z^2)\tilde{R}_1\rangle_{t_u})\frac{\Delta_{K\pi}\left(\Delta_{\ell\pi} - 2u\right) + u\left(\Sigma_0 - u\right)}{8u^2}$$

$$- (2\langle(1 - z^2)z\tilde{N}_1\rangle_{t_u} + \langle(1 - z^2)z\tilde{R}_1\rangle_{t_u})\frac{\lambda_{K\pi}^{1/2}(u)\lambda_{\ell\pi}^{1/2}(u)}{8u^2}, \tag{C.16}$$

where

Table 10 NA48/2 data [6,9], corrected by additional radiative and isospin-breaking mass effects [33]. The uncertainties of the isospin corrections (without the higher-order estimate) are added in quadrature to the systematic error. The fully correlated error of the normalisation increases from 0.62 to 0.70 %. The normalisation of F_s is increased by 0.77 % to take the dependence on s_ℓ into account

$\sqrt{s}$/MeV	$\sqrt{s_\ell}$/MeV	F_s	F_p	G_p	$\tilde{G}_p$
286.06	92.61	5.6941 (85) (185)	−0.181 (67) (15)	5.035 (257) (66)	4.317 (74) (20)
295.95	92.01	5.7878 (90) (170)	−0.324 (62) (34)	5.168 (142) (84)	4.404 (53) (32)
304.88	91.51	5.8410 (89) (171)	−0.209 (60) (33)	4.924 (108) (59)	4.532 (46) (26)
313.48	90.65	5.8905 (91) (171)	−0.156 (58) (32)	4.879 (91) (51)	4.627 (41) (24)
322.02	88.32	5.9275 (90) (166)	−0.366 (55) (41)	5.227 (80) (58)	4.692 (38) (29)
330.80	85.59	5.9557 (93) (168)	−0.383 (54) (40)	5.265 (73) (56)	4.748 (35) (28)
340.17	81.02	5.9915 (92) (166)	−0.218 (55) (46)	5.036 (68) (59)	4.762 (34) (31)
350.94	76.16	6.0161 (92) (163)	−0.302 (54) (35)	5.246 (62) (37)	4.889 (34) (21)
364.57	69.80	6.0351 (91) (162)	−0.309 (54) (33)	5.338 (57) (31)	5.000 (35) (20)
389.95	58.96	6.1155 (93) (224)	−0.264 (59) (35)	5.400 (55) (34)	5.144 (36) (22)

$$\langle z^n X\rangle_{t_s} := \frac{1}{2}\int_{-1}^{1} z^n X(t(s,z))\mathrm{d}z,$$

$$\langle z^n X\rangle_{s_t} := \frac{1}{2}\int_{-1}^{1} z^n X(s(t,z))\mathrm{d}z,$$

$$\langle z^n X\rangle_{u_t} := \frac{1}{2}\int_{-1}^{1} z^n X(u(t,z))\mathrm{d}z, \qquad \text{(C.17)}$$

$$\langle z^n X\rangle_{s_u} := \frac{1}{2}\int_{-1}^{1} z^n X(s(u,z))\mathrm{d}z,$$

$$\langle z^n X\rangle_{t_u} := \frac{1}{2}\int_{-1}^{1} z^n X(t(u,z))\mathrm{d}z.$$

and

$$
\begin{aligned}
t(s,z) &= \frac{1}{2}\left(\Sigma_0 - s - 2X\sigma_\pi z\right), \\
s(t,z) &= \frac{1}{2}\left(\Sigma_0 - t + \frac{1}{t}(z\,\lambda_{K\pi}^{1/2}(t)\lambda_{\ell\pi}^{1/2}(t) - \Delta_{K\pi}\Delta_{\ell\pi})\right), \\
u(t,z) &= \frac{1}{2}\left(\Sigma_0 - t - \frac{1}{t}(z\,\lambda_{K\pi}^{1/2}(t)\lambda_{\ell\pi}^{1/2}(t) - \Delta_{K\pi}\Delta_{\ell\pi})\right), \\
s(u,z) &= \frac{1}{2}\left(\Sigma_0 - u + \frac{1}{u}(z\,\lambda_{K\pi}^{1/2}(u)\lambda_{\ell\pi}^{1/2}(u) - \Delta_{K\pi}\Delta_{\ell\pi})\right), \\
t(u,z) &= \frac{1}{2}\left(\Sigma_0 - u - \frac{1}{u}(z\,\lambda_{K\pi}^{1/2}(u)\lambda_{\ell\pi}^{1/2}(u) - \Delta_{K\pi}\Delta_{\ell\pi})\right).
\end{aligned}
$$
$$\text{(C.18)}$$

We recall the abbreviations

$$\Delta_{K\pi} = M_K^2 - M_\pi^2, \quad \Delta_{\ell\pi} = s_\ell - M_\pi^2,$$
$$\Sigma_0 = M_K^2 + 2M_\pi^2 + s_\ell,$$
$$PL = \frac{1}{2}(M_K^2 - s - s_\ell), \quad X = \frac{1}{2}\lambda^{1/2}(M_K^2, s, s_\ell),$$
$$\sigma_\pi = \sqrt{1 - \frac{4M_\pi^2}{s}}. \qquad \text{(C.19)}$$

Table 11 E865 data [7,8], corrected by isospin-breaking mass effects [33]. The uncertainties of the isospin corrections (without the higher-order estimate) are added in quadrature to the systematic error. The fully correlated error of the normalisation is 1.2 %

$\sqrt{s}$/MeV	$\sqrt{s_\ell}$/MeV	F_s	G_p
287.6	106.8	5.781 (13) (42)	4.702 (89) (40)
299.5	105.7	5.825 (14) (48)	4.693 (62) (37)
311.2	103.8	5.914 (14) (56)	4.771 (54) (41)
324.0	101.1	5.974 (16) (62)	4.999 (51) (56)
339.6	96.3	6.097 (17) (63)	5.002 (49) (57)
370.0	84.6	6.151 (20) (41)	5.104 (50) (42)

D Isospin-breaking corrected data input

In this appendix, we list the isospin-corrected data sets on the $K_{\ell4}$ form factors that we use for the fits of the dispersion relation. These are the NA48/2 [6,9] and E865 data sets [7,8], corrected for isospin-breaking mass effects and (in the case of NA48/2) the additional radiative effects that were calculated in [33].

More detailed explanations can be found in Sect. 4.1.

D.1 One-dimensional NA48/2 and E865 data sets

See Tables 10 and 11.

D.2 Two-dimensional NA48/2 data set

For the fits of the dispersion relation to the data, we do not use the above NA48/2 data set on F_s consisting of 10 bins, but the two-dimensional data set, which was recently published as an addendum to [9]. Here, we list the isospin-corrected values of F_s that we use as input in our fits. The values and uncertainties, shown in Table 12, are constructed as follows:

Table 12 Values of F_s for the two-dimensional data set of NA48/2 [9] including isospin-breaking corrections [33]. The fully correlated error of the normalisation of 0.70 % has to be treated separately

F_s	1	2	3	4	5	6
1	5.641 (51) (55)	5.628 (30) (35)	5.700 (24) (30)	5.687 (22) (28)	5.744 (21) (27)	5.707 (22) (28)
2	5.753 (51) (30)	5.716 (30) (22)	5.747 (24) (20)	5.777 (22) (20)	5.807 (22) (20)	5.833 (23) (20)
3	5.785 (52) (33)	5.775 (31) (24)	5.831 (25) (21)	5.837 (22) (21)	5.841 (22) (20)	5.875 (23) (21)
4	5.908 (52) (33)	5.809 (31) (23)	5.877 (25) (21)	5.874 (22) (20)	5.910 (22) (20)	5.894 (23) (20)
5	5.910 (52) (24)	5.903 (31) (19)	5.891 (25) (18)	5.909 (22) (18)	5.924 (21) (18)	5.961 (22) (18)
6	5.831 (51) (29)	5.925 (30) (22)	5.912 (24) (20)	5.919 (22) (19)	5.971 (21) (19)	6.032 (22) (19)
7	6.031 (50) (25)	5.927 (29) (20)	5.941 (23) (18)	5.970 (21) (18)	6.024 (20) (18)	6.045 (22) (18)
8	6.026 (47) (21)	5.976 (28) (18)	5.990 (22) (17)	6.020 (20) (17)	6.024 (20) (17)	6.067 (23) (17)
9	6.023 (44) (22)	5.987 (26) (18)	6.037 (20) (17)	6.059 (19) (17)	6.044 (20) (17)	6.077 (25) (18)
10	6.163 (38) (67)	6.128 (22) (41)	6.107 (18) (34)	6.120 (18) (34)	6.139 (23) (42)	6.130(45) (79)

	7	8	9	10
1	5.703 (25) (30)	5.721 (30) (35)	5.717 (43) (47)	5.709 (82) (86)
2	5.817 (26) (21)	5.828 (31) (23)	5.872 (43) (27)	5.929 (84) (45)
3	5.843 (26) (22)	5.934 (31) (24)	5.911 (43) (29)	5.923 (117) (68)
4	5.905 (26) (21)	5.957 (31) (24)	6.111 (50) (32)	
5	6.004 (25) (18)	5.942 (33) (20)	6.074 (70) (29)	
6	6.025 (26) (20)	6.009 (38) (24)		
7	6.042 (28) (20)	6.124 (54) (26)		
8	6.086 (33) (19)	6.024 (122) (39)		
9	6.058 (54) (25)			

- With the number of data and Monte Carlo events for each 2D bin [9], we compute the relative values and statistical uncertainty of the relative values of F_s.
- We fix the normalisation by requiring $f_s = 5.705$ in a parametric fit of the form (111).
- Unfortunately, systematic errors are not available for the 2D data set. We guess a systematic error by assuming that the ratio of systematic and statistical error does not depend on s_ℓ.
- We apply isospin corrections due to photonic and mass-difference effects [33]. The uncertainty from the mass effects is added in quadrature to the systematic error.

E Matching equations

E.1 Subtraction constants at $\mathcal{O}(p^4)$ in χPT

In the following expressions for the subtraction constants at NLO, we have used the Gell-Mann–Okubo (GMO) formula $M_\eta^2 = (4M_K^2 - M_\pi^2)/3$ to simplify the analytic expressions considerably. This introduces an error only at NNLO. In practice, we use the physical η mass and not the GMO relation. We do not show the analytic expressions for this case because they are much larger. We have

$$m_{0,\text{NLO}}^0 = \frac{M_K}{\sqrt{2}F_\pi} \left(1 + \frac{1}{F_\pi^2} \left(-64L_1^r M_\pi^2 + 16L_2^r (M_K^2 + M_\pi^2) \right. \right.$$

$$+ 4L_3^r (M_K^2 - 3M_\pi^2) + 32L_4^r M_\pi^2 + 4L_5^r M_\pi^2 + 2L_9^r s_\ell$$

$$- \frac{161M_K^6 + 42M_K^4 M_\pi^2 - 27M_K^2 M_\pi^4 + 4M_\pi^6}{384\pi^2 \Delta_{K\pi}^2}$$

$$- s_\ell \frac{73M_K^4 - 14M_K^2 M_\pi^2 + M_\pi^4}{384\pi^2 \Delta_{K\pi}^2} + \ln\left(\frac{M_\pi^2}{\mu^2}\right)$$

$$\times \left(\frac{3M_\pi^2(3M_K^6 - 8M_K^4 M_\pi^2 + 2M_K^2 M_\pi^4 + M_\pi^6)}{128\pi^2 \Delta_{K\pi}^3} \right.$$

$$\left. - s_\ell \frac{M_\pi^4(3M_K^2 - M_\pi^2)}{128\pi^2 \Delta_{K\pi}^3} \right) - \ln\left(\frac{M_K^2}{\mu^2}\right)$$

$$\times \left(\frac{M_K^2(92M_K^6 - 15M_K^2 M_\pi^4 + M_\pi^6)}{64\pi^2 \Delta_{K\pi}^3} \right.$$

$$\left. + s_\ell \frac{M_K^4(41M_K^2 - 15M_\pi^2)}{64\pi^2 \Delta_{K\pi}^3} \right) + \ln\left(\frac{M_\eta^2}{\mu^2}\right)$$

$$\times \left(\frac{172M_K^8 + 17M_K^6 M_\pi^2 - 12M_K^4 M_\pi^4 - 22M_K^2 M_\pi^6 + 7M_\pi^8}{128\pi^2 \Delta_{K\pi}^3} \right.$$

$$+ s_\ell \frac{(4M_K^2 - M_\pi^2)^2(5M_K^2 + M_\pi^2)}{128\pi^2\Delta_{K\pi}^3}\bigg)\bigg)\bigg), \tag{E.1}$$

$$m_{0,\text{NLO}}^1 = \frac{M_K}{\sqrt{2}F_\pi^3}\bigg(32L_1^r M_K^2 + 8L_3^r M_K^2$$

$$+ \frac{M_K^2(116M_K^6 + 273M_K^4 M_\pi^2 - 258M_K^2 M_\pi^4 + 49M_\pi^6)}{384\pi^2\Delta_{K\pi}^2(4M_K^2 - M_\pi^2)}$$

$$- \ln\left(\frac{M_\pi^2}{\mu^2}\right)\frac{M_K^2(8M_K^6 - 24M_K^4 M_\pi^2 + 21M_K^2 M_\pi^4 - 7M_\pi^6)}{128\pi^2\Delta_{K\pi}^3}$$

$$+ \ln\left(\frac{M_K^2}{\mu^2}\right)\frac{M_K^2(38M_K^6 - 6M_K^4 M_\pi^2 - 9M_K^2 M_\pi^4 + 3M_\pi^6)}{64\pi^2\Delta_{K\pi}^3}$$

$$- \ln\left(\frac{M_\eta^2}{\mu^2}\right)\frac{M_K^2(4M_K^2 - M_\pi^2)^2(5M_K^2 + M_\pi^2)}{128\pi^2\Delta_{K\pi}^3}\bigg), \tag{E.2}$$

$$m_{1,\text{NLO}}^0 = \frac{M_K}{\sqrt{2}F_\pi^3}\bigg(-8L_2^r M_K^2$$

$$+ \frac{M_K^2(79M_K^4 - 2M_K^2 M_\pi^2 + 7M_\pi^4)}{384\pi^2\Delta_{K\pi}^2}$$

$$+ \ln\left(\frac{M_\pi^2}{\mu^2}\right)\frac{5M_K^2 M_\pi^4(3M_K^2 - M_\pi^2)}{128\pi^2\Delta_{K\pi}^3}$$

$$+ \ln\left(\frac{M_K^2}{\mu^2}\right)\frac{M_K^6(43M_K^2 - 21M_\pi^2)}{64\pi^2\Delta_{K\pi}^3}$$

$$- \ln\left(\frac{M_\eta^2}{\mu^2}\right)\frac{M_K^2(4M_K^2 - M_\pi^2)^2(5M_K^2 + M_\pi^2)}{128\pi^2\Delta_{K\pi}^3}\bigg), \tag{E.3}$$

$$\tilde{m}_{1,\text{NLO}}^0 = \frac{M_K}{\sqrt{2}F_\pi}\bigg(1 + \frac{1}{F_\pi^2}\bigg(-8L_2^r(M_K^2 + 2M_\pi^2 + s_\ell)$$

$$- 4L_3^r(M_K^2 + M_\pi^2) + 4L_5^r M_\pi^2 + 2L_9^r s_\ell$$

$$+ \frac{16M_K^6 - 3M_K^4 M_\pi^2 + 3M_K^2 M_\pi^4 + 2M_\pi^6}{96\pi^2\Delta_{K\pi}^2}$$

$$+ s_\ell \frac{(M_K^2 + M_\pi^2)^2}{64\pi^2\Delta_{K\pi}^2} - \ln\left(\frac{M_\pi^2}{\mu^2}\right)$$

$$\times\bigg(\frac{M_\pi^2(3M_K^2 - M_\pi^2)(M_K^4 - 8M_K^2 M_\pi^2 - 5M_\pi^4)}{128\pi^2\Delta_{K\pi}^3}$$

$$- s_\ell \frac{M_\pi^4(3M_K^2 - M_\pi^2)}{32\pi^2\Delta_{K\pi}^3}\bigg) + \ln\left(\frac{M_K^2}{\mu^2}\right)$$

$$\times\bigg(\frac{M_K^2(37M_K^6 - 35M_K^4 M_\pi^2 - 17M_K^2 M_\pi^4 + 3M_\pi^6)}{64\pi^2\Delta_{K\pi}^3}$$

$$+ s_\ell \frac{M_K^4(M_K^2 - 3M_\pi^2)}{32\pi^2\Delta_{K\pi}^3}\bigg) - \ln\left(\frac{M_\eta^2}{\mu^2}\right)$$

$$\times \frac{68M_K^6 + 7M_K^4 M_\pi^2 - 2M_K^2 M_\pi^4 - M_\pi^6}{128\pi^2\Delta_{K\pi}^2}\bigg)\bigg), \tag{E.4}$$

$$\tilde{m}_{1,\text{NLO}}^1 = \frac{M_K}{\sqrt{2}F_\pi^3}\bigg(8L_2^r M_K^2 - \frac{M_K^2(M_K^4 + M_\pi^4)}{32\pi^2\Delta_{K\pi}^2}$$

$$- \ln\left(\frac{M_\pi^2}{\mu^2}\right)\frac{M_K^2(M_K^6 - 3M_K^4 M_\pi^2 + 12M_K^2 M_\pi^4 - 4M_\pi^6)}{96\pi^2\Delta_{K\pi}^3}$$

$$- \ln\left(\frac{M_K^2}{\mu^2}\right)\frac{M_K^2(7M_K^6 - 21M_K^4 M_\pi^2 + 3M_K^2 M_\pi^4 - M_\pi^6)}{192\pi^2\Delta_{K\pi}^3}\bigg), \tag{E.5}$$

$$n_{0,\text{NLO}}^1 = \frac{M_K}{\sqrt{2}F_\pi^3}\bigg(-24L_2^r M_K^2 - 6L_3^r M_K^2$$

$$- \frac{M_K^2(16613M_K^6 - 2179M_K^4 M_\pi^2 + 29M_K^2 M_\pi^4 + 69M_\pi^6)}{2048\pi^2\Delta_{K\pi}^3}$$

$$+ \ln\left(\frac{M_\pi^2}{\mu^2}\right)\frac{3M_K^2 M_\pi^4(37M_K^4 - 80M_K^2 M_\pi^2 + 20M_\pi^4)}{512\pi^2\Delta_{K\pi}^4}$$

$$+ \ln\left(\frac{M_K^2}{\mu^2}\right)\frac{3M_K^6(-4840M_K^4 + 1216M_K^2 M_\pi^2 + 83M_\pi^4)}{512\pi^2\Delta_{K\pi}^4}$$

$$+ \ln\left(\frac{M_\eta^2}{\mu^2}\right)\frac{3M_K^2(4M_K^2 - M_\pi^2)(304M_K^6 - 6M_K^4 M_\pi^2 - M_\pi^6)}{128\pi^2\Delta_{K\pi}^4}\bigg). \tag{E.6}$$

E.2 Matching at NNLO

E.2.1 Decomposition of the two-loop result

E.2.1.1 NLO contribution We have already decomposed the NLO contributions. We apply a gauge transformation to convert the expressions to the second gauge and evaluate the result numerically:

$$m_{0,L}^{0,\text{NLO}} = \frac{M_K}{\sqrt{2}F_\pi}\bigg(-0.1466 \cdot 10^3 L_1^r + 0.4953 \cdot 10^3 L_2^r$$

$$+ 0.0872 \cdot 10^3 L_3^r + 0.0733 \cdot 10^3 L_4^r$$

$$+ 0.0092 \cdot 10^3 L_5^r + 0.0573 \cdot 10^3 L_9^r \frac{s_\ell}{M_K^2}\bigg),$$

$$m_{0,L}^{1,\text{NLO}} = \frac{M_K}{\sqrt{2}F_\pi}(0.9173 \cdot 10^3 L_1^r + 0.2293 \cdot 10^3 L_3^r),$$

$$m_{0,L}^{2,\text{NLO}} = 0,$$

$$m_{1,L}^{0,\text{NLO}} = \frac{M_K}{\sqrt{2}F_\pi}(-0.2293 \cdot 10^3 L_2^r),$$

$$m_{1,L}^{1,\text{NLO}} = 0,$$

$$\tilde{m}_{1,L}^{0,\text{NLO}} = \frac{M_K}{\sqrt{2}F_\pi}\bigg(-0.2660 \cdot 10^3 L_2^r$$

$$- 0.1238 \cdot 10^3 L_3^r + 0.0092 \cdot 10^3 L_5^r$$

$$- (0.2293 \cdot 10^3 L_2^r - 0.0573 \cdot 10^3 L_9^r)\frac{s_\ell}{M_K^2}\bigg),$$

$$\tilde{m}_{1,L}^{1,\mathrm{NLO}} = \frac{M_K}{\sqrt{2}F_\pi}(0.2293 \cdot 10^3 L_2^r),$$

$$\tilde{m}_{1,L}^{2,\mathrm{NLO}} = 0,$$

$$n_{0,L}^{1,\mathrm{NLO}} = \frac{M_K}{\sqrt{2}F_\pi}(-0.6880 \cdot 10^3 L_2^r - 0.1720 \cdot 10^3 L_3^r),$$

$$n_{0,L}^{2,\mathrm{NLO}} = n_{1,L}^{1,\mathrm{NLO}} = \tilde{n}_{1,L}^{1,\mathrm{NLO}} = 0, \tag{E.7}$$

$$m_{0,R}^{0,\mathrm{NLO}} = \frac{M_K}{\sqrt{2}F_\pi}\left(0.1393 + 0.0444\frac{s_\ell}{M_K^2} + 0.0256\frac{s_\ell^2}{M_K^4}\right),$$

$$m_{0,R}^{1,\mathrm{NLO}} = \frac{M_K}{\sqrt{2}F_\pi}\left(0.3413 - 0.0512\frac{s_\ell}{M_K^2}\right),$$

$$m_{0,R}^{2,\mathrm{NLO}} = \frac{M_K}{\sqrt{2}F_\pi}(0.4080),$$

$$m_{1,R}^{0,\mathrm{NLO}} = \frac{M_K}{\sqrt{2}F_\pi}\left(-0.0916 - 0.0512\frac{s_\ell}{M_K^2}\right),$$

$$m_{1,R}^{1,\mathrm{NLO}} = \frac{M_K}{\sqrt{2}F_\pi}(0.0512),$$

$$\tilde{m}_{1,R}^{0,\mathrm{NLO}} = \frac{M_K}{\sqrt{2}F_\pi}\left(-0.0902 - 0.0595\frac{s_\ell}{M_K^2} - 0.0256\frac{s_\ell^2}{M_K^4}\right),$$

$$\tilde{m}_{1,R}^{1,\mathrm{NLO}} = \frac{M_K}{\sqrt{2}F_\pi}\left(0.1545 + 0.0512\frac{s_\ell}{M_K^2}\right),$$

$$\tilde{m}_{1,R}^{2,\mathrm{NLO}} = \frac{M_K}{\sqrt{2}F_\pi}(0.0137),$$

$$n_{0,R}^{1,\mathrm{NLO}} = \frac{M_K}{\sqrt{2}F_\pi}\left(-0.1376 - 0.0384\frac{s_\ell}{M_K^2}\right),$$

$$n_{0,R}^{2,\mathrm{NLO}} = \frac{M_K}{\sqrt{2}F_\pi}(-0.0796),$$

$$n_{1,R}^{0,\mathrm{NLO}} = \frac{M_K}{\sqrt{2}F_\pi}(0.0384),$$

$$\tilde{n}_{1,R}^{1,\mathrm{NLO}} = \frac{M_K}{\sqrt{2}F_\pi}(-0.0282). \tag{E.8}$$

E.2.1.2 NNLO LECs   First, we consider the contribution of the NNLO LECs, the C_i^r. We decompose this contribution into the form of the polynomial part in (69):

$$m_{0,C}^{0,\mathrm{NNLO}} = \frac{M_K}{\sqrt{2}F_\pi}\frac{1}{F_\pi^4}(4M_K^4$$
$$\times(C_1^r - 2C_3^r - 2C_4^r + 2C_5^r + 4C_6^r$$
$$+ 2C_{10}^r + 8C_{11}^r - 4C_{12}^r - 8C_{13}^r + 2C_{22}^r + 4C_{23}^r - 2C_{34}^r)$$
$$- M_\pi^2 M_K^2(4C_1^r + 64C_2^r + 56C_3^r + 34C_4^r - 8C_5^r + 40C_6^r$$
$$+ 64C_7^r + 24C_8^r - 16C_{10}^r - 48C_{11}^r - 8C_{12}^r + 112C_{13}^r$$
$$+ 16C_{14}^r - 80C_{15}^r - 64C_{17}^r + 8C_{22}^r - 16C_{23}^r + 16C_{25}^r$$
$$+ 16C_{26}^r + 32C_{29}^r + 64C_{30}^r + 32C_{36}^r$$
$$+ C_{66}^r + 2C_{67}^r - C_{69}^r - C_{88}^r + C_{90}^r) + M_\pi^4$$
$$\times(-24C_1^r - 128C_2^r - 32C_3^r - 18C_4^r - 32C_5^r - 24C_6^r$$

$$-64C_7^r + 8C_8^r + 8C_{10}^r + 16C_{11}^r - 80C_{12}^r - 80C_{13}^r$$
$$+32C_{14}^r + 8C_{15}^r + 128C_{16}^r - 48C_{17}^r + 16C_{22}^r + 32C_{23}^r$$
$$+32C_{26}^r + 128C_{28}^r - 5(C_{66}^r + 2C_{67}^r - C_{69}^r - C_{88}^r + C_{90}^r))$$
$$+s_\ell(M_K^2(4C_1^r - 8C_3^r - 6C_4^r - 8C_{12}^r - 32C_{13}^r - 8C_{63}^r$$
$$-8C_{64}^r + C_{66}^r + 2C_{67}^r + 3C_{69}^r - C_{88}^r - 3C_{90}^r) - M_\pi^2$$
$$\times(12C_1^r + 64C_2^r + 72C_3^r + 10C_4^r - 48C_{13}^r - 8C_{22}^r$$
$$-32C_{23}^r + 8C_{25}^r + 4C_{64}^r + 4C_{65}^r + 9C_{66}^r + 2C_{67}^r$$
$$+16C_{68}^r + 3C_{69}^r + 8C_{83}^r + 16C_{84}^r + 3C_{88}^r + C_{90}^r))$$
$$-2s_\ell^2(8C_3^r + 2C_4^r + C_{66}^r + 2C_{67}^r - C_{69}^r + C_{88}^r - C_{90}^r)), \tag{E.9}$$

$$m_{0,C}^{1,\mathrm{NNLO}} = \frac{M_K}{\sqrt{2}F_\pi}\frac{1}{F_\pi^4}$$
$$\times(8M_K^4(C_1^r + 4C_2^r + 4C_3^r + 2C_4^r + 4C_6^r + 4C_7^r + 2C_8^r$$
$$+2C_{12}^r + 8C_{13}^r - 2C_{23}^r + C_{25}^r)$$
$$+ 2M_\pi^2 M_K^2(24C_1^r + 96C_2^r + 32C_3^r - 6C_4^r + 8C_5^r$$
$$+8C_6^r + 16C_7^r - 16C_{13}^r - 16C_{23}^r + 8C_{25}^r$$
$$+C_{66}^r + 2C_{67}^r - C_{69}^r - C_{88}^r + C_{90}^r)$$
$$+ 2s_\ell M_K^2(4C_1^r + 16C_2^r + 16C_3^r - 2C_4^r$$
$$+3C_{66}^r + 2C_{67}^r + 4C_{68}^r + C_{69}^r + C_{88}^r - C_{90}^r)),$$

$$m_{0,C}^{2,\mathrm{NNLO}} = \frac{M_K}{\sqrt{2}F_\pi}\frac{1}{F_\pi^4}16M_K^4(-C_1^r - 4C_2^r - C_3^r + C_4^r),$$

$$m_{1,C}^{0,\mathrm{NNLO}} = \frac{M_K}{\sqrt{2}F_\pi}\frac{1}{F_\pi^4}2M_K^2$$
$$\times(M_K^2(4C_3^r + 2C_4^r - 4C_{10}^r - 16C_{11}^r + 12C_{12}^r + 32C_{13}^r$$
$$-2C_{22}^r - 4C_{23}^r + 2C_{63}^r + C_{66}^r + C_{67}^r - C_{69}^r - 2C_{83}^r + C_{90}^r)$$
$$+M_\pi^2(16C_3^r + 16C_4^r - 4C_{10}^r - 8C_{11}^r + 4C_{12}^r + 16C_{13}^r$$
$$-10C_{22}^r + 6C_{25}^r - 8C_{23}^r + 6C_{25}^r - 2C_{63}^r + 4C_{67}^r + 2C_{83}^r - C_{88}^r)$$
$$+s_\ell(12C_3^r + 2C_4^r + C_{66}^r + C_{67}^r - C_{69}^r + C_{88}^r - C_{90}^r)),$$

$$m_{1,C}^{1,\mathrm{NNLO}} = \frac{M_K}{\sqrt{2}F_\pi}\frac{1}{F_\pi^4}2M_K^4$$
$$\times(-16C_3^r - 6C_4^r + C_{66}^r - C_{67}^r - C_{69}^r - C_{88}^r + C_{90}^r),$$

$$\tilde{m}_{1,C}^{0,\mathrm{NNLO}} = \frac{M_K}{\sqrt{2}F_\pi}\frac{1}{F_\pi^4}$$
$$\times(M_\pi^4(-8C_1^r + 10C_4^r - 8C_6^r - 8C_8^r - 8C_{10}^r - 16C_{11}^r + 16C_{12}^r$$
$$+16C_{13}^r + 8C_{15}^r + 16C_{17}^r - 16C_{22}^r - 32C_{23}^r$$
$$+C_{66}^r + 2C_{67}^r - C_{69}^r - C_{88}^r + C_{90}^r)$$
$$+M_\pi^2 M_K^2(-12C_1^r + 24C_3^r + 34C_4^r - 8C_5^r$$
$$-24C_6^r - 8C_8^r - 8C_{10}^r - 32C_{11}^r + 16C_{12}^r + 16C_{13}^r$$
$$+16C_{14}^r + 16C_{15}^r - 36C_{22}^r - 32C_{23}^r + 20C_{25}^r + 16C_{26}^r$$
$$-32C_{29}^r + 4C_{63}^r + C_{66}^r - 6C_{67}^r - C_{69}^r - 4C_{83}^r + C_{88}^r + C_{90}^r)$$
$$-2M_K^4(2C_1^r - 2C_4^r + 4C_5^r + 8C_6^r + 12C_{12}^r + 16C_{13}^r + 2C_{22}^r$$
$$+4C_{23}^r + 4C_{34}^r + 2C_{63}^r + C_{66}^r + C_{67}^r - C_{69}^r - 2C_{83}^r + C_{90}^r)$$
$$+s_\ell(M_\pi^2(-4C_1^r + 40C_3^r + 26C_4^r - 8C_{10}^r - 16C_{11}^r$$
$$+8C_{12}^r + 16C_{13}^r - 12C_{22}^r - 16C_{23}^r + 4C_{25}^r - 4C_{63}^r - 4C_{64}^r$$

$$-4C_{65}^r + C_{66}^r - 6C_{67}^r - 5C_{69}^r - 4C_{83}^r + C_{88}^r - 7C_{90}^r)$$
$$-M_K^2(4C_1^r + 8C_3^r - 6C_4^r + 8C_{10}^r + 32C_{11}^r - 16C_{12}^r - 32C_{13}^r$$
$$+4C_{22}^r + 8C_{23}^r + 4C_{63}^r + 8C_{64}^r + C_{66}^r + 2C_{67}^r + 3C_{69}^r$$
$$+4C_{83}^r + C_{88}^r + C_{90}^r)) + s_\ell^2(8C_3^r - 2C_{67}^r)),$$

$$\tilde{m}_{1,C}^{1,\text{NNLO}} = \frac{M_K}{\sqrt{2}F_\pi}\frac{1}{F_\pi^4}2M_K^2$$
$$\times(-M_K^2(4C_3^r + 8C_4^r - 4C_{10}^r - 16C_{11}^r + 4C_{12}^r + 32C_{13}^r$$
$$-6C_{22}^r - 4C_{23}^r + 4C_{25}^r - 2C_{63}^r - 2C_{67}^r + 2C_{83}^r - C_{88}^r)$$
$$-M_\pi^2(16C_3^r + 10C_4^r - 4C_{10}^r - 8C_{11}^r$$
$$+12C_{12}^r + 16C_{13}^r - 6C_{22}^r - 8C_{23}^r + 2C_{25}^r$$
$$+2C_{63}^r + C_{66}^r - 2C_{67}^r - C_{69}^r - 2C_{83}^r + C_{90}^r)$$
$$-s_\ell(12C_3^r + 2C_4^r + C_{66}^r - 2C_{67}^r - C_{69}^r + C_{88}^r - C_{90}^r)),$$

$$\text{(E.10)}$$

$$\tilde{m}_{1,C}^{2,\text{NNLO}} = \frac{M_K}{\sqrt{2}F_\pi}\frac{1}{F_\pi^4}2M_K^4$$
$$\times(8C_3^r + 2C_4^r + C_{66}^r - C_{67}^r - C_{69}^r - C_{88}^r + C_{90}^r),$$

$$n_{0,C}^{1,\text{NNLO}} = \frac{M_K}{\sqrt{2}F_\pi}\frac{1}{F_\pi^4}3M_K^2(-2M_K^2$$
$$\times(3C_1^r - 4C_4^r + 2C_5^r + 4C_6^r$$
$$+2C_{10}^r + 8C_{11}^r - 2C_{12}^r - 8C_{13}^r + 2C_{22}^r + 4C_{23}^r)$$
$$-\frac{1}{2}M_\pi^2(16C_1^r + 8C_3^r - 18C_4^r + 8C_6^r + 8C_8^r$$
$$+8C_{10}^r + 16C_{11}^r - 16C_{12}^r - 16C_{13}^r + 16C_{22}^r + 32C_{23}^r$$
$$-C_{66}^r - 2C_{67}^r + C_{69}^r + C_{88}^r - C_{90}^r)$$
$$-\frac{1}{2}s_\ell(4C_1^r - 8C_3^r - 6C_4^r + C_{66}^r + 2C_{67}^r + 3C_{69}^r$$
$$-C_{88}^r + C_{90}^r)),$$

$$n_{0,C}^{2,\text{NNLO}} = \frac{M_K}{\sqrt{2}F_\pi}\frac{1}{F_\pi^4}12M_K^4(C_1^r + C_3^r - C_4^r),$$

$$n_{1,C}^{0,\text{NNLO}} = \frac{M_K}{\sqrt{2}F_\pi}\frac{1}{F_\pi^4}\frac{-3M_K^4}{2}(16C_3^r + 6C_4^r - C_{66}^r - 2C_{67}^r$$
$$+C_{69}^r + C_{88}^r - C_{90}^r),$$

$$\tilde{n}_{1,C}^{1,\text{NNLO}} = \frac{M_K}{\sqrt{2}F_\pi}\frac{1}{F_\pi^4}3M_K^4(8C_3^r + 2C_4^r + C_{66}^r$$
$$+2C_{67}^r - C_{69}^r - C_{88}^r + C_{90}^r).$$

Unfortunately, a lot of NNLO LECs enter the polynomial. In total, there appear 24 linearly independent combinations of the C_i^r.

If we use the resonance estimate of [50], we obtain the following values for the NNLO counterterm contribution:

$$m_{0,\text{reso}}^{0,\text{NNLO}} = \frac{M_K}{\sqrt{2}F_\pi}\left(-0.1546 - 0.1716\frac{s_\ell}{M_K^2} + 0.0316\frac{s_\ell^2}{M_K^4}\right),$$

$$m_{0,\text{reso}}^{1,\text{NNLO}} = \frac{M_K}{\sqrt{2}F_\pi}\left(0.1747 - 0.0316\frac{s_\ell}{M_K^2}\right),$$

$$m_{0,\text{reso}}^{2,\text{NNLO}} = \frac{M_K}{\sqrt{2}F_\pi}(0.0310),$$

$$m_{1,\text{reso}}^{0,\text{NNLO}} = \frac{M_K}{\sqrt{2}F_\pi}\left(0.1657 - 0.0316\frac{s_\ell}{M_K^2}\right),$$

$$m_{1,\text{reso}}^{1,\text{NNLO}} = \frac{M_K}{\sqrt{2}F_\pi}(-0.0104),$$

$$\tilde{m}_{1,\text{reso}}^{0,\text{NNLO}} = \frac{M_K}{\sqrt{2}F_\pi}\left(-0.0900 - 0.0135\frac{s_\ell}{M_K^2}\right),$$

$$\tilde{m}_{1,\text{reso}}^{1,\text{NNLO}} = \frac{M_K}{\sqrt{2}F_\pi}\left(-0.1712 - 0.0316\frac{s_\ell}{M_K^2}\right),$$

$$\tilde{m}_{1,\text{reso}}^{2,\text{NNLO}} = \frac{M_K}{\sqrt{2}F_\pi}(0.1805),$$

$$n_{0,\text{reso}}^{1,\text{NNLO}} = \frac{M_K}{\sqrt{2}F_\pi}\left(0.1502 - 0.0237\frac{s_\ell}{M_K^2}\right),$$

$$n_{0,\text{reso}}^{2,\text{NNLO}} = \frac{M_K}{\sqrt{2}F_\pi}(-0.0233),$$

$$n_{1,\text{reso}}^{0,\text{NNLO}} = \frac{M_K}{\sqrt{2}F_\pi}(-0.0078),$$

$$\tilde{n}_{1,\text{reso}}^{1,\text{NNLO}} = \frac{M_K}{\sqrt{2}F_\pi}(0.2707). \qquad \text{(E.11)}$$

Alternatively, if we use the 'preferred values' of the BE14 fit [45] (complemented with $C_{88}^r - C_{90}^r = -55 \cdot 10^{-6}$ [48] and the remaining LECs that appear in the s_ℓ-dependence set to zero), we obtain the following values for the NNLO counterterm contribution:

$$m_{0,\text{BE14}}^{0,\text{NNLO}} = \frac{M_K}{\sqrt{2}F_\pi}\left(-0.4108 - 0.1823\frac{s_\ell}{M_K^2} - 0.0033\frac{s_\ell^2}{M_K^4}\right),$$

$$m_{0,\text{BE14}}^{1,\text{NNLO}} = \frac{M_K}{\sqrt{2}F_\pi}\left(0.7959 + 0.0986\frac{s_\ell}{M_K^2}\right),$$

$$m_{0,\text{BE14}}^{2,\text{NNLO}} = \frac{M_K}{\sqrt{2}F_\pi}(-0.1709),$$

$$m_{1,\text{BE14}}^{0,\text{NNLO}} = \frac{M_K}{\sqrt{2}F_\pi}\left(0.2627 + 0.0296\frac{s_\ell}{M_K^2}\right),$$

$$m_{1,\text{BE14}}^{1,\text{NNLO}} = \frac{M_K}{\sqrt{2}F_\pi}(-0.1709),$$

$$\tilde{m}_{1,\text{BE14}}^{0,\text{NNLO}} = \frac{M_K}{\sqrt{2}F_\pi}\left(0.0356 + 0.1050\frac{s_\ell}{M_K^2} + 0.0263\frac{s_\ell^2}{M_K^4}\right),$$

$$\tilde{m}_{1,\text{BE14}}^{1,\text{NNLO}} = \frac{M_K}{\sqrt{2}F_\pi}\left(-0.2942 - 0.0296\frac{s_\ell}{M_K^2}\right),$$

$$\tilde{m}_{1,\text{BE14}}^{2,\text{NNLO}} = \frac{M_K}{\sqrt{2}F_\pi}(0.1841),$$

$$n_{0,\text{BE14}}^{1,\text{NNLO}} = \frac{M_K}{\sqrt{2}F_\pi}\left(0.3505 + 0.0296\frac{s_\ell}{M_K^2}\right),$$

$$n_{0,\text{BE14}}^{2,\text{NNLO}} = \frac{M_K}{\sqrt{2}F_\pi}(0.0099),$$

$$n_{1,\text{BE14}}^{0,\text{NNLO}} = \frac{M_K}{\sqrt{2}F_\pi}(-0.1282),$$

$$\tilde{n}_{1,\text{BE14}}^{1,\text{NNLO}} = \frac{M_K}{\sqrt{2}F_\pi}(0.2761). \tag{E.12}$$

E.2.1.3 Vertex integrals   Let us study in more detail the contribution of the vertex integrals. They can be decomposed into functions of one Mandelstam variable according to

$$F_V^{\text{NNLO}}(s,t,u) = F_{VS,0}^{\text{NNLO}}(s,s_\ell) + \frac{u-t}{M_K^2}F_{VS,1}^{\text{NNLO}}(s,s_\ell)$$

$$+ F_{VT,0}^{\text{NNLO}}(t,s_\ell) + \frac{s-u}{M_K^2}F_{VT,1}^{\text{NNLO}}(t,s_\ell) + F_{VU}^{\text{NNLO}}(u,s_\ell),$$

$$G_V^{\text{NNLO}}(s,t,u) = G_{VS}^{\text{NNLO}}(s,s_\ell) + G_{VT,0}^{\text{NNLO}}(t,s_\ell)$$

$$+ \frac{s-u}{M_K^2}G_{VT,1}^{\text{NNLO}}(t,s_\ell) + G_{VU}^{\text{NNLO}}(u,s_\ell). \tag{E.13}$$

The u-channel vertex integrals fulfil $F_{VU}^{\text{NNLO}} = G_{VU}^{\text{NNLO}}$. In the following, we treat them numerically. The contribution to R_0 is obtained by subtracting the constant, linear and quadratic terms:

$$R_0^V(u,s_\ell) = F_{VU}^{\text{NNLO}}(u,s_\ell) - P_{VU}^{\text{NNLO}}(u,s_\ell),$$

$$P_{VU}^{\text{NNLO}}(u,s_\ell) = F_{VU}^{\text{NNLO}}(0,s_\ell)$$

$$+ uF_{VU}^{\text{NNLO}\prime}(0,s_\ell) + \frac{1}{2}u^2F_{VU}^{\text{NNLO}\prime\prime}(0,s_\ell), \tag{E.14}$$

where $\prime$ stands for the derivative with respect to the first argument (u). The polynomial P_{VU}^{NNLO} has to be lumped into the overall polynomial and finally reshuffled into the subtraction constants. Numerically, we find

$$P_{VU}^{\text{NNLO}}(u,s_\ell) \approx \frac{M_K}{\sqrt{2}F_\pi}\left(0.4008 + 0.0119\frac{s_\ell}{M_K^2}\right.$$

$$\left. + \left(-0.2521 - 0.0130\frac{s_\ell}{M_K^2}\right)\frac{u}{M_K^2} + 0.0569\frac{u^2}{M_K^4}\right). \tag{E.15}$$

As we have checked again numerically, the polynomial-subtracted u-channel contribution of the vertex integrals fulfils the dispersion relation

$$R_0^V(u,s_\ell) = \frac{u^3}{\pi}\int_{u_0}^\infty \frac{\text{Im}R_0^V(u',s_\ell)}{(u'-u-i\epsilon)u'^3}du'. \tag{E.16}$$

Next, we consider the s-channel vertex integrals: apart from a polynomial, they belong to either M_0, M_1 or $\tilde{M}_1$. Again, we subtract the first few terms of the Taylor expansion:

$$M_0^V(s,s_\ell) = F_{VS,0}^{\text{NNLO}}(s,s_\ell) - P_{F,VS0}^{\text{NNLO}}(s,s_\ell),$$

$$M_1^V(s,s_\ell) = F_{VS,1}^{\text{NNLO}}(s,s_\ell) - P_{F,VS1}^{\text{NNLO}}(s,s_\ell),$$

$$\tilde{M}_1^V(s,s_\ell) = G_{VS}^{\text{NNLO}}(s,s_\ell) - P_{G,VS}^{\text{NNLO}}(s,s_\ell),$$

$$P_{F,VS0}^{\text{NNLO}}(s,s_\ell) = F_{VS,0}^{\text{NNLO}}(0,s_\ell) + sF_{VS,0}^{\text{NNLO}\prime}(0,s_\ell)$$

$$+ \frac{1}{2}s^2F_{VS,0}^{\text{NNLO}\prime\prime}(0,s_\ell),$$

$$P_{F,VS1}^{\text{NNLO}}(s,s_\ell) = F_{VS,1}^{\text{NNLO}}(0,s_\ell) + sF_{VS,1}^{\text{NNLO}\prime}(0,s_\ell),$$

$$P_{G,VS}^{\text{NNLO}}(s,s_\ell) = G_{VS}^{\text{NNLO}}(0,s_\ell) + sG_{VS}^{\text{NNLO}\prime}(0,s_\ell)$$

$$+ \frac{1}{2}s^2G_{VS}^{\text{NNLO}\prime\prime}(0,s_\ell). \tag{E.17}$$

We find numerically

$$P_{F,VS0}^{\text{NNLO}}(s,s_\ell) \approx \frac{M_K}{\sqrt{2}F_\pi}\left(0.2663 + 0.0992\frac{s_\ell}{M_K^2}\right.$$

$$+ \left(-1.7763 - 0.0450\frac{s_\ell}{M_K^2}\right)\frac{s}{M_K^2} - 0.5385\frac{s^2}{M_K^4}\right),$$

$$P_{F,VS1}^{\text{NNLO}}(s,s_\ell) \approx \frac{M_K}{\sqrt{2}F_\pi}$$

$$\times \left(0.0029 + 0.0006\frac{s_\ell}{M_K^2} + 0.0006\frac{s}{M_K^2}\right),$$

$$P_{G,VS}^{\text{NNLO}}(s,s_\ell) \approx \frac{M_K}{\sqrt{2}F_\pi}\left(-0.3197 - 0.0727\frac{s_\ell}{M_K^2}\right.$$

$$+ \left(0.1457 + 0.0163\frac{s_\ell}{M_K^2}\right)\frac{s}{M_K^2} + 0.0003\frac{s^2}{M_K^4}\right). \tag{E.18}$$

A numerical check shows that the polynomial-subtracted s-channel contributions of the vertex integrals fulfil the dispersion relations

$$M_0^V(s,s_\ell) = \frac{s^3}{\pi}\int_{s_0}^\infty \frac{\text{Im}M_0^V(s',s_\ell)}{(s'-s-i\epsilon)s'^3}ds',$$

$$M_1^V(s,s_\ell) = \frac{s^2}{\pi}\int_{s_0}^\infty \frac{\text{Im}M_1^V(s',s_\ell)}{(s'-s-i\epsilon)s'^2}ds', \tag{E.19}$$

$$\tilde{M}_1^V(s,s_\ell) = \frac{s^3}{\pi}\int_{s_0}^\infty \frac{\text{Im}\tilde{M}_1^V(s',s_\ell)}{(s'-s-i\epsilon)s'^3}ds'.$$

Finally, we consider the t-channel, which is a bit more intricate: the reason is that not all linear and quadratic terms of a simple Taylor expansion in t belong to the subtraction polynomial. The t-channel contributions can be written as

$$F_{VT,0}^{\text{NNLO}}(t,s_\ell) = \frac{2}{3}N_0^V(t,s_\ell) + \frac{2}{3}\frac{\Delta_{K\pi}\Delta_{\ell\pi}}{M_K^4}N_1^V(t,s_\ell)$$

$$- \frac{2}{3}\frac{\Delta_{K\pi}-3t}{2M_K^2}\tilde{N}_1^V(t,s_\ell) + \frac{1}{3}R_0^V(t,s_\ell) + P_{F,VT0}^{\text{NNLO}}(t,s_\ell),$$

$$F_{VT,1}^{\text{NNLO}}(t,s_\ell) = \frac{2t}{3M_K^2}N_1^V(t,s_\ell) + P_{F,VT1}^{\text{NNLO}}(t,s_\ell),$$

$$G_{VT,0}^{\text{NNLO}}(t,s_\ell) = -\frac{2}{3}N_0^V(t,s_\ell) - \frac{2}{3}\frac{\Delta_{K\pi}\Delta_{\ell\pi}}{M_K^4}N_1^V(t,s_\ell)$$

$$+ \frac{2}{3}\frac{\Delta_{K\pi}+t}{2M_K^2}\tilde{N}_1^V(t,s_\ell) - \frac{1}{3}R_0^V(t,s_\ell) + P_{G,VT0}^{\text{NNLO}}(t,s_\ell),$$

$$G_{VT,1}^{\text{NNLO}}(t, s_\ell) = -\frac{2t}{3M_K^2} N_1^V(t, s_\ell) + P_{G,VT1}^{\text{NNLO}}(t, s_\ell),$$

$$\text{(E.20)}$$

where $P_{F,VT0}^{\text{NNLO}}$, $P_{G,VT0}^{\text{NNLO}}$ are second order and $P_{F,VT1}^{\text{NNLO}}$, $P_{G,VT1}^{\text{NNLO}}$ are first-order polynomials. The Taylor expansion of N_0^V starts with a cubic term, the one of $\tilde{N}_1^V$ with a quadratic and the one of N_1^V with a linear term. Numerically, we find

$$P_{F,VT1}^{\text{NNLO}}(t, s_\ell) = -P_{G,VT1}^{\text{NNLO}}(t, s_\ell) \approx \frac{M_K}{\sqrt{2}F_\pi}$$

$$\times \left(0.0044 + 0.0002 \frac{s_\ell}{M_K^2} + 0.0003 \frac{t}{M_K^2} \right) \quad \text{(E.21)}$$

and also identify the linear and the quadratic term of the Taylor expansion of N_1^V. In the sum

$$F_{VT,0}^{\text{NNLO}}(t, s_\ell) + G_{VT,0}^{\text{NNLO}}(t, s_\ell)$$

$$= \frac{4t}{3M_K^2} \tilde{N}_1^V(t, s_\ell) + P_{F,VT0}^{\text{NNLO}}(t, s_\ell) + P_{G,VT0}^{\text{NNLO}}(t, s_\ell),$$

$$\text{(E.22)}$$

we can easily separate $\tilde{N}_1^V$ from the sum of the polynomials. After having identified $\tilde{N}_1^V$ (in particular the quadratic term of its Taylor expansion), we can also separate the difference of the polynomials using

$$F_{VT,0}^{\text{NNLO}}(t, s_\ell) - G_{VT,0}^{\text{NNLO}}(t, s_\ell) = \frac{4}{3} N_0^V(t, s_\ell)$$

$$+ \frac{4}{3} \frac{\Delta_{K\pi} \Delta_{\ell\pi}}{M_K^4} N_1^V(t, s_\ell) - \frac{2}{3} \frac{\Delta_{K\pi} - t}{M_K^2} \tilde{N}_1^V(t, s_\ell)$$

$$+ \frac{2}{3} R_0^V(t, s_\ell) + P_{F,VT0}^{\text{NNLO}}(t, s_\ell) - P_{G,VT0}^{\text{NNLO}}(t, s_\ell). \quad \text{(E.23)}$$

Numerically, we find

$$P_{F,VT0}^{\text{NNLO}}(t, s_\ell) \approx \frac{M_K}{\sqrt{2}F_\pi} \left(-0.6831 - 0.1136 \frac{s_\ell}{M_K^2} - 0.0013 \right.$$

$$\left. \times \frac{s_\ell^2}{M_K^4} + \left(0.2841 - 0.0006 \frac{s_\ell}{M_K^2} \right) \frac{t}{M_K^2} + 0.0190 \frac{t^2}{M_K^4} \right),$$

$$P_{G,VT0}^{\text{NNLO}}(t, s_\ell) \approx \frac{M_K}{\sqrt{2}F_\pi} \left(-0.0055 - 0.0146 \frac{s_\ell}{M_K^2} - 0.0006 \right.$$

$$\left. \times \frac{s_\ell^2}{M_K^4} + \left(0.0131 + 0.0095 \frac{s_\ell}{M_K^2} \right) \frac{t}{M_K^2} - 0.0356 \frac{t^2}{M_K^4} \right).$$

$$\text{(E.24)}$$

Again, the following dispersion relations can be checked numerically:

$$N_0^V(t, s_\ell) = \frac{t^3}{\pi} \int_{t_0}^\infty \frac{\text{Im} N_0^V(t', s_\ell)}{(t' - t - i\epsilon)t'^3} dt',$$

$$N_1^V(t, s_\ell) = \frac{t}{\pi} \int_{t_0}^\infty \frac{\text{Im} N_1^V(t', s_\ell)}{(t' - t - i\epsilon)t'} dt',$$

$$\tilde{N}_1^V(t, s_\ell) = \frac{t^2}{\pi} \int_{t_0}^\infty \frac{\text{Im} \tilde{N}_1^V(t', s_\ell)}{(t' - t - i\epsilon)t'^2} dt'. \quad \text{(E.25)}$$

Reshuffling the polynomial contributions into the subtraction constants leads to

$$m_{0,V}^{0,\text{NNLO}} = \frac{M_K}{\sqrt{2}F_\pi} \left(0.0705 + 0.0667 \frac{s_\ell}{M_K^2} - 0.0539 \frac{s_\ell^2}{M_K^4} \right),$$

$$m_{0,V}^{1,\text{NNLO}} = \frac{M_K}{\sqrt{2}F_\pi} \left(-1.7841 + 0.0648 \frac{s_\ell}{M_K^2} \right),$$

$$m_{0,V}^{2,\text{NNLO}} = \frac{M_K}{\sqrt{2}F_\pi} (-0.5954),$$

$$m_{1,V}^{0,\text{NNLO}} = \frac{M_K}{\sqrt{2}F_\pi} \left(-0.2658 + 0.0969 \frac{s_\ell}{M_K^2} \right),$$

$$m_{1,V}^{1,\text{NNLO}} = \frac{M_K}{\sqrt{2}F_\pi} (-0.1132),$$

$$\tilde{m}_{1,V}^{0,\text{NNLO}} = \frac{M_K}{\sqrt{2}F_\pi} \left(-0.1310 - 0.2580 \frac{s_\ell}{M_K^2} + 0.0435 \frac{s_\ell^2}{M_K^4} \right),$$

$$\tilde{m}_{1,V}^{1,\text{NNLO}} = \frac{M_K}{\sqrt{2}F_\pi} \left(0.2570 - 0.0849 \frac{s_\ell}{M_K^2} \right),$$

$$\tilde{m}_{1,V}^{2,\text{NNLO}} = \frac{M_K}{\sqrt{2}F_\pi} (0.0572),$$

$$n_{0,V}^{1,\text{NNLO}} = \frac{M_K}{\sqrt{2}F_\pi} \left(-0.2587 + 0.0519 \frac{s_\ell}{M_K^2} \right),$$

$$n_{0,V}^{2,\text{NNLO}} = \frac{M_K}{\sqrt{2}F_\pi} (0.0898),$$

$$n_{1,V}^{0,\text{NNLO}} = \frac{M_K}{\sqrt{2}F_\pi} (-0.0849),$$

$$\tilde{n}_{1,V}^{1,\text{NNLO}} = \frac{M_K}{\sqrt{2}F_\pi} (0.0729). \quad \text{(E.26)}$$

E.2.1.4 Remaining two-loop integrals   Next, we consider the remaining two-loop parts, X_P^{NNLO}. It is easy to decompose them into functions of one Mandelstam variable:

$$F_P^{\text{NNLO}}(s, t, u) = F_{PS}^{\text{NNLO}}(s, s_\ell) + F_{PT,0}^{\text{NNLO}}(t, s_\ell)$$

$$+ \frac{s - u}{M_K^2} F_{PT,1}^{\text{NNLO}}(t, s_\ell) + F_{PU}^{\text{NNLO}}(u, s_\ell) + P_{F,P}^{\text{NNLO}}(s, t, u),$$

$$G_P^{\text{NNLO}}(s, t, u) = G_{PS}^{\text{NNLO}}(s, s_\ell) + G_{PT,0}^{\text{NNLO}}(t, s_\ell)$$

$$+ \frac{s - u}{M_K^2} G_{PT,1}^{\text{NNLO}}(t, s_\ell) + G_{PU}^{\text{NNLO}}(u, s_\ell) + P_{G,P}^{\text{NNLO}}(s, t, u),$$

$$\text{(E.27)}$$

where $P_{F,P}^{\text{NNLO}}$ and $P_{G,P}^{\text{NNLO}}$ are second-order polynomials. The remaining steps are analogous to the case of the ver-

tex integrals. Again, we apply subtractions to the different functions:

$$
M_0^P(s, s_\ell) = F_{PS}^{\mathrm{NNLO}}(s, s_\ell) - P_{F,PS}^{\mathrm{NNLO}}(s, s_\ell),
$$

$$
\tilde{M}_1^P(s, s_\ell) = G_{PS}^{\mathrm{NNLO}}(s, s_\ell) - P_{G,PS}^{\mathrm{NNLO}}(s, s_\ell),
$$

$$
R_0^P(u, s_\ell) = F_{PU}^{\mathrm{NNLO}}(u, s_\ell) - P_{F,PU}^{\mathrm{NNLO}}(u, s_\ell)
$$

$$
= G_{PU}^{\mathrm{NNLO}}(u, s_\ell) - P_{G,PU}^{\mathrm{NNLO}}(u, s_\ell), \quad (E.28)
$$

where

$$
P_{F,PS}^{\mathrm{NNLO}}(s, s_\ell) = F_{PS}^{\mathrm{NNLO}}(0, s_\ell) + s F_{PS}^{\mathrm{NNLO}'}(0, s_\ell)
$$
$$
+ \frac{1}{2} s^2 F_{PS}^{\mathrm{NNLO}''}(0, s_\ell),
$$

$$
P_{G,PS}^{\mathrm{NNLO}}(s, s_\ell) = G_{PS}^{\mathrm{NNLO}}(0, s_\ell) + s G_{PS}^{\mathrm{NNLO}'}(0, s_\ell)
$$
$$
+ \frac{1}{2} s^2 G_{PS}^{\mathrm{NNLO}''}(0, s_\ell),
$$

$$
P_{F,PU}^{\mathrm{NNLO}}(u, s_\ell) = F_{PU}^{\mathrm{NNLO}}(0, s_\ell) + u F_{PU}^{\mathrm{NNLO}'}(0, s_\ell)
$$
$$
+ \frac{1}{2} u^2 F_{PU}^{\mathrm{NNLO}''}(0, s_\ell),
$$

$$
P_{G,PU}^{\mathrm{NNLO}}(u, s_\ell) = G_{PU}^{\mathrm{NNLO}}(0, s_\ell) + u G_{PU}^{\mathrm{NNLO}'}(0, s_\ell)
$$
$$
+ \frac{1}{2} u^2 G_{PU}^{\mathrm{NNLO}''}(0, s_\ell). \quad (E.29)
$$

Numerically, we find

$$
P_{F,PS}^{\mathrm{NNLO}}(s, s_\ell) \approx \frac{M_K}{\sqrt{2} F_\pi} \left(-0.1660 + 0.0002 \frac{s_\ell}{M_K^2} + 0.0007 \right.
$$
$$
\times \frac{s_\ell^2}{M_K^4} + \left(1.1629 + 0.0343 \frac{s_\ell}{M_K^2} \right) \frac{s}{M_K^2} + 0.7815 \frac{s^2}{M_K^4} \left. \right),
$$

$$
P_{G,PS}^{\mathrm{NNLO}}(s, s_\ell) \approx \frac{M_K}{\sqrt{2} F_\pi} \left(0.0609 + 0.0118 \frac{s_\ell}{M_K^2} \right.
$$
$$
+ \left(-0.0514 - 0.0058 \frac{s_\ell}{M_K^2} \right) \frac{s}{M_K^2} - 0.0007 \frac{s^2}{M_K^4} \left. \right),
$$

$$
P_{F,PU}^{\mathrm{NNLO}}(u, s_\ell) = P_{G,PU}^{\mathrm{NNLO}}(u, s_\ell) \approx \frac{M_K}{\sqrt{2} F_\pi} \left(0.0585 - 0.0089 \right.
$$
$$
\times \frac{s_\ell}{M_K^2} + \left(0.0165 + 0.0069 \frac{s_\ell}{M_K^2} \right) \frac{u}{M_K^2} - 0.0442 \frac{u^2}{M_K^4} \left. \right). \quad (E.30)
$$

The t-channel contributions can be written as

$$
F_{PT,0}^{\mathrm{NNLO}}(t, s_\ell) = \frac{2}{3} N_0^P(t, s_\ell) + \frac{2}{3} \frac{\Delta_{K\pi} \Delta_{\ell\pi}}{M_K^4} N_1^P(t, s_\ell)
$$
$$
- \frac{2}{3} \frac{\Delta_{K\pi} - 3t}{2M_K^2} \tilde{N}_1^P(t, s_\ell) + \frac{1}{3} R_0^P(t, s_\ell) + P_{F,PT0}^{\mathrm{NNLO}}(t, s_\ell),
$$

$$
F_{PT,1}^{\mathrm{NNLO}}(t, s_\ell) = \frac{2t}{3M_K^2} N_1^P(t, s_\ell) + P_{F,PT1}^{\mathrm{NNLO}}(t, s_\ell),
$$

$$
G_{PT,0}^{\mathrm{NNLO}}(t, s_\ell) = -\frac{2}{3} N_0^P(t, s_\ell) - \frac{2}{3} \frac{\Delta_{K\pi} \Delta_{\ell\pi}}{M_K^4} N_1^P(t, s_\ell)
$$
$$
+ \frac{2}{3} \frac{\Delta_{K\pi} + t}{2M_K^2} \tilde{N}_1^P(t, s_\ell) - \frac{1}{3} R_0^P(t, s_\ell) + P_{G,PT0}^{\mathrm{NNLO}}(t, s_\ell),
$$

$$
G_{PT,1}^{\mathrm{NNLO}}(t, s_\ell) = -\frac{2t}{3M_K^2} N_1^P(t, s_\ell) + P_{G,PT1}^{\mathrm{NNLO}}(t, s_\ell), \quad (E.31)
$$

where $P_{F,PT0}^{\mathrm{NNLO}}$, $P_{G,PT0}^{\mathrm{NNLO}}$ are second order and $P_{F,PT1}^{\mathrm{NNLO}}$, $P_{G,PT1}^{\mathrm{NNLO}}$ are first-order polynomials. Numerically, we find

$$
P_{F,PT1}^{\mathrm{NNLO}}(t, s_\ell) = -P_{G,PT1}^{\mathrm{NNLO}}(t, s_\ell)
$$
$$
\approx \frac{M_K}{\sqrt{2} F_\pi} \left(-0.0010 - 0.0001 \frac{t}{M_K^2} \right) \quad (E.32)
$$

and also identify the linear and the quadratic term of the Taylor expansion of N_1^P. In the sum

$$
F_{PT,0}^{\mathrm{NNLO}}(t, s_\ell) + G_{PT,0}^{\mathrm{NNLO}}(t, s_\ell) = \frac{4t}{3M_K^2} \tilde{N}_1^P(t, s_\ell)
$$
$$
+ P_{F,PT0}^{\mathrm{NNLO}}(t, s_\ell) + P_{G,PT0}^{\mathrm{NNLO}}(t, s_\ell) \quad (E.33)
$$

we can separate $\tilde{N}_1^P$ from the polynomials. We obtain the difference of the polynomials with

$$
F_{PT,0}^{\mathrm{NNLO}}(t, s_\ell) - G_{PT,0}^{\mathrm{NNLO}}(t, s_\ell)
$$
$$
= \frac{4}{3} N_0^P(t, s_\ell) + \frac{4}{3} \frac{\Delta_{K\pi} \Delta_{\ell\pi}}{M_K^4} N_1^P(t, s_\ell)
$$
$$
- \frac{2}{3} \frac{\Delta_{K\pi} - t}{M_K^2} \tilde{N}_1^P(t, s_\ell)
$$
$$
+ \frac{2}{3} R_0^P(t, s_\ell) + P_{F,PT0}^{\mathrm{NNLO}}(t, s_\ell) - P_{G,PT0}^{\mathrm{NNLO}}(t, s_\ell)
$$
$$
\quad (E.34)
$$

and find numerically

$$
P_{F,PT0}^{\mathrm{NNLO}}(t, s_\ell) \approx \frac{M_K}{\sqrt{2} F_\pi} \left(0.2047 + 0.0339 \frac{s_\ell}{M_K^2} \right.
$$
$$
+ \left(-0.1781 + 0.0019 \frac{s_\ell}{M_K^2} \right) \frac{t}{M_K^2} - 0.0211 \frac{t^2}{M_K^4} \left. \right),
$$

$$
P_{G,PT0}^{\mathrm{NNLO}}(t, s_\ell) \approx \frac{M_K}{\sqrt{2} F_\pi} \left(-0.0662 + 0.0085 \frac{s_\ell}{M_K^2} \right.
$$
$$
+ \left(0.0757 - 0.0054 \frac{s_\ell}{M_K^2} \right) \frac{t}{M_K^2} + 0.0251 \frac{t^2}{M_K^4} \left. \right). \quad (E.35)
$$

Finally, the additional polynomials are given by

$$
P_{F,P}^{\mathrm{NNLO}}(s, t, u) \approx \frac{M_K}{\sqrt{2} F_\pi} \left(0.2640 - 0.0510 \frac{s_\ell}{M_K^2} \right.
$$
$$
- 0.0002 \frac{s_\ell^2}{M_K^4} + 0.0561 \frac{s}{M_K^2} - 0.0700 \frac{t}{M_K^2} \left. \right),
$$

$$P_{G,P}^{\text{NNLO}}(s,t,u) \approx \frac{M_K}{\sqrt{2}F_\pi}\left(0.0686 + 0.0287\frac{s_\ell}{M_K^2}\right.$$
$$\left. +0.0006\frac{s_\ell^2}{M_K^4} - 0.0396\frac{s}{M_K^2} + 0.0169\frac{t}{M_K^2}\right). \quad \text{(E.36)}$$

Reshuffling all polynomial contributions into the subtraction constants leads to

$$m_{0,P}^{0,\text{NNLO}} = \frac{M_K}{\sqrt{2}F_\pi}\left(0.3349 - 0.0426\frac{s_\ell}{M_K^2} + 0.0429\frac{s_\ell^2}{M_K^4}\right),$$

$$m_{0,P}^{1,\text{NNLO}} = \frac{M_K}{\sqrt{2}F_\pi}\left(1.1922 - 0.0523\frac{s_\ell}{M_K^2}\right),$$

$$m_{0,P}^{2,\text{NNLO}} = \frac{M_K}{\sqrt{2}F_\pi}(0.8257),$$

$$m_{1,P}^{0,\text{NNLO}} = \frac{M_K}{\sqrt{2}F_\pi}\left(-0.0083 - 0.0797\frac{s_\ell}{M_K^2}\right),$$

$$m_{1,P}^{1,\text{NNLO}} = \frac{M_K}{\sqrt{2}F_\pi}(0.0884),$$

$$\tilde{m}_{1,P}^{0,\text{NNLO}} = \frac{M_K}{\sqrt{2}F_\pi}\left(0.0771 + 0.0016\frac{s_\ell}{M_K^2} - 0.0367\frac{s_\ell^2}{M_K^4}\right),$$

$$\tilde{m}_{1,P}^{1,\text{NNLO}} = \frac{M_K}{\sqrt{2}F_\pi}\left(-0.0030 + 0.0757\frac{s_\ell}{M_K^2}\right),$$

$$\tilde{m}_{1,P}^{2,\text{NNLO}} = \frac{M_K}{\sqrt{2}F_\pi}(-0.0449),$$

$$n_{0,P}^{1,\text{NNLO}} = \frac{M_K}{\sqrt{2}F_\pi}\left(-0.2217 - 0.0478\frac{s_\ell}{M_K^2}\right),$$

$$n_{0,P}^{2,\text{NNLO}} = \frac{M_K}{\sqrt{2}F_\pi}(-0.0693),$$

$$n_{1,P}^{0,\text{NNLO}} = \frac{M_K}{\sqrt{2}F_\pi}(0.0662),$$

$$\tilde{n}_{1,P}^{1,\text{NNLO}} = \frac{M_K}{\sqrt{2}F_\pi}(-0.0633). \quad \text{(E.37)}$$

E.2.1.5 NNLO one-loop integrals The last NNLO piece that we have to decompose is the part containing the L_i^r. Similar to the two-loop parts, it can easily be decomposed into functions of one variables. Since this contribution contains only one-loop integrals, we can express it in terms of A_0 and B_0 functions, which can be treated analytically. After decomposing the NNLO one-loop part according to

$$F_L^{\text{NNLO}}(s,t,u) = F_{LS,0}^{\text{NNLO}}(s,s_\ell) + \frac{u-t}{M_K^2}F_{LS,1}^{\text{NNLO}}(s,s_\ell)$$
$$+ F_{LT,0}^{\text{NNLO}}(t,s_\ell) + \frac{s-u}{M_K^2}F_{LT,1}^{\text{NNLO}}(t,s_\ell)$$
$$+ F_{LU}^{\text{NNLO}}(u,s_\ell) + P_{F,L}^{\text{NNLO}}(s,t,u),$$

$$G_L^{\text{NNLO}}(s,t,u) = G_{LS}^{\text{NNLO}}(s,s_\ell) + G_{LT,0}^{\text{NNLO}}(t,s_\ell)$$
$$+ \frac{s-u}{M_K^2}G_{LT,1}^{\text{NNLO}}(t,s_\ell)$$
$$+ G_{LU}^{\text{NNLO}}(u,s_\ell) + P_{G,L}^{\text{NNLO}}(s,t,u),$$
$$\text{(E.38)}$$

the polynomial contribution is found in analogy to the two-loop part. Reshuffling the polynomial gives very long expressions for the subtraction constants. We perform a Taylor expansion in s_ℓ and evaluate the expressions numerically, using the physical masses and $\mu = 770$ MeV:

$$m_{0,L}^{0,\text{NNLO}}$$
$$= \frac{M_K}{\sqrt{2}F_\pi}\left((0.0243 + 0.0155\cdot 10^3 L_5^r)\cdot 10^3 L_1^r\right.$$
$$+ (0.3528 - 0.0523\cdot 10^3 L_5^r)\cdot 10^3 L_2^r$$
$$+ (0.0831 - 0.0092\cdot 10^3 L_5^r)\cdot 10^3 L_3^r$$
$$+ (0.0400 + 0.0350\cdot 10^3 L_4^r - 0.0020\cdot 10^3 L_5^r)\cdot 10^3 L_4^r$$
$$+ (0.0066 + 0.0048\cdot 10^3 L_5^r)\cdot 10^3 L_5^r$$
$$- (0.0012 + 0.0699\cdot 10^3 L_4^r + 0.0087\cdot 10^3 L_5^r)\cdot 10^3 L_6^r$$
$$+ 0.0213\cdot 10^3 L_7^r + (0.0100 - 0.0027\cdot 10^3 L_4^r$$
$$- 0.0003\cdot 10^3 L_5^r)\cdot 10^3 L_8^r + \frac{s_\ell}{M_K^2}$$
$$\times (0.0213\cdot 10^3 L_1^r - 0.0161\cdot 10^3 L_2^r + 0.0230\cdot 10^3 L_3^r$$
$$+ 0.0139\cdot 10^3 L_4^r + 0.0018\cdot 10^3 L_5^r$$
$$- 0.0017\cdot 10^3 L_6^r - 0.0008\cdot 10^3 L_8^r$$
$$+ (0.0229 - 0.0060\cdot 10^3 L_5^r)\cdot 10^3 L_9^r)$$
$$+ \frac{s_\ell^2}{M_K^4}(-0.0053\cdot 10^3 L_1^r - 0.0029\cdot 10^3 L_2^r$$
$$- 0.0029\cdot 10^3 L_3^r + 0.0065\cdot 10^3 L_4^r + 0.0010\cdot 10^3 L_5^r$$
$$\left. - 0.0012\cdot 10^3 L_6^r - 0.0006\cdot 10^3 L_8^r + 0.0025\cdot 10^3 L_9^r\right),$$

$$m_{0,L}^{1,\text{NNLO}} = \frac{M_K}{\sqrt{2}F_\pi}\left(-(0.1644 + 0.0968\cdot 10^3 L_5^r)\cdot 10^3 L_1^r\right.$$
$$- 0.2921\cdot 10^3 L_2^r - (0.1665 + 0.0242\cdot 10^3 L_5^r)\cdot 10^3 L_3^r$$
$$- 0.0353\cdot 10^3 L_4^r + 0.0049\cdot 10^3 L_5^r + 0.0185\cdot 10^3 L_6^r$$
$$- 0.0033\cdot 10^3 L_7^r + 0.0076\cdot 10^3 L_8^r$$
$$+ \frac{s_\ell}{M_K^2}(0.0138\cdot 10^3 L_1^r - 0.0575\cdot 10^3 L_2^r - 0.0087\cdot 10^3 L_3^r$$
$$- 0.0130\cdot 10^3 L_4^r - 0.0020\cdot 10^3 L_5^r + 0.0024\cdot 10^3 L_6^r$$
$$\left. + 0.0012\cdot 10^3 L_8^r + 0.0196\cdot 10^3 L_9^r\right), \quad \text{(E.39)}$$

$$m_{0,L}^{2,\text{NNLO}} = \frac{M_K}{\sqrt{2}F_\pi}$$

$$\times (0.3345 \cdot 10^3 L_1^r + 0.2734 \cdot 10^3 L_2^r$$
$$+ 0.1618 \cdot 10^3 L_3^r + 0.0863 \cdot 10^3 L_4^r$$
$$+ 0.0096 \cdot 10^3 L_5^r + 0.0067 \cdot 10^3 L_6^r$$
$$- 0.0003 \cdot 10^3 L_7^r + 0.0032 \cdot 10^3 L_8^r),$$

$$m_{1,L}^{0,\text{NNLO}} = \frac{M_K}{\sqrt{2}F_\pi}\Big(-0.1203 \cdot 10^3 L_1^r$$
$$+ \big(-0.2247 + 0.0242 \cdot 10^3 L_5^r\big) \cdot 10^3 L_2^r$$
$$- 0.0727 \cdot 10^3 L_3^r - 0.0241 \cdot 10^3 L_4^r$$
$$- 0.0046 \cdot 10^3 L_5^r + 0.0078 \cdot 10^3 L_6^r + 0.0039 \cdot 10^3 L_8^r$$
$$+ \frac{s_\ell}{M_K^2}(0.0121 \cdot 10^3 L_1^r + 0.0044 \cdot 10^3 L_2^r$$
$$+ 0.0063 \cdot 10^3 L_3^r - 0.0130 \cdot 10^3 L_4^r - 0.0020 \cdot 10^3 L_5^r$$
$$+ 0.0024 \cdot 10^3 L_6^r + 0.0012 \cdot 10^3 L_8^r - 0.0053 \cdot 10^3 L_9^r)\Big),$$

$$m_{1,L}^{1,\text{NNLO}} = \frac{M_K}{\sqrt{2}F_\pi}(-0.0198 \cdot 10^3 L_1^r$$
$$- 0.0059 \cdot 10^3 L_2^r - 0.0056 \cdot 10^3 L_3^r + 0.0130 \cdot 10^3 L_4^r$$
$$+ 0.0020 \cdot 10^3 L_5^r - 0.0024 \cdot 10^3 L_6^r - 0.0012 \cdot 10^3 L_8^r),$$

$$\tilde{m}_{1,L}^{0,\text{NNLO}} = \frac{M_K}{\sqrt{2}F_\pi}\Big(0.0440 \cdot 10^3 L_1^r$$
$$+ (-0.1488 + 0.0281 \cdot 10^3 L_5^r) \cdot 10^3 L_2^r$$
$$+ (-0.0140 + 0.0131 \cdot 10^3 L_5^r) \cdot 10^3 L_3^r$$
$$+ (0.0001 + 0.0044 \cdot 10^3 L_5^r) \cdot 10^3 L_4^r$$
$$+ (-0.0033 + 0.0048 \cdot 10^3 L_5^r) \cdot 10^3 L_5^r$$
$$+ (0.0186 - 0.0087 \cdot 10^3 L_5^r) \cdot 10^3 L_6^r - 0.0135 \cdot 10^3 L_7^r$$
$$+ (0.0026 - 0.0003 \cdot 10^3 L_5^r) \cdot 10^3 L_8^r$$
$$+ \frac{s_\ell}{M_K^2}(-0.0957 \cdot 10^3 L_1^r$$
$$- (0.2423 - 0.0242 \cdot 10^3 L_5^r) \cdot 10^3 L_2^r - 0.0520 \cdot 10^3 L_3^r$$
$$- 0.0134 \cdot 10^3 L_4^r - 0.0033 \cdot 10^3 L_5^r + 0.0067 \cdot 10^3 L_6^r$$
$$+ 0.0033 \cdot 10^3 L_8^r + (0.0098 - 0.0060 \cdot 10^3 L_5^r) \cdot 10^3 L_9^r)$$
$$+ \frac{s_\ell^2}{M_K^4}(0.0057 \cdot 10^3 L_1^r + 0.0010 \cdot 10^3 L_2^r$$
$$+ 0.0029 \cdot 10^3 L_3^r - 0.0065 \cdot 10^3 L_4^r$$
$$- 0.0010 \cdot 10^3 L_5^r + 0.0012 \cdot 10^3 L_6^r$$
$$+ 0.0006 \cdot 10^3 L_8^r - 0.0034 \cdot 10^3 L_9^r)\Big),$$

$$\tilde{m}_{1,L}^{1,\text{NNLO}} = \frac{M_K}{\sqrt{2}F_\pi}\Big(0.0987 \cdot 10^3 L_1^r$$
$$+ (0.2328 - 0.0242 \cdot 10^3 L_5^r) \cdot 10^3 L_2^r$$
$$+ 0.0581 \cdot 10^3 L_3^r + 0.0213 \cdot 10^3 L_4^r$$
$$+ 0.0062 \cdot 10^3 L_5^r - 0.0078 \cdot 10^3 L_6^r - 0.0039 \cdot 10^3 L_8^r$$
$$+ \frac{s_\ell}{M_K^2}(-0.0138 \cdot 10^3 L_1^r - 0.0029 \cdot 10^3 L_2^r$$
$$- 0.0026 \cdot 10^3 L_3^r + 0.0130 \cdot 10^3 L_4^r$$
$$+ 0.0020 \cdot 10^3 L_5^r - 0.0024 \cdot 10^3 L_6^r$$
$$- 0.0012 \cdot 10^3 L_8^r + 0.0089 \cdot 10^3 L_9^r)\Big),$$

$$\tilde{m}_{1,L}^{2,\text{NNLO}} = \frac{M_K}{\sqrt{2}F_\pi}$$
$$(-0.0070 \cdot 10^3 L_1^r + 0.0114 \cdot 10^3 L_2^r$$
$$- 0.0097 \cdot 10^3 L_3^r - 0.0044 \cdot 10^3 L_4^r$$
$$+ 0.0001 \cdot 10^3 L_5^r + 0.0012 \cdot 10^3 L_6^r + 0.0006 \cdot 10^3 L_8^r),$$

$$n_{0,L}^{1,\text{NNLO}} = \frac{M_K}{\sqrt{2}F_\pi}\Big(-0.0796 \cdot 10^3 L_1^r$$
$$+ (-0.4712 + 0.0726 \cdot 10^3 L_5^r) \cdot 10^3 L_2^r$$
$$+ (-0.1097 + 0.0181 \cdot 10^3 L_5^r) \cdot 10^3 L_3^r$$
$$- 0.0262 \cdot 10^3 L_4^r - 0.0049 \cdot 10^3 L_5^r$$
$$+ 0.0075 \cdot 10^3 L_6^r - 0.0117 \cdot 10^3 L_7^r - 0.0021 \cdot 10^3 L_8^r$$
$$+ \frac{s_\ell}{M_K^2}(0.0095 \cdot 10^3 L_1^r + 0.0035 \cdot 10^3 L_2^r$$
$$+ 0.0040 \cdot 10^3 L_3^r - 0.0098 \cdot 10^3 L_4^r$$
$$- 0.0015 \cdot 10^3 L_5^r + 0.0018 \cdot 10^3 L_6^r$$
$$+ 0.0009 \cdot 10^3 L_8^r - 0.0079 \cdot 10^3 L_9^r)\Big),$$

$$n_{0,L}^{2,\text{NNLO}} = \frac{M_K}{\sqrt{2}F_\pi}(-0.0003 \cdot 10^3 L_1^r$$
$$- 0.0010 \cdot 10^3 L_2^r + 0.0101 \cdot 10^3 L_3^r - 0.0007 \cdot 10^3 L_4^r$$
$$- 0.0022 \cdot 10^3 L_5^r + 0.0003 \cdot 10^3 L_6^r$$
$$- 0.0010 \cdot 10^3 L_7^r - 0.0004 \cdot 10^3 L_8^r),$$

$$n_{1,L}^{0,\text{NNLO}} = \frac{M_K}{\sqrt{2}F_\pi}(-0.0125 \cdot 10^3 L_1^r$$
$$- 0.0051 \cdot 10^3 L_2^r - 0.0069 \cdot 10^3 L_3^r + 0.0098 \cdot 10^3 L_4^r$$
$$+ 0.0015 \cdot 10^3 L_5^r - 0.0018 \cdot 10^3 L_6^r$$
$$- 0.0009 \cdot 10^3 L_8^r),$$

$$\tilde{n}_{1,L}^{1,\text{NNLO}} = \frac{M_K}{\sqrt{2}F_\pi}(0.0059 \cdot 10^3 L_1^r$$
$$+ 0.0096 \cdot 10^3 L_2^r \cdot + 0.0051 \cdot 10^3 L_3^r - 0.0072 \cdot 10^3 L_4^r$$
$$- 0.0012 \cdot 10^3 L_5^r + 0.0018 \cdot 10^3 L_6^r$$
$$+ 0.0009 \cdot 10^3 L_8^r). \tag{E.40}$$

Note that there are no quadratic terms in L_1^r, L_2^r or L_3^r.

E.2.2 Chiral expansion of the Omnès representation

In order to derive the NNLO chiral expansion of the Omnès representation (C.1), we first expand the Omnès function chirally:

$$
\Omega^{\text{NNLO}}(s) = 1 + \omega \frac{s}{M_K^2} + \bar{\omega} \frac{s^2}{M_K^4} + \frac{s^3}{\pi} \int_{s_0}^{\infty} \frac{\delta_{\text{NLO}}(s')}{(s'-s-i\epsilon)s'^3} ds'
$$
$$
+ \frac{1}{2} \left(\omega \frac{s}{M_K^2} + \frac{s^2}{\pi} \int_{s_0}^{\infty} \frac{\delta_{\text{LO}}(s')}{(s'-s-i\epsilon)s'^2} ds' \right)^2 , \quad \text{(E.41)}
$$

where the subtraction terms ω and $\bar{\omega}$ are defined in (147).

In the quadratic term of the expansion, only the LO phase enters and therefore only two subtractions are needed. The NLO expansion of the modulus of the inverse Omnès function is given by

$$
\frac{1}{|\Omega^{\text{NLO}}(s)|} = 1 - \omega \frac{s}{M_K^2}
$$
$$
- \frac{s^2}{\pi} \mathcal{P}\!\!\!\int_{s_0}^{\infty} \frac{\delta_{\text{NLO}}(s')}{(s'-s-i\epsilon)s'^2} ds'. \quad \text{(E.42)}
$$

Therefore, the NNLO chiral expansion of the argument of the dispersive integrals reads

$$
\left. \frac{\hat{M}(s)\sin\delta(s)}{|\Omega(s)|} \right|_{\text{NNLO}} = \hat{M}^{\text{LO}}(s)\delta_{\text{NLO}}(s) + \hat{M}^{\text{NLO}}(s)\delta_{\text{LO}}(s)
$$
$$
- \hat{M}^{\text{LO}}(s)\delta_{\text{LO}}(s) \left(1 + \omega \frac{s}{M_K^2} + \frac{s^2}{\pi}\mathcal{P}\!\!\!\int_{s_0}^{\infty} \frac{\delta_{\text{LO}}(s')}{(s'-s-i\epsilon)s'^2} ds' \right).
$$
$$\quad \text{(E.43)}$$

This leads to

$$
M_0^{\text{NNLO}}(s)
$$
$$
= a_{\text{LO}}^{M_0} \left(\omega_0^0 \frac{s}{M_K^2} + \bar{\omega}_0^0 \frac{s^2}{M_K^4} + \frac{s^3}{\pi} \int_{s_0}^{\infty} \frac{\delta_{0,\text{NLO}}^0(s')}{(s'-s-i\epsilon)s'^3} ds' \right.
$$
$$
\left. + \frac{1}{2} \left(\omega_0^0 \frac{s}{M_K^2} + \frac{s^2}{\pi} \int_{s_0}^{\infty} \frac{\delta_{0,\text{LO}}^0(s')}{(s'-s-i\epsilon)s'^2} ds' \right)^2 \right)
$$
$$
+ \left(\Delta a_{\text{NLO}}^{M_0} + b_{\text{NLO}}^{M_0} \frac{s}{M_K^2} + c_{\text{NLO}}^{M_0} \frac{s^2}{M_K^4} \right)
$$
$$
\times \left(\omega_0^0 \frac{s}{M_K^2} + \frac{s^2}{\pi} \int_{s_0}^{\infty} \frac{\delta_{0,\text{LO}}^0(s')}{(s'-s-i\epsilon)s'^2} ds' \right)
$$
$$
+ a_{\text{NNLO}}^{M_0} + b_{\text{NNLO}}^{M_0} \frac{s}{M_K^2} + c_{\text{NNLO}}^{M_0} \frac{s^2}{M_K^4} + d_{\text{NNLO}}^{M_0} \frac{s^3}{M_K^6}
$$
$$
+ \frac{s^4}{\pi} \int_{s_0}^{\infty} \frac{\hat{M}_0^{\text{NLO}}(s')\delta_{0,\text{LO}}^0(s')}{(s'-s-i\epsilon)s'^4} ds',
$$
$$
M_1^{\text{NNLO}}(s) = \left(a_{\text{NLO}}^{M_1} + b_{\text{NLO}}^{M_1} \frac{s}{M_K^2} \right)
$$
$$
\times \left(\omega_1^1 \frac{s}{M_K^2} + \frac{s^2}{\pi} \int_{s_0}^{\infty} \frac{\delta_{1,\text{LO}}^1(s')}{(s'-s-i\epsilon)s'^2} ds' \right)
$$
$$
+ a_{\text{NNLO}}^{M_1} + b_{\text{NNLO}}^{M_1} \frac{s}{M_K^2} + c_{\text{NNLO}}^{M_1} \frac{s^2}{M_K^4}
$$
$$
+ \frac{s^3}{\pi} \int_{s_0}^{\infty} \frac{\hat{M}_1^{\text{NLO}}(s')\delta_{1,\text{LO}}^1(s')}{(s'-s-i\epsilon)s'^3} ds',
$$
$$
\tilde{M}_1^{\text{NNLO}}(s) = a_{\text{LO}}^{\tilde{M}_1} \left(\omega_1^1 \frac{s}{M_K^2} + \bar{\omega}_1^1 \frac{s^2}{M_K^4} + \frac{s^3}{\pi} \right.
$$
$$
\times \int_{s_0}^{\infty} \frac{\delta_{1,\text{NLO}}^1(s')}{(s'-s-i\epsilon)s'^3} ds'
$$
$$
\left. + \frac{1}{2} \left(\omega_1^1 \frac{s}{M_K^2} + \frac{s^2}{\pi} \int_{s_0}^{\infty} \frac{\delta_{1,\text{LO}}^1(s')}{(s'-s-i\epsilon)s'^2} ds' \right)^2 \right)
$$
$$
+ \left(\Delta a_{\text{NLO}}^{\tilde{M}_1} + b_{\text{NLO}}^{\tilde{M}_1} \frac{s}{M_K^2} + c_{\text{NLO}}^{\tilde{M}_1} \frac{s^2}{M_K^4} \right)
$$
$$
\times \left(\omega_1^1 \frac{s}{M_K^2} + \frac{s^2}{\pi} \int_{s_0}^{\infty} \frac{\delta_{1,\text{LO}}^1(s')}{(s'-s-i\epsilon)s'^2} ds' \right)
$$
$$
+ a_{\text{NNLO}}^{\tilde{M}_1} + b_{\text{NNLO}}^{\tilde{M}_1} \frac{s}{M_K^2} + c_{\text{NNLO}}^{\tilde{M}_1} \frac{s^2}{M_K^4} + d_{\text{NNLO}}^{\tilde{M}_1} \frac{s^3}{M_K^6}
$$
$$
+ \frac{s^4}{\pi} \int_{s_0}^{\infty} \frac{\hat{\tilde{M}}_1^{\text{NLO}}(s')\delta_{1,\text{LO}}^1(s')}{(s'-s-i\epsilon)s'^4} ds',
$$
$$
N_0^{\text{NNLO}}(t) = \left(b_{\text{NLO}}^{N_0} \frac{t}{M_K^2} + c_{\text{NLO}}^{N_0} \frac{t^2}{M_K^4} + \frac{t^3}{\pi} \right.
$$
$$
\left. \times \int_{t_0}^{\infty} \frac{\hat{N}_0^{\text{LO}}(t')\delta_{0,\text{LO}}^{1/2}(t')}{(t'-t-i\epsilon)t'^3} dt' \right)
$$
$$
\times \left(\omega_0^{1/2} \frac{t}{M_K^2} + \frac{t^2}{\pi} \int_{t_0}^{\infty} \frac{\delta_{0,\text{LO}}^{1/2}(t')}{(t'-t-i\epsilon)t'^2} dt' \right)
$$
$$
+ b_{\text{NNLO}}^{N_0} \frac{t}{M_K^2} + c_{\text{NNLO}}^{N_0} \frac{t^2}{M_K^4} + \frac{t^3}{\pi}
$$
$$
\times \int_{t_0}^{\infty} \frac{\hat{N}_0^{\text{LO}}(t')\delta_{0,\text{NLO}}^{1/2}(t')}{(t'-t-i\epsilon)t'^3} dt'
$$
$$
+ \frac{t^3}{\pi} \int_{t_0}^{\infty} \frac{\hat{N}_0^{\text{NLO}}(t')\delta_{0,\text{LO}}^{1/2}(t')}{(t'-t-i\epsilon)t'^3} dt'
$$
$$
- \frac{t^3}{\pi} \int_{t_0}^{\infty} \frac{\hat{N}_0^{\text{LO}}(t')\delta_{0,\text{LO}}^{1/2}(t')}{(t'-t-i\epsilon)t'^3}
$$
$$
\times \left(1 + \omega_0^{1/2} \frac{t'}{M_K^2} + \frac{t'^2}{\pi} \mathcal{P}\!\!\!\int_{t_0}^{\infty} \frac{\delta_{0,\text{LO}}^{1/2}(t'')}{(t''-t'-i\epsilon)t''^2} dt'' \right) dt',
$$
$$
N_1^{\text{NNLO}}(t) = a_{\text{NLO}}^{N_1}
$$
$$
\times \left(\omega_1^{1/2} \frac{t}{M_K^2} + \frac{t^2}{\pi} \int_{t_0}^{\infty} \frac{\delta_{1,\text{LO}}^{1/2}(t')}{(t'-t-i\epsilon)t'^2} dt' \right)
$$
$$
+ a_{\text{NNLO}}^{N_1} + \frac{t}{\pi} \int_{t_0}^{\infty} \frac{\hat{N}_1^{\text{NLO}}(t')\delta_{1,\text{LO}}^{1/2}(t')}{(t'-t-i\epsilon)t'} dt',
$$
$$
\tilde{N}_1^{\text{NNLO}}(t) = \left(b_{\text{NLO}}^{\tilde{N}_1} \frac{t}{M_K^2} + \frac{t^2}{\pi} \int_{t_0}^{\infty} \frac{\hat{\tilde{N}}_1^{\text{LO}}(t')\delta_{1,\text{LO}}^{1/2}(t')}{(t'-t-i\epsilon)t'^2} dt' \right)
$$

$$\times\left(\omega_1^{1/2}\frac{t}{M_K^2}+\frac{t^2}{\pi}\int_{t_0}^{\infty}\frac{\delta_{1,\mathrm{LO}}^{1/2}(t')}{(t'-t-i\epsilon)t'^2}\mathrm{d}t'\right)$$

$$+b_{\mathrm{NNLO}}^{\tilde{N}_1}\frac{t}{M_K^2}+\frac{t^2}{\pi}\int_{t_0}^{\infty}\frac{\hat{\tilde{N}}_1^{\mathrm{LO}}(t')\delta_{1,\mathrm{NLO}}^{1/2}(t')}{(t'-t-i\epsilon)t'^2}\mathrm{d}t'$$

$$+\frac{t^2}{\pi}\int_{t_0}^{\infty}\frac{\hat{\tilde{N}}_1^{\mathrm{NLO}}(t')\delta_{1,\mathrm{LO}}^{1/2}(t')}{(t'-t-i\epsilon)t'^2}\mathrm{d}t'$$

$$-\frac{t^2}{\pi}\int_{t_0}^{\infty}\frac{\hat{\tilde{N}}_1^{\mathrm{LO}}(t')\delta_{1,\mathrm{LO}}^{1/2}(t')}{(t'-t-i\epsilon)t'^2}$$

$$\times\left(1+\omega_1^{1/2}\frac{t'}{M_K^2}+\frac{t'^2}{\pi}\,\rlap{\;/}{\int}_{t_0}^{\infty}\frac{\delta_{1,\mathrm{LO}}^{1/2}(t'')}{(t''-t'-i\epsilon)t''^2}\mathrm{d}t''\right)\mathrm{d}t',$$

$$R_0^{\mathrm{NNLO}}(t)=\left(\frac{t^3}{\pi}\int_{t_0}^{\infty}\frac{\hat{R}_0^{\mathrm{LO}}(t')\delta_{0,\mathrm{LO}}^{3/2}(t')}{(t'-t-i\epsilon)t'^3}\mathrm{d}t'\right)$$

$$\times\left(\omega_0^{3/2}\frac{t}{M_K^2}+\frac{t^2}{\pi}\int_{t_0}^{\infty}\frac{\delta_{0,\mathrm{LO}}^{3/2}(t')}{(t'-t-i\epsilon)t'^2}\mathrm{d}t'\right)$$

$$+\frac{t^3}{\pi}\int_{t_0}^{\infty}\frac{\hat{R}_0^{\mathrm{LO}}(t')\delta_{0,\mathrm{NLO}}^{3/2}(t')}{(t'-t-i\epsilon)t'^3}\mathrm{d}t'$$

$$+\frac{t^3}{\pi}\int_{t_0}^{\infty}\frac{\hat{R}_0^{\mathrm{NLO}}(t')\delta_{0,\mathrm{LO}}^{3/2}(t')}{(t'-t-i\epsilon)t'^3}\mathrm{d}t'-\frac{t^3}{\pi}\int_{t_0}^{\infty}\frac{\hat{R}_0^{\mathrm{LO}}(t')\delta_{0,\mathrm{LO}}^{3/2}(t')}{(t'-t-i\epsilon)t'^3}$$

$$\times\left(1+\omega_0^{3/2}\frac{t'}{M_K^2}+\frac{t'^2}{\pi}\,\rlap{\;/}{\int}_{t_0}^{\infty}\frac{\delta_{0,\mathrm{LO}}^{3/2}(t'')}{(t''-t'-i\epsilon)t''^2}\mathrm{d}t''\right)\mathrm{d}t',$$

$$R_1^{\mathrm{NNLO}}(t)=0,$$
$$\tilde{R}_1^{\mathrm{NNLO}}(t)=0,\tag{E.44}$$

where we use the following notation for the contributions to the subtraction constants:

$$a_{\mathrm{NLO}}=a_{\mathrm{LO}}+\Delta a_{\mathrm{NLO}},$$
$$a_{\mathrm{NNLO}}=a_{\mathrm{LO}}+\Delta a_{\mathrm{NLO}}+\Delta a_{\mathrm{NNLO}}.\tag{E.45}$$

Remember that $b_{\mathrm{NLO}}^{M_1}$ and $a_{\mathrm{NLO}}^{N_1}$ are non-zero after the gauge transformation.

We further define

$$b_{\mathrm{NLO}}^{M_0}=:-\omega_0^0\frac{M_K}{\sqrt{2}F_\pi}+\bar{b}_{\mathrm{NLO}}^{M_0},$$
$$b_{\mathrm{NNLO}}^{M_0}=:-\omega_0^0\frac{M_K}{\sqrt{2}F_\pi}+\bar{b}_{\mathrm{NNLO}}^{M_0},$$
$$b_{\mathrm{NLO}}^{\tilde{M}_1}=:-\omega_1^1\frac{M_K}{\sqrt{2}F_\pi}+\bar{b}_{\mathrm{NLO}}^{\tilde{M}_1},$$
$$b_{\mathrm{NNLO}}^{\tilde{M}_1}=:-\omega_1^1\frac{M_K}{\sqrt{2}F_\pi}+\bar{b}_{\mathrm{NNLO}}^{\tilde{M}_1},\tag{E.46}$$

which allows for the simplifications

$$M_0^{\mathrm{NNLO}}(s)=\frac{M_K}{\sqrt{2}F_\pi}$$

$$\times\left(\left(\bar{\omega}_0^0-\frac{1}{2}\omega_0^{0\,2}\right)\frac{s^2}{M_K^4}+\frac{s^3}{\pi}\int_{s_0}^{\infty}\frac{\delta_{0,\mathrm{NLO}}^0(s')}{(s'-s-i\epsilon)s'^3}\mathrm{d}s'\right.$$

$$\left.+\frac{1}{2}\left(\frac{s^2}{\pi}\int_{s_0}^{\infty}\frac{\delta_{0,\mathrm{LO}}^0(s')}{(s'-s-i\epsilon)s'^2}\mathrm{d}s'\right)^2\right)$$

$$+\left(\Delta a_{\mathrm{NLO}}^{M_0}+\bar{b}_{\mathrm{NLO}}^{M_0}\frac{s}{M_K^2}+c_{\mathrm{NLO}}^{M_0}\frac{s^2}{M_K^4}\right)$$

$$\times\left(\omega_0^0\frac{s}{M_K^2}+\frac{s^2}{\pi}\int_{s_0}^{\infty}\frac{\delta_{0,\mathrm{LO}}^0(s')}{(s'-s-i\epsilon)s'^2}\mathrm{d}s'\right)$$

$$+a_{\mathrm{NNLO}}^{M_0}+b_{\mathrm{NNLO}}^{M_0}\frac{s}{M_K^2}+c_{\mathrm{NNLO}}^{M_0}\frac{s^2}{M_K^4}+d_{\mathrm{NNLO}}^{M_0}\frac{s^3}{M_K^6}$$

$$+\frac{s^4}{\pi}\int_{s_0}^{\infty}\frac{\hat{M}_0^{\mathrm{NLO}}(s')\delta_{0,\mathrm{LO}}^0(s')}{(s'-s-i\epsilon)s'^4}\mathrm{d}s',$$

$$M_1^{\mathrm{NNLO}}(s)=\left(a_{\mathrm{NLO}}^{M_1}+b_{\mathrm{NLO}}^{M_1}\frac{s}{M_K^2}\right)$$

$$\times\left(\omega_1^1\frac{s}{M_K^2}+\frac{s^2}{\pi}\int_{s_0}^{\infty}\frac{\delta_{1,\mathrm{LO}}^1(s')}{(s'-s-i\epsilon)s'^2}\mathrm{d}s'\right)$$

$$+a_{\mathrm{NNLO}}^{M_1}+b_{\mathrm{NNLO}}^{M_1}\frac{s}{M_K^2}+c_{\mathrm{NNLO}}^{M_1}\frac{s^2}{M_K^4}$$

$$+\frac{s^3}{\pi}\int_{s_0}^{\infty}\frac{\hat{M}_1^{\mathrm{NLO}}(s')\delta_{1,\mathrm{LO}}^1(s')}{(s'-s-i\epsilon)s'^3}\mathrm{d}s',$$

$$\tilde{M}_1^{\mathrm{NNLO}}(s)=\frac{M_K}{\sqrt{2}F_\pi}$$

$$\times\left(\left(\bar{\omega}_1^1-\frac{1}{2}\omega_1^{1\,2}\right)\frac{s^2}{M_K^4}+\frac{s^3}{\pi}\int_{s_0}^{\infty}\frac{\delta_{1,\mathrm{NLO}}^1(s')}{(s'-s-i\epsilon)s'^3}\mathrm{d}s'\right.$$

$$\left.+\frac{1}{2}\left(\frac{s^2}{\pi}\int_{s_0}^{\infty}\frac{\delta_{1,\mathrm{LO}}^1(s')}{(s'-s-i\epsilon)s'^2}\mathrm{d}s'\right)^2\right)$$

$$+\left(\Delta a_{\mathrm{NLO}}^{\tilde{M}_1}+\bar{b}_{\mathrm{NLO}}^{\tilde{M}_1}\frac{s}{M_K^2}+c_{\mathrm{NLO}}^{\tilde{M}_1}\frac{s^2}{M_K^4}\right)$$

$$\times\left(\omega_1^1\frac{s}{M_K^2}+\frac{s^2}{\pi}\int_{s_0}^{\infty}\frac{\delta_{1,\mathrm{LO}}^1(s')}{(s'-s-i\epsilon)s'^2}\mathrm{d}s'\right)$$

$$+a_{\mathrm{NNLO}}^{\tilde{M}_1}+\bar{b}_{\mathrm{NNLO}}^{\tilde{M}_1}\frac{s}{M_K^2}+c_{\mathrm{NNLO}}^{\tilde{M}_1}\frac{s^2}{M_K^4}+d_{\mathrm{NNLO}}^{\tilde{M}_1}\frac{s^3}{M_K^6}$$

$$+\frac{s^4}{\pi}\int_{s_0}^{\infty}\frac{\hat{\tilde{M}}_1^{\mathrm{NLO}}(s')\delta_{1,\mathrm{LO}}^1(s')}{(s'-s-i\epsilon)s'^4}\mathrm{d}s',$$

$$N_0^{\mathrm{NNLO}}(t)=b_{\mathrm{NNLO}}^{N_0}\frac{t}{M_K^2}+c_{\mathrm{NNLO}}^{N_0}\frac{t^2}{M_K^4}+\omega_0^{1/2}\frac{t}{M_K^2}$$

$$\times\left(b_{\mathrm{NLO}}^{N_0}\frac{t}{M_K^2}+\delta c_{\mathrm{NLO}}^{N_0}\frac{t^2}{M_K^4}\right)$$

$$+\left(\frac{t^2}{\pi}\int_{t_0}^{\infty}\frac{\delta_{0,\mathrm{LO}}^{1/2}(t')}{(t'-t-i\epsilon)t'^2}\mathrm{d}t'\right)$$

$$\times \left(b_{\mathrm{NLO}}^{N_0} \frac{t}{M_K^2} + c_{\mathrm{NLO}}^{N_0} \frac{t^2}{M_K^4} + \frac{t^3}{\pi} \int_{t_0}^{\infty} \frac{\hat{N}_0^{\mathrm{LO}}(t')\delta_{0,\mathrm{LO}}^{1/2}(t')}{(t'-t-i\epsilon)t'^3} dt' \right)$$

$$+ \frac{t^3}{\pi} \int_{t_0}^{\infty} \frac{\hat{N}_0^{\mathrm{LO}}(t')\delta_{0,\mathrm{NLO}}^{1/2}(t')}{(t'-t-i\epsilon)t'^3} dt'$$

$$+ \frac{t^3}{\pi} \int_{t_0}^{\infty} \frac{\hat{N}_0^{\mathrm{NLO}}(t')\delta_{0,\mathrm{LO}}^{1/2}(t')}{(t'-t-i\epsilon)t'^3} dt'$$

$$- \frac{t^3}{\pi} \int_{t_0}^{\infty} \frac{\hat{N}_0^{\mathrm{LO}}(t')\delta_{0,\mathrm{LO}}^{1/2}(t')}{(t'-t-i\epsilon)t'^3}$$

$$\times \left(1 + \frac{t'^2}{\pi} \mathcal{P}\!\!\int_{t_0}^{\infty} \frac{\delta_{0,\mathrm{LO}}^{1/2}(t'')}{(t''-t'-i\epsilon)t''^2} dt'' \right) dt',$$

$$N_1^{\mathrm{NNLO}}(t) = a_{\mathrm{NNLO}}^{N_1} + a_{\mathrm{NLO}}^{N_1} \omega_1^{1/2} \frac{t}{M_K^2}$$

$$+ a_{\mathrm{NLO}}^{N_1} \frac{t^2}{\pi} \int_{t_0}^{\infty} \frac{\delta_{1,\mathrm{LO}}^{1/2}(t')}{(t'-t-i\epsilon)t'^2} dt'$$

$$+ \frac{t}{\pi} \int_{t_0}^{\infty} \frac{\hat{N}_1^{\mathrm{NLO}}(t')\delta_{1,\mathrm{LO}}^{1/2}(t')}{(t'-t-i\epsilon)t'} dt',$$

$$\tilde{N}_1^{\mathrm{NNLO}}(t) = b_{\mathrm{NNLO}}^{\tilde{N}_1} \frac{t}{M_K^2} + \omega_1^{1/2} \delta b_{\mathrm{NLO}}^{\tilde{N}_1} \frac{t^2}{M_K^4}$$

$$+ \left(\frac{t^2}{\pi} \int_{t_0}^{\infty} \frac{\delta_{1,\mathrm{LO}}^{1/2}(t')}{(t'-t-i\epsilon)t'^2} dt' \right)$$

$$\times \left(b_{\mathrm{NLO}}^{\tilde{N}_1} \frac{t}{M_K^2} + \frac{t^2}{\pi} \int_{t_0}^{\infty} \frac{\hat{\tilde{N}}_1^{\mathrm{LO}}(t')\delta_{1,\mathrm{LO}}^{1/2}(t')}{(t'-t-i\epsilon)t'^2} dt' \right)$$

$$+ \frac{t^2}{\pi} \int_{t_0}^{\infty} \frac{\hat{\tilde{N}}_1^{\mathrm{LO}}(t')\delta_{1,\mathrm{NLO}}^{1/2}(t')}{(t'-t-i\epsilon)t'^2} dt'$$

$$+ \frac{t^2}{\pi} \int_{t_0}^{\infty} \frac{\hat{\tilde{N}}_1^{\mathrm{NLO}}(t')\delta_{1,\mathrm{LO}}^{1/2}(t')}{(t'-t-i\epsilon)t'^2} dt'$$

$$- \frac{t^2}{\pi} \int_{t_0}^{\infty} \frac{\hat{\tilde{N}}_1^{\mathrm{LO}}(t')\delta_{1,\mathrm{LO}}^{1/2}(t')}{(t'-t-i\epsilon)t'^2}$$

$$\times \left(1 + \frac{t'^2}{\pi} \mathcal{P}\!\!\int_{t_0}^{\infty} \frac{\delta_{1,\mathrm{LO}}^{1/2}(t'')}{(t''-t'-i\epsilon)t''^2} dt'' \right) dt',$$

$$R_0^{\mathrm{NNLO}}(t) = -\omega_0^{3/2} \frac{t}{M_K^2} \frac{t^2}{\pi} \int_{t_0}^{\infty} \frac{\hat{R}_0^{\mathrm{LO}}(t')\delta_{0,\mathrm{LO}}^{3/2}(t')}{t'^3} dt'$$

$$+ \left(\frac{t^2}{\pi} \int_{t_0}^{\infty} \frac{\delta_{0,\mathrm{LO}}^{3/2}(t')}{(t'-t-i\epsilon)t'^2} dt' \right)$$

$$\times \left(\frac{t^3}{\pi} \int_{t_0}^{\infty} \frac{\hat{R}_0^{\mathrm{LO}}(t')\delta_{0,\mathrm{LO}}^{3/2}(t')}{(t'-t-i\epsilon)t'^3} dt' \right)$$

$$+ \frac{t^3}{\pi} \int_{t_0}^{\infty} \frac{\hat{R}_0^{\mathrm{LO}}(t')\delta_{0,\mathrm{NLO}}^{3/2}(t')}{(t'-t-i\epsilon)t'^3} dt'$$

$$+ \frac{t^3}{\pi} \int_{t_0}^{\infty} \frac{\hat{R}_0^{\mathrm{NLO}}(t')\delta_{0,\mathrm{LO}}^{3/2}(t')}{(t'-t-i\epsilon)t'^3} dt' - \frac{t^3}{\pi} \int_{t_0}^{\infty} \frac{\hat{R}_0^{\mathrm{LO}}(t')\delta_{0,\mathrm{LO}}^{3/2}(t')}{(t'-t-i\epsilon)t'^3}$$

$$\times \left(1 + \frac{t'^2}{\pi} \mathcal{P}\!\!\int_{t_0}^{\infty} \frac{\delta_{0,\mathrm{LO}}^{3/2}(t'')}{(t''-t'-i\epsilon)t''^2} dt'' \right) dt',$$

$$R_1^{\mathrm{NNLO}}(t) = 0,$$

$$\tilde{R}_1^{\mathrm{NNLO}}(t) = 0, \tag{E.47}$$

where $\delta c_{\mathrm{NLO}}^{N_0}$ and $\delta b_{\mathrm{NLO}}^{\tilde{N}_1}$ are given by (146) and the remaining subtraction constants denote the quantities after the gauge transformation. Note that ω and $\bar{\omega}$ appear only in polynomial terms. In M_0, M_1 and $\tilde{M}_1$, they can be reabsorbed into the NNLO subtraction constants. However, this is not the case for N_0, N_1, $\tilde{N}_1$ and R_0. Here, we are required to fix the ω-terms by imposing the requirement that the chirally expanded Omnès representation agree with the standard dispersive representation (or finally the two-loop representation). This somewhat awkward situation is just another manifestation of the fact that we identify the chiral representation with the Omnès dispersion relation although the phase shifts of the former have a wrong asymptotic behaviour.

The comparison of the Taylor expansions of (E.47) and (69) leads to the relation (148) for the subtraction constants.

References

1. S. Weinberg, Phys. Rev. **166**, 1568 (1968)
2. J. Gasser, H. Leutwyler, Ann. Phys. **158**, 142 (1984)
3. J. Gasser, H. Leutwyler, Nucl. Phys. B **250**, 465 (1985)
4. E.P. Shabalin, J. Exp. Theor. Phys. (USSR) **44**, 765 (1963) [Sov. Phys. JETP **17**, 517 (1963)]
5. N. Cabibbo, A. Maksymowicz, Phys. Rev. **137**, B438 (1965) (erratum-ibid. 168, 1926, 1968)
6. J. Batley et al., NA48-2 Collaboration, Eur. Phys. J. C **70**, 635 (2010)
7. S. Pislak et al., BNL-E865 Collaboration, Phys. Rev. Lett. **87**, 221801 (2001) (erratum-ibid. 105, 019901, 2010). arXiv:hep-ex/0106071
8. S. Pislak et al., BNL-E865 Collaboration, Phys. Rev. D **67**, 072004 (2003) (erratum-ibid. D81, 119903, 2010). arXiv:hep-ex/0301040
9. J. Batley et al., NA48/2 Collaboration, Phys. Lett. B **715**, 105 (2012). arXiv:1206.7065 [hep-ex] (addendum-ibid. B740, 364, 2015)
10. J. Bijnens, G. Colangelo, J. Gasser, Nucl. Phys. B **427** (1994). arXiv:hep-ph/9403390
11. G. Amoros, J. Bijnens, P. Talavera, Nucl. Phys. B **585**, 293 (2000). arXiv:hep-ph/0003258
12. P. Stoffer, A Dispersive Treatment of $K_{\ell 4}$ Decays. Master's thesis, University of Bern (2010)
13. G. Colangelo, E. Passemar, P. Stoffer, EPJ Web Conf. **37**, 05006 (2012). arXiv:1209.0755 [hep-ph]
14. P. Stoffer, G. Colangelo, E. Passemar, PoS CD **12**, 058 (2013)
15. P. Stoffer, Dispersive Treatments of $K_{\ell 4}$ Decays and Hadronic Light-by-Light Scattering. PhD thesis, University of Bern (2014). arXiv:1412.5171 [hep-ph]
16. F. Berends, A. Donnachie, G. Oades, Phys. Rev. **171**, 1457 (1968)
17. C. Riggenbach, Formfaktoren und Zerfallsbreite von K_{l4}-Zerfällen in der chiralen Störungstheorie. PhD thesis, University of Bern (1992)
18. M. Jacob, G. Wick, Ann. Phys. **7**, 404 (1959)
19. A.D. Martin, T.D. Spearman, *Elementary Particle Theory* (North-Holland, Amsterdam, 1970)

20. C. Kacser, Phys. Rev. **132**, 2712 (1963)
21. J. Stern, H. Sazdjian, N.H. Fuchs, Phys. Rev. D **47**, 3814 (1993). arXiv:hep-ph/9301244
22. B. Ananthanarayan, P. Buettiker, Eur. Phys. J. C **19**, 517 (2001). arXiv:hep-ph/0012023
23. M. Zdráhal, J. Novotný, Phys. Rev. D **78**, 116016 (2008). arXiv:0806.4529 [hep-ph]
24. V. Bernard, S. Descotes-Genon, M. Knecht, Eur. Phys. J. C **73**, 2478 (2013). arXiv:1305.3843 [hep-ph]
25. M. Froissart, Phys. Rev. **123**, 1053 (1961)
26. N.I. Muskhelishvili, *Singular Integral Equations* (Wolters-Noordhoff, Groningen, 1953)
27. R. Omnès, Nuovo Cim. **8**, 316 (1958)
28. B. Ananthanarayan, G. Colangelo, J. Gasser, H. Leutwyler, Phys. Rep. **353**, 207 (2001). arXiv:hep-ph/0005297
29. I. Caprini, G. Colangelo, H. Leutwyler, Eur. Phys. J. C **72**, 1860 (2012). arXiv:1111.7160 [hep-ph]
30. J.A. Oller, L. Roca, Phys. Lett. B **651**, 139 (2007). arXiv:0704.0039 [hep-ph]
31. P. Buettiker, S. Descotes-Genon, B. Moussallam, Eur. Phys. J. C **33**, 409 (2004). arXiv:hep-ph/0310283
32. D. Boito, R. Escribano, M. Jamin, JHEP **1009**, 031 (2010). arXiv:1007.1858 [hep-ph]
33. P. Stoffer, Eur. Phys. J. C **74**, 2749 (2014). arXiv:1312.2066 [hep-ph]
34. C. Callan, S. Treiman, Phys. Rev. Lett. **16**, 153 (1966)
35. S. Weinberg, Phys. Rev. Lett. **17**, 336 (1966)
36. S.B. Treiman, E. Witten, R. Jackiw, B. Zumino, *Current Algebra and Anomalies* (World Scientific, Singapore, 1985)
37. V. de Alfaro, S. Fubini, G. Furlan, C. Rossetti, *Currents in Hadron Physics* (North-Holland, Amsterdam, 1973)
38. S. Biswas, R. Dutt, K. Gupta, Ann. Phys. **52**, 366 (1969)
39. J. Bijnens, P. Talavera, Nucl. Phys. B **669**, 341 (2003). arXiv:hep-ph/0303103
40. G. D'Agostini, Nucl. Instrum. Method **A346**, 306 (1994)
41. R.D. Ball et al., NNPDF Collaboration, JHEP **1005**, 075 (2010). arXiv:0912.2276 [hep-ph]
42. V. Bernard, N. Kaiser, U.-G. Meißner, Nucl. Phys. B **357**, 129 (1991)
43. J. Bijnens, Nucl. Phys. B **337**, 635 (1990)
44. C. Riggenbach, J. Gasser, J.F. Donoghue, B.R. Holstein, Phys. Rev. D **43**, 127 (1991)
45. J. Bijnens, G. Ecker, Ann. Rev. Nucl. Part. Sci. **64**, 149 (2014). arXiv:1405.6488 [hep-ph]
46. A. Bazavov et al., MILC Collaboration, PoS CD **09**, 007 (2009). arXiv:0910.2966 [hep-ph]
47. S. Aoki et al., Eur. Phys. J. C **74**, 2890 (2014). arXiv:1310.8555 [hep-lat]
48. J. Bijnens, P. Talavera, JHEP **0203**, 046 (2002). arXiv:hep-ph/0203049
49. S.-Z. Jiang, Y. Zhang, C. Li, Q. Wang, Phys. Rev. D **81**, 014001 (2010). arxiv:0907.5229 [hep-ph]
50. J. Bijnens, I. Jemos, Nucl. Phys. B **854**, 631 (2012). arXiv:1103.5945 [hep-ph]